DICAL Records of oceanog. works in Japan

(2)

LIBRARY

JAN 19 1961

FISH & WILDLIFE SERVICE

AD
C
D

5(2)

Volume 5, No. 2
New Series

Feb. 1960

RECORDS OF OCEANOGRAPHIC WORKS IN JAPAN

Published by

Science Council of Japan

BOARD OF EDITORS

Editor-in Chief

Shinkichi HATAI

Editors

Yoshio HIYAMA — Kōji HIDAKA
Yasuo MIYAKE — Hiroshi NIINO

With the Co-operation of

Physical Oceanography

Kōji FUKUTOMI — Shōichirō HAYAMI
Mashito NAKANO — Tadayoshi SASAKI
Kanji SUDA — Ryūtarō TAKAHASHI
Michitaka UDA

Chemical Oceanography

Masayoshi ISHIBASHI — Yasuo MATSUDAIRA
Ken SUGAWARA

Geological Oceanography

Shōzaburō HANZAWA

Biological Oceanography

Denzaburō MIYADI — Yō K. OKADA
Isao TAKI — Yukio YAMADA

Fisheries

Hiroaki AIKAWA — Motosaku FUJINAGA
Takeo IMAI

Secretary

Buei ARAYA

SUGGESTION TO AUTHORS OF PAPERS FOR THE RECORDS OF OCEANOGRAPHIC WORKS IN JAPAN

An author wishing to contribute a paper to the RECORDS OF OCEANOGRAPHIC WORKS IN JAPAN should submit in compliance with the following suggestions:

1. Manuscripts will be accepted within the scope of
   Physical Oceanography — Geological Oceanography
   Chemical Oceanography — Biological Oceanography and Fisheries
2. An original and a copy of his manuscript should be type-written double-spaced in 21×29.5 cm paper, within 12 sheets, making 6 printed pages including plates and tables.
3. The manuscript should be addressed to the competent editor and mailed to the official in charge of the Science Council of Japan, Ueno Park, Tokyo, Japan.
4. The author is asked to follow this publication for forms of headings and references, etc.
5. The editors reserve the right to accept the manuscripts and to make minor editorial changes in them, so that all paper may conform to over-all style of this publication.

CONTENTS

Angular Distribution of Scattered Light in Deep Sea Water 1

The Oceanic Waves of Days to Manths' Periods 11

On the Distribution of Divergence and Convergence of Surface Drift Vectors in the Western Pacific Oceans 25

The Thickness of the Upper Homogeneous Layer 44

Existence of a Contra Solem Vortical Motion in the Coral Sea 52

Inorganic Constituents in Seaweeds 55

Determination of Manganese in Sea — Water 63

Determination of Arsenic in Sea — Water 66

Studies of Vitamin B_{12} in Natural Water 71

Biology of Sebastiscus Marmoratus CUVIER et Valenciennes 77

Biology of Sebastes Inermis Cuvier et Valenciennes 86

An Ider on the Maximum Permissible Concentration of Radio — Active Materials in Sea — Water 98

Morphometric Comparison of the Yellowfin Tuna From the Banda Sea and its Adjacent Waters* 105

Strontium — Calcium Discrimination in the Rainbow Trout 120

The Feeding Mechanism in Young Fishes 132

The Relationship of the Gill Structure and Food Habits of Some Coastal Fishes in Japan. 139

The Feeding Mechanism in Some Carnivorous Fishes 153

Notes on Some Edible Marine Fishes Collected Between The Bonin Islands and The Mouth of Sagami Bay. II 161

On The Larva Possibly Referable to Marlina Marlina (JORDAN & HILL) 167

Digitized by the Internet Archive
in 2025

https://archive.org/details/records-of-oceanographic-works-in-japan-new-series_1960-02_5_2

Records of Oceanographic Works
in Japan Vol. 5, No. 2,
March, 1960

Angular Distribution of Scattered Light in Deep Sea Water

By
Tadayoshi SASAKI, Noboru OKAMI,
Gohachiro OSHIBA and Seiichi WATANABE

1. Introduction

The knowledge about the angular distribution of scattered light in sea-water is one of the most important matters having to be learned by researchers investigating various optical problems in the ocean.

Measurements for this purpose have already been performed by some researchers using water taken up from the sea.(1)(2) From these results it is found that the intensity of forward scattered light is much larger than that of backward scattered light. The results which we obtained from the measurements using sea-water taken up from the deep layers of the Japan Trench show also the larger intensity of forward scattered lgiht. This larger forward scattering is obviously owing to the light scattering by suspended particles in sea-water. The scattering theory which is introduced by MIE and applicable to spherical particles having diameters about the same as the wave-length of incident light was applied to light scattering by suspended particles in sea-water and the angular distribution of scattered light was calculated. Comparing the curves of angular distribution obtained by theoretical calculation with those obtained by measurements it was found that the formers are very similar to the latters.

2. Apparatus and Water Samples

The scattering meter used in the determination of the angular distribution of scattered light is similar in construction to the apparatus, which B. H. ZIMM(3) used in the determination of the intensity of light scattering of dilute polymer solution. The diagram of our apparatus and projective optical system are shown in Fig. 1. In this apparatus, the monochromatic beams (546 mμ) fall in the cell full of a water sample and the scattered light is received by the multiplier phototube (RCA, 931-A) and the value of the photo-current is read by the galvanometer having a sensitivity of 10^{-10} A. A mercury lamp

*Tokyo University of Fisheries and RIKAGAKU KENKYUSHO.
**RIKAGAKU KENKYUSHO (The Institute of Physical and Chemical Research), Tokyo.

(Matsuda, SHL-100UV) is used as the light source and the monochromatic light is obtained through an interference filter and the intensity of the incident light is adjusted by a neutral density filter.

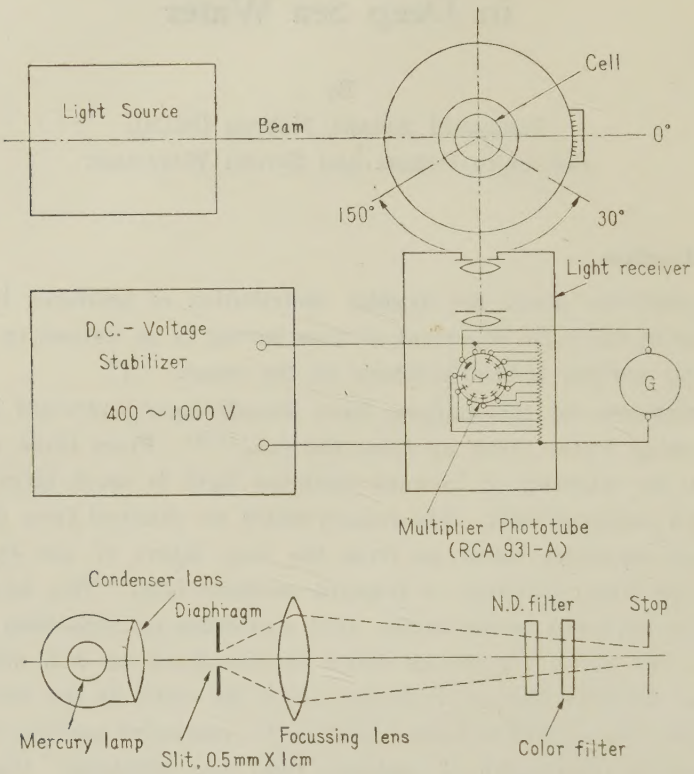

Fig. 1. Block diagram of light scattering apparatus and projective optical system.

The light receiver can rotate around the cell full of the water sample in the range from 30° to 150°. The angle of rotation can be read by the angular graduation on the table where the cell is placed. The optical system of the receiver consists of two lens-diaphragm combinations. In Fig. 2, the scattered light from the volume scattering of the water sample is focused on the rectangular diaphragm in front of lens S by the objective lens R. The image of diaphragm A is formed on the cathode of the multiplier phototube by means of lens S.

In this optical system, the size and the position of the image on the cathode is not changed by rotating the light receiver and changing light intensity can be measured. And therefore, the sensitivity is not changed by the position of the cathode of the multiplier phototube at all and the measurement can be prevented from contaminating stray light.

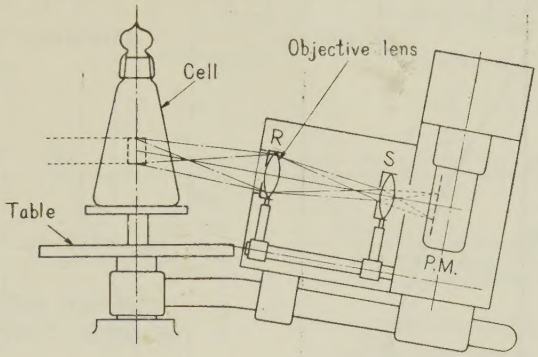

Fig. 2. Conical cell and light receiver.

The cell is of conical shape made of glass and has a capacity of about 50 cc. The conical cell is preferable to that of other shapes because reflected light on the glass surface of the cell does not reach the light receiver. In order to examine the contaminating stray light and the error caused by the unevenness of the walls of the cell, the cell is filled with aqueous solution containing 0.5 mg of fluorescein per l. The fluctuations from $1/\sin\theta$ to $F_\theta/F_{90°}$ of the cell used in the measurement in the range of the angles of scattering light from 30° to 150° are within 3%, where F_θ is the intensity of fluorescence at any angle of scattering light and $F_{90°}$ is that at 90°.

By means of "the Bathyscaphe", the French Navy's underwater exploration vessel, 15 water samples were taken out of deep sea-water at depths down to 3,000 m, in the neighborhood of the Japan Trench in June-August, 1958. These 15 samples were examined by apparatus described above.

The apparatus of sampling sea-water was made of plastics, attached to the Bathyscaphe and could take up sea-water of 6 different layers at a single submersion. The quantity of the water sample of each layer was 4,000 cc, from which 300 cc was used in the determination of suspended matter. Each water sample was placed in a sterile glass bottle and brought to the laboratory and the bottles were placed in a dark cool place until they were examined.

3. Results of Measurements and Discussion

The angular distribution curve of each sample is obtained from the results of measuring the intensity of scattered light at every 10° from 30° to 150° of scattering angle. The intensity at each scattering angle is multiplied by the volume correction factor $\sin\theta$ and plotted by the unit which is the intensity at scattering angle of 90°.

Results of measurement at depths of 600, 1,500, 2,650 and 3,000 m are shown respectively by dotted lines in Figs. 3-6.

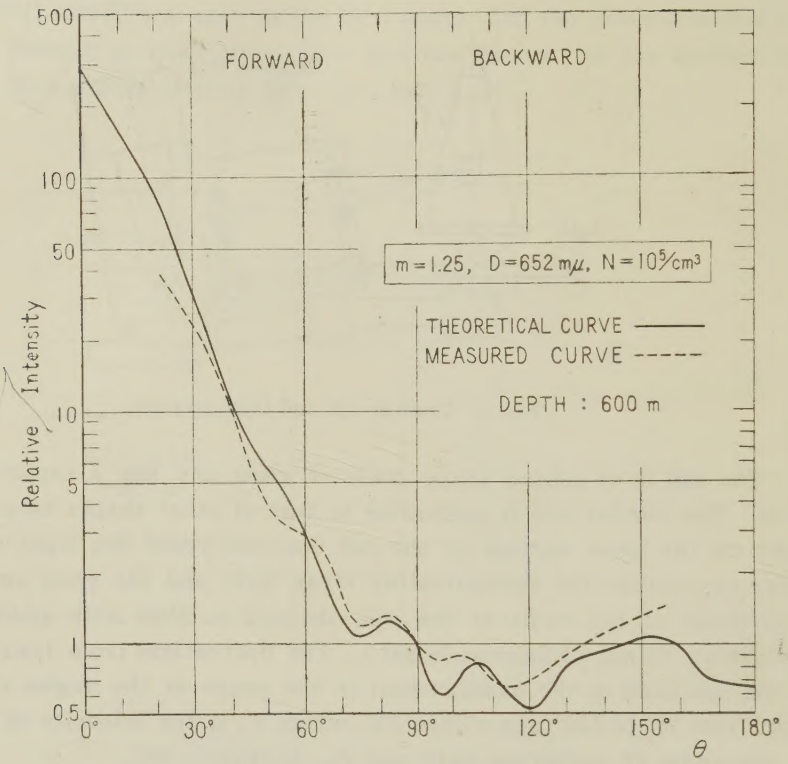
FORWARD
BACKWARD
m=1.25, D=652 mμ, N=10⁵/cm³
THEORETICAL CURVE
MEASURED CURVE
DEPTH : 600 m
Relative Intensity
500
100
50
10
5
1
0.5
0°
30°
60°
90°
120°
150°
180°
θ

Fig. 3.

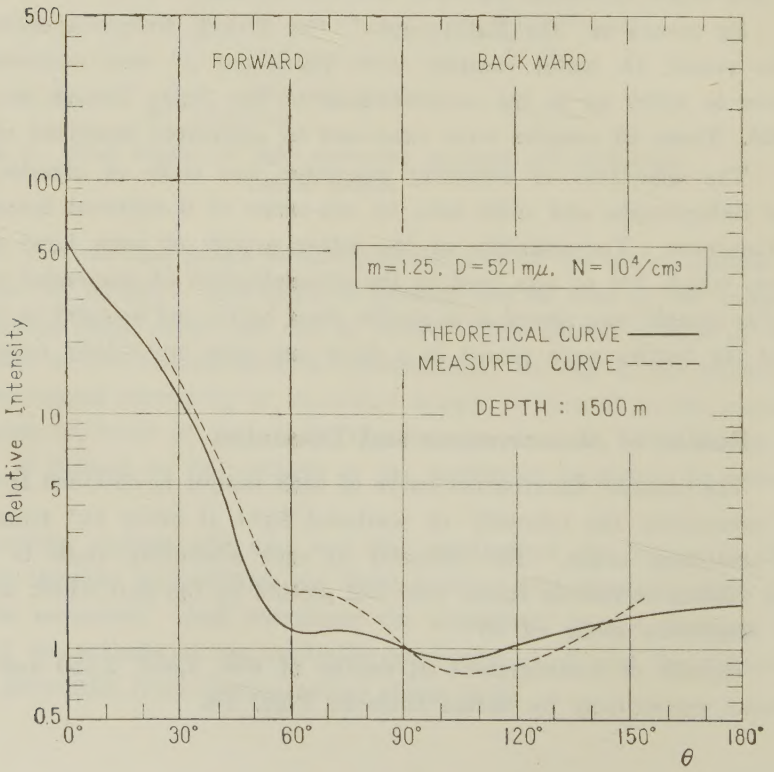
FORWARD
BACKWARD
m=1.25, D=521 mμ, N=10⁴/cm³
THEORETICAL CURVE
MEASURED CURVE
DEPTH : 1500 m
Relative Intensity
500
100
50
10
5
1
0.5
0°
30°
60°
90°
120°
150°
180°
θ

Fig. 4.

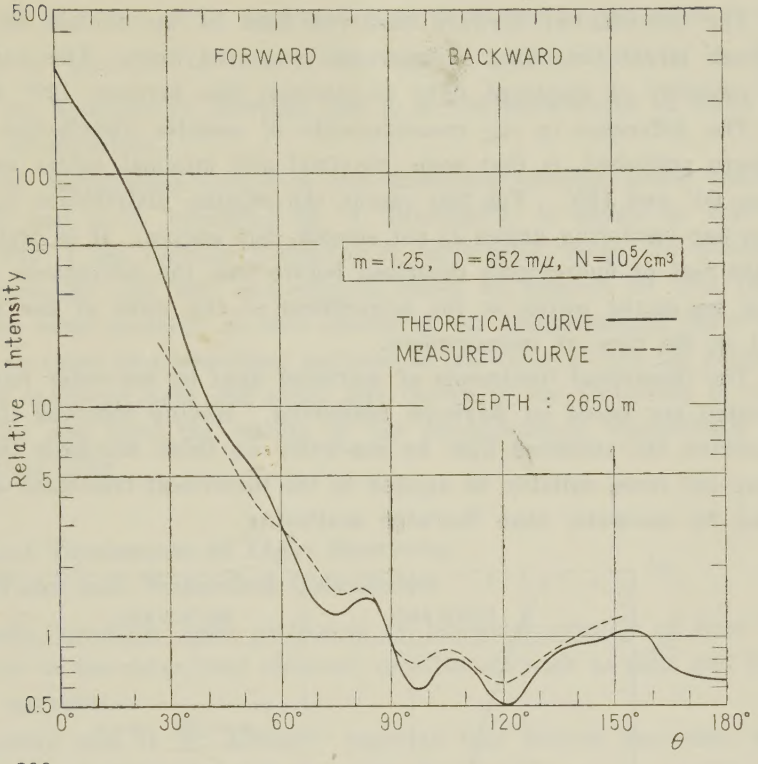
FORWARD
BACKWARD
m=1.25, D=652 mμ, N=10⁵/cm³
THEORETICAL CURVE
MEASURED CURVE
DEPTH : 2650 m
Relative Intensity
500
100
50
10
5
1
0.5
0°
30°
60°
90°
120°
150°
180°
θ

Fig. 5.

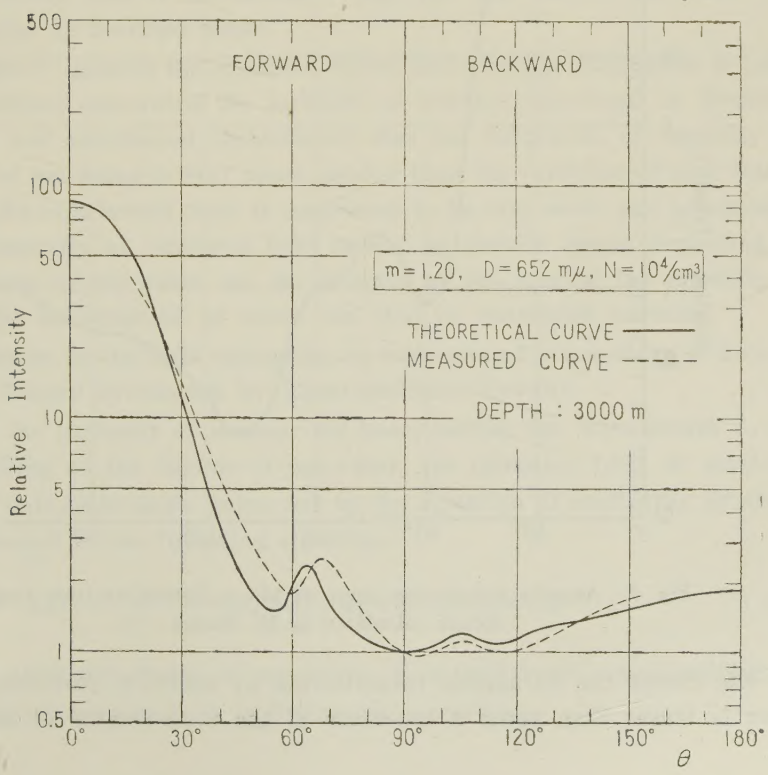
FORWARD
BACKWARD
m=1.20, D=652 mμ, N=10⁴/cm³
THEORETICAL CURVE
MEASURED CURVE
DEPTH : 3000 m
Relative Intensity
500
100
50
10
5
1
0.5
0°
30°
60°
90°
120°
150°
180°
θ

Fig. 6.

The intensity of forward scattered light of the sample at every depth is much larger than that of backward scattered light. The angle at which the intensity of scattered light is minimal, lies between 120° and 90°.

The difference in our measurements of angular distribution from those hitherto published, is that some maximal and minimal values are found between 60° and 120°. For this reason the angular distribution curve between these two scattering angles is not smooth, but uneven. It is decidedly proved by the test of fluorescence described before that the unevenness of the curve is by no means owing to the unevenness of the walls of the cell or stray light at the time of measurement.

The theoretical treatments of scattered light by sea-water having hitherto appeared are based on Rayleigh scattering. Having observed the results of measuring the scattered light by sea-water we think decidedly that Mie scattering can more suitably be applied to the theoretical treatment of light scattering by sea-water than Rayleigh scattering.

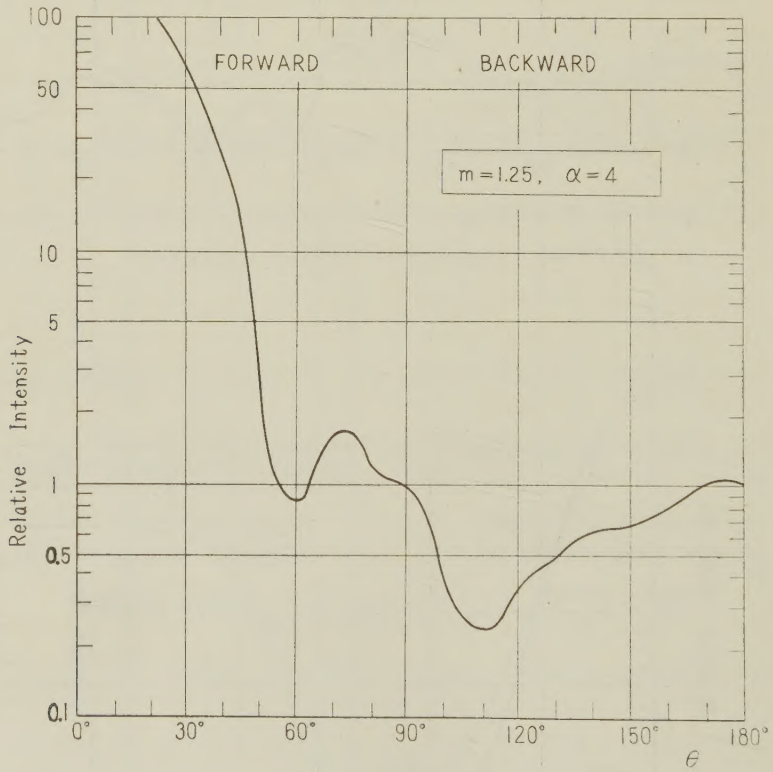

Fig. 7. Angular distribution curve of Mie scattering treating single sphere calculated by H. Blumer.

Mie theory can be applied to scattering by spherical particles, whose diameter is larger than about a twentieth of the wave-lengths of incident light

and the angular distribution of scattered light is varied by the ratio of refractive index of particles to that of surrounding medium and by $\alpha=\frac{\pi D}{\lambda}$ (where D is the diameter of particles and λ is the wave-length of light in the medium), as variables.

The angular distribution curves of Mie scattering treating single sphere, where m=1.25 and $\alpha=4$, calculated by H. BLUMER[4], is shown in Fig. 7. As shown in Fig. 7 the forward scattering is remarkably large, the minimal value lies between 90° and 120° and extreme values lie between 60° and 120°. These show the same tendency as that shown by our measurements described before. Now we think that suspended particles in sea-water govern the angular distribution of scattered light and apply Mie theory to the scattering of suspended particles and treat the results of our measurements theoretically as will be described later.

4. Theoretical Treatments of Light Scattering by Sea-Water and Numerical Calculation

Theoretically speaking, light scattering by sea-water consists of term by water molecules in sea-water, that chemical constituents such as salts and that by suspended particles.

G. L. CLARKE and H. R. JAMES[5] reported that filtered sea-water was optically similar to destilled water.

K. HISHIDA[6] applied the equation, where concentration fluctuation is taken into consideration, concerning the turbidity of solution introduced by EINSTEIN to sea-water and ascertained theoretically that the fluctuation of turbidity by the salinity of sea-water is very much smaller than the turbidity of pure water. From these the said second term is considered to be very small and is neglected here. The intensity of scattered light caused by parallel beams projecting on the unit volume of sea-water can be obtained as the sum of the intensity of scattered light by molecules of water and that by suspended particles.

With respect to the light scattering by molecules of water there is Density Fluctuation Theory introduced by EINSTEIN-SMOLUKOWSKY.

If I_0 be the intensity of unpolarized beam having the wave-length λ_0 per unit area falling on the volume of sea-water, the intensity $I_a(\theta)$, of scattered light in the unit solid angle going out in the direction of scattering angle (θ) will be expressed in the following equation.

$$I_a(\theta)=\frac{\pi^2}{18}\frac{\eta kT}{\lambda_0^4}(m_0^2-1)^2(m_0^2+2)^2(1+\cos^2\theta)I_0\,. \qquad (1)$$

where m_0 is refractive index of sea-water, η is isothermal compressibility, T is the absolute temperature, k is Boltzmann's constant.

From the scattering theory it follows that light scattered at $\theta=\frac{\pi}{2}$ was not completely polarized. However, observations[7] have shown that for pure water the light sacttered at $\theta=\frac{\pi}{2}$ was not completely polarized, the ratio δ of the weak to the strong polarized component being some value and approximately constant with wave-length. δ was termed "the polarization defect". When this term was introduced into the scattering theory (1) became[8].

$$I_a(\theta)=\frac{\pi^2}{18}\frac{\eta kT}{\lambda_0^4}(m_0^2-1)^2(m_0^2+2)^2\frac{6(1+\delta)}{6-7\delta}\left[1+\frac{1-\delta}{1+\delta}\cos^2\theta\right] \qquad (2)$$

Mie theory can only be applied to scattered light by nonabsorbing spherical particles and if this theory be applied to that by suspended particles in sea-water these particles will be assumed to satisfy these conditions.

If the suspended particles in sea-water be treated physicochemically, they will be of polydisperse-system instead of monodisperse-systems, wherein particles are not necessarily spheres. Therefore, the suspended particles in sea-water samples are assumed to be homogeneous nonabsorbing spherical particles and thinly dispersed and belong to the monodisperse-system and Mie theory is applied to the light scattered by disperse-system.

If N being the number of homogeneous spherical particles having a diameter D, be equally dispersed in the unit volume of sea-water, the intensity $I_b(\theta)$ of scattered light in the unit solid angle in the direction θ, will be introduced to the following equation by Mie theory.

$$I_b(\theta)=\frac{\lambda^2 N}{8\pi^2}(i_\perp+i_\parallel)\theta \qquad (3)$$

provided that

$$(i_\perp)\theta=\left|\sum_{n=1}^{\infty}\left[\frac{a_n}{n(n+1)}\pi_n+\frac{p_n}{n(n+1)}\{v\pi_n-(1-v^2)\pi'_n\}\right]\right|^2 \qquad (4)$$

$$(i_\parallel)\theta=\left|\sum_{n=1}^{\infty}\left[\frac{a_n}{n(n+1)}\{v\pi_n-(1-v^2)\pi'_n\}+\frac{p_n}{n(n+1)}\pi_n\right]\right|^2 \qquad (5)$$

where a_n and p_n are complex function of α and m, relative refractive index of the particle relative to sea-water. $\pi_n=\partial p_n(v)/\delta v$, $\pi'_n=\partial^2 p_n(v)/\partial v^2$ and $p_n(v)$ is Legendre's function and $v=\cos(\pi-\theta)$.

When natural light having a wave-length $\lambda_0=546$ mμ is projected on sea-water the angular distribution of scattered light can be calculated from the sum of the said equations (2) and (3).

For the purpose of comparison, the theoretical value of the intensity at each scattering angle (θ) is obtained as the relative value to the intensity of the scattering angle of 90°.

Each constant necessary for the equation (1) with respect to sea-water is shown below.

$m_0=1.33$, $\eta=4.95\times10^{-11}$ dyne^{-1} cm^2, $k=1.38\times10^{-16}$ erg deg^{-1}, $T=298°$ K, $\delta=0.1$[8].

For calculating the euqation (2) it is necessary first of all to determine the value of m, namely, the kind of suspended matter. Assuming that the suspended particles in sea-water of deep layers consist largely of inorganic matter we performed calculations using three different values, m=1.20, m=1.25 and m=1.33.

The value of $(i_\perp+i_\parallel)$ necessary for the calculation of the equation (3) was obtained in the case of m=1.20 from the table calculated by L. E. ASHLEY and C. M. COBB[9] and in the case of m=1.25 and m=1.33 from the table calculated by BLUMER[4].

5. Comparison of Theoretical Curves with Those Obtained by Measurement

The most similar curve to that obtained by measurement with respect to each sample of sea-water is selected from a lot of theoretical angular distribution curves obtained by calculation. The most similar theoretical curve to that obtained by measuring each sample of sea-water is shown by solid lines in Figs. 3-6. The values of relative refractive index, diameter and the number of particles in the unit volume of each sea-water sample, from which the theoretical curve is obtained, are shown by values in the Figures.

The most angular distribution curves obtained by measurement are similar to the theoretical curves obtained by calculation using the refractive index, m=1.25. The angular distribution curves of the sample sea-water collected at the depth of 3,000 m. is, however, rather similar to the theoretical curve obtained by calculation using the refractive index, m=1.20.

Observing the similarity of the curves obtained by measurement to those obtained by calculation using 15 kinds of sample water, we surmise that the more increase the depth, where sample water is collected, the greater becomes the similarity. Because the dissimilarity of theoretical curves to those obtained by measurement may be considered to be owing to the assumption that suspended particles are spherical particles of equal quality and the same diameter, the nature of scattered particles in sea-water must more approximate that satisfying this assumption with increase of the depth.

There is a report by W. V. BURT[10] on the light scattering by suspended particles in sea-water, to which Mie theory is applied. He applied Mie theory to the results of measuring the optical density of the visible range of wavelength of scattered light in sea-water sampled. In application of theory he adapted the value, m=1.15, as the relative refractive index of suspended particles to sea-water. This value, m=1.15, is somewhat less than those, m=1.20~1.25, which can be assumed from the results of our measurements. The difference

may be owing to the diversity between particles in bay-water measured by Burt and those in deep sea-water measured by us.

Generally speaking, the angular distribution curves obtained by measurement are much similar to those obtained by applying Mie theory to the light scattering by suspended particles. It is found by comparing the angular distribution courves obtained by measurement with those theoretical that the difference of angular distribution curves obtained by measuring each sample from each other is due to the diversity in size, kind, number and others of suspended particles in the unit volume. It is also found that the unevenness of the angular distribution curves between 60° and 120° of scattering angles is due to the phenomenon caused by a considerable amount of particles having diameters about the same as wave-length of incident light contained in the unit volume of sea-water.

The authors wish to express their hearty thanks to Dr. E. Wada and Dr. S. Iwayanagi of Laboratory of Polymer Physics, the Institute of Physical and Chemical Research, for their kind advice on construction of the photometer for scattered light. We also wish to thank Messrs. K. Arai and T. Arakawa, who helped us in calculating numerical values of theoretical equations.

References

(1) E. O. Hulburt, J. Opt. Soc. Amer., 35 (1945), 698.
(2) W. R. G. Atkins and H. H. Poole, Sci. Proc., R. D. S., 26 (1954), 313.
(3) B. H. Zimm, J. Chem. Phys., 16 (1948), 1099.
(4) H. Blumer, Zs. f. Phys., 38 (1926), 304.
(5) G. L. Clarke and H. R. James, J. Opt. Soc. Amer., 29 (1939), 43.
(6) K. Hishida, J. Ocean. Soc. Japan, 9 (1953), 143.
(7) W. H. Martin and S. Lehrman, J. Phys. Chem., 26 (1922), 113.
(8) L. H. Dawson and E. O. Hulburt, J. Opt. Soc. Amer., 31 (1941), 554.
(9) L. E. Ashley and C. M. Cobb, J. Opt. Soc. Amer., 48 (1958), 261.
(10) W. V. Burt, J. Marine Res., 14 (1955), 33.

Records of Oceanographic Works
in Japan Vol. 5, No. 2,
March, 1960

The Oceanic Waves of Days to Months' Periods

by

Kozo Yoshida

(Geophysical Institute, Tokyo Univ., Tokyo)

Abstract

The responses of the two-layered ocean to variable winds with days to months' period are examined for the meridionally bounded oceans.

The importance of the coastal boundaries to the density fluctuations as well as to the sea level changes is discussed. Particular attention was paid to the internal Kelvin waves generated along coasts and the long barotropic waves of wavelengths as large as ocean width.

So far, only the baroclinic waves along the coasts could be compared with the observed features of transient coastal upwelling and of the sea level fluctuations.

1. Introduction

The present article deals with the behaviors of the long waves in the bounded ocean which have the period range between *a few days and a few months*. They are of particular interest from their linking to the short-period fluctuations in the circulation as well as in the mean sea level. Their practical importance may emerge especially from the facts that such variations nearly correspond to those over the time scale for a single oceanographic cruise usually taken and should therefore be essential to interpret the observed results as well as to make plans for those observations. Very little has been worked as yet on these variations of intermediate period range, while their occurrence in actual oceans has been indicated by eventual observations in various occasions.

Alike the motions of water associated with ordinary ocean waves, tsunamis and tides inferred from the measurements of pressure changes or changes in sea level, some of the oceanic currents and their variations can be found from the measurements of pressure distributions and changes. Hence a study of the distributions and changes in depths of certain representative density layers and in the sea level would be essential to our understanding of these oceanic motions. The motions of the two-layered ocean contain baroclinic and barotropic modes of which the relative importance depends upon the scales of the phenomena. Evidently, the appreciably large displacement of the thermocline depth and con-

sequently the variations in the density structure should essentially be associated with the baroclinic modes of the motions. The variations in the circulation which could be detected from oceanographic observations will principally be those characterized by baroclinic waves.

As the period range of interest is as short as days to months, wind variations with scales much larger than such as 100 km would not produce appreciable forced waves of baroclinic modes in the central ocean regions. However, large baroclinic waves will take place along the coastal edges of the ocean even when the wind variations are of much larger scale. Such large free baroclinic waves may also be generated along the edges of the strong currents and also along the equator, although they will not be discussed in the present article. It may be of some interest to see that the internal waves of such longer periods may also be enlarged to a large extent in nearshore regions due to the Earth's rotation, in some similarity to the shorter gravity waves due to the shoaling depths of the water. Some cases of the baroclinic motions along coasts have been well observed as coastal upwelling at various coasts (See Section 8).

2. A Theoretical Model

The model ocean is assumed to be two-layered. The mean density in each layer, the mean depth of thermocline and of the ocean are assumed to be uniform horizontally. Although the considerable variations in density distributions across the strong current are in actuality likely to be responsible for the waves such as meander waves, they are not included in the present consideration. The effects of the variations in the ocean depth are also disregarded, although they may modify the motions to some large extent. For the period range of the present interest, frictional effects except for wind stirring in the upper layer are disregarded. The meridional coast boundaries are only considered. The meridional variations are confined only to those in winds with wavelengths of the order of about 6,000 km.

The basic equations as well as some of the derivations to be used for the following considerations are given in the Appendix.

3. Free Motions

It can be seen from the analysis given in the Appendix that the dynamical system under the present model contains *four* different types of waves, of which two are baroclinic and the other two are barotropic. All the four motions represent the waves which propagate toward west.

Consider a free motion of the form*

$$(w_0)_{ij} \propto e^{i(\sigma t+ly)+a_{ij}x} \qquad (1)$$

* The symbols employed are explained in the list which appears at the end of this paper.

where σ is the frexuency, $T=2\pi/\sigma$ being the period, and l is the meridional wave number, $L_y=2\pi/l$ is the meridional wavelength. Substitution of (1) in the homogeneous vorticity equation [(13′) : $G_1(\tau)=0$] gives the following four values of d_{ij} as the approximate roots of the equation:

$$\left.\begin{aligned} d_{11} &\sim -k+i\frac{\beta}{2\sigma} \\ d_{12} &\sim k+i\frac{\beta}{2\sigma} \end{aligned}\right\} \vartheta_1 \text{ waves (baroclinic)}$$

$$\left.\begin{aligned} d_{21} &\sim i\frac{\beta}{\sigma} \\ d_{22} &\sim i\left(\frac{f^2}{gD}+l^2\right)\frac{\sigma}{\beta} \end{aligned}\right\} \vartheta_2 \text{ waves (barotropic)} \qquad (2)$$

where

$$k=\frac{f}{\sqrt{gH\Delta\rho}}\sqrt{\frac{D}{H'}}$$

The first two, d_{11} and d_{12}, are the roots of the equation $\vartheta=-k^2/\beta$ which gives $w_{H1}\simeq -D/H'\Delta\rho\cdot w_{01}$ and hence the baroclinic modes. The last two, d_{21} and d_{22}, are the roots of $\vartheta=-f^2/g\beta D$ which gives $w_{H2}\simeq H'/D\cdot w_{02}$ and hence the barotropic.

From (1) and (2), it is seen that the baroclinic motions, d_{1j}, have appreciable amplitudes only at either edge of the ocean. One of them is appreciable at the western edge of the ocean, and the other one at the eastern, both being confined within the distances of about 100 kilometers from the coast since k is the order of 10^{-6} cm^{-1}. The barotropic motions, d_{2j}, have uniform magnitudes over the whole ocean. The longer wave, d_{22}, has a very large wavelength of the order of ocean width, while the wavelength of the shorter wave, d_{21}, is nearly 600 km. Of these four waves, only the longest barotropic wave transmits its energy westward. (Arons and Stommel, 1956).

The free motions are of particular interest because they may be excited, due to the presence of the coastal boundaries, for the wind stress variations of various wavelengths. Another importance of the free modes would of course be related to resonance phenomena in the forced waves or at least to the growth of the forced waves.

4. Forced Motions

From the derivation given in the Appendix, only the forced motions will be taken up here with a subscript τ.

From (13′)

$$w_{0\tau}=\frac{G_1(\tau)}{f}\frac{1+\dfrac{g\beta H'\Delta\rho}{f^2}\vartheta_\tau}{\left(1+\dfrac{\beta}{k^2}\vartheta_\tau\right)\left(1+\dfrac{g\beta D}{f^2}\vartheta_\tau\right)},$$

From (12')

$$w_{H\tau} = -w_{0\tau} \frac{\frac{g\beta H'}{f^2}\vartheta_\tau}{1+\frac{\beta g H' \Delta\rho}{f^2}\vartheta_\tau},$$

Hence

$$w_{0\tau}+\omega_H \Delta\rho \simeq w_{0\tau} \frac{1}{1+\frac{\beta g H' \Delta\rho}{f^2}\vartheta_\tau}$$

It follows from the above that

$$\left.\begin{aligned} &w_{H\tau} \simeq -\frac{1}{\Delta\rho} w_{0\tau} \\ &| w_{0\tau}+w_{H\tau}\Delta\rho | \ll w_{0\tau} \end{aligned}\right\} \quad \text{for} \quad \vartheta_\tau \gg \frac{k^2}{\beta}\frac{H}{D},$$

and

$$\left.\begin{aligned} &| w_{H\tau} | \ll | w_{0\tau} | \frac{H'}{D} \\ &w_{0\tau}+w_{H\tau}\Delta\rho \simeq w_{0\tau} \end{aligned}\right\} \quad \text{for} \quad \vartheta_\tau \ll \frac{f^2}{g\beta D}.$$

Thus the forced motions with very short wavelengths such as $| d_\tau | \gg k$ are baroclinic, and those with very long wavelengths are barotropic. The dependence of the response of the two-layer ocean upon the scale of the disturbances has been discussed previously by the present author (Yoshida, 1959) and more thoroughly by Veronis and Stommel (1956).

5. The Motions along the Edges of the Oceans

Some of the nature of the solutions can be obtained simply without going into the details of the solutions for each separated modes of the motions. Let us put the subscripts 1 and 2 the baroclinic and barotropic motions, resepectively. Let us confine ourselves to the case for which no meridional variations in the conditions occur except for the change in Coriolis parameter with latitudes. Of course, the model under this assumption is *not* quite realistic. However, this simpler treatment may be desirable to see somewhat qualitative nature of the problem more clearly.

The assumption is that (1) the winds are purely meridional and vary only zonally and (2) the two-layered ocean is bounded by the meridional coasts.

The original equations are linear and can be separated into the free baroclinic, free barotropic and the forced motions, with subscripts 1, 2 and τ, respectively.

From the approximate equations

$$\frac{\partial v_1}{\partial t} = -\frac{g}{f}\frac{\partial w_{01}}{\partial x}, \qquad (3)$$

$$\frac{\partial v_1'}{\partial t} = -\frac{g}{f}\frac{\partial}{\partial x}(w_{01}+w_{H1}\Delta\rho)\,, \tag{4}$$

and

$$w_{H1} \simeq -\frac{D}{\hat{H}\Delta\rho}\,w_{01}\,, \tag{5}$$

it immediately follows that

$$H\frac{\partial v_1}{\partial t}+H'\frac{\partial v_1'}{\partial t}\equiv 0\,, \tag{6}$$

for all values of x.

This indicates that the meridional masstransport for the free baroclinic motions vanishes everywhere and always. In other words there is always and everywhere the current in the lower layer of which the direction is opposite to that in the surface layer, or opposite to the wind direction. The free baroclinic motions are significant only at the edges of the ocean, so that such countercurrents in the lower layers which could be detected by dynamic computations would only be confined within small distances from the coasts. This may give an immediate account for the vertical divergence feature of isotherms observed for the coastal upwelling areas such as off the California coasts (Yoshida et al, 1957). As far as there is no zonal component of wind stress along the coasts, the above is true whether or not the forced motions occur.

From the original equations

$$H\frac{\partial v}{\partial t}+H'\frac{\partial v'}{\partial t}+f(uH+u'H')=\tau_y\,, \tag{7}$$

Along the edges of the ocean

$$uH+u'H'=0\,, \tag{8}$$

and, further, owing to (4),

$$D\frac{\partial v_2}{\partial t}+\left(H\frac{\partial v_\tau}{\partial t}+H'\frac{\partial v_\tau'}{\partial t}\right)=\tau_y\,. \tag{8}$$

We can also see

$$H\frac{\partial v_\tau}{\partial t}+H'\frac{\partial v_\tau'}{\partial t}=\tau_y\frac{d_\tau^2}{d_\tau^2+\dfrac{\beta}{i\sigma}d_\tau-\dfrac{f^2}{gD}}\,. \tag{9}$$

Table 1 shows the approximate magnitudes for each motion at the coasts.

These results at either one of the boundaries are obtained independently of the conditions at each other boundary.

It then follows that the meridional winds of very short wavelengths ($|\vartheta_\tau| \gg k^2/\beta$) will produce only the baroclinic forced motions and no free motions, whereas those of much longer wavelengths will cause no appreciable forced motions but baroclinic and barotropic free motions.

Table 1. The magnitudes of $\partial v/\partial t$ at the coast for various ranges of wavelengths of winds.

$d_\tau \rightarrow$	$k(10^{-6})$	$\frac{\beta}{\sigma}(10^{-7})$	$\frac{f^2}{gD}\frac{\sigma}{\beta}(10^{-9})$
$\frac{\partial v_\tau}{\partial t}$	$\frac{\tau}{H}$	$\frac{\tau}{D}$	0	0
$\frac{\partial v_\tau'}{\partial t}$	0	$\frac{\tau}{D}$	0	0
$\frac{\partial v_2}{\partial t}$	0	0	$\frac{\tau}{D}$	$\frac{\tau}{D}$
$\frac{\partial v_1}{\partial t}$	0	$\frac{\tau}{H}\frac{H'}{D}$	$\frac{\tau}{H}\frac{H'}{D}$	$\frac{\tau}{H}\frac{H'}{D}$
$\frac{\partial v_1'}{\partial t}$	0	$-\frac{\tau}{D}$	$-\frac{\tau}{D}$	$-\frac{\tau}{D}$

For longer wavelengths of the disturbing winds, the forced motions are relatively small. It can be seen that, for the wavenumbers much lower than β/σ , the forced waves are negligibly small compared with the free waves generated at the coastal boundaries. Meridional winds parallel to the coasts produce surface offshore or onshore transports which lead to coastal vertical motions. During the period of upwelling, the surface offshore transport is partially compensated by the onshore transport in the lower layer. The longshore component of the currents in the lower layer is also opposite to the surface windward currents. This free motion is thus the baroclinic motion and the total masstransport in meridional direction vanishes at all the time. The meridional winds must produce certain significant amount of meridional masstransport, so that this must be provided by barotropic free waves generated at the coasts. Therefore, the free baroclinic wave should be associated with the barotropic waves which are free motions for the wave numbers of the disturbing winds much lower than β/σ The free baroclinic waves are generated for all wave numbers of the winds except for thos extremely high, higher than k. As far as the wavenumbers are lower than k, the characteristics of the free baroclinic motions do not depend upon the wavenumbers of the winds.

For very short wavelengths ($d_\tau \gg k$), the forced motions are baroclinic and are purely meridional! As the forced motions are closely related to the wind stress vorticity (curl), the magnitude of this meriodional forced motion is large. The wave satisfying always the boundary conditions at the coast, no free motion is to be generated ot the coasts.

The forced motions are barotropic for all wavelengths $d_\tau \ll k$. Unless the forced motions of baroclinic modes are dominant, either the barotropic forced

motions or free motions are dominant. The free baroclinic motions are generated for all wavelengths in this range as stated above. Whether the forced barotropic motions are dominant or the free barotropic motions are dominant depend upon the wave numbers. The barotropic forced motions are dominant for wave numbers $k \gg d_\tau \gg \beta/\sigma$, and the barotropic free motions are dominant for $d_\tau \ll \beta/\sigma$. Thus the energy of the barotropic forced waves are absorbed into the barotropic free waves for $d_\tau \ll \beta/\sigma$.

6. Magnitudes of the Motions and the d_{22} Wave

Let estimate the order of magnitude of the velocities for the simplest case described in § 5. Each of the velocities are expressed as shown in Table 2.

Table 2. Velocities at the coast for each mode of the motions.

	d_1	d_2	
		d_{21}	d_{22}
$\lvert w_0 \rvert$	$\frac{\tau}{\sqrt{gH}} \sqrt{\Delta\rho} \left(\frac{H'}{D}\right)^{3/2}$	$\frac{f\tau}{gD} \frac{\sigma}{\beta}$	$\frac{\beta}{\sigma} \frac{\tau}{f}$
$\lvert w_H \rvert$	$\frac{\tau}{\sqrt{gH\Delta\rho}} \sqrt{\frac{H'}{D}}$	$\frac{f\tau}{gD} \frac{\sigma}{\beta} \frac{H'}{D}$	$\frac{\beta}{\sigma} \frac{\tau}{f} \frac{H'}{D}$
$\lvert v \rvert$	$\frac{\tau}{\sigma H} \frac{H'}{D}$	$\frac{\tau}{\sigma D}$	
$\lvert v' \rvert$	$\frac{\tau}{\sigma D}$	$\frac{\tau}{\sigma D}$	
$\lvert u \rvert$	$\frac{\tau}{fH} \frac{H'}{D}$	$\frac{\tau}{fD}$	
$\lvert u' \rvert$	$\frac{\tau}{fD}$	$\frac{\tau}{fD}$	

Putting the numerical values (all in C.G.S. units): $\tau=1$, $f=10^{-4}$, $\beta=2\times10^{-13}$, $g=10^3$, $\Delta\rho=10^{-3}$, $H=10^4$, $H'=10^5$ and $D\simeq10^5$, the order of magnitudes of the velocities are given as illustrated in Table 3.

Table 3. Numerical Values for the velocities at the coast (rough order of magnitude)

	d_1	d_2	
		d_{21}	d_{22}
$\lvert w_0 \rvert$	10^{-5}	10^{-5}	10^{-3}!
$\lvert w_H \rvert$	$10^{-}{}_2$	10^{-5}	10^{-3}!
$\lvert v \rvert$	10^2	10	
$\lvert v' \rvert$	10	10	
$\lvert u \rvert$	1	0.1	
$\lvert u' \rvert$	0.1	0.1	

From this table, it is readily seen that the longer barotropic waves, d_{22}, may have very large amplitude of the sea level oscillations. This amplitude may amount to the order of 1 to 10 meters for the periods considred. Such large variations have *not* been observed in usual conditions and may not, therefore, be very realistic. There are various possibilities that actual conditions of the real ocean would reduce the amplitudes of the waves appreciably. For instance, it will be seen in next section that such large waves would not occur if the meridional variations in the motions as usually encountered should exist. Nevertheless, this wave might still contain some considerable part of the level changes under certain conditions and might therefore deserve more attention. A physical interpretation of this d_{22} wave is given briefly in the Appendix 2.

7. Effects of Meridional Variations

In the real oceans, there *are* meridional variations in conditions to a considerable extent. As far as the most general features are concerned, the length scale in the meridional directions may be taken to be of the order of several thousand kms and hence $l \sim 10^{-8}\,\mathrm{cm}^{-1}$.

The characteristic numbers for the free modes, d_{ij}, are not altered by the introduction of such meridional variations, except for d_{22}. The number d_{22} is, in this case, given by

$$d_{22} \sim i\left(\frac{f^2}{gD}+l^2\right)\frac{\sigma}{\beta}\,.$$

However, the effects of the meridional variations in winds are considerable, especially on the amplitudes of the d_{22} wave as well as the behaviors of the baroclinic waves along the coastal boundaries. In the first place, unreasonably large amplitudes of the d_{22} waves will *not* occur in this case as will be shown later. This seems to give a right interpretation for the absence of such large d_{22} oscillations in the real oceans. Another outstanding phenomenon which emerges under the presence of meridional variations in the conditions would be the *internal Kelvin wave* (Proudman, 1953: 346-349) travelling southward along the western edge of the ocean and northward along the eastern edge. Although no observational evidence has ever been found to prove the occurrence of such travelling waves, it might be worthwhile to suggest their importance in the actual ocean.

Simple derivation and illustration for this wave are given in Appendix 2. The phase speed of this wave along the coast is given by $C=\sqrt{gH\Delta\rho}\sqrt{\frac{H'}{D}}$ which is the speed for the ordinary internal wave. With the numerical values as used before,* $C \simeq 10^2\,\mathrm{cm/sec}$. If the winds have the wave lengths of 6,000 km and vary with the periods of about a few months, there will be large

* $H=10^4$, $\Delta\rho=10^{-3}$, $H'=10^5$, $D\simeq 10^5$, all in C.G.S. units.

possibility that this wave will develop to a great extent.

Finally, let us consider a theoretical model of the problem to see some more realistic solution which has been described somewhat separately before.

Assume the wind stress distribution to be given by

$$\tau_x = \tau_1 e^{i\sigma t} \sin ly \sin mx$$

$$\tau_y = \tau_2 e^{i\sigma t} \cos ly \cos mx$$

where $m = \pi/L$

The ocean is assumed to be bounded by the western coast at $x=0$ and the eastern coast at $x=L$. Numerically, $|\tau_1|=|\tau_2|=1$, $l=10^{-8}$, $L=10^9$. The boundary conditions are

$$u = u' = 0 \quad \text{at} \quad x = 0 \quad \text{and} \quad L,$$

where u and u' are the velocity components normal to the boundaries in the upper and lower layer, respectively.

The solutions for vertical velocities at the ocean surface, w_0 and at the interface, ω_H, are given by

$$w_0 = w_{01} + w_{02} + w_{0\tau}$$

$$w_H = -\frac{D}{H\Delta\rho} w_{01} + \frac{H'}{D} \omega_{02} + \omega_{H\tau}$$

where

$$w_{01} = \frac{\frac{H'}{D}}{k^2 - f^2\frac{l^2}{\sigma^2}} \frac{f\tau_2}{2gH} \begin{Bmatrix} \left\{\left(k - \frac{fl}{\sigma}\right)\cos(\sigma t - ly) + \left(k + \frac{fl}{\sigma}\right)\cos(\sigma t + ly)\right\} e^{-kx} \\ + \left\{\left(k + \frac{fl}{\sigma}\right)\cos(\sigma t - ly) + \left(k - \frac{fl}{\sigma}\right)\cos(\sigma t + ly)\right\} e^{-k(L-x)} \end{Bmatrix} \tag{10}$$

$$w_{02} = \frac{\tau_1 m}{gD} \frac{f\beta l}{\sigma} \frac{1}{\left(\frac{f^2}{gD} + l^2\right)^2 - \frac{m^2\beta^2}{\sigma^2}} \cos ly \cdot R,$$

$$w_{0\tau} = -\frac{fl\tau_1}{gD} \frac{\cos ly}{\left(\frac{f^2}{gD} + l^2\right)^2 - m^2\frac{\beta^2}{\sigma^2}} \begin{Bmatrix} l^2 + \frac{f^2}{gD} \sin mx \cos \sigma t \\ + \frac{m\beta}{\sigma} \cos mx \sin \sigma t \end{Bmatrix},$$

$$w_{H\tau} = \frac{lH'}{fD} \tau_1 \frac{\cos ly}{\left(\frac{f^2}{gD} + l^2\right)^2 - m^2\frac{\beta^2}{\sigma^2}} \begin{Bmatrix} \left\{l^2\left(l^2 + \frac{f^2}{gD}\right) - \frac{m^2\beta^2}{\sigma^2}\right\} \sin mx \cos \sigma t \\ -m\frac{\beta}{\sigma}\frac{f^2}{gD} \cos mx \sin \sigma t \end{Bmatrix},$$

$$R = \frac{1}{\sqrt{2\{1 - \cos(S_2 - S_1)L\}}} \begin{bmatrix} \sin\{\sigma t + S_2 x - S_1 L + \tan^{-1}\theta + \tan^{-1}\theta_1\} \\ -\sin\{\sigma t + S_1 x - S_1 L + \tan^{-1}\theta + \tan^{-1}\theta_2\} \end{bmatrix},$$

$$\theta=\frac{\sin(S_2-S_1)L}{1-\cos(S_2-S_1)L},$$

$$\theta_1=\frac{\sin S_1L}{1+\cos S_1L},$$

$$\theta_2=\frac{\sin S_2L}{1+\cos S_2L},$$

$$S_1=\frac{\beta}{\sigma},\qquad S_2=\left(l^2+\frac{f^2}{gD}\right)\frac{\sigma}{\beta},$$

The solution for the uniform meridional winds, $\tau_x\equiv 0$ and $\tau_y\equiv\tau$, is approximately

$$w_0=\frac{\tau_2}{\sqrt{gH}}\sqrt{\Delta\rho}\left(\frac{H'}{D}\right)^{3/2}[e^{-kx}+e^{-k(L-x)}]+\frac{f\tau_2}{gD}\frac{\sigma}{\beta}R_1-\frac{\tau_2\beta}{f\sigma}R_2,$$

$$w_H=-\frac{\tau_2}{\sqrt{gH\Delta\rho}}\sqrt{\frac{H'}{D}}[e^{-kx}+e^{-k(L-x)}]+\frac{H'}{D}\frac{f\tau_2}{gD}\frac{\sigma}{\beta}R_1-\frac{H'}{D}\frac{\tau_2\beta}{f\sigma}R_2,$$

where

$$R_1=\frac{1}{\sqrt{2\{1-\cos(S_2-S_1)L\}}}\sin\left\{\begin{array}{l}\sigma t+\dfrac{\beta}{\sigma}(x-L)\\ \quad+\tan^{-1}\dfrac{\sin(S_2-S_1)L}{1-\cos(S_2-S_1)L}\\ \quad+\tan^{-1}\dfrac{\sin S_2L}{1+\cos S_2L}\end{array}\right\},$$

$$R_2=\frac{1}{\sqrt{2\{1-\cos(S_2-S_1)L\}}}\sin\left\{\begin{array}{l}\sigma t+\dfrac{f^2}{gD}\dfrac{\sigma}{\beta}x-\dfrac{\beta}{\sigma}L\\ \quad+\tan^{-1}\dfrac{\sin(S_2-S_1)L}{1-\cos(S_2-S_1)L}\\ \quad+\tan^{-1}\dfrac{\sin S_1L}{1+\cos S_1L}\end{array}\right\}.$$

From the results, two outstanding points will be noted. The behaviors of the baroclinic coastal waves expressed in (10) depend upon $fl/\sigma k$, that is, $\frac{l}{\sigma}Ci$, where $Ci=\sqrt{gH\Delta\rho}\sqrt{\frac{H'}{D}}$. When $\sigma\simeq lC_i$, the waves at both boundaries become very large, showing resonance. In this case, the wave becomes purely progressive wave travelling southward along the western boundary and that travelling northward along the eastern boundary. For $l=10^{-8}$, $k=10^{-6}$ and $f=10^{-4}$, the resonance frequency is $\sigma=10^{-6}\,\mathrm{sec}^{-1}$. If σ differs much from $10^{-6}\,\mathrm{sec}^{-1}$, both edge waves become standing waves.

Another point of interest is that the amplitudes of thd d_{22} wave are not considerably large in the presence of the meridional variations. Hence the question raised in the section 2 concerning unreasonably large amplitudes for theoretical d_{22} waves is now answered. That is, it is now seen that such

unreasonable result has followed from our assumption of no meridional variations which is not realistic as there are generally meridional variations of the order of $10^{-8}\,cm^{-1}$. However, there might be some cases in which the d_{22} wave is of considerable significance. For an example, the motions in the waters on which are seasonal winds (monsoon) blow almost uniformly may contain large d_{22} wave.

8. Summary

As a result of the examination of a theoretical model for the responses of the stratified, bounded ocean to variable winds of days to months' periods, four types of free waves as well as the forced waves due to somewhat specific wind stress distributions have been discussed. Particular attention was paid to the free baroclinic waves confined within distances as small as 100 km, travelling to the left (facing coast from the sea in the northern hemisphere). Attention is also paid to the barotropic waves of the largest wavelengths which might contribute some important portion of rise and fall to the sea level oscillations.

In all cases, there are pronounced interface oscillations along the coasts. In nearly all the cases, there are counter-currents in the lower layer as usually found in the coastal upwelling regions. The mechanism for the occurrence of these waves is what has long been known to account for the upwelling along coasts.

The actual occurrence of the baroclinic response of the ocean edge motions to the local winds of the duration of the order of a month has been indicated from the observations of the coastal upwelling in various parts of the oceans (SVERDRUP and FLEMING, 1941: TAYLOR and STEWART, 1959). The propagation of such baroclinic disturbances along the coast as the internal Kelvin waves has not yet been observed. However, a study of daily mean sea level along the coasts of Japan by SHOJI (1954, 1957) and by SHOJI and WATANABE (unpublished) appears to give a possibility that the progressive disturbances of the sea level observed might be such waves. Further speculation might lead to a possibility that the westward propagation of such baroclinic waves might be related to the offshore movement of the boundary region continually being re-formed as pointed out by SVERDRUP (SVERDRUP, 1938: SVERDRUP and FLEMING, 1941). The observed speed of the westward movement was about 2 cm/sec according to SVERDRUP and FLEMING, in close agreement with the theoretical value given by for the duration of favorable winds of a month to two. On the other hand, the barotropic waves derived in the present article have not yet been detectd from obsrvations.

References

Arons, A. B. and Henry Stommel (1956): A-plane analysis of free periods of the second class in meridional and zonal oceans. Deep-Sea Res. 4 : 23-31.

Shioji, Daitaro (1954): On the variations in daily mean sea level and in oceanographic conditions. Hydrogr. Bull., Spec. No. 14.

(1957): Kuroshio during 1955. Rec. Oceanogr. Works Japan, Spec. No. 21-26.

Sverdrup, H. U. (1938): On the process of upwelling, J. Mar. Res., 1 : 155-164.

Sverdrup, H. U. and R. H. Fleming (1941): The waters off the coast of Southern California, March to July, 1937. Bull. Scripps Inst. Oceanogr., Vol. 4, No. 10 : 261-378.

Taylor, C. B. and H. B. Stewart, Jr. (1959): Summer upwelling along the East Coast of Florida. J. Geophys. Res. 64 (1) : 33-40.

Veronis, G. and H. Stommel (1956): The action of variable wind stresses on a stratified ocean. J. Mar. Res. 15 (1) : 43-75.

Yoshida, Kozo (1955): Coastal upwelling off the California coast. Rec. Oceanogr. Works Japan, 2 (2) : 8-20.

(1958): Coastal upwelling, coastal currents and their variation. Rec. Oceanogr. Works Japan, (Spec. no. 2) : 85-89.

Yoshida, Kozo and Mizuki Tsuchiya (1957): Northward flow in lower layers as an indicator of coastal upwelling. Rec. Oceanogr. Works Japan, 4 (1) : 14-22.

Appendix 1

The basic equations are

$$\frac{\partial u}{\partial t} - v = g\frac{\partial z_0}{\partial x} + \frac{\tau_x}{H}, \qquad (1)'$$

$$\frac{\partial v}{\partial t} + fu = g\frac{\partial z_0}{\partial y} + \frac{\tau_y}{H}, \qquad (2)'$$

$$\frac{\partial u'}{\partial t} - fv' = g\frac{\partial}{\partial x}(z_0 + h\Delta\rho), \qquad (3)'$$

$$\frac{\partial v'}{\partial t} + fu' = g\frac{\partial}{\partial y}(z_0 + h\Delta\rho), \qquad (4)'$$

$$\frac{\partial u}{\partial x} + \frac{\partial v}{\partial y} + \frac{\partial w}{\partial z} = 0, \qquad (5)'$$

$$w_H = \partial h/\partial t, \qquad w_0 = \partial z_0/\partial t, \qquad (6)'$$

$$w_D = 0. \qquad (7)'$$

The vorticity equations derived from (1′), (2′), (3′) and (4′) are

$$\frac{\partial \zeta}{\partial t} - f\frac{w_H - w_0}{H} + \beta v = \frac{1}{H}\,\mathrm{cual}\,\underline{\tau}, \qquad (8)'$$

$$\frac{\partial \zeta'}{\partial t} + f\frac{w_H}{H'} + \beta v' = 0, \qquad (9)'$$

where $\zeta = \partial v/\partial x - \partial u/\partial y$, and $\zeta' = \partial v'/x - \partial u'/\partial y$.

Based on the equations above, the equation for w_0 is

$$w_0\left[1+\frac{g\beta D}{f^2-\tau^2}\vartheta+\frac{g\beta^2 D}{(f^2-\sigma^2)k^2}\vartheta^2\right]=\frac{f}{f^2-\sigma^2}G_1(\tau)\left[1+\frac{g\beta H'\Delta\rho}{f^2-\sigma^2}\vartheta_\tau\right], \qquad (10)'$$

where

$$\vartheta=-\frac{l_1^2+d^2}{\beta}+\frac{2fl_1}{f^2-\sigma^2}-\frac{d}{i\sigma}\frac{f^2+\sigma^2}{f^2-\sigma^2},$$

$$l_1=\frac{\partial}{\partial y}, \quad d=\frac{\partial}{\partial x},$$

$$G_1(\tau)=\mathrm{curl}\,\underline{\tau}+\frac{i\sigma}{f}\,\mathrm{div}\,\underline{\tau}-\frac{\beta}{f(f^2-\sigma^2)}\{2if\sigma\tau_y-(f^2+\sigma^2)\tau_x\}, \qquad (11)'$$

$$k^2=\frac{f^2-\sigma^2}{gH\Delta\rho}\frac{D}{H'},$$

We also have

$$w_H=w_0\left(1+\frac{gH\beta}{f^2-\sigma^2}\vartheta\right)-\frac{f}{f^2-\sigma^2}G_1(\tau), \qquad (12')$$

Assuming at this point, $l_1=il$, $l\simeq10^{-8}$, $d\simeq10^{-6}\sim10^{-9}$, $\sigma\simeq10^{-5}\sim10^{-7}$, equations (10) and (11) can be approximated by

$$w_0\left(1+\frac{\beta}{k^2}\vartheta\right)\left(1+\frac{g\beta D}{f^2}\vartheta\right)=\frac{1}{f}G_1(\tau)\left[1+\frac{g\beta H'\Delta\rho}{f^2}\vartheta_\tau\right], \qquad (13')$$

and

$$\vartheta\simeq-\left(\frac{d^2-l^2}{\beta}\right)-\frac{d}{i\sigma},$$

$$G_1(\tau)\simeq\mathrm{curl}\,\underline{\tau}-\frac{\beta i\sigma}{f^2}\left(2\tau_y-\frac{f}{i\sigma}\tau_x\right).$$

Appendix 2

The d_{22} wave

This long wave comes essentially from a vorticity balance

$$-f\frac{\partial w}{\partial z}+\beta v=0,$$

for the barotropic motion, so that

$$fw_0+\beta vD=0,$$

and then

$$\frac{\partial w_0}{\partial t}-\frac{g\beta D}{f^2}\frac{\partial w_0}{\partial x}=0.$$

indicating that the wave travels westward with a phase velocity $g\beta D/f^2$ ($\sim10^3$cm/sec$\sim10^9$cm/10^6sec). For this wave to occur, the occurrence of convergence associated with the poleward flow is essential. Let us take a portion of the ocean of which the surface sea level rise from west toward east. Geostrophically balanced to this surface slope, there is northward current (in the Northern hemisphere) from surface to bottom as far as the barotropic motions are concerned. The northward current tends, on the otherhand, to produce the horizontal convergence and consequently the rising of the sea surface. Then it immediately follows that the surface deviation must propagate toward west in form of a wave.

If the surface is lower toward north, along the western edge of the ocean, the northward current is accelerated due to this surface slope. Geostrophically balanced then, the horizontal gradient of vertical velocity will be negative, that is, w_0 decrease toward east. As the vorticity balance for the baroclinic motions near the coast requires that $|w_0|$ decreases exponentially with an increasing distrnce from the coast, w_0 must be dositive. In other word, the surface will tend to be lowered wherever the surface is lower toward north. Thus the wave will travel southward.

List of Symbols

x horizontal distance from western edge of the ocean
y horizontal coordinate eirected positively toward north from the equator
z vertical coordinate directed positiveły downward from the mean sea surface
t time
u, u' x component of currnte velocity in the upper layer, and lower layer
v, v' y component of current velocity in the upper layer, and lower layer
w z component of current velocity (vertical velocity)
z_0 elevation of the sea surface
h dəviation of the interface
w_0 vertical velocity at the sea surface ($z=O$)
w_H vertical velocity at the interface ($z=H$)
f Coriols parameter 2ω sin ϕ, wher ω is the angular speed of the earth, ϕ the latitude
β df/dy
H, H' mean depth of the upper layer, and of the lower layer
τ wind stress uector, with x and y components denoted by τ_x and τ_y, respectively
σ wave frequency
$\Delta\rho$ density difference between the upper and lower layer
g acckleration due to gravity
D total depth of water
L width of the ocean

The subscripts 1 and 2 refer to the baroclinic mode and brotropic mode, respectively.

Records of Oceanographic Works
in Japan Vol. 5, No. 2,
March, 1960

On the Distribution of Divergence and Convergence of Surface Drift Vectors in the Western Pacific Oceans

By
Hideo SUDO
(Geophysical Institute, University of Tokyo)

Abstract

The distribution of surface divergence and convergence in the Western Pacific Ocean has been calculated directly from the current chart and its seasonal variation is discussed. Though the result of calculation shows very complicated patterns, it is expected that there exist the deep currents balanced with surface divergence or convergence as the result of comparison with the Norpac observation data.

1. Introduction

An attempt to compute the transport of water due to the wind system was carried out for the North Atlantic Ocean by R. B. MONTGOMERY (1936) and later K. HIDAKA (1955) derived a method to calculate the divergence of surface drift vectors in terms of wind stresses over the oceans and obtained the charts of surface divergence areas for the three oceans (HIDAKA and OGAWA, 1958). But yet these results have not been confirmed to represent the magnitudes and patterns of the surface divergence of the actual oceans and this method has a defect that the absolute value of divergence becomes infinite at the equator; the direct calculation of the divergence from surface current vectors should be much better than the method to use wind stresses, if we could get sufficient data for surface currents. Already F. G. Walton SMITH (1951) and W. van DIJK (1956) directly calculated the distribution of divergence for the Gulf of Mexico and for the Indian Ocean, respectively, and both of them proved that there appeared some relations between the water divergence and the sea surface temperature in some parts of those areas. Besides, the direct computation by S. HIKOSAKA et al. (1955) shows that in the Northwestern Pacific near Japan there three divergence zones, that is, the equatorial divergence zone, the small divergence area off the south coast of Honshu, and the elongated divergence zone towards the east off Sanriku districts. With less accurate data in some region, the author directly computed the surface divergence and convergence in the Western Pacific Ocean from the current charts.

2. Calculation of Divergence of the Surface Drift Vectors from Current Charts

As data, the author used the Current Charts of the Northwestern Pacific Ocean (H. O. Misc. No. 10,058A) and the Southwestern Pacific Ocean (H. O. Misc. No. 10,058), published by the Hydrographic Office United States Navy in 1944. These charts show monthly surface currents by information compiled from observations of the vessels' drifts made during the month for all years prior to 1935 by the co-operating observers of the Hydrographic Office. So they do not always represent the true surface sea currents, and on them it is remarked that observations were not considered reliable in four cases of followings:

(1) where tidal currents prevailed,
(2) where winds, seas, or swells were strong,
(3) where the leeway driftage were excessive, and
(4) when the report was "no current."

By Z. Yasui et al. (1942) there is little need to consider the driftage by wind for the ship running in over than about 12 knots when wind force is less than 5 or 6, and the direction correction is less than 2 degrees for the wind of force 7 or above.

On these current charts the mean direction by an arrow, the resultant drift in miles per day to the nearest tenth of a mile, and the numbers of the total current observations used in the computation are given in each 1-degree quadrangle for the month under the average normal condition. Therefore, of course, there is sufficient accuracy for the regions along the routes because of a lot of data, while the accuracy is bad for the districts with a small number of data off the course, Numbers of observations in each 5-degrees quadrangle for January and July are shown in Table 1. On the whole observed numbers in the southern hemisphere are smaller than those in the northern hemisphere and there are few observations in the region south of 15°N, west of 175°W except near Marianas Is. and Caroline Is. The most numerous observations were carried out in the region of 20°N to 35°N which corresponds to the ordinary course and in that of 45°N to 50°N to the great circle route.

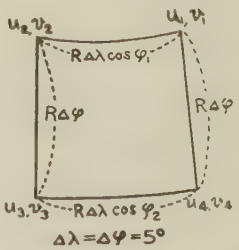

Fig. 1. The 5-degrees quadrangle used for the calculation.

Now, after the author decomposed the current velocity vector in each 1-degree quadrangle given on the current chart to the W-E component and the S-N component, he averaged two components over 5-degrees quadrangle containing 25 given quadrangles by multiplying number of observations as

Table 1–a. Numbers of observations in each 5-degrees quadrangle for January. The parenthesized number shows the total number of observations for December, January and February used for the calculation.

	120°E	125	130	135	140	145	150	155	160	165	170	175	180	175	170	165	160	155°W	
55°N									3(7)	2(10)	8	27	30	42	52	46	69		55°N
50							17	43	70	107	94	62	76	57	42	39	34		50
45						77	165	102	65	38	20	23	42	24	16	29	29		45
40					271	222	83	41	40	38	39	34	25	33	27	43	24		40
35				129	210	199	190	147	138	115	114	135	139	85	89	84	102	111	35
30		146	60	47	32	47	65	112	140	139	122	99	138	111	112	93	50	52	30
25		74	56	41	42	53	42	42	53	66	62	80	95	107	1261	151	196	317	25
20		31	46	83	63	62	45	42	29	22	18	16	10	5	4(19)	6	60	53	20
15			102	35	35	20	29	7	2(15)	3(15)	0(7)	6	1(4)	1(5)	8	27	81	23	15
10			33	8	14	10	7	3(8)	4(21)	7	3(8)	7(4)	6	8	14	39	44	36	10
5°N			22	5	1(4)	3(7)	3(21)	5(16)	2(5)	2(6)	3(10)	9	2(7)	14	34	51	53	23	5°N
0°						5	4(15)	12	5	4(10)	22	6	5	27	45	78	25	20	0°
5°S								14	6	1(5)	8	5	6	25	62	21	14	19	5°N
10								11	3(20)	9	8	6	36	45	19	23	28	20	10
15								6	14	5	4(9)	33	39	32	34	38	42	28	15
20								16	19	5	54	50	41	14	17	21	29	18	20
25								48	54	61	62	27	36	19	27	38	16	3(27)	25
30								84	59	37	32	21	42	22	51	20	11	18	30
35		31	18	25	19	19	25	35	10	9	8	3(22)	20	36	14	14	14	12	35
40		3(6)	55		4(7)	2(4)	2(10)	7	11	5	12	10	9	5	10	9	9	11	40
45°S	120°E	125	130	135	140	145	150	155	160	165	170	175	180	175	170	165	160	155°W	45°S

Table 1-b. Numbers of observations in each 5-degrees quadrangle for July. The parenthesized number shows the total number of observations for June, July and August used for the calculation.

	120°E	125	130	135	140	145	150	155	160	165	170	175	180	175	170	165	160	155°W	
55°N									2(10)	3(9)	8	28	76	108	112	116	126		55°N
50							15	57	116	141	157	115	104	107	105	116	120		50
45						126	270	220	103	61	41	38	24	39	30	46	61		45
40					494	484	181	93	62	52	55	53	63	54	65	54	51		40
35				237	313	281	208	224	226	202	214	192	243	113	87	72	79	76	35
30		284	124	57	30	25	25	30	42	48	51	56	56	136	193	163	6	16	30
25		109	45	41	38	41	24	29	44	38	43	31	43	59	88	107	233	378	25
20		35	26	40	35	45	39	44	35	22	18	18	10	13	6	3(19)	76	98	20
15			81	30	30	30	31	16	13	6	4(8)	0(2)	3(6)	3(10)	7	26	150	52	15
10			33	21	18	20	8	7	8	9	2(3)	2(5)	9	5	18	58	92	50	10
5°N			49	9	2(13)	7	5(20)	9	3(10)	9	9	11	9	5	40	102	70	30	5°N
0°						6	5	13	7	8	22	11	11	35	85	119	26	21	0°
5°S								8	9	16	13	13	19	70	70	76	13	43	5°S
10								14	9	19	16	6	72	67	31	43	31	45	10
15								9	32	13	17	67	48	58	60	46	64	38	15
20								17	22	10	67	59	44	22	33	36	36	22	20
25								37	58	81	43	53	49	35	29	39	40	17	25
30								81	97	74	60	30	44	54	49	21	22	17	30
35		28	28	33	21	20	34	61	33	13	12	12	27	40	15	16	12	11	35
40		1(2)	3(5)	3(6)	3(8)	1(1)	2(2)	1(9)	2(10)	7	6	12	17	7	3(12)	6	4(11)	2(7)	40
45°S	120°E	125	130	135	140	145	150	155	160	165	170	175	180	175	170	165	160	155°W	45°S

weight to the velocity components, and made these averages the mean values of the current at the center of the 5-degrees quadrangle. Namely we regard them rather as the averages in the region within neighboring several hundred kilometers than as the velocity components at the center of the quadrangle and so all the following discussions concerning divergence or convergence must be restricted only to phenomena of the large scale over several hundred kilometers.

Regarding the 5-degrees quadrangle as an isosceles trapezoid, we obtain the divergence formula (1) by dividing differences of outgoing fluxes from incoming fluxes by the area (see Fig. 2).

$$\frac{\partial u}{\partial x}+\frac{\partial v}{\partial y} = \frac{\left(\frac{v_1+v_2}{2}\cos\varphi_1-\frac{v_3+v_4}{2}\cos\varphi_1\right)R\Delta\lambda+\left(\frac{u_1+u_4}{2}-\frac{u_2+n_3}{2}\right)R\Delta\varphi}{\frac{1}{2}R^2(\cos\varphi_1+\cos\varphi_2)\Delta\lambda\cdot\Delta\varphi}, \quad (1)$$

where x is eastward positive, y northward positive, u and v horizontal components of current velocity in x and y directions respectively, φ and λ the geographical latitude and longitude respectively, and R the mean radius of the earth. Since neglect of the difference between $\cos\varphi_1$ and $\cos\varphi_2$ has little influence upon the computation of divergence, the expression (1) is simplified as follows:

$$\frac{\partial u}{\partial x}+\frac{\partial v}{\partial y}=\frac{1}{R\Delta\lambda}\left[\frac{u_1-u_2-u_3+u_4}{2\cos\varphi}+\frac{v_1+v_2-v_3-v_4}{2}\right], \quad (2)$$

The calculation is practiced for the middle months of four seasons, namely, January, April, July and October, and the annual mean averaged over above four months. However, for the quadrangle for the month when number of observations is less than five, the data for before and after months (for example, December and February for January) besides that month were used. The parenthesized number in Table 1 shows the total number of observations for these months used for this calculation.

3. Consideration of Seasonal Veriation of Surface Divergence Field

As divergence has been computed by the directly numerical differentiation, the result has caused the complicated distributions and it is not considered that the distinctive features of the small scales are actually significant. Therefore, it is necessary to smooth these calculated results for time and space, but on account of considerable difficulty of smoothing concretely, divergence contours were drawn being supposed that the value at each point indicates the true value

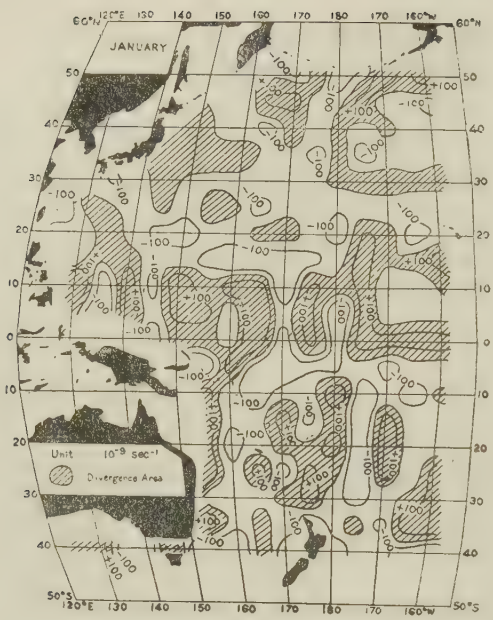

Fig. 2–a. Distribution of divergence and convergence areas at the sea surface (unit 10^{-9} sec^{-1})—January. Shaded areas show the divergence zones.

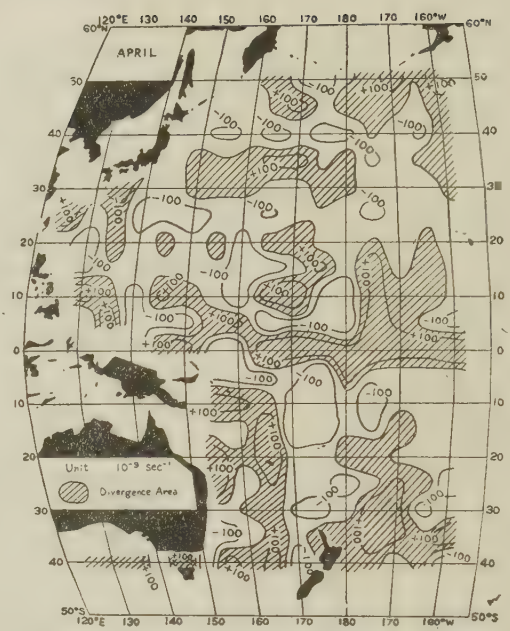

Fig. 2–b. Distribution of divergence and convergence areas at the sea surface (unit 10^{-9} sec^{-1})—April. Shaded areas show the divergence zones.

Fig. 2–c. Distribution of divergence and convergence areas at the sea surface (unit 10^{-9} sec^{1})—July. Shaded areas show the divergence zones.

Fig. 2–d. Distribution of divergence and convergence areas at the sea surface (unit 10^{-9} sec^{1})—October. Shaded areas show the divergence zones.

at the very intersecting point of each 5-degrees lines. So we should pay considerable attention to reading of these distributions so that we may interpretate these results in fairly large scale.

Distributions of divergences and convergences in four months and the annual mean are shown in Fig. 2 and Table 2. The unit is 10^{-9} sec^{-1}. Hatched areas of the figures are the divergent areas that denote the positive values in the expression (2). Besides the contours which denote $+100$ or -100 ($\times 10^{-9}$ sec^{-1}) were drawn as a criterion of magnitude of upwelling or sinking. Namely, the magnitude of divergence or convergence is the order of 10^{-7} to 10^{-8}. Integrating the equation of continuity for a homogeneous water with respect to z from the surface to the depth $z=h$, we have

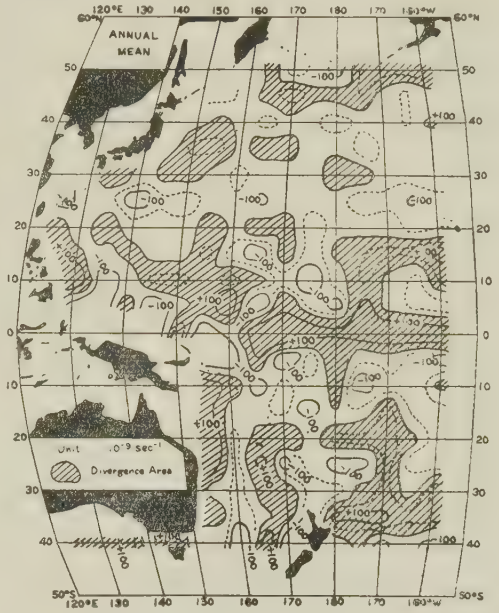

Fig. 2-e. Distribution of divergence and convergence at the sea surface (unit 10^{-9} sec^{-1})—The annual mean. Shaded areas show the divergence zones.

$$w=-\int_0^h\left(\frac{\partial u}{\partial x}+\frac{\partial v}{\partial y}\right)dz=-\int_0^h div\, \boldsymbol{v}_0\, dz\ , \qquad (3)$$

where z is taken positive vertically downward, and $\boldsymbol{v}_0$ denotes the current vector at the surface. When the average value of divergence within a top layer of thickness h is $div\, \boldsymbol{v}$, we obtain the vertical velocity w_h at the level $z=h$, putting $W_0=0$,

$$w_h=-h\, div\, \boldsymbol{v}\ . \qquad (4)$$

For example, for $div\, \boldsymbol{v}=10^{-7}$ sec^{-1}, and $h=100$ m$=10^4$ cm

$$w_h=-10^{-3}\ \text{cm/sec}\ .$$

The intensity of upwelling is 86.4cm per day or about 25m per month.

Now, let us see the feature of divergence and convergence of the surface currents in each season.

January: (i) Divergences exist south of Aleutian Is., though the area is separated to two regions of the eastern and western parts. It is considered that these regions correspond to the cylone near 50°N, 170°E. (ii) The center of the high pressure belt in the North Pacific Ocean is found, much easterly, near 30°N,

Table 2–a. Divergence of surface currents in the Western Pacific Ocean (in 10^{-9} sec^{-1})—January.

	125°E	130	135	140	145	150	155	160	165	170	175	180	175	170	165	160°W	
50°N									−7	−114	70	−247	−29	135	92	222	50°N
45							−97	−5	184	236	−32	−16	155	−38	−81	−105	45
40						86	−36	−52	−121	58	−49	16	−54	25	−36	−94	40
35					31	95	38	63	−18	−7	−114	20	−128	−81	−61	−13	35
30			−106	−18	61	−14	−11	−34	−49	−4	−22	34	65	79	27	22	30
25	−308	36	0	−47	34	−61	68	4	−160	−29	−9	−99	−94	−77	−63	−56	25
20	−25	−77	63	−31	−108	−196	−23	−52	29	63	−72	−146	121	56	−191	−88	20
15		−41	5	27	−34	−20	−112	−232	−236	−211	−148	−16	175	2	67	225	15
10		745	−346	132	−184	306	18	150	153	−322	220	13	121	−110	−146	7	10
5°N		23	−719	236	−45	177	155	−63	310	−70	348	−502	173	−135	−142	−94	5°N
0°					−175	29	11	−49	442	−211	353	−141	294	191	366	414	0°
5°S							−567	144	−106	−481	−144	−119	−11	−130	−63	−52	5°S
10							119	−72	−478	−125	−9	196	−171	−76	−160	16	10
15							173	−22	−14	178	−117	68	−146	112	−50	−77	15
20							117	−270	−45	32	7	162	−222	261	−31	−77	20
25							241	−85	162	−195	103	36	−301	193	−72	159	25
30							−38	−99	−45	29	133	−83	−124	−77	29	108	30
35							186	−74	36	−70	−162	−32	31	−103	230	328	35
40°S	119	204	−265	−412	488	−243	−223	−338	20	−186		−514	−72	−67	−130	−388	40°S
	125°E	130	135	140	145	150	155	160	165	170	175	180	175	170	165	160°W	

Table 2-b. Divergence of surface currents in the Western Pacific Ocean (in 10^{-9} sec^{-1})—April.

	125°E	130	135	140	145	150	155	160	165	170	175	180	175	170	165	160°W	
50°N									47	−132	−139	−4	54	146	0	168	50°N
45							−16	−47	36	117	−20	86	79	29	−34	38	45
40						−99	−121	−70	−198	−79	−146	−110	7	−72	−119	88	40
35					−32	49	0	63	132	150	−13	34	−126	−47	23	36	35
30			225	−86	−96	99	36	25	−14	−34	36	22	−43	−76	−70	22	30
25	252	−52	31	−193	−121	−193	−70	−68	−106	−47	−2	−65	−124	−81	−40	−7	25
20	−74	−164	54	−85	36	−59	18	−133	25	86	−22	−36	7	−88	39	−85	20
15		−128	−5	−41	−22	−94	−2	−209	−180	−97	112	−76	232	−47	81	−14	15
10		344	34	−157	126	97	−88	−319	222	768	−173	−141	135	62	47	−29	10
5°N		−883	333	−260	−110	−209	76	119	−539	−101	−133	−321	301	52	−20	−148	5°N
0°					99	164	−182	−386	765	905	236	117	337	218	256	432	0°
5°S							−188	−204	−191	−70	−438	175	−27	−31	−38	−36	5°S
10							260	132	27	−132	−193	−52	−214	−7	−70	0	10
15							−25	−29	182	−290	−159	−7	−106	108	−67	−52	15
20							220	2	369	−25	−78	49	67	−11	−76	−7	20
25							285	−175	112	−74	−96	−126	−14	115	59	−270	25
30							−50	7	72	−103	−202	−81	212	106	−142	−40	30
35							−123	−92	29	−13	160	79	278	148	7	232	35
40°S	207	177	230	−81	300	−193	142	65	187	−840		86	88	−63	7	−220	40°S
	125°E	130	135	140	145	150	155	160	165	170	175	180	175	170	165	160°W	

Table 2-c. Divergence of surface currents in the Western Pacific Ocean (in 10^{-9} sec^{-1})—July.

	125°E	130	135	140	145	150	155	160	165	170	175	180	175	170	165	160°W	
50°N									−4	−135	−11	−193	61	5	58	−16	50°N
45							−20	−7	−74	61	74	−45	63	−41	−79	−99	45
40						−20	50	74	−23	−45	−108	−155	−148	−43	−85	18	40
35					−14	106	128	−72	40	77	−59	58	−2	−11	−20	−9	35
30			−58	−128	−27	68	−31	−211	−101	9	−47	65	−13	−117	−115	13	30
25	−409	−59	−49	−85	−68	41	−41	−112	−61	−31	−36	95	−77	−4	−169	−47	25
20	−92	59	−27	13	40	97	88	79	49	−63	−268	164	38	−103	58	23	20
15		88	−11	−40	−97	−20	153	14	−101	434	−326	72	−22	41	130	160	15
10		685	−240	−92	294	−54	317	97	−180	−225	−218	112	4	−95	−18	−7	10
5°N		63	−621	288	−276	−36	474	456	−416	49	−333	27	67	−36	−32	−86	5°N
0°					−528	32	−324	124	−126	297	−270	168	−97	261	265	108	0°
5°S							95	−281	207	50	9	209	22	0	14	−391	5°S
10							233	16	−90	−27	−133	13	−81	−128	70	−25	10
15							103	49	−333	−162	−207	−47	124	0	−99	−148	15
20							101	0	−151	178	54	97	232	−99	198	−76	20
25							366	117	178	59	−58	−175	−97	−29	31	−139	25
30							58	−41	63	58	−90	−146	−32	62	7	101	30
35							126	−180	−81	70	−151	267	132	177	52	−193	35
40°S	81	173	38	243	−85	360	−187	−353	234	−77		178	108	−85	263	45	40°S
	125°E	130	135	140	145	150	155	160	165	170	175	180	175	170	165	160°W	

Table 2-d. Divergence of surface currents in the Western Pacific Ocean (in 10^{-9} sec^{-1})—October.

	125°E	130	135	140	145	150	155	160	165	170	175	180	175	170	165	160°W	
50°N									−23	−18	−27	−67	94	92	90	−5	50°N
45							−187	−25	0	−83	−5	34	−96	−32	−35	7	45
40						−16	157	−16	79	7	92	−112	63	−45	13	7	40
35					−16	4	76	−67	−54	−135	−4	−139	−38	−52	23	−59	35
30			130	133	122	−85	−54	−52	47	−52	−59	81	92	23	14	−63	30
25	−150	−86	−159	−279	−76	−139	−56	−9	−110	41	2	−23	−65	−78	−132	−195	25
20	247	70	67	−20	−97	58	18	90	18	18	−31	18	−268	49	−157	−50	20
15		86	−72	132	52	22	189	103	−50	−2	59	45	−198	247	−29	108	15
10		800	−97	−211	4	−78	−182	371	−119	−512	−393	−70	−52	94	−166	279	10
5°N		−141	−169	−106	−242	−47	−526	241	−474	467	−164	338	22	−4	−47	−18	5°N
0°					−229	86	−231	191	248	735	362	288	20	187	256	178	0°
5°S							−725	−670	584	−142	283	23	−114	86	−155	−32	5°S
10							494	5	16	−50	141	−74	−112	−58	−182	18	10
15							250	−32	−18	−23	−36	−20	−59	31	−114	−29	15
20							258	11	−45	171	−88	−59	242	159	−40	−59	20
25							23	−68	−11	−268	−117	−196	−133	−70	−254	−13	25
30							23	−135	18	124	−59	−18	−4	141	−7	187	30
35							34	−40	−16	81	−236	157	7	252	−65	9	35
40°S	378	306	346	101	2	−117	112	−99	65	164		72	−128	−49	−243	76	40°S
	125°E	130	135	140	145	150	155	160	165	170	175	180	175	170	165	160°W	

Table 2-e. Divergence of surface currents in the Western Pacific Ocean (in 10^{-9} sec^{-1})—The annual mean.

	125°E	130	135	140	145	150	155	160	165	170	175	180	175	170	165	160°W	
50°N									2	−96	−27	−130	50	90	56	101	50°N
45							−78	−22	36	83	5	13	50	−18	−54	−38	45
40						−14	13	−13	−70	−18	−49	−88	−32	−36	−54	2	40
35					−11	65	59	−5	25	18	−47	−7	−74	−47	−13	−7	35
30			49	−25	16	16	−16	−68	−29	−18	−22	50	27	−22	−38	−2	30
25	−151	−41	−45	−150	−58	−90	−23	−45	−110	−14	−13	−22	−92	−11	−101	−76	25
20	12	−25	40	−32	−31	−23	27	−2	32	23	−97	−2	−29	−22	−63	−50	20
15		2	−23	20	−23	−29	56	−81	−142	31	−76	5	49	59	63	119	15
10		645	−162	−83	61	67	16	72	18	−76	−144	−22	52	−13	−68	61	10
5°N		−234	−296	43	−168	−43	47	191	−281	86	−68	−115	141	−31	−59	−86	5°N
0°					−209	76	−178	−29	332	432	171	106	137	220	283	278	0°
5°S							−348	−252	124	−160	−72	72	−31	−20	−62	−128	5°S
10							276	22	−132	−58	−45	20	−146	−68	−86	4	10
15							128	−11	−47	−74	−132	0	−49	61	−78	−78	15
20							171	−65	32	92	−27	65	78	78	14	−56	20
25							231	−52	108	−121	−45	−117	−135	52	−58	−65	25
30							−4	−65	29	27	−54	−79	13	58	−31	90	30
35							54	−97	−7	18	−103	119	110	119	58	96	35
40°S	196	214	86	−34	177	−49	−38	−182	126	−234		−45	2	−65	−23	−123	40°S
	125°E	130	135	140	145	150	155	160	165	170	175	180	175	170	165	160°W	

140°W, rnd corresponding to it, the convergence zone having the axis near 25°N expands from the east. Because thə mass tarnsport of the sea water by the wind is a right angle to the right hand with the direction of the wind in the northern hemisphere, always the cyclone must cause divergence of the surface currents and the ʊnticyclone must make the convergence area. (iiī) Divergence appears in the Kuroshio region east of Honshu, too. Although the origin of it is unknown, it is mainly caused by $\partial v/\partial y$, namely, what the eastern currents slightly disperse to north and south. (iv) Moreover strong divergence appears near the quator all the year round, and we can find the areas with strong divergences east of Australia and north of New Zealand, respectively.

April: (i) In response to moving of the cyclone in higher latitude of the Northern Pacific eastward (to 55°N, 155°W), the divergence area has moved eastward. (ii) Since the anticyclone has grown a little and has moved westward (to 30°N, 155°W), the convergence area has stretched widely to east and west centered at about 25°N. (iii) The divergence area east of Honshu has moved eastward and has extended. (iv) The divergence area south of 20°N, west of 180° has been connected with the equatorial divergence zone. (v) The divergence zone east of Australia has removed eastward, and a large divergence area appears northeast of New Zealand.

July: (i) As the cyclone has disappeared, the divergence south of Aleutian Is. has been weakened. (ii) Corresponding to the growth of the anticyclone over the Northern Pacific, the convergence area spreads to the extent of 20°N to 40°N. (iii) The divergence area east of Honshu slenderly stretches from north to south, and convergence exists south of Honshu. (iv) A divergence zone stretches along the meridian of 180°. (v) The divergence east of Australia has grown strong and the divergence still continues northeast of New Zealand.

October: (i) Although the center of the cyclone is situated near 55°N, 160°W, the divergence south of Aleutian Is has not yet grown. (ii) A part of the anticyclone is outstretched near 30°N, 170°E and in its neighborhood convergence exists. (iii) The divergence area east of Honshu has become narrow and divergence appears south of Honshu, too. (iv) There are divergences still near 20°N, 150°E to 170°E and to the south of it. (v) Convergence has developed near 25°S and the divergence region near New Zealand has been divided into the northeast and the northwest of New Zealand.

Moreover, intermediate contors denotes +50 or −50 is drawn in the distribution map of the annual mean. (i) First, we see divergence south of Aleutian Is., and it is considered that it originates because the current velocity increases where the Alaska Current changes into the West Wind Drift turning the direction counterclockwise from south into southeast. (ii) Corresponding to the middle latitude high pressure belt, the area to the extent of 20°N to 40°N forms a great convergence zone, and the subtropical convergence exists near 25°N. (iii) Diver-

gence appears east of Honshu, and mainly, it is caused by $\partial v/\partial y$, that is to say, the southern part of currents off the east coast of Honshu so turns into about eastsoutheast that the currents diverge since the Kuroshio has become the eastward current. (iv) Besides the strong divergence near the equator, divergences appear centered at 15°N in the eastern part and at 10°N in the western part. These divergences are caused by that which the velocity of the North Equatorial Current increases westward. Because the South Equatorial Current runs nearly to the westnorthwest having the north component and nearly to westsouthwest having the south component, north and south of equator, respectively, by the Southeast Trade Wind crossing the equator, the strong divergence is generated centered at the equator. (v) There is the divergence zone east of Australia, and it seems to be caused that in the northern part of the East Australia Current which runs to the west increases its velocity westward, and along the shore in the southern part the southerly current become rapid southward. (iv) It is considered that the divergence northeast of New Zealand is caused by dispersion of the South Equatorial Current westerly to southwesterly.

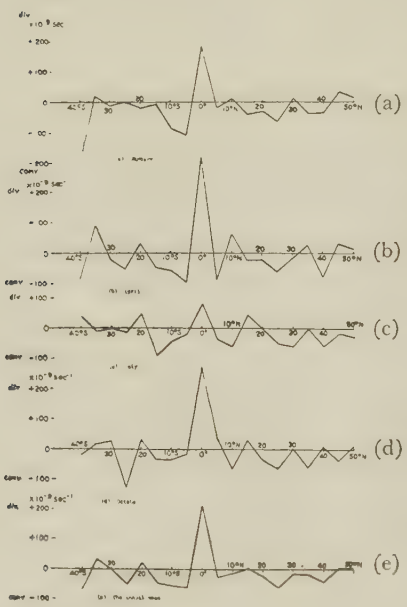

Fig. 3. Mean seasonal divergenec along the meridian 160°E–160°W.
(a) January, (b) April, (c) July
(d) Octobər, (e) The annual mean

So far as this result of direct calculation means, above considerations tell us that main patterns of divergence and convergence areas are caused chiefly by $\partial v/\partial y$, namely, meridional variations of the S-N components of currents. Therefore, the author averaged the values of divergences or convergences over 160°E to 160°W for each latitude and the meridional variations of them for four months and the annual mean are shown in Fig. 3 From these figures following facts are explained. (i) There is the remarkable strong divergence at the equator all the year round. (ii) In the Doldrum at 5°N convergence exists, and at the southern boundary of the North Equatorial Current at 10°N to 15°N divergence appears. These facts agree with the knowledge that has been accepted widely up to the present. (iii) The convergence zone by the middle latitude high pressure belt is centered at 25°N, and in July it removes a little north in response to movement of the high pressure zone. (iv) Accordingly to the rise and fall of the low pressure belt, the divergence at 45°N to 50°N is stronger in January and April than in July and October. (v) Divergences appear at 20°S and 35°S.

4. Comparison with the Divergence Field as Computed from the Distribution of Wind Sfresses

Last year HIDAKA and OGAWA computed divergence of surface drift currents using the distribution of wind stresses. As absolute values may depend upon the coefficient of eddy viscosity μ which is rather uncertain, let us compare above results with the distributions by HIDAKA and OGAWA only concerning patterns of divergences and convergences. The latters show strong or weak divergences east of Japan, south of Aleutian Is., and east of Australia, but comparing with results by the author's direct calculation, they are much shifted. Moreover almost the Northern Pacific Ocean is the convergence area, though lacking in data in part, and the clear correspondences cannot be found. Especially, in the Southern Pacific Ocean, the distributions completely differ, although a part of the reasons may be shortage of data. These values by HIDAKA and OGAWA are given for the northern hemisphere by following formula,

$$\left(\frac{\partial u}{\partial x}+\frac{\partial v}{\partial y}\right)_{z=0}=\frac{\operatorname{div}\tau+\operatorname{curl}_z\tau}{2\sqrt{\rho\omega\sin\varphi\cdot\mu}}+\frac{\tau_x-\tau_y}{4\sqrt{\rho\omega\sin\varphi\cdot\mu}}\frac{\cos\varphi}{R}\,, \qquad (5)$$

where τ_x and τ_y are the wind stress components in x and y directions, respectively, and ρ density of sea water.

It is expected that there may be some correspondences between the distributions of the divergence of surface currents and of the curl of wind stresses, as the author explained in the proceding chapter that the seasonal variation of divergence depends upon the distribution of atmospheric pressure. Then distributions of the rations of wind stresses

$$\operatorname{curl}_z\tau=\frac{\partial\tau_y}{\partial x}-\frac{\partial\tau_x}{\partial y} \qquad (6)$$

distributions of the rotation of wind stresses in the Northern Pacific Ocean for winter (December to February) and summer (June to August) are shown in Fig. 4. This rotation was computed by K. YOSHIDA from the Oceanographic Report No. 14 by Scripps Institution of Oceanography. Using the expression (6), positive areas and negative areas denote the cyclonic and anticyclonic rotations, respectively, and they are regarded as causing divergence and convergence of surface water. In winter the positive area in higher latitude which extends north of 40°N stretches into the east of Honshu, on the other hand the positive area near the equator which occupies south of 10°N spreads to the extent of the east of Philippines. In summer the positive area in higher latitude becomes small, and a part of it retreats northeastward of 50°N, 160°W, another part stretches from northeast to southwest to the east of Japan. And then the positive area east of Philippines is separated from the equatorial positive area, and the northern boundary of the positive area goes up north to the

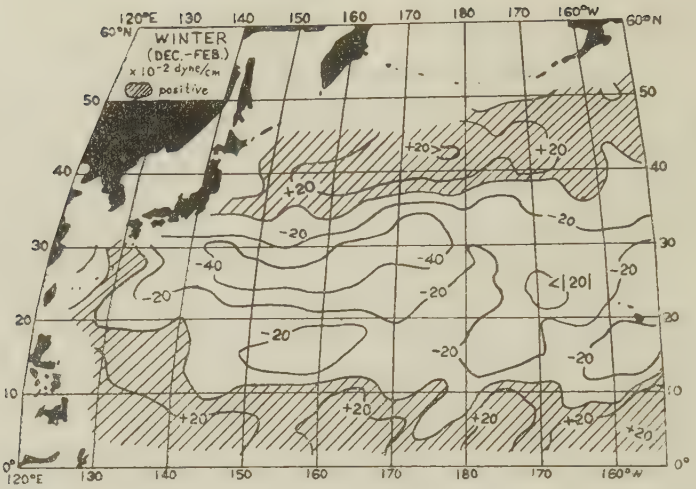

Fig. 4–a. Distribution of the curl of wind stresses (unit 10^{-2} dyne·cm^{-3})—Winter. Shaded areas show the zones of the cyclonic rotation.

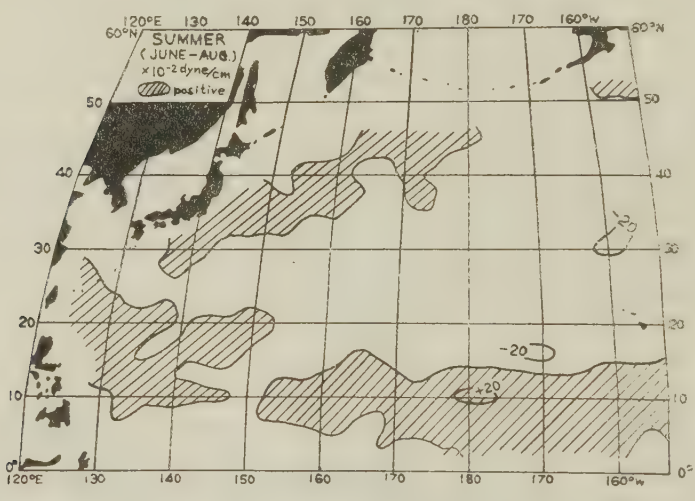

Fig. 4–b. Distribution of the curl of wind stresses (unit 10^{-2} dyne·cm^{-3})—Summer. Shaded areas show the zones of the cyclonic rotation.

extent of 15°N, but the negative area appears near the equator west of about 170°W. Although these charts do not express minor features owing to pretty smoothing procedure, it is considered that they are close upon the actual distributions of divergences and convergences in large scale.

5. Relation between Distributions of Divergences and Convergences and Some Observed Oceanic Conditions

Although distributions of divergences and convergences directly computed were compared with distributions of sea surface temperatures by World Atlas

of Sea Surface Temperatures published by U. S. Hydrographic Office, significant results could not be obtained. Since on these charts isotherms are drawn for every 5°F (about 2.8°C), minor features of temperatures at the surface of great variability do not appear. Besides, the surface temperature may be much influenced by meteorological conditions, and so it seems to be very difficult that we would find any significant relations between the divergence field and the temperature field at the sea surface on the ocean.

Then it is required to compare with the trustworthy observed results which are completely independent upon these current charts and for that purpose it is proper to use the result of the co-operative observation of the whole North Pacific Ocean by Japan, the United States of America, and Canada (the Norpac observation). As this observation was operated in July to October in 1955, namely, extending over summer and autumn, and the oceanic condition near the surface is changeable, it was attempted to consider what currents may happen in the deep layer according to divergence or convergence at the sea surface.

It may be considered that it is improper to compare the divergence or the convergence that is the average over the long period with the only once observation. But, arranging the Norpac observation data, we have been able to verify that there is little variation in the lower layer of more than several hundred meters all the year round over long years. Accordingly it has no objection to regard that in the Norpac projection more the averaged condition over the long period was observed than the condition extending over summer and autumn was observed.

The deep currents corresponding to the divergence or convergence were discussed by H. STOMMEL (1956) and K. YOSHIDA at al. (1957). Generally in the deep layer except the top layer of about 100 to 200 meters from the surface, there must be convergenc or divergence to compensate upwelling or to dissipate sinking. Now, geostrophic flow is given as the following equations,

$$-fv=-\frac{1}{\rho}\frac{\partial p}{\partial x} \qquad fu=-\frac{1}{\rho}\frac{\partial p}{\partial y}, \tag{7}$$

where f denotes the Coriolis parameter. Eliminating the pressure term p from above equations, we obtain

$$v=-\frac{f}{\beta}\operatorname{div} v, \tag{8}$$

where $\beta=\frac{\partial f}{\partial y}$.

Since it is considered that in deep layer this dynamical balance as geostrophic flow is realized well, the expression (8) means that in the northern hemisphere there must be deep currents with the north component, if divergence exists near the surface, and with the south component, if convergence exists.

Though geostrophic flow can be obtained by dynamic computation, it is not always proper for discussion on deep currents to apply dynamic computation because of that only the relative currents, in general on the basis of the depth of 1,000 meters or 1,500 meters, can be calculated. As in the deep layer the density of sea water is more dependent upon the temperature than upon the salinity, the author assumed that the pressure gradient is represented by the sea water temperature at the depth of 1,000 meters, for simplicity. Namely, the current must run looking the higher temperature side to the righthand in the northern hemisphere, because of that the higher temperature of the sea water means the smaller density, namely the rise of the isobaric surface.

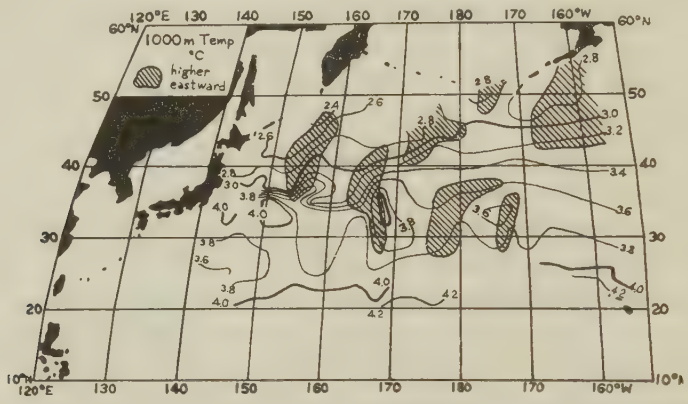

Fig. 5. Distribution of the sea water temperature at the depth of 1000 m by the Norpac observation in July to October, 1955 (°C). Shaded areas show the zones where it grows higher to the eastward.

Now let us compare the area of the current with the north component or with the south component in the deep layer with the area of divergence or convergence at the surface (compare Fig. 5 with Fig. 2). Although for the annual mean divergence field a little discrepancy between two patterns is found, we can preceive that the north flow area near 35°N to 45°N, 155°E corresponds to the divergence area near 30°N to 40°N, 150°E to 160°E and the north flow area north of 40°N, east of 170°E, but divided to three regions, seems to be corresponding to the divergence area spreading from east to west near 45°N. Besides there is some probability that the north flow areas near 30°N to 40°N, 165°E and 30°N to 35°N, 175°E to 180° correspond to the divergence areas near 35°N, 165°E to 170°E and 30°N, 180° to 175°W, respectively, though these areas are smaller. Moreover, considering rough correspondence of the large areas of the south flow and of the surface convergence nearly south of 40°N, east of 170°W, it has been found that the both patterns of surface devergence and of deep water temperature in the Northwestern Pacific Ocean agree generally well. Relatively good agreement between the two patterns is seen for July too, however, for October the degree of correspondence is more or less bad. From these

facts we can confirm that the deep currnts do not respond to the seasonal variation of the divergence near the surface. It is the greatly interesting fact that the agreement to the considerable extent like above between the results computed from the current chart and the Norpac observation data, completely independent one another, has been seen.

6. Conclusion

From the above consideration, though mainly on the Northwestern Pacific Ocean, following conclusions are obtained.

(i) The magnitude of divergence or convergence of the sea surface water calculated directly from the current chart is the order of 10^{-8} to 10^{-7}.

(ii) There is the remarkably strong divergence near the equator all the year round.

(iii) The convergence zone exists in the middle latitude centered at 25°N to 30°N and its situation or area changes to some extent according to rise and fall of the Northern Pacific Anticyclone.

(iv) The deep currents with the north or south component appear to balance with divergence or convergence of surface currents in the middle latitude in the North Pacific Ocean.

Acknowledgements

The author wishes to express his sincerest gratitude to Prof. K. HIDAKA for his cordial guidance and encouragement through the course of this investigation. Thanks are also due to Dr. K. YOSHIDA and the other members of the laboratory for their many helpful advices. And he is indebted to the Japanese Hydrographic Office for furnishing the basic data.

References

DIJK, W. van (1956): An investigation of the vergence field of the wind and ocean currents of the Indian Ocean. Arch. met. Geoph. Biokl., A. **9** (1), 158-177.

HIDAKA, Koji (1955): Divergence of surface drift currents in terms of wind stresses, with special application to the location of upwelling and sinking. Japanese Journal of Geophysics, **1** (2), 47-56.

HIDAKA, Koji and OGAWA, Kiheiji (1958): On the seasonal variations of surface divergence of the ocean currents in terms of wind stresses over the oceans. Records of Oceanog. Works in Japan, **4** (2), 124-169.

HIKOSAKA, Shigeo and WATANABE, Ryuzo (1955): Areas of divergence and convergence of surface currents in the North-Western Pacific. Proceedings of the Unesco Symposium on Phys. Oceanog., 101-103.

SMITH, F. G. Walton (1951): Distribution of vertical water movement caluculated from surface drift vectors. Bull. Marine Science of the Gulf and Caribbean, **1** (3), 187-195.

YASUI, Zen'ichi and SAKATA, Makoto (1942): On the leeway current of ships (2) (in Japanese). Umi to Sora, **22** (9), 309-322.

YOSHIDA, Kozo and MAO, Han-Lee (1957): A theory of upwelling of large horizontal extent. Journ. Mar. Res., **16** (1), 40-54.

Records of Oceanographic Works
in Japan Vol. 5, No. 2,
March, 1960

The Thickness of the Upper Homogeneous Layer*

By
Shigeo MORIYASU
(Kōbe Marine Observalory)

Abstract

We give a simple model to the vertical distribution of density in the sea for the region off Enshū-nada, Japan, and then find a linear relation between the thickness of the upper homogeneous layer and the dynamic depth anomaly. The thickness fluctuates under the influence of the wind stress. However, the fluctuation is dependent upon the relation between the thickness and the depth to which the wind stress extends. This discussion is based upon a vertical distribution of the stress, which is more or less hypothetical but seems to be conceivable. Furthermore, the result is compared with the condition off California, though it is not quantitatively found.

1. Introduction

We have discussed the vertical distribution of density in the sea south of Honshū, Japan, separating the upper layer from the transitional layer below (MORIYASU, 1958 a). The vertical distribution of water temperature can be known in detail with the bathythermograph. Consequently, we can measure the thickness of the upper layer and discuss its fluctuations.

In the area under consideration, NAN'NITI (1958) gave a model of the vertical distribution of density. We shall admit his model and consider a relation between the thickness and the dynamic depth anomaly. YOSHIDA (1955) discussed the fluctuation of the thickness and made clear the relation between the vertical velocity at the thermocline and the wind stress by using the data off California. We are going to inspect whether the relation is valid for the region off Enshū-nada or not. YOSHIDA assumed that the mean of the thickness (h) was the depth (H) to which the wind stress extended, but the spatial change of the thickness is remarkable in the region under consideration. Therefore, we assume H to be independent of h and discuss the fluctuation of h.

2. The Model of the Vertical Distribution of Density

As stated in the previous paper, the vertical distribution is not simple and the seasonal variation is found in the upper layer, while the seasonal variation

*On the fluctuation of the Kuroshio south of Honshū (6).

is not distinct and the T-Cl relations are nearly constant below the layer. In the upper layer, the vertical gradient almost vanishes and the homogeneous layer is found in winter. The feature was verified by using the results of observations in March, 1956 and we showed that $\rho_d-\rho$ below the upper homogeneous layer was represented by an exponential function of the depth (MORIYASU, 1958 b). Therefore, we take the following distribution of density:

$$\begin{cases} \rho=\rho_0=\rho_d-\Delta\rho & \text{at} \quad z\leqq h \\ \rho=\rho_d-\Delta\rho e^{-\frac{1}{\alpha}(z-h)} & \text{at} \quad z\geqq h\,. \end{cases}$$

Here, h is the thickness of the upper homogeneous layer and z is positive downward and α is a constant. In other seasons, the homogeneous layer is not so distinct as in winter and the stratification appears in summer, but the same model as mentioned above may be applied to the distribution in every season, when the mean density in the upper layer is approximately substituted for the constant density. This model was adopted and the seasonal variations of $\Delta\rho$ and h were discussed by NAN'NITI (loc. cit.).

REID (1948 a) introduced a relation between the thickness of the upper homogeneous layer and the elevation of the sea surface in the equatorial region. We attempt to obtain the relation between them in the same way as REID's. If the elevation of the sea surface is indicated by

$$z=-\eta\,,$$

the pressure in the depth of $z\,(z>h)$ is

$$p=\int_{-\eta}^{z} g\rho dz=g\{\rho_d(\eta+z)-\Delta\rho(\eta+h)+\alpha\Delta\rho(e^{-\frac{1}{\alpha}(z-h)}-1)\}\,.$$

When it is assumed that the horizontal pressure gradient vanishes at $d\gg h$ and that $\Delta\rho$ is constant, we have

$$\eta=\frac{\Delta\rho}{\rho_0}h\,.$$

Here, the constant of integration is chosen so that we may have $\eta=0$ at $h=0$. Fig. 1 shows the relation between the thickness of upper homogeneous layer and the dynamic depth anomaly of the 1000 db surface in March, 1956 on the basis of an assumption that η is proportional to the dynamic depth anomaly. The linear relation is not satisfied at some stations, where $\Delta\rho$ is less. Though there are some deviations, we may expect the existence of the relation. Consequently, if the change of $\Delta\rho$ is taken into account, the deviation will be eliminated. In this case, we

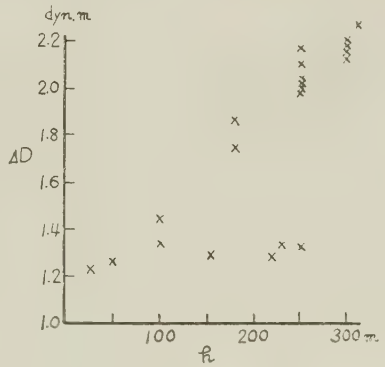

Fig. 1. The relation between dynamic depth anomaly (ΔD) and h in March, 1956.

have

$$\eta = \frac{\Delta\rho}{\rho_0}(h+\alpha),$$

where $\alpha = 3.5\times10^4$ cm is given by the method of least squares. The relation between $\frac{\Delta\rho}{\rho_0}(h+\alpha)$ and the dynamic depth anomaly is illustrated in Fig. 2, which proves that the relation is nearly satisfied. At the station with great value of ΔD, h is greater than 250 m and we can not determine h with bathythermograph, but we estimate h from serial observations. Therefore, the scattering is striking for great value of ΔD in Figs. 1 and 2.

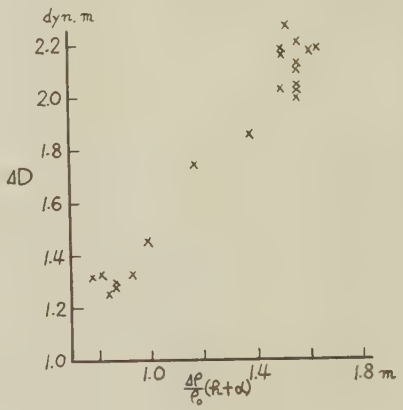

Fig. 2. The relation between dynamic depth anomaly (ΔD) and $\frac{\Delta\rho}{\rho_0}(h+\alpha)$ in March, 1956, on the assumption that $\Delta\rho$ is notconstant. Here, $\alpha = 350$ m is taken.

3. The Variation in the Thickness of the Upper Homogeneous Layer

The variation in the thickness of the upper homogeneous layer gives the vertical velocity at the thermocline. We shall consider a simple model, in which we assume that there is no variation in the east-west direction. Then, the equation of motion in the upper homogeneous layer is approximately given as follows after Yoshida (loc. cit.):

$$-fv = -\frac{\partial\tau}{\partial z},$$

$$fu = -\frac{\partial p}{\partial y}.$$

Furthermore, it may be assumed that the absolute value of τ decreases linearly with the depth. If τ_0 is the eastward component of the wind stress, the vertical gradient of τ is a constant, $-\frac{\tau_0}{H}$. Here, H is the depth where the influence of the wind stress vanishes. However, when h is greater than H, τ vanishes and so $\frac{\partial\tau}{\partial z}$ also vanishes below H in the upper homogeneous layer, because $\frac{\partial u}{\partial z}$ and the influence of the wind stress do not exist. Accordingly, we assume the distribution of τ as illustrated in Fig. 3. Then, we have

$$h>H: \begin{cases} v = -\frac{1}{f}\frac{\tau_0}{H} & \text{at} \quad z<H, \\ v=0 & \text{at} \quad H<z<h, \end{cases}$$

$$h<H: \quad v = -\frac{1}{f}\frac{\tau_0}{H} \quad \text{at} \quad z<h.$$

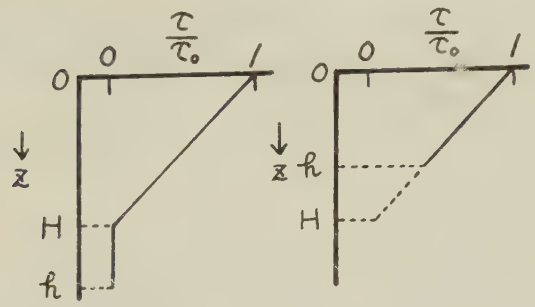

Fig. 3. The model of the vertical distribution of the stress in the upper homogeneous layer.

Now, we will discuss the variation in the thickness of the upper homogeneous layer in two cases, that is, $h>H$ and $h<H$. When h is greater than H, the following relations are simply obtained:

$$\int_0^h \operatorname{div} V dz = \int_0^H \operatorname{div} V dz = QH ,$$

$$w_h = \frac{\partial h}{\partial t} = -\int_0^h \operatorname{div} V dz = -QH = \frac{1}{f}\frac{\partial \tau_0}{\partial y} ,$$

$$\Delta h = h - h_0 = -H\int_0^t Q dt ,$$

where h_0 is the thickness of the layer at $t=0$ and Q is the divergence of velocity. When h is less than H, the following relations are obtained in the same manner:

$$\int_0^h \operatorname{div} V dz = Qh ,$$

$$w_h = \frac{\partial h}{\partial t} = -\int_0^h \operatorname{div} V dz = -Qh = \frac{1}{f}\frac{h}{H}\frac{\partial \tau_0}{\partial y} ,$$

$$\Delta h = h - h_0 = h_0(e^{-\int_0^t Q dt} - 1) .$$

Therefore, the vertical velocity at the thermocline and the amount of the variation in the thickness are independent of the thickness in the former case, while they are related to the thickness in the latter case. In Fig. 4, we show

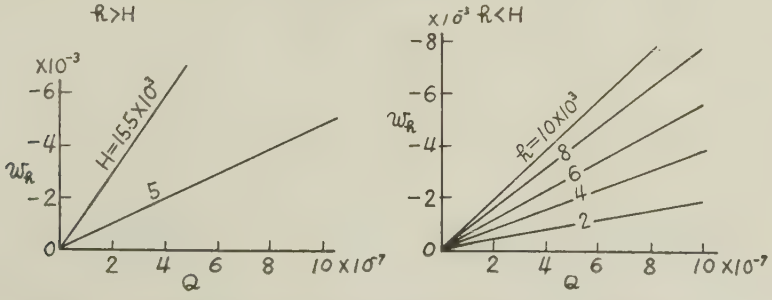

Fig. 4. The vertical velocity at the thermocline in C.G.S. units.

the relations between w_h and Q. For this reason, if the divergence is constant, the amount of the variation in the thickness is given in four cases as follows:

(1) $h_0 > H$, $Q < 0$:

$$\Delta h = -HQt,$$

(2) $h_0 > H$, $Q > 0$:

$$\Delta h = -HQt \quad \text{for} \quad t < t_1,$$

$$\Delta h = -h_0 + He^{-Q(t-t_1)} \quad \text{for} \quad t > t_1, \quad \text{where} \quad t_1 = -\frac{H-h_0}{HQ},$$

(3) $h_0 < H$, $Q > 0$:

$$\Delta h = h_0(e^{-Qt}-1),$$

(4) $h_0 < H$, $Q < 0$:

$$\Delta h = h_0(e^{-Qt}-1) \quad \text{for} \quad t < t_1,$$

$$\Delta h = (H-h_0) - HQ(t-t_1) \quad \text{for} \quad t > t_1, \quad \text{where} \quad e^{-Qt_1} = \frac{H}{h_0}.$$

The values of Δh and t are obtained by the observations, but the value of H can not be determined. According to Yoshida (loc. cit.), H is the mean thickness of the upper layer and the vertical velocity at the themorcline is given by $\frac{1}{f}\frac{\partial \tau_0}{\partial y}$. This corresponds to the case for $h > H$ in the above expressions. If the deviation of h from the mean value is a little, w_h is nearly equal to $\frac{1}{f}\frac{\partial \tau_0}{\partial y}$ for $h < H$, while it is equal to $\frac{1}{f}\frac{\partial \tau_0}{\partial y}$ for $h > H$. On the other hand, if the deviation is great, w_h is equal to $\frac{1}{f}\frac{\partial \tau_0}{\partial y}$ for $h > H$, while its absolute value is considerably less than $\left|\frac{1}{f}\frac{\partial \tau_0}{\partial y}\right|$ for $h < H$. Therefore, the expression mentioned above is significant where h is much less as compared with H, for example, in the cold water region. If h is 50 m and H is assumed to be 150 m, w_h is a third of the vertical velocity $\left(\frac{1}{3}\frac{1}{f}\frac{\partial \tau_0}{\partial y}\right)$ when h is equal to or greater than H. $\frac{\partial \tau}{\partial z}$ is not verified by the observations and is based on an assumption, which seems to be conceivable because the magnitude of the stress can be considered to decrease with the depth. Consequently, we can admit the result derived above though it is based on the hypotheses.

In Fig. 5, we show two examples. The one is in the case for $h_0 = 65$m, $H = 50$ m and $Q = 4 \times 10^{-7}$ sec^{-1}, and the other is in the case for $h_0 = 25$ m, $H = 50$ m and $Q = -4 \times 10^{-7}$ sec^{-1}. The depth of 50 m is nearly equivalent to the depth of frictional influence for $\nu = 100$ cm^2 sec^{-1} in the latitude of 35°N. In the first example, h decreases at a constant rate and amounts to H at $t_1 = 7.5 \times 10^5$ sec $= 8.66$ days and then the rate is diminished with time, that is, the decrease in h for $h < H$ is less than that for $h > H$. In the second example, h

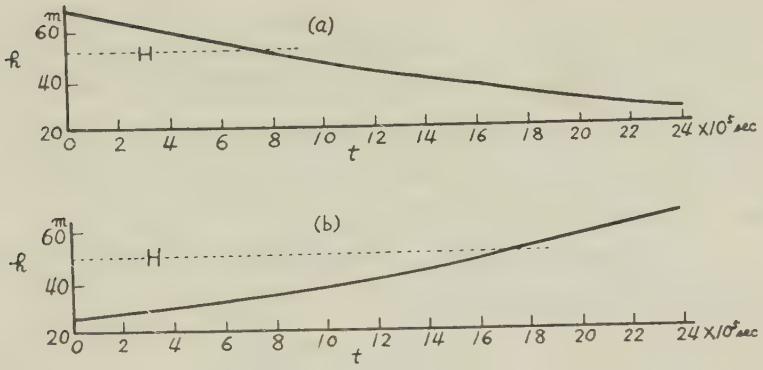

Fig. 5. Two examples of the variation in the thickness of the upper homogeneous layer.
(a) $h_0=65$ m, $H=50$ m, $Q=4.0\times10^{-7}$ sec^{-1}.
(b) $h_0=25$ m, $H=50$ m, $Q=-4.0\times10^{-7}$ sec^{-1}.

increases at a rate which increases with time, and amounts to H at $t_1=17\times10^5$sec$=19.7$ days and then the rate is constant and less than that for $h<H$. The value of Q in both examples is of equal absolute value and of opposite sign. It takes about 25×10^5sec to diminish h from 65m to 25m, while it takes about 24.5×10^5sec to enlarge h from 25m to 65m, and the difference between them is about 5×10^4sec, that is about 0.6 day. Accordingly, the time required for the decrease of a given magnitude in h is not equal to that for the increase of the same magnitude in h even when the magnitude of divergence is equal to the magnitude of convergence. This is due to the difference in the rate when h is less than H, but the difference is not great in the examples. When h is less than H and a constant divergence occurs, the ascending velocity decreases with time and, finally, h vanishes theoretically. However, h is hardly less than 30m in general, and such observed results seem to imply the decreasing in ascending velocity for a little value of h.

From the above consideration, the vertical velocity at the thermocline is given as follows:

$$w_h=\frac{1}{fc}\frac{\partial\tau_0}{\partial y},$$

where $c=1$ for $h>H$ and $c=\dfrac{H}{h}$ for $h<H$. Integrating this from y_0 to y_1 and from 0 to t, we have

$$\int_0^t \tau_0|_{y_1}dt-\int_0^t \tau_0|_{y_0}dt=f\int_0^t dt\int_y^{y_1} c\,w_h\,dy\,.$$

Though the value of c is constant for $h>H$ and is inversely proportional to h for $h<H$, the right hand side is transformed into $f\int_{y_0}^{y_1}\overline{c}\,\Delta h\,dy$ by using the mean value of c in the latter case. Therefore, if τ_0 and Δh are known from

the observations, c and then H can be computed. However, if h is greater than H everywhere, we have $c=1$ and H can not be determined. In Fig. 6, we show Δh and $\int_0^t \tau_0\,dt$. Δh is obtained by repeated observations on the meridian of about 138°E: the one was made on February 20~21, 1956 by Hydrographic Office and the other was made on March 14~15, 1956 by Kobe Marine Observatory. $\int_0^t \tau_0\,dt$ is based on the data at $9h$ and $21h$ at each weather station and τ_0 is computed according to the following formula (Reid, 1948 b):

$$\tau_0 = 0.8\,\rho_a' u^2 \times 10^{-3} \quad \text{for} \quad u < 6.6\ \text{m/sec},$$
$$\tau_0 = 2.6\,\rho_a' u^2 \times 10^{-3} \quad \text{for} \quad u > 6.6\ \text{m/sec}.$$

The figure shows that Δh seems to correspond to $\frac{\partial}{\partial y}\int_0^t \tau_0\,dt$ qualitatively, but the computed value of the left hand side is about 1/12 of the value in the right hand side of the above formula even when $c=1$ is taken (Table 1). This discrepancy is due to many causes. Though we can not determine them, the followings may be considered: that the steady state is not formed and that we substitute the wind velocity at the weather station for the wind velocity at a height of 15 m and that the weather station is not situated on the meridian of 138°E. Since the data used here are not sufficient as mentioned above, it is not significant to discuss the discrepancy, but the qualitative relation between them may be admitted in this case. If $c=1$ and a constant divergence are assumed, we have the constant value of w_h. Using the data in the example, we compute w_h and Q on the assumption, $H=50$ m (Table 2). The orders of w_h and Q are 10^{-3} cm/sec and 10^{-7} sec^{-1}, respectively.

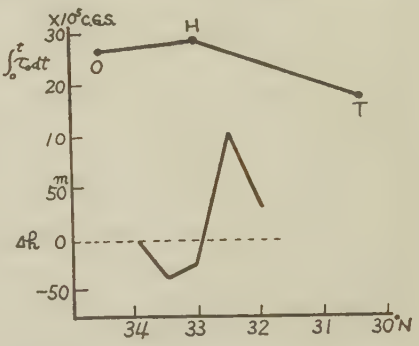

Fig. 6 The wind stress and variation in the thickness of the upper homogeneous layer on the meridian of about 138°E from February 20–21 to March 14–15, 1956. O: Omaesaki; H: Hachijo-shima; T: Tori-shima.

Table 1. The relation between the wind stress and the variation in the thickness of the upper homogeneous layer in February 20~March 15, 1956. Here, $\delta\tau_0$ is $\int_{y_0}^{y_1} dy \int_0^t \tau_0 dt$ and the units are in C.G.S.

	34°~33°	33°~32° N
$\delta\tau_0$	-1.8×10^{5}	4.0×10^{5}
$\frac{1}{f}\delta\tau_0$	-0.226×10^{10}	0.502×10^{10}
$\int_{y_0}^{y_1}\Delta h\,dy$	-2.91×10^{10}	6.25×10^{10}

Table 2. The computed values of Q and w_h in the example. Here, $H=50$ m is assumed and so h is greoter than H.

	34°	33°	32°30′	32° N
h_0	100	100	190	290 m
h	100	75	300	320 m
Δh	0	−25	110	30 m
Q	0	2.51	−11.2	-3.03×10^{-7} sec^{-1}
w_h	0	−1.26	5.60	1.52×10^{-3} cm sec^{-1}

4. Summary

When we assume a simple vertical distribution of density, the thickness of the upper homogeneous layer is proportional to the dynamic depth anomaly and the relation is available for the rough estimation of the dynamic depth anomaly. The relation between the vertical velocity at the thermocline and the wind stress derived by YOSHIDA is qualitatively found in the sea area under consideration. Here, we use the data of repeated observations which were made with interval of about 20 days. Though the variation of the thickness for the given divergence or convergence is dependent upon the relation between h and H, we can not find a remarkable quantitative difference between them. However, if h is less than H, the decrease in h is not conspicuous as compared with the case that h is greater than H.

We use a hypothetical vertical distribution of stress in the upper homogeneous layer. However, we have no observations which prove the model used in this paper and so the discussion is not justified by the fact.

Acknowledgement

The author wishes to express his gratitude to Dr. K. HIDAKA, Dr. T. NAN'NITI and Dr. K. YOSHIDA for their guidance.

References

MORIYASU, S. (1958 a): On the fluctuation of the Kuroshio south of Honshu (2). Mem. Kobe Mar. Obs. *12*, 2.

MORIYASU, S. (1958 b): An attempt to estimate the dynamic depth anomaly. Journ. Mar. Meteor. Soc. (Umi to Sora). *34*, 2. (In Japanese).

NAN'NITI, T. (1958): A theory of the mechanism of the generation of the cold water region in the offing of Enshunada. Pap. Met. Geophys. *8*, 4.

REID, R. O. (1948 a): A model of the vertical structure of mass in equatorial wind-driven currents of a baroclinic ocean. Journ. Mar. Res. *7*, 3.

REID, R. O. (1948 b): The equatorial currents of the eastern Pacific as maintained by the stress of the wind. Journ. Mar. Res. *7*, 2.

YOSHIDA, K. (1955): Coastal upwelling off the California coast. Rec. Oceanogr. Works, Japan. *2*, 2.

Records of Oceanographic Works
in Japan Vol. 5, No. 2,
March, 1960

Existence of a *Contra Solem* Vortical Motion in the Coral Sea

By
Tadao TAKAHASHI
(Faculty of Fisheries, Kagoshima University)

Abstract

A *contra solem* vortical motion is found in the Coral Sea from the results of the oceanographic observations in November-December 1954 taken by the Keiten-maru, Kagoshima University, and the fact is consistent with the EQUAPAC materials obtained by the Horizon, Scripps Institution of Oceanography.

A series of tuna-fishing experiments by the long line method was carried out in the Coral Sea by the Keiten-maru, Kagoshima University, in November-December of 1954 (T. MORITA, T. GENKA, and T. TAKAHASHI 1959), and part of the results concerning hydrographical conditions was presented by the present author (T. TAKAHASHI 1959) in the preliminary report, which contained also some other hydrographic results obtained by the Keiten-maru and by the Kagoshima-maru, Kagoshima University, during their several other research cruises in the western Equatorial Pacific.

It was deduced in the previous paper stated above that a *contra solem* vortical motion existed in the Coral Sea, on the base of the dynamic topography of the sea surface and of the 150 deci-bar surfaces referred to the 500 deci-bar surface in the western Equatorial Pacific. However, the materials used for the conclusion of the existence of the vortical motion might be insufficient, because no observation was taken by the Keiten-maru in the areas of the north-eastern part of the deduced vortical motion. In the areas under consideration, EQUAPAC materials obtained by the Horizon, Scripps Institution of Oceanography (preliminary informations for preparing the EQUAPAC data table to the participant agencies) are available, though the observations were taken during late southern winter of 1956, a quite different season.

The dynamic topography of the sea surface in dynamic meters referred to the 500 deci-bar surface in the Coral Sea and its adjacent areas is given in the following Figure, using the Keiten-maru materials in the region and some of the Horizon materials stated above. A *contra solem* vortical motion in the Coral Sea is found clearly in the figure. The eastward flow next to the northern side of the *contra solem* vortical motion can be more clearly defined than that discussed in previous paper and is consistent with J. L. REID's conclusion (1959),

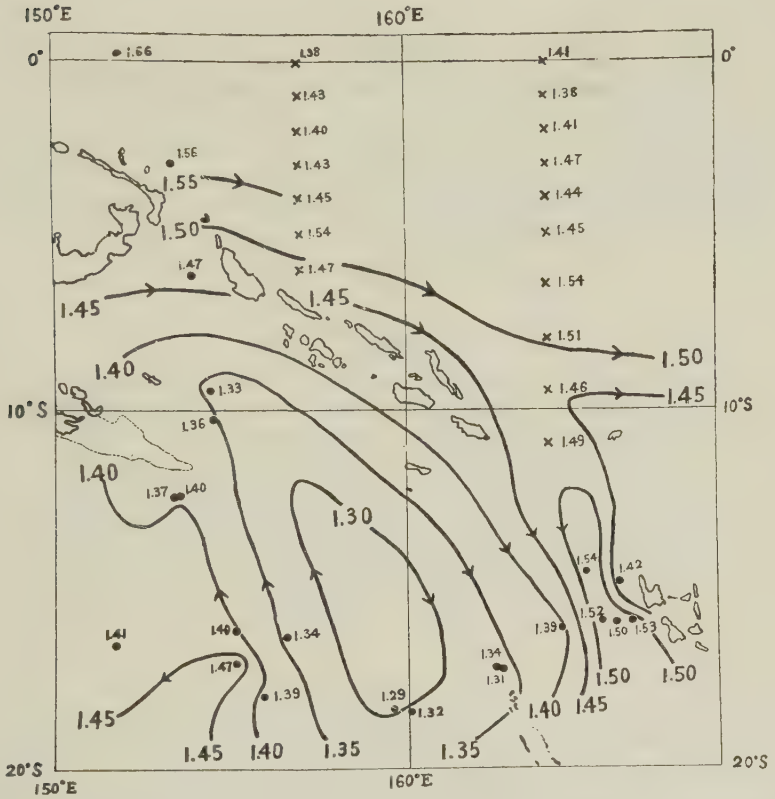

The dynamic topographic chart of the sea surface in dynamic meters referred to the 500 deci-bar surface. Observing stations of the Keiten-maru and of the Horizon are indicated by dots and by crosses respectively. Approximate current directions are indicated by arrows.

in which he considers it part of a South Equatorial Countercurrent.

In the areas near the Equator, contour lines of the dynamic height anomaly are not drawn in the figure on account of the inconsistency between the two vessels' materials, which appears in their numerical values entered in the figure at each observing station. This inconsistency may be rather natural, since the two kinds of materials were obtained in quite different seasons and besides different years.

It is quite necessary to discuss in future whether the Equatorial inconsistency is associated with the simple seasonal displacement of the Equatorial currents or with any other serious problems. Anyway, the eastward flow near the Solomon Islands is a fact recognized by observations and supports the existence of the *contra solem* vortical motion in the Coral Sea.

The author is indebted to Mr. J. L. Reid, Jr., Scripps Institution of Oceanography, for his kind information concerning his unpublished manuscript on a South Equatorial Countercurrent.

References

Morita, T., T. Genka, and T. Takahashi (1959): Tuna-fishing experiments in the Coral Sea (unpublished manuscript).

Reid, Jr., J. L. (1959): Evidence of a South Equatorial Countercurrent in the Pacific Ocean, Nature (to be published).

Takahashi, T. (1959): Hydrographical researches in the western Equatorial Pacific, Mem. Fac. Fish. Kagoshima Univ., Vol. 7.

Records of Oceanographic Works
in Japan Vol. 5, No. 2,
March, 1960

Inorganic Constituents in Seaweeds

By
Masayoshi ISHIBASHI
and
Toshio YAMAMOTO

Summary

(Institute of Chemistry, Faculty of Science, University of Kyoto.)

83 samples of seaweeds composed of 44 species, have been collected from Tomoga-Shima (Wakayama Pref., Japan) area through all the seasons. Total ashes, and sodium, potassium, calcium, magnesium and phosphorus contents in these samples have been determined by the gravimetric method and iron, manganese and chromium contents by the spectrophotometric method. The atomic ratios of K/Na, Ca/Mg, Fe/Mn and Fe/Cr in these seaweeds have been calculated and discussed.

Introduction

There are few detailed investigations on the contents of various elements in seaweeds. W. A. P. BLACK and R. L. MITCHELL[1] summarized the related works of this field. M. ISHIBASHI and R. SAHARA[2] reported on the spectrographic analysis and qualitatively determined 21 elements including major constituents, later the same workers[3] determined chlorine, bromine and iodine in seaweeds using colorimetric method.

In the present paper, the analysis of major constituents (Na, K, Ca, Mg, P and total ash) together with some minor constituents (Cr, Mn and Fe which are successional in atomic number) in various seaweeds are reported.

The content of inorganic constituents in seaweeds will probably change by species, by seasons and by habitats. We are to investigate the details of these subjects. In this connection, the analysis were made with samples of different species and different seasons.

Experimental

Treatment: Collected seaweed samples were first washed with sea-water, dried in the shade, and then washed carefully with distilled water until the washing showed absence of chloride ions. The wet materials were dried at 40°C to 50°C. Samples were specially so selected as to avoid any contamination

* (Institute of Chemistry, Faculty of Science, University of Kyoto.)

before use, and dried at 105°C for about two hours. After the dried samples were weighed, they were ashed gradually at 400°C to 500°C in an electric-furnace.

Determination: Total amounts of ashes were determined in all the samples. Next, following elements were determined by the methods described.

Na	Uranyl-magnesium acetate	method
K	Sodium-cobaltnitrite	method
Ca	Ammonium oxalate	method
Mg	Oxine	method
P	Magnesium pyrophosphate	method
Fe	O-phenanthrorin	method
Mn	Permanganate	method[4]
Cr	Diphenyl-carbazide	method[5]

In the analysis of manganese and chromium a modified method of oxidation were applied; small amount of silver nitrate was added as a catalyser to oxidize manganese and chromium by sodium bismuthate.

Results

The results obtained are summarized in Tables I, II, III, IV and V. It is seen from the tables, that following analysis were made:

Ash	83 samples of 44 spieces
Na, K	39 samples of 27 spieces
Ca, Mg, P	42 samples of 30 spieces
Fe	72 samples of 41 spieces
Mn	70 samples of 39 spieces
Cr	16 samples of 15 spieces

And that considerable variation in the contents of these element by season and by species even though taken from the same habitat.

1) Generally, the seaweeds contain much more Na, Mg and Fe than those of the land plants. Especially *Ulva s. p.* contains much of Mg.
2) Generally, the brown seaweeds are rich in K and Ca contents and the green seaweeds are rich in Fe and Cr contents.
3) There are remarkable difference in the contents of Fe and Mn by species, however little difference is observed with P.
4) Seaweeds which have rich Fe contents have rich Mn and Cr contents as a whole. Approximately half of the analysed species showed the value of 3-7 in the Fe/Mn atomic ratio. The Fe/Cr atomic ratio also showed considerable concentration of iron.
5) The atomic ratio of K/Na is near 1 in all species. The Ca/Mg atomic ratio is below 2 except one species. (*Desmarestia viridus*)

Table 1. Brown Sea-weeds (1)

Sample	Date of Collection	Contents in dry matter in mg./g.									Atomic ratio in ashes			
		Total ash	Na	K	Ca	Mg	P	Fe	Mn	Cr	K/Na	Ca/Mg	Fe/Mn	Fe/Cr
Myelophycus caespitosus	Jan. 26, 1956	142.						1.193	0.054				21.69	
Scytosiphon lomentarius	Feb. 29, 1956	293.	9.9	8.7	31.9	10.7	1.8	3.410	0.078		0.52	1.81	43.20	
Desmarestia virids	May. 16, 1956	39.	0.4	0.7	8.7	0.3	0.9	0.420	0.009		0.99	17.21	47.29	
Eudesme crassa	Oct. 16, 1955	110.	2.3	1.4	6.3	7.9	1.1	2.136	0.227		0.37	0.48	9.24	
Chordaria sp.	Oct. 16. 1955	114.	5.4	11.2	11.9	6.7	0.7	0.584	0.122		1.22	1.09	4.73	
Eisenia bicyclis	Jan. 26. 1956	161.	16.6	23.1				0.106	0.009		0.82		12.18	
	May. 16, 1956	161.	17.1	26.3	18.8	9.1	1.1	0.144	0.012		0.91	1.26	12.03	
	May. 26, 1957	138.	12.3	22.5	13.1	7.9	1.1	0.090	0.004	0.00074	1.02	1.01	23.65	112.5
	Aug. 1, 1958	144.						0.076						
	Aug. 28, 1956	142.	14.7	21.1	17.8	9.9	0.6	0.077	0.007		0.84	1.09	11.11	
	Oct. 16, 1955	130.	13.1	17.7	11.4	6.6	0.8	0.106	0.010		0.79	1.04	10.79	
Padina arborescens	Jan. 26, 1956	130.												
	Feb. 29, 1956	125.						0.353	0.094				3.68	
	May. 16, 1956	188.	16.1	35.7	12.8	11.6	0.9	0.643	0.198	.000142	1.31	0.67	3.20	422.7
	Aug. 8, 1955	145.						0.627						
	Aug. 28, 1956	158.						0.649	0.147				4.74	
	Oct. 16, 1955	133.												

Table 2. Brown Sea-weeds (2)

Sample	Date of Collection	Contents in dry matter in mg./g.									Atomic ratio in ashes			
		Total ash	Na	K	Ca	Mg	P	Fe	Mn	Cr	K/Na	Ca/Mg	Fe/Mn	Fe/Cr
Hizikia fusiforme	Jan. 1955	158.						0.270	0.042				6.37	
	Jan. 26, 1956	178.						0.133	0.024				5.36	
	Feb. 1954	155.						0.187	0.033				5.62	
	Feb. 1955	164.							0.025					
	Feb. 17, 1953	210.			18.8	8.4	1.2	0.112	0.028			1.36	3.93	
	Feb. 29, 1956	196.												
	Mar. 15, 1953	195.						0.258	0.031				8.30	
	May. 16, 1956	192.	16.9	34.3	19.4	11.8	0.6	0.167	0.019	0.00063	1.19	1.00	8.54	246.4
Neurocarpus Prolifera	Aug. 28, 1956	105.	4.7	7.0	14.0	5.8	1.8	0.900	0.070		0.89	1.48	12.61	
Sargassum enerve	Oct. 16, 1955	125.	7.1	13.4	19.8	12.6	0.9	0.152	0.028		1.11	0.95	5.43	
Sargassum giganteifolium	Jan. 26, 1956	119.	4.8	8.5	15.7	13.6	1.1	0.158	0.013	0.00052	1.05	0.70	11.57	285.8
Sargassum Ringgoldianum	Jan. 26, 1956	153.	6.9	16.8				0.070	0.010		1.44		6.61	
	Jan. 26, 1956	155.						0.154	0.009				17.10	
	May. 16, 1956	153.	7.0	19.5	24.4	12.1	0.8	0.113	0.019	0.00047	1.65	1.23	5.85	222.4
	Aug. 8, 1955	138.						0.080	0.009				8.36	
	Aug. 28, 1956	136.	7.6	16.0	23.1	9.7	0.7	0.070	0.017		1.24	1.45	4.09	
Sargassum Serratifolium	Aug. 8, 1955	164.			29.2	16.5	0.2	0.092	0.004			1.07	25.22	

Table 3. Brown Sea-weeds (3)

Sample	Date of Collection	Contents in dry matter in mg./g.								Atomic ratio in ashes			
		Total ash	Na	K	Ca	Mg	P	Fe	Mu	Cr	K/Na	Ca/Mg	Fe/Mn	Fe/Cr
Sargassum piluliferum	Aug. 8, 1955	96.	4.0	3.7	19.0	6.8	0.7	0.493	0.033		0.55	1.69	14.69	
	Aug. 8, 1955	121.						0.739	0.043				17.03	
Sargassum Horneri	Jan. 26, 1956	102.	3.6	6.4	16.4	16.9	1.2	0.142	0.014		1.05	0.59	9.75	
Sargassum tortile	Oct. 16, 1955	112.	2.7	5.4	26.6	7.8	0.7	0.119	0.020		1.19	2.06	5.95	
Ishige Okamurai	Feb. 29, 1956	124.	15.3	7.6	14.8	8.4	1.7	0.088	0.007	0.00089	0.29	1.06	11.59	92.1
Ishige foliacea	Feb. 29, 1956	115.						0.144	0.031				4.61	
Sargassum micaracanthum	Aug. 28, 1956	137.	6.7	12.5	24.1	11.8	0.5	0.367	0.120	0.00124	1.09	1.24	3.02	274.4
Sargassum Thumbergii	Jan. 26, 1956	161.	7.1	19.4	12.3	7.5	1.2	0.813	0.257		1.59	0.99	3.11	
	Feb. 29, 1956	177.	8.2	23.5	22.8	6.9	1.5	0.660	0.235	0.00150	1.68	2.01	2.76	409.4
	Mar. 1954	195.	7.2	13.8	28.7	7.5	0.9	1.935	0.305		1.14	2.31	6.23	
	May. 16, 1956	164.	11.0	19.3	22.4	10.6	0.9	0.695	0.184		1.04	1.29	3.71	
	May. 16, 1956	205.	11.8	32.6	42.1	12.8	0.8	0.291	0.100		1.62	1.99	2.85	
	Aug. 8, 1955	178.						1.089	0.172				6.22	
	Aug. 13, 1954	207.	7.2	17.0	27.5	9.5	0.8	1.203	0.478		1.39	1.77	2.48	
	Aug. 28, 1956	223.							0.266					
	Oct. 16, 1955	194.						0.584	0.263				2.19	
	Oct. 18, 1952	189.			34.0	8.8	1.6	0.438	0.169	0.00152		2.35	2.55	268.6

Table 4. Green Sea-weeds

Sample	Date of Collection	Contents in dry matter in mg./g.									Atomic ratio in ashes			
		Total ash	Na	K	Ca	Mg	P	Fe	Mn	Ca	K/Na	Ca/Mg	Fe/Mn	Fe/Cr
Monostroma nitidum	Jan. 26, 1956	238.	17.9	7.6	17.2	14.3	0.9	1.434	0.055	0.00207	0.25	0.73	25.54	644.8
Ulva conglobata	Aug. 28, 1956	159.	1.0	1.7	8.3	36.5	0.8	0.609	0.097	0.00121	0.95	0.14	6.14	467.8
Ulva sp.	Oct. 16, 1955	168.	3.6	4.7	5.7	38.3	1.2	0.500	0.168	0.00104	0.77	0.09	2.93	449.0
Ulva sp.	Jan. 26, 1956	190.	3.6	5.5	5.6	44.3	1.7	0.526	0.012	0.00134	0.89	0.08	42.53	365.5
	Aug. 1, 1958	177.						0.363						
Ulva sp.	Oct. 16, 1955	126.						0.334	0.111				2.96	
Cladophora Wrightiana	Oct. 16, 1955	180.						0.582	0.087				6.54	
Chaetomorpha crassa	Jan. 26, 1956	102.						0.376	0.102				3.63	
	May. 16, 1956	121.	6.5	13.2	11.3	8.6	0.8	0.561	0.199	0.00182	1.20	0.79	2.77	287.3
Cavlerpa Okamurai Weber	Aug. 1. 1958	182.						3.079						
Codium fragile	Oct. 16, 1955	150.			11.4	11.1	1.5	2.497	0.299			0.62	8.23	
Codium pugniformis	May. 16, 1956	360.	66.6	25.8	8.6	15.4	2.8	0.591	0.052	0.00253	0.23	0.34	11.14	217.8

Table 5. Red Sea.weeds

Sample	Date of Collection	Contents in dry matter in mg./g.									Atomic ratio in ashes			
		Total ash	Na	K	Ca	Mg	P	Fe	Mn	Cr	K/Na	Ca/Mg	Fe/Mn	Fe/Cr
Gelidium sp.	Jan. 26, 1956	27.							0.019					
	Aug. 1955	32.	0.2	0.3	3.5	5.0	0.2	0.224	0.041	0.00050	0.89	0.43	5.36	416.3
Gelidium sp.	Aug. 1, 1958	61.						0.534						
	Oct. 16. 1955	66.			7.7	10.4	1.6	0.255	0.070			0.45	3.56	
Acanthopeltis japonica	Jan. 26, 1956	139.						0.293	0.080				3.62	
	May. 16, 1956	103.	1.7	1.1					0.054		0.39			
	Aug. 28, 1956	137.	1.9	1.1	4.7	2.2	1.3		0.065		0.34	1.28		
	Oct. 16, 1955	108.			3.1	2.5	0.8	0.183	0.042			0.75	4.32	
Meristotheca papulosa	Aug. 28, 1956	164.			6.2	8.4	1.3	0.465	0.337			0.45	1.36	
Sarcodia ceylanica	Feb. 29, 1956	100.						0.343	0.048				7.01	
Hypnea Saidana	Jan. 26, 1956	110.						0.424						
Hypnea sp.	Jan. 26, 1956	164.						1.013						
Plocamium Telfairiae	Jan. 26, 1956	199.						1.504						
Gloiosiphonia Capillaris	May. 16, 1956	131.							0.076					
Grateloupia filicina	Aug. 28, 1956	303.												
Carpopeltis flabellate	Mar. 1955	99.	10.7	6.5	3.8	7.8	1.2	0.221	0.028		0.36	0.29	7.76	
	Aug. 1, 1958	106.						0.139						
Carpopeltis rigida	May. 16, 1956	36.	1.1	1.0					0.044		0.52			
Chondrococcus japonica	Oct. 16. 1955	127.						1.091	0.270				3.97	
Zostera Marina	Oct. 16, 1955	168.						1.235	0.194				6.26	

6) Chromium is much more condensed in the seaweed than in the sea-water.
7) Most species contained 10-20% of ash. The content of minor constituents is almost indifferent to the amount of total ashes.
For the details see figures in Table I, II, III, IV and V.

Literature Cited

1) W. A. P. Black, B. L. Mitchell, J. Mar. Biol. Ass. U.K. 30, 575 (1952)
2) M. Ishibashi, R. Sahara, J. Chem. Soc. Japan, Pure Chem. Sec., 61, 277 (1940)
3) M. Ishibashi, R. Sahara, ibid. 61, 513 (1940)
4) M. Ishibashi, T. Yamamoto, ibid. 79, 1184 (1958)
5) T. Yamamoto, J. Chem. Soc. Japan, Pure Chem. Sec., 81, No. 3 (1960).

Records of Oceanographic Works
in Japan Vol. 5. No. 2,
March, 1960

Determination of Manganese in Sea-Water

By
Masayoshi ISHIBASHI, Tsunenobu SHIGEMATSU
and Yasuharu NISHIKAWA

Abstract

The manganese content of sea-water was investigated. Manganese was separated with aluminum hydroxide, and determined by periodate method. The greater part of manganese in sea-water was removed by filtration, and about 1 ~ 3 μg of manganese per litre of sea-water was found in the filtrate.

Introduction

The amount of manganese in sea-water obtained by THOMPSON and WILSON[1] is about 1~10 μg per liter of sea water. Formerly, 5 μg/L of manganese content was refered as the amount of manganese in sea water by WATTENBERG[2].

The authors determined the amount of manganese in sea-water by potassium

μg of manganese was found in a liter of sea waters sampled at Shuma and Shirahama.

Enrichment and Colorimetric Determination of Mn.

The minuteness of manganese content in sea water makes its direct determination difficult. In order to concentrate and separate the Mn in sea water, the authors utilized the coprecipitation method where aluminium hydroxide was used as a collector. The procedure was designed as follows.

Analytical procedure: To 5~10 liter of the sample water acidified with 5 ml of hydrochloric acid, and 5~10 mg of aluminium ion as $AlCl_3$, mix throughly and add ammonium hydroxide solution (1 : 5) to make the solution slightly alkaline. After standing for 1~2 days, filter the precipitate and dissolve with 20 *ml* of sulfuric acid, containing a minute amount of hydrogen peroxide. Evaporate the sulfuric acid solution to fume SO_3 gas, cool, add 1 *ml* of 80% phosphoric acid and dilute to 8~9 *ml* with water. Add 0.2~0.5 g of Potassium periodate crystal, heat for 20~30 minutes, cool, transfer the solution into a 10 *ml* measuring flask and then dilute to the mark with water. The resulting reddish violet of permanganate ion was measured colorimetrically.

Colorimetric determination was made by using Pulfrich photometer with the cell of 2 *cm* length and the filter S_{61}. The amount of manganese was calculated

from the following equation.

$$\text{Mn } \mu g = 105 \times E$$

where E is color intensity, i.e. extinction.

It was found that through this procedure 5～10 μg of manganese can be determined within the error of ±5%. The results obtained with the artifical sea-water according to the above mentioned procedure are shown in Table I.

Table I.

Artifical sea water taken	Mn added (μg)	Mn found (μg)	Difference (μg)
5 l	0.0	0.0	—
5	30	28.7	−0.3
5	30	30.0	0.0
5	30	29.9	−0.1

The recovery of Mn in this procedure was more than about 95 per cent.

On the amounts of Manganese in Sea-Water

The sea-water were collected off shore of Suma, Hiyogo, on July 18th, 1949 (I) and off shore of Shirahama, Wakayama, Japan on August 12th, 1949 (II). The results of analysis are shown in Table II.

These sample of sea-water was almost clear, but the brown muddy residue appeared slightly when the sample water was filtered through a Toyo Roshi Co. filter paper No. 5.

Table II.

Sample No.	Sample sea water taken (l)	Mn		Remarks
		Found (μg)	μg/l	
I	18	257.4	14.3	Not filtered
I	16	15.5	0.97	filtered
II	5	50.5	10.1	Not filtered
II	3	9.0	3.0	filtered

The loss of manganese in sea-water by filtration was found different dependent on the samples; 90 % and 70 % of manganese was lost by the filtration of sample I and sample II, respectively. It was shown that the greater part of manganese in sea-water was contained in suspended materials. The value of manganese in a filtered sea-water is 1 and 3 μg/L and shows good accordance with that obtained by Thompson and Wilson.

The authors wish to express their thanks to Dr. T. Tokioka for his help in sampling of sea-water.

References

(1) Thompson and Wilson, J.A.C.S., **57**, 233 (1935).
(2) Wattenberg, Z. anorg. Chem., **251**, 86 (1943).
(3) Willard and Greathause, J.A.C.S., **89**, 2366 (1917).

(The work was read before the meeting of the Institute for Chemical Research, Kyoto University, 1951).

Records of Oceanographic Works
in Japan Vol. 5, No. 2,
March, 1960

Determination of Arsenic in Sea-Water

By
Masayoshi ISHIBASHI, Tsunenobu SHIGEMATSU
Yasuharu NISHIKAWA and Yoshihiro ISHIBASHI.
(Institute of Chemistry, Faculty of Science, University of Kyoto.)

Abstract

Arsenic in sea-water was separated by precipitating with ferric hydroxide as carrier, and then determined by Gutzeit method. The value obtained from different samples was ranging from 3 μg to 6 μg per litre of sea-water, and the mean was about 4 μg/1 L.

Introduction

The amount of arsenic in sea-water obtained by GAUTIER[1], and by RAKESTRAW and LUTZ[2] are about 10 μg, and 6~28 μg per liter of sea-water respectively. RAKESTRAW and LUTZ determined the arsenic content in sea-water by Gutzeit method, and showed the mean being about 15 μg. They stated that although the arsenic content increased at 10~15 m below the surface, there was no general increase with depth; hence the distribution was quite unlike that of phosphorous.

On the other hand, ATKINS and WILSON[3] described that the amount of arsenic in sea-water were varied with phosphorous content, and changed with regard to depth.

At the present time, the amount of arsenic in sea-water is recognized to be about 10~20 μg per liter.

The purpose of the present investigation was to study the application of the Gutzeit method to the determination of arsenic and to obtain the quantitative data from some different samples of sea-water.

Determination of Arsenic by Gutzeit method.

The authors studied on the Gutzeit method for trace amount of arsenic and established the conditions necessary and satisfactory to obtaine accurate results.

1. Reagents and Apparatus

Standard arsenic solution: A known amount of pure arsenious oxide was dissolved in sodium hydroxide solution and neutralized with sulfuric acid. The solution containing 100 μg arsenic per milliliter was obtained, and then it was diluted to proper concentration of arsenic as needed.

Ferric alum solution: 8.4 gram of ferric ammonium alum was dissolved in water containing 2 ml of sulfuric acid and diluted to 100 ml.

Stannous chloride solution: 40 g of pure stannous chloride was dissolved in 25ml of concentrated hydrochloric acid and diluted to 50 ml.

Lead acetate solution: 1 gram of lead acetate was dissolved in water, containing enough quantity of acetic acid to make the clear solution, and diluted to 100 ml.

Zinc metal granule: Granular zinc metal which was 2~3 mm in diameter and was free from arsenic, was used.

Sensitized mercuric chloride paper: The strips having 3×120 mm uniform width and length was prepared with filter paper No. 1 from Toyo Roshi Co. Such strips were dyed by drawing through a 5 % solution of recrystalized mercuric chloride and dried at room temperature. This test paper was stored in desiccater and kept in the dark.

Apparatus for the determination of arsenic: The apparatus employed in this investigation is shown in Figure 1. A is a reduction bottle. Tube B is packed with absorbent cotton moistened with lead acetate solution to remove the trace of hydrogen sulphide and to moisten the arsine. This absorbent cotton must be exchanged in each test. The mercuric chloride paper must be carefully set in the center of the upper tube C.

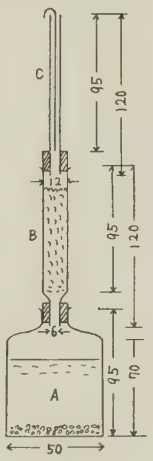

Fig. 1.

2. Analytical procedure

50 ml of sample-solution was taken into the reduction bottle A, then 3 ml of concentrated sulfuric acid, 3 ml ferric alum solution, and 1 ml of stannous chloride solution were added. Warm to approximately 25°C. Charge the tube B with lead acetate cotton, connect with the upper tube C furnished with strip of the mercuric chloride paper, add 20 g of zinc granule shot to the solution and insert the stopper carrying the tubes. Shake gently and allow to stand in a bath at 25°C for 45 minutes. Remove the mercuric chloride paper and compare with the length of standard yellowish brown stains. Table I shows a relationship between the arsenic content and the length of stains. It was found that by this procedure 0~40 μg of arsenic could be determined within the error of $\pm$ 1 μg.

Table I.

As (μg)	0	5	10	15	20	30	40
length of stain (mm)	0 0.2	4.0	7.5	12.0	15.5	23.0	32

Enrichment of Arsenic in Sea-Water

The minuteness of arsenic content in sea-water makes its direct determination difficult. In order to concentrate and separate arsenic from the major constituents of sea-water such as chloride, sulfate, sodium, calcium and magnesium, coprecipitation method with ferric hydroxide as collector is used.

For the preliminary survey, the following experiments were made.

The definite amount of standard arsenic solution and a known amount of ferric iron solution were added to one liter of artificial sea-water. 20 ml of ammonium hydroxide (1 : 10) was added, and then the resulting solution was allowed to stand over night to settle the precipitate. The precipitate was filtered, and dissolved with sulfuric acid. This solution was determined according to the procedure mentioned above.

The results are shown in Table II.

Table II.

Arsenic added	Arsenic found μg		Mean value	Recovery
0.0 μg	0.0	0.4	0.2 μg	—
10.0	8.7	8.0	8.4	84 %
15.0	17.3		17.3	115
20.0	19.4	18.0	19.1	95
	19.4	19.4		
30.0	25.0	26.1	25.6	85

These data indicate that arsenic is almost completely coprecipitated with ferric hydroxide, and its recovery in this procedure was more than 85 per cent.

In order to test the absorption of arsenic by filter paper used for the removal of suspended material and plankton, the author conducted the experiments as follows.

One liter of artificial sea-water containing 20 μg of arsenic was filtered through the filter paper No. 5A (9 cm). Then the filtrate was treated according to the procedure mentioned above. The analytical results were about 18.6 μg arsenic. As seen in Table II, these data showed that the absorption of arsenic by filtration can be disregarded.

Determination of Arsenic in Sea-Water

1~2 liters of the sample-water was taken, and acidified with 5~6 drops of sulfuric acid. In order to decompose the organic matter, 1~2 ml of bromine water was added and heated for about 10 minutes. Then was added 20 mg of ferric iron as ferric chloride to every one liter of sea-water, and mixed thoroughly. To the solution, 20 ml of ammonium hydroxide solution (1 : 10) was

Table III. Arsenic in Sea-Water.

Sample Sea-Water	Chlorinity and Density	Filtration	Sample taken	Arsenic taken	Amount of arsenic/l	Run. No.
Shionomisaki Promontory on the Pacific 32.5°N, 135°E, Aug. 20th, 1949	Cl=19.10‰ d=1.025	Non	1 l	3.3 μg	3.3 μg	1
		Filtered	〃	0.0	0	2
Off the coast of Setozaki in Wakayama Prefecture. (1 m below the surface) Feb. 21st, 1950	Cl=19.25‰ d=1.027	Non	1 l	6.6	6.6	3
		Filtered	〃	5.0	5.0	4
		〃	〃	6.0	6.0	5
		〃	〃	6.6	6.6	6
		〃	2	10.6	5.3	7
		〃	1 (+5μgAs)	11.3	6.3	8
The Japan Sea 35°44′46″N, 135°30′E Apr. 27th, 1950	Cl=19.12‰	Non	1	4.4	4.4	9
		〃	1 (+5μgAs)	8.7	3.7	10
		Filtered	1	0	0	11
		—		4.0	〃	12
Off the bay of Tanabe in Wakayama Prefecture 33°42′N, 135°19′E Oct. 17th, 1950	Cl=18.77‰ d=1.025	Non	1	2.5	2.5	13
		〃	2	7.3	3.6	14
		Filtered	1	3.0	3.0	15
		〃	2	6.3	3.2	16
Off the bay of Tanabe in Wakayama Prefecture 33°42′N, 135°19′E Oct. 18th, 1950	Cl=18.77‰ d=1.025 1 m below the surface	Non	1	3.0	3.0	17
	10 m 〃	〃	2	6.5	3.3	18
	15 m 〃	〃	1	5.0	5.0	19
	20 m 〃	〃	〃	3.5	3.5	20
	30 m 〃	〃	〃	4.0	4.0	21

added and allowed to stand over night. The precipitate was filtered and dissolved with 18 ml of sulfuric acid (1 : 5) and transfered to the Gutzeit reduction apparatus and diluted to 50 ml. This solution was determined by Gutzeit method.

The results of analysis are shown in Table III.

On the Amount of Arsenic in Sea-Water

As seen in Table III, the arsenic content in the surface sea-water is believed to be 3~6 μg/L, and it seems that the arsenic content is changed by the sampling place.

When the sea-water was filtered through a filter paper, occasionally the arsenic was not found in the filtrate (Run. No. 2 and 11). In this case, the total arsenic was found in the residue on the filter paper as seen in Table III (Run. No. 12).

However, the authors already described that the adsorption of arsenic by filtration can be disregarded. Accordingly, the diminution of arsenic by filtration may be due to a removal of suspended material and plankton in sea-water, which absorbs arsenic.

The samples used at Run. No. 2 was elapsed at about three monthes after sampling, and so the colloidal precipitate formed and the arsenic was absorbed by them. Hence in the newly sampled sea-water, the diminution of arsenic by filtration was disregarded.

The facts described above showed that the arsenic in sea-water was principally in the form of arsenite as Atkins[3] stated.

The amount of arsenic in surface sea-water are about 3~6 μg/L, the mean being about 4μg/L.

The variation of arsenic content with depth was not so particular, but it seems to increase gradually from 15 m to 30 m below the surface as shown in Table III.

The authors wish to express their thanks to Dr. T. Tokioka for his help in sampling of sea water.

References

(1) Gautier, Compt. rend. **137**, 232 (1903).
(2) N. W. Rakestraw and F. B. Lutz, Biol. Bull., **65**, 397 (1933).
(3) W. R. G. Atkins and E. G. Wilson, J. Marine Biol. Assoc., **14**, 609 (1927).
(The work was read at the meeting of the Institute for Chemical Research, Kyoto Univ., 1951)

Records of Oceanographic Works
in Japan Vol. 5, No. 2,
March, 1960

Studies of Vitamin B_{12} in Natural Water

By
Ken-ichi KASHIWADA, Daiichi KAKIMOTO and Akio KANAZAWA
(Faculty of Fisheries, Kagoshima University)

Summary

1. In order to ascertain the distribution of B_{12} in the oceanic front, some random surveys of sea lying along the line of Long. 130°E from Lat. 0° to 30°N in the North Pacific Ocean with the depth of 1,200 m below the surface were carried out; the distribution being fixed to be within the range on 26 m γ/1. The maximum was ascertained to be within the water depth of 500 m.

2. The maximum point of B_{12} content in the lake was at 20 m below the surface; this being in agreement with the dissolved oxygen. The influence of land-water over the sea-water was proved to have not a small influence over the latter.

3. In order to ascertain the B_{12} distribution state under the action of light passed through the water layer B_{12} solution put into the polyethylene sack was immersed in sea-water and the decreasing ratio of B_{12} through sunlight during about 10 hours from sunrise to sunset was examined, with the result that at the sea-depth 0 m (surface), 2.5 m, 5 m, 10 m, 15 m, 20 m, 25 m, 30 m, it was ascertained to be about 81 %, 79 %, 72 %, 65 %, 63 %, 54 %, 31 %, 9 % respectively.

It has been well known that vitamin B_{12} acts as a growth-stimulating factor to certain kinds of creatures.

As to the natural distribution of vitamin B_{12}, it is said that it covers a wide biological area from micro-organisms to the higher animals with the exception of the botanical field. From the results of the recent research performed on the marine products it was ascertained that B_{12} was contained in seaweed and that B_{12} played an essential part as nutritive element for the growth of some kinds of marine bacteria. But, only a few researchers know that how much amount of B_{12} distribute in ocean, lake and river until recent time.

In this paper, the authors are going to make some explanations on the distribution state of B_{12} in sea, lake and river water, as well as discussing the stability of B_{12} in them.

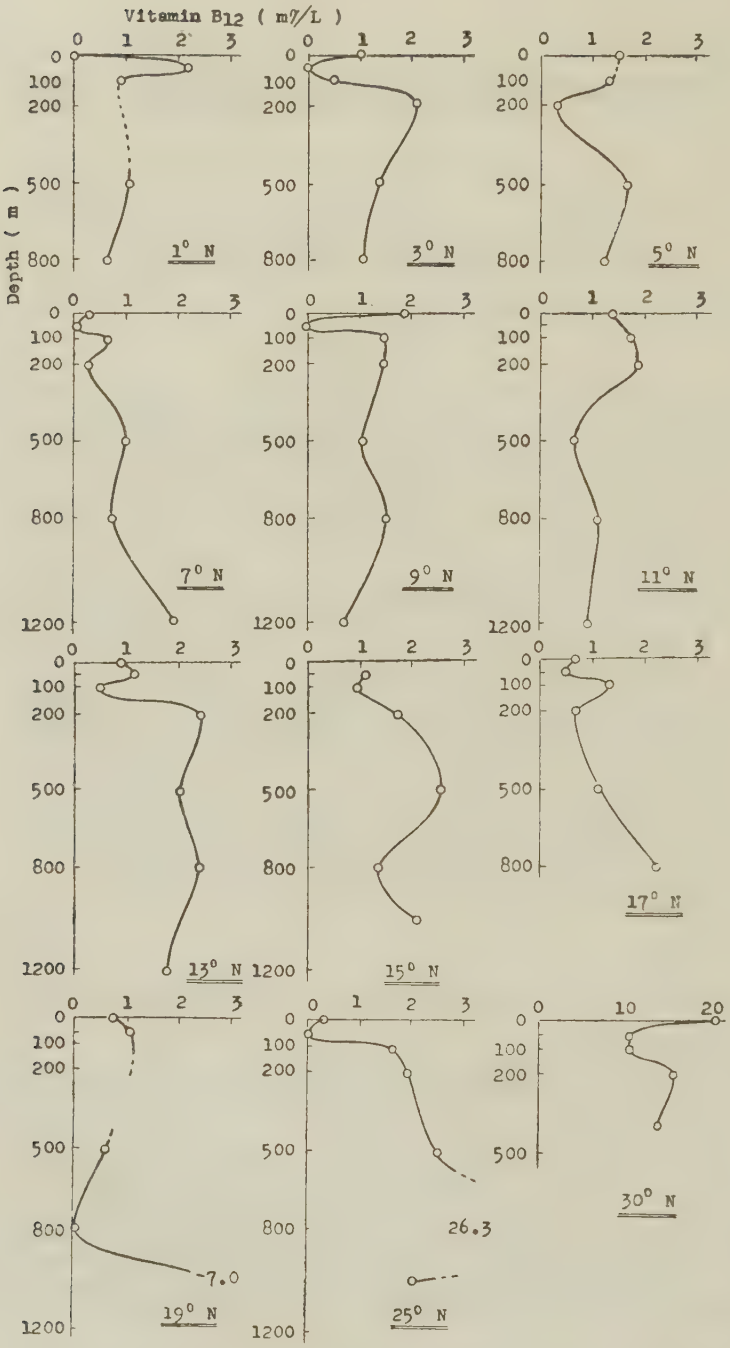

Fig. 1. Vertical distribution of vitamin B_{12} in sea water.
(0°—30°N along 130°E)

1. Vitamin B_{12} Content in Sea-Water

Vitamin B_{12} content in sea-water was measured by the authors' method.[1]. As the result of surveying the surface water in the North Sea and the Atlantic Ocean, the regional and seasonal variations of B_{12} in sea water reported by DROOP[2] and COWEY[3]. According to those reports, the B_{12} content in sea-water was fixed to be in the neighbourhood of 5-10 mγ/l, which coincided with the results determined by the authors in the water taken from the Pacific Ocean as was shown in Fig. 1.

Not only the surface water but the sea-water of several regions with various depths was measured by the authors with the conformation of a certain difference in the density, which perhaps may be attributed to the variation of the place where the measurement was done.

In this experiment, the delicate errors due to the variations of the days and times or decrease derived from the effect of the light which were noticed in the record after the finish of the experiment were put out of the consideration. As to the decrease of B_{12} in the natural water caused by sunlight, reference is going to be made in another section of this paper.

2. Vitamin B_{12} Content in Lake Ikeda and River Kōtsuki

Although as mentioned above some results were obtained from sea-water, in the ocean, such obstacles as rolling waves and tide currents prevent us from gaining a genuine result. So lake-water free from these influences was adopted as the sample, and after determining its vertical distributions a comparative research was done about these two kinds of waters. With the same project and in order to ascertain the origin B_{12} in sea-water, B_{12} content in the river was also measured (Table 1).

Table 1. Diurnal fluctuation of vitamin B_{12} content in Kōtsuki River.

Time	Weather	Appearance of sample water	B_{12}(mγ/l)	B_{12} in stord water*
5.30 A.M.	Cloudy	Clear	2.7	2.7
7.30 〃	〃	〃	1.2	1.5
9.30 〃	〃	〃	0.4	0.7
2.30 P.M.	Rainy	Muddy	4.5	0.7

Remarks; It began to rain at about 10 A.M.

* The river water collected at 5.30 A.M. was stored out doors in polyethylene sack.

Lake Ikeda is situated at the southern most end of Japan, with the length of 4.5 km from East to West, and of 3 km from South to North, having a depth of 250 m, located at the height of 66 m above sea level.

Sample of water was taken on 22nd of Oct., 1956 at 3 P.M. in the neighbourhood of the lake center, from the surface to 120 m depth. A comparative research of B_{12} was done according to the fixed temperature and the result obtained is as follows. Namely, the B_{12} content in the lake reaches its maximum at the point 62.5 mγ/l. The difference between the highest and the lowest is quite remarkable: Comparatively speaking, the largest fluctuation is to be seen between the surface and a depth of 20 m. Along the surface of the lake even a slight difference in the depth causes not a small difference in B_{12} content. For example, within the depth of 10 m the B_{12} content is 0 and 7.5 mγ/l respectively, and that of 2-8 m the same tendency was seen.

The cause of such an extreme difference as this in the density was left unsettled, but this might probably be attributed to some water mass formation or to the existence of a certain water circle. As to the vertical distribution of water temperature as was shown in the figure in the lying within 20 m from the surface little difference was seen between that of surface water, the standard value being about 21°C. Beyond 20 m, a sudden lowering tendency set in, and it reached 12°C at the depth of 30 m. In the neighbourhood of 40 m, a rise in the water temperature was observed together with the rising tendency in the density of B_{12}. In a nutshell, it can be safely sald that the fluctuation of B_{12} is remarkable at the shallow regions of the lake.

Again, in August 1958, the second measurement was done at the same lake with the results shown in Fig. 2. In this investigation, temperature, pH value, the amount of dissolved oxygen, nitrate, phosphate and silicate etc. were measured together with B_{12}. The measurement was done both at the deepest region and around the lake at the depth of about 30 m. As a result, maximum B_{12} content was fixed at the depth of 20 m, and the close relationship between the vertical distribution of B_{12} and the amount of the dissolved oxygen was also confirmed. The investigation done with

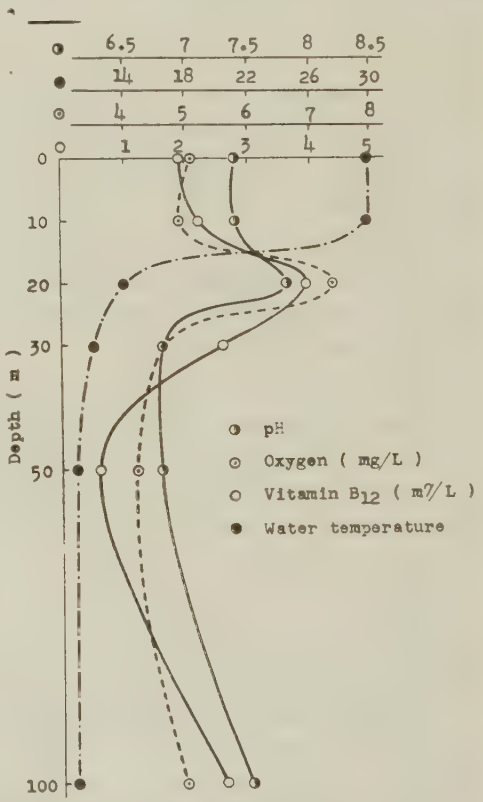

Fig. 2. The vertical distribution of vitamin B_{12}, pH value, dissolved oxygen and water temperature in the Lake Ikeda.

the aid of radar, also, confirmed the existence of fish schools in this neighbourhood.

River Kōtsuki runs across Kagoshima city into Kinko bay and its lengths is 15 km and width at river mouth is 120 m. On 15th of June, 1958 surveys were done along this river. At regular intervals consecutive of about 500 m was done under cloudy skies.

It was ascertained that at 0.1-0.2 mγ/l, each point along the river side over a region covering 5 km showed generally the same account. There is almost no difference between the houseless sections and the thickly populated urban districts, while on the sea front about 100 m off the river mouth it showed the content of 1-3 mγ/l.

On 15th of Oct., 1958 an observation was done at a point at upper stream, 2 km from the river mouth. Before the illumination of sunlight the B_{12} content was fixed at 2.7 mγ/l but in the lapse of time it began to decrease. However, rainfall prevented the decreasing tendency, regaining the count of 4.5 mγ/l after the beginning of the rainfall. A part of water took from the river at 5.30 A.M. in the morning was put into a polyethylene bag and it was left outdoors. It decreased to 0.7 mγ/l at 9.30 A.M. This experiment shows that B_{12} in the river-water decreases quickly under the open state and increases under the rainfall. The increase of precipitation may be attributed to B_{12} being carried into the water from the banks. Simple and incomplete as this is, by this experiment some relationships between the B_{12} in sea-water and river-water might be safely assumed. (Table 1)

3. Stability of B_{12} in Sea-Water

Much has been known about the instability of B_{12} in relation to the influence of light, but little is known about its decomposition process in the natural state by sunlight, and about the range of sunlight influence throughout the respective depth of the water. In order to ascertain this, B_{12} solution of known density (52.5 mγ/l) was put into a polyethylene bag and suspended at a fixed depth of sea-water. The decrease amount of the B_{12} was measured. Fig. 3 shows the decomposing degree measured on 5th of Dec., 1958 during fine weather. During 10 hours from sunrise to sunset, 81% of B_{12} was destroyed on the surface. At the depth

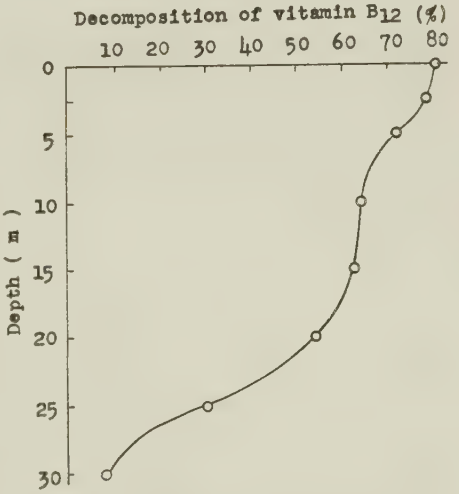

Fig. 3. Decomposition of vitamin B_{12} at each depth of the sea.

of 20 m, more than 50% destruction was observed, but at layers deeper than that no remarkable destruction was to be seen. This shows that, at least, near the water surface, sunlight has not a small relationship with the destruction of B_{12}. Thus, vitamin B^{12} distribution covers the wide area of the natural waters, and has some important role in the productivity of the sea. And it may be loked upon as one of the essential nutritive elements of the living organisms in their growing process. But seen from the general nutritive point of view the role of B_{12} is not so great. It is needless to say that other nutritive substances such as general vitamins and amino acids are far more momentous as the object of research.

This research on B_{12} will be pursued successively and by other comprehensive and thorough researches on the productivity of sea. Some contributions might be made to the promotion of the world-wide researches on the 'biological active substance in the ocean,' and if so, our efforts will have been amply rewarded.

Literature

(1) Ken-ichi Kashiwada, Daiichi Kakimoto, Tomokazu Morita, Akio Kanazawa and Kazunori Kawagoe: Bulletin of the Japanese Society of Scientific Fisheries, 22, 637 (1957)
(2) M. R. Droop: J. Mar. biol. Ass. U.K. 34, 435 (1955)
(3) C. B. Cowey: Ibid. 35, 609 (1956)

Records of Oceanographic Works
in Japan Vol. 5. No. 2,
March, 1960

BIOLOGY OF *Sebastiscus marmoratus* CUVIER et VALENCIENNES

By
Shin-ichi MIO
(Fisheries Department, Faculty of Agriculture, Kyushu University)

The scale and otolith show similarity in mark-size, but otolith-marks are better for age-determination than scale-marks. The relationship of total length (L) to otolith-size (R) is isometric and each mark-sizes are standardized by L — R equation. The marks are formed in May every year.

The growth of this species is fitted the Pütter-von Bertalanffy's equation to length data, the Buch-Andresen-Fischer's equation to weight data.

This ovoviviparous fish copulates in October and the eggfertilization and progeny-production occur from December to February. This fish produces the progenies at several times throughout the spawning season. The number of progenies increases with age, ranging from 10,000 to 20,000 at one time.

The present author tries some biological analysis of *Sebastiscus marmoratus* as the second part of the population study of the coastal fish. 390 specimens were collected during the period from March, 1956 to February, 1957, off Tuyazaki near Fukuoka, from landings mostly caught by gill-net and a few by line and hook. Here, I wish to thanks Professor H. AIKAWA, for his critically reading and commenting on preparing this paper.

1. Growth

The scales of ctenoid type are cleaned by putting in 5 percent solution of potassium hydroxide for about 10 hours and then by washing well. The dried scales held between two slide glasses are presented for observation.

The scale picture is of cutting-over type in both lateral sectors, but rather of concrescent type in the anterior sector. The marks are definable as those comprised zones of wide bands in the anterior sector and corresponding with them, stoppage of ridges concurrently in the lateral ones. Scale-size (R) and mark-size (r) are measured on the longitudinal-axis from the origin of growth (center of nucleus) by means of projector (magnified 20 times).

Otoliths washed with water and cleaned well, are immersed in creosote

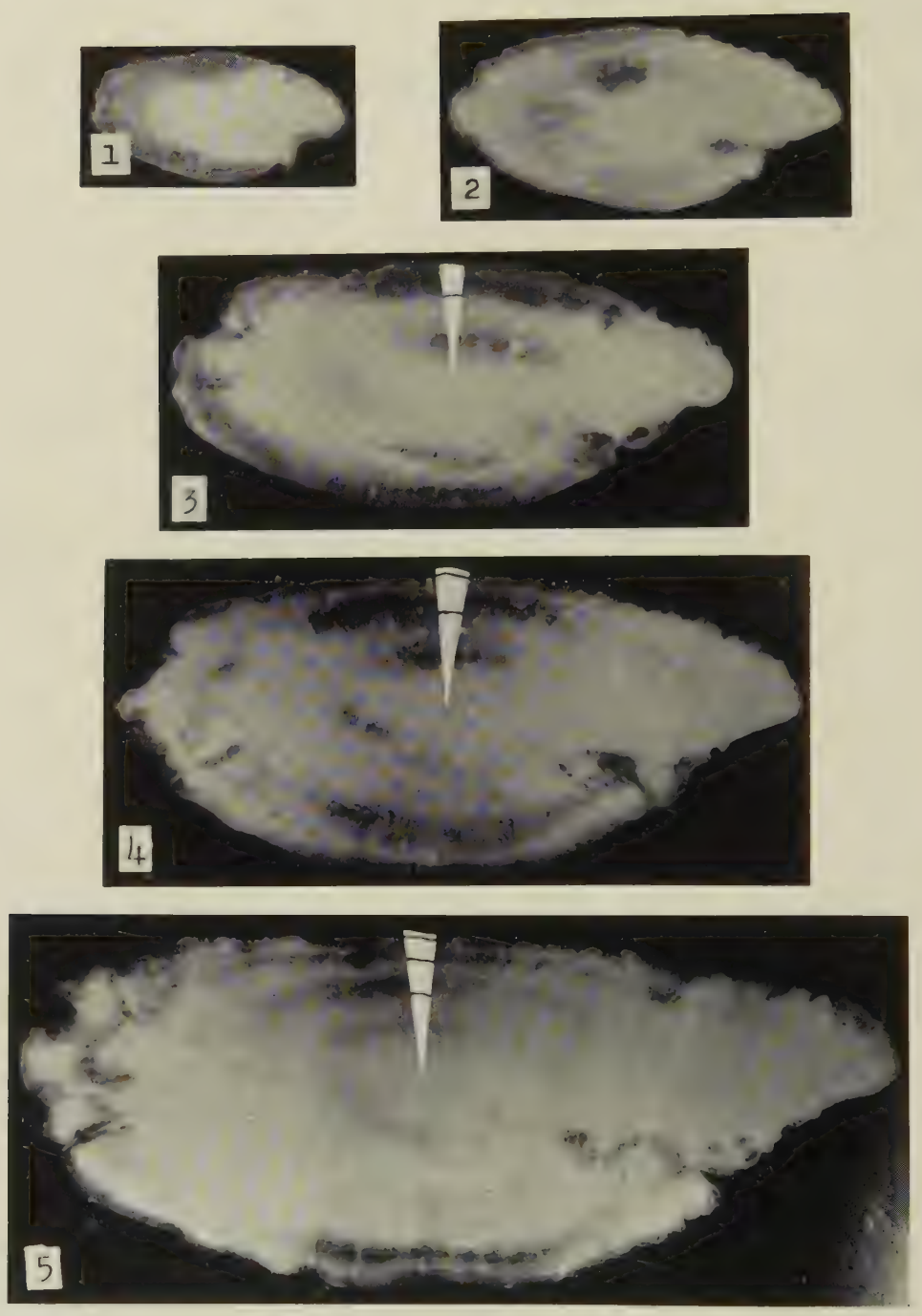

Fig. 1. Photographs of the otolith.

1: Sep., 20, 1956. L=65 mm. 2: May, 17, 1957. L=95 mm.
3: Feb., 26, 1957. L=144 mm. 4: Aug., 7, 1957. L=210 mm.
5: Aug., 7, 1957. L=252 mm.

xylol for about 30 seconds and mounted with Canada balsam on the slide glass. The otolith is elliptical in shape and provided with the transparent and the opaque zones alternately around opaque central portion, all zones running in parallel with margin (Fig. 1). The marks are defined as the bounderies from outer margin of the opaque zone to transparent one. Otolith-size (R) and mark-size (r) are measured from the center of growth in the short axis.

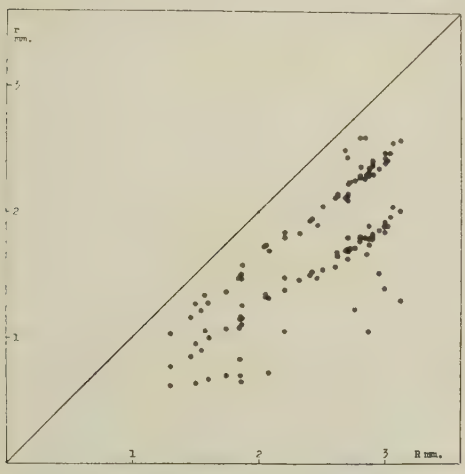

Fig. 2. Similarity of the marks of scale.

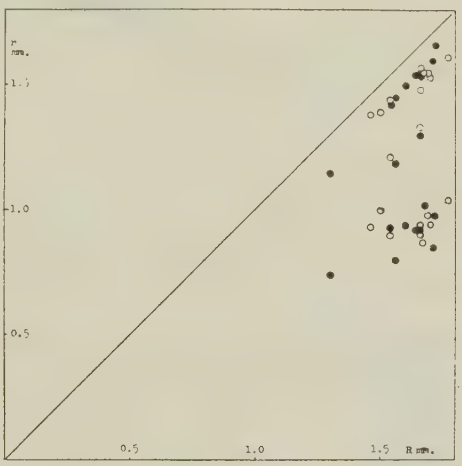

Eig. 3. Similarity of the marks of otolith of nine specimens (150–180mm. in February)

The relationship of scale-size (otolith-size) to mark-size shows similarity (Fig. 2 and 3), being expressed by a linear regression. Here, the otolith-method is used for age determination, since the probability of mark-formation is higher than in scale. The right and left otoliths are equal in the probability of mark-formation (Table 1).

Table 1. The probability of mark-formation.

	No. of specimens	genuine marks		
		I	II	III
Scale	151	0.54	0.91	0.95
Otolith	18	1.00	1.00	—

Although the points of l against R are considerably scattered, relationship of total length to otolith-size (Fig. 4) is approximatly expressed as follows,

$$l = 121.3\,\hat{R} - 40.0 \quad \ldots\ldots\ldots\ldots\ldots\ldots \quad 1$$

All R and r measurments had better be standardized by multiplying with factor, $\hat{R}/R$, because the ssmilarity is recognizable as mentioned above. This

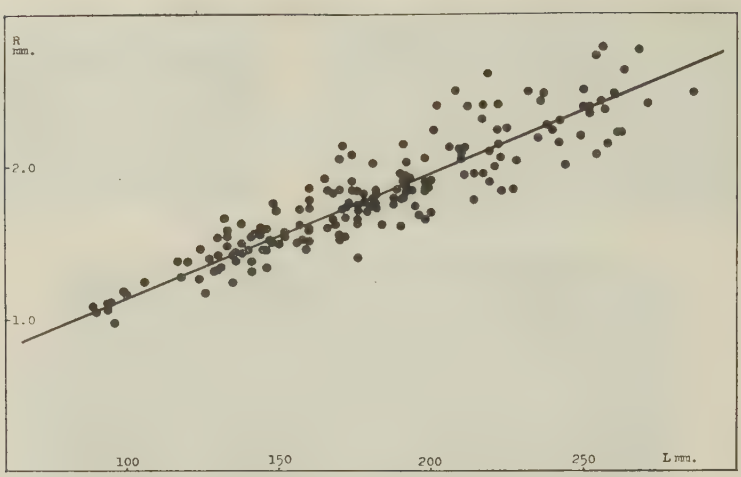

Fig. 4. Relationship of total length to otolith-size.

treatment is also tries here for each different size group in every 10 millimeter unit and the relationship of standardized mark-size to total body length (correspondency) is expressed linearly (Fig. 5, Table 2).

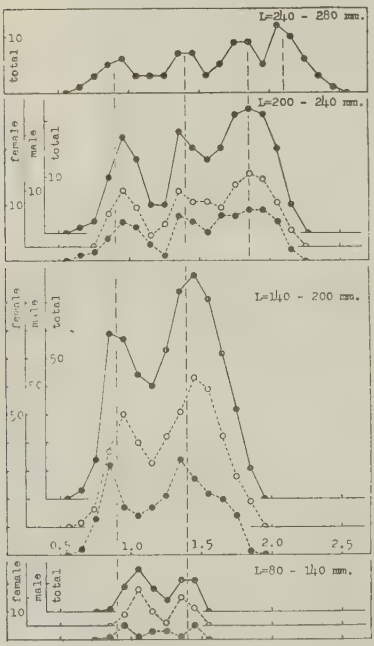

Fig. 5. Correspondency of otolith marks size.

Table 2. Modes of standard mark-sizes in each mark group.

mark-group	r_1	r_2	r_3	r_4
I	1.05 mm.	mm.	mm.	mm.
II	0.85	1.50		
III	0.95	1.35	1·85	
IV	0.95	1.45	1.80	2.15
mode	0.95	1.45	1.85	2.15
(l)	(78)	(138)	(186)	(222)

Lastly following to Walford's graphic method is obtained the equation as below,

$$r_{n+1}=0.78\ r_n+0.7 \quad \ldots\ldots\ldots\ldots\ldots\ldots\ 2$$

Then, these marks are formed at the same time interval. The value of $R-r_1/R$ and $R-r_n/r_n-r_{n-1}=\alpha$ change seasonally, attaining the minimum value in May (Fig. 6).

The height of spawning season is considered in January. Here, l_1 with the first mark (r_1) just formed is not attained in May 5 months after spawned, but in May of next year (after 1·5/12 years). Thus,

puttinng $t=0$ at the spawning time, the equation is given,

$$L_t=345\ (1-e^{-0.256t+0.0768}) \quad \ldots\ldots 3$$

where L_t is the total length after t years since hatched.

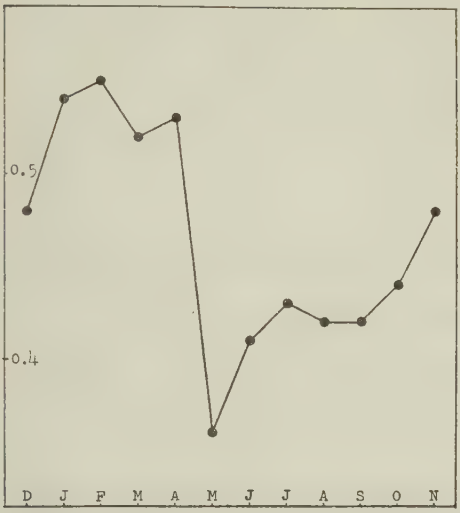

Fig. 6. Monthly changes of marginal growth rate.

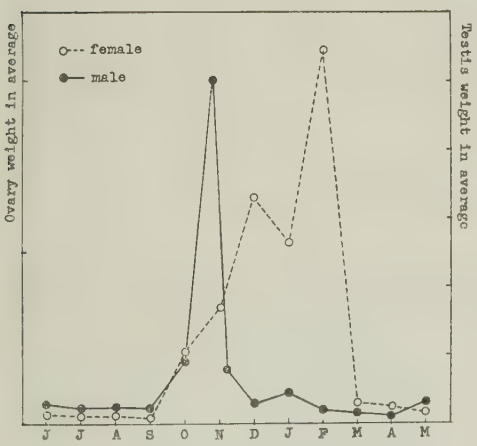

Fig. 7. Monthly changes of the average of gonad weight.

Relationship of body weight to total length is expressed as follow,

$$W=1.76\cdot10^{-2}\cdot L^3 \quad \ldots\ldots 4$$

Hence, the growth of body weight is derived from the equation as (Table 3),

$$W_t=722\ (1-e^{-0.256t+0.0768})^3 \quad \ldots\ldots 5$$

Where the time of the maximum growth rate (T), is 4.50 years ($L_T=$ 228 mm. and $W_T=208$ g.).

Table 3. Total length and body weight at t years after spawning

t	L_t mm.	W_t g.
1	67	5.3
2	122	31.6
3	174	90.0
4	211	165
5	241	245

2. Maturity

Testis weight attains maximum value of 2.5 g. in October, while ovary weight of this ovoviviparous species 21.8 g of maximum in February (Fig. 7).

The right and left ovaries are nearly same in weight and in egg-size composition with each another as a whole, while the latter is different between the egg masses of different portions (Table 4).

The ovaries of type A have one or two modal batches of unfertlized eggs. The first batch of eggs, after fertlized, becomes rapidly larger and embryo develops in egg. Mass of unfertlized eggs becomes again two modal. Such ovaries are of type B. Ovaries of type C are provided with two modes of unfertlized eggs in addition to mass of progenies. Ovaries of type C, just after

Table 4, a. Comparison of egg-size composition at right and left ovary.

Sp. No.	side	egg-size (mm.)			
		-0.2	0.2–0.3	0.3–0.4	0.4–0.5
8	right %		17.5	13.8	9.4
	(d.c.f.)		(13.4–22.0)	(9.9–17.8)	(7.9–12.1)
	left %		20.5	15.7	8.2
	(d.c.f.)		(17.9–24.2)	(12.0–20.0)	(5.8–11.7)
13	right %	15.7	18.1	6.4	1.7
	(d.c.f.)	(12.4–19.3)	(14.7–22.0)	(4.4–9.0)	(0.5–3.0)
	left %	19.8	13.6	6.5	1.1
	(d.c.f.)	(16.0–22.9)	(10.0–16.0)	(4.6–8.8)	(0.1–1.9)

Sp. No.	side	egg-size (mm.)			
		0.5–0.6	0.6–0.7	0.7–0.8	progenies
8	right %		23.7	35.6	
	(d.c.f.)		(18.6–28.0)	(29.8–40.7)	
	left %	0.2	20.9	34.5	
	(d.c.f.)	(0–1.0)	(16.4–25.0)	(29.2–39.0)	
13	right %	19.0	14.2		23.4
	(d.c.f.)	(15.6–23.0)	(11.2–17.9)		(19.1–27.2)
	left %	20.5	12.2		26.2
	(d.c.f.)	(17.1–23.4)	(9.3–15.4)		(22.3–30.5)

Not: Sample No. refer to Table 5.

Table 4, b. Comparison of egg-size compositions between different portions of right ovary.

Sp. No.	portion	egg-size (mm.)					
		0.2	0.2–0.3	0.3–0.4	0.4–0.5	0.5–0.6	0.6–0.7
19	a %	13.0	10.5	8.1	5.0	0.7	
	(d.c.f.)	(12.2–13.4)	(10.0–11.0)	(7.4–8.5)	(4.2–5.4)	(0–2.0)	
	b %	14.8	15.7	11.9	6.6	1.9	
	(d.c.f.)	(14.0–15.2)	(15.0–16.0)	(11.1–12.2)	(6.0–6.8)	(0.9–2.0)	
	c %	23.7	22.0	11.7	5.0	2.0	
	(d.c.f.)	(22.2–25.0)	(21.8–23.4)	(10.4–12.2)	(3.9–5.8)	(1.4–2.4)	
12	a %	21.8	10.9	10.9	13.0	15.6	0.6
	(d.c.f.)	(20.0–23.3)	(9.8–12.0)	(9.8–12.0)	(11.8–14.2)	(14.0–16.8)	(0–2.0)
	b %	20.2	12.1	12.1	12.3	13.2	
	(d.c.f.)	(19.3–21.4)	(11.2–12.8)	(11.2–12.8)	(11.8–13.2)	(12.2–13.8)	
	c %	25.7	15.9	6.4	10.3	14.9	1.2
	(d.c.f.)	(24.1–27.1)	(14.6–17.6)	(5.3–7.2)	(9.4–11.2)	(13.7–16.0)	(0.7–2.0)

Sp. No.	portion	egg-size (mm.) 0.7–0.8	0.8–0.9	0.9–1.0	1.0–1.1	progenies
19	a %	31.3				
	(d.c.f.)	(30.1–32.0)				
	b %	49–2				
	(d.c.f.)	(48.4–50.1)				
	c %	35.7				
	(d.c.f.)	(34.0–37.2)				
12	a %		0.6	4.6	6.7	13.9
	(d.c.f.)		(0–2.0)	(3.3– 5.2)	(5.4–7.4)	(12.8–14.5)
	b %			9.7	8.3	16.2
	(d.c.f.)			(8.6–10.2)	(7.6–9.2)	(15.2–17.2)
	c %			2.5	4.9	18.1
	(d.c.f.)			(1.8– 2.8)	(3.2–5.2)	(17.0–19.8)

the progenies are produced, are similar to ovaries of type A in egg-size composition. Process of egg maturation may probably be repeated at several times during a spawning season. Then, this species, different from *Sebastes inermis*, is multiple spawner (Fig. 8 and 9).

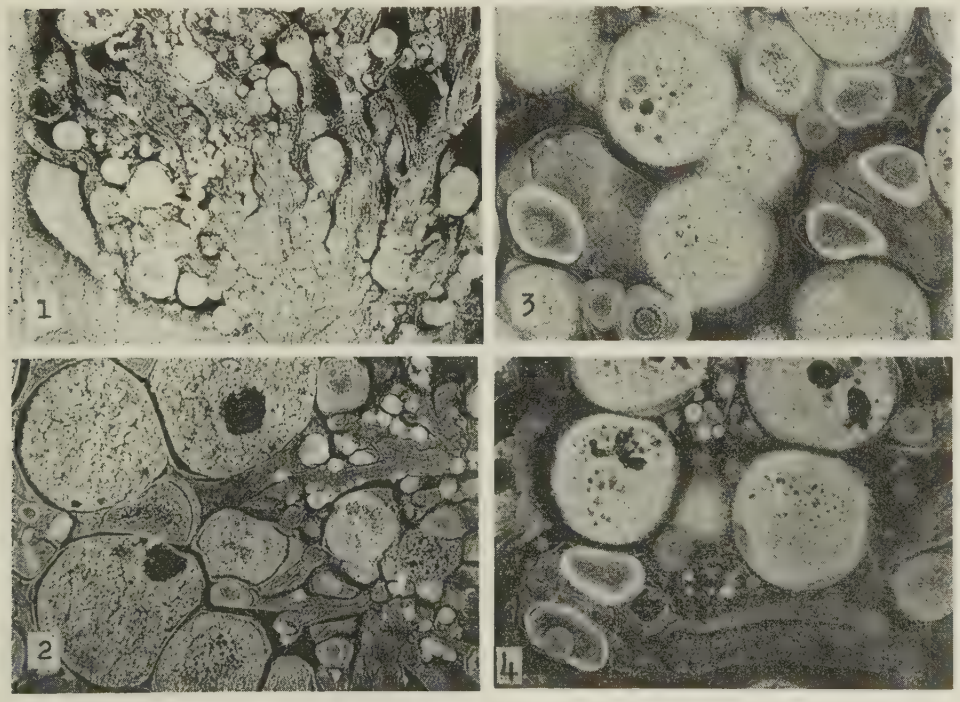

Fig. 8. Photographs of the intra-ovarian eggs of *Sebastiscus marmoratus*.

1: Eggs of immatured ovary in type A.
2: Eggs of matured ovary in type A.
3: Eggs of immatured, matured and advanced embryos in ovary of type B.
4: Eggs and progenies in ovary of type C.

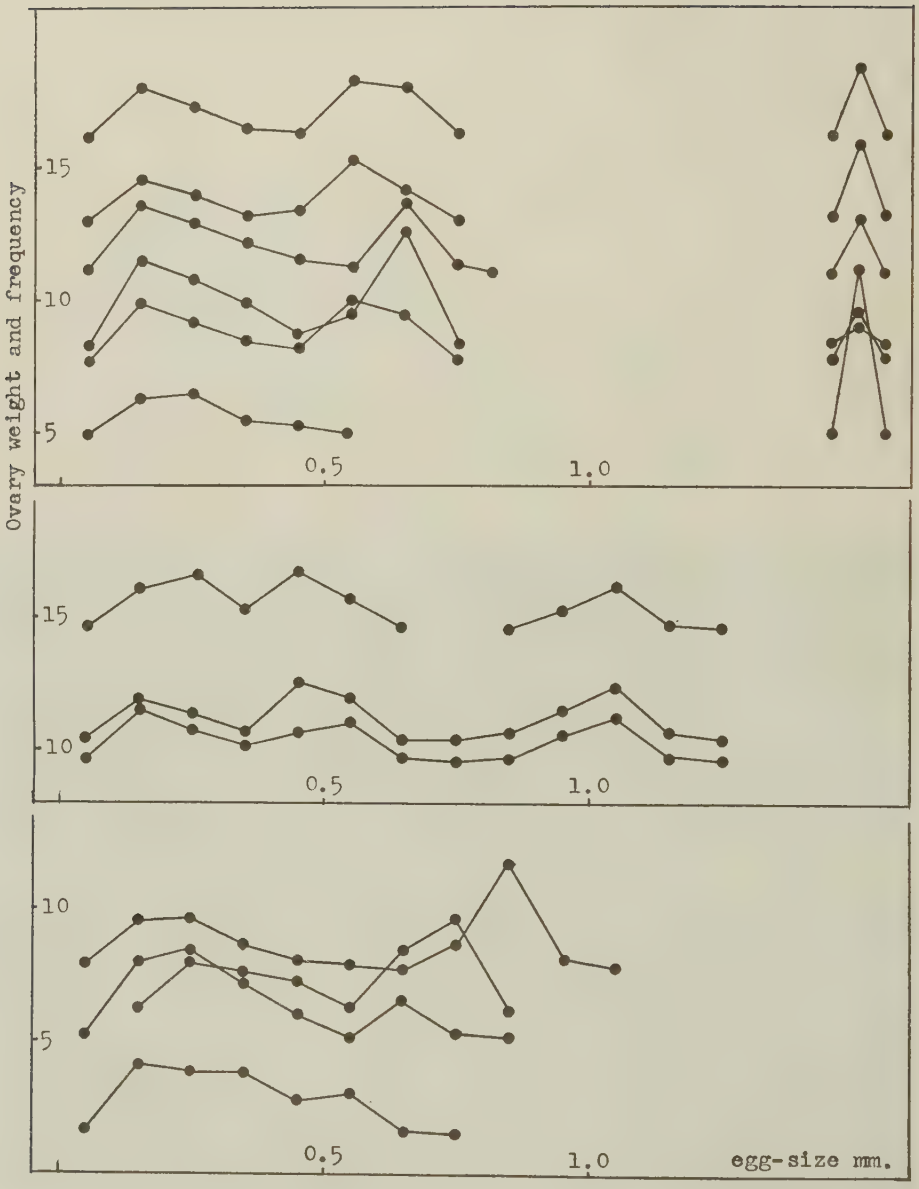

Fig. 9. Relationship of egg-size to gonad weight in each age group.

Table 5. Estimates of ovaries.

Sp. No.	date	length (mm.)	ovary weight	type	age	number of eggs	egg diameter in each mode	
							I	II
1	Dec. 27. '56	154	1.6	A	II	22,375	0.2	0.5
2	Feb. 18. '56	162	8.3	C	II	22,150	0.5	—
3	Feb. 26. '57	144	4.9	C	II	16,300	0.2	—
4	Feb. 18. '57	149	7.7	A	II	35,150	0.2	0.5
5	Feb. 26. '57	155	8.5	A	II	38,345	0.5	0.8
6	Dec. 4. '56	187	9.7	B	III	57,800	0.5	1.0
7	〃	180	10.3	B	III	54,020	0.4	1.0
8	〃	190	6.2	A	III	57,100	0.2	0.7
9	Dec. 27. '56	191	9.1	A	III	60,400	0.7	0.7
10	〃	189	16.2	C	III	57,010	0.2	0.5
11	〃	193	7.8	C	III	33,692	0.2	0.5
12	〃	172	6.7	B	III	21,557	0.5	1.1
13	Feb. 26. '57	179	12.8	C	III	42,560	0.2	0.5
14	Feb. 25. '58	168	7.7	A	III	18,750	0.2	0.8
15	Dec. 4. '56	201	13.6	A	IV	69,800	0.2	0.7
16	Dec. 27. '56	211	14.6	B	IV	70,665	0.2	1.0
17	〃	214	12.9	C	IV	45,940	0.2	0.5
18	〃	217	8.4	C	IV	57,440	0.2	0.4
19	〃	218	10.5	A	IV	29,978	0.2	0.7
20	〃	203	11.2	C	IV	22,515	0.2	0.6
21	〃	234	5.2	A	V	38,000	0.2	0.6

Entire females of 2-age first become functional. The number of progenies increases with age, 10,000 in 2-age, 15,000 in 3-age and 20,000 in 4-age.

Records of Oceanographic Works
in Japan Vol. 5. No. 2,
March, 1960

BIOLOGY OF *Sebastes inermis* CUVIER et VALENCIENNES

By

Shin-ichi MIO

(Fisheries Department, Faculty of Agriculture, Kyushu University)

Summery

This paper presents contributions to the biology of *Sebastes inermis* (C. *et* V.).

For the age-determination can be used the scale and the otolith, and the similarity of mark-size is proved. The relationship of total length (L) to scale-size (R) and also to otolith-size (R) is linear, and each mark-sizes are standardized by L — R equation. The marks are formed periodically on scale in September, while on otolith in April.

The growth of the fish is fitted the Pütter-von Bertalanffy's equation to length data, Buch-Andresen-Fischer's equation to weight data.

This ovoviviparous fish copulates in November and the egg-fertilization and progeny-production occur from December to January. The fish produces the progenies at one time. The sexual maturity is first attained at 2-age and the main spawning group is the 3-age group. The number of progenies is proportional to 5.56 power of total length of mother fish.

The present author tries some biological analysis of *Sebastes inermis* as a part of the population study of the coastal fish, since none of fishery-biological studies about this species has been done. 644 specimens were collected during the period from July, 1955 to April, 1958 off Tuyazaki near Fukuoka, from landings mostly caught by gill-net and a few by line and hook. Here, I wish to thanks Professor H. AIKAWA for his critically reading and commenting on preparing this paper.

1. Age-determination by scale method

The scales of ctenoid type are cleaned by putting in 5 per cent solution of potassium hydroxide for about 10 hours and after then washing well. The dried scales held between two slide glasses are presented for observation.

The scale picture is of cutting-over type in both lateral sectors, but rather of concrescent type in the anterior sector. The marks are definable as those comprised of zones of wide bands in the anterior sector, and concurrently with them stoppage of ridges in the lateral ones (Fig. 1). Scale-size (R) and mark-

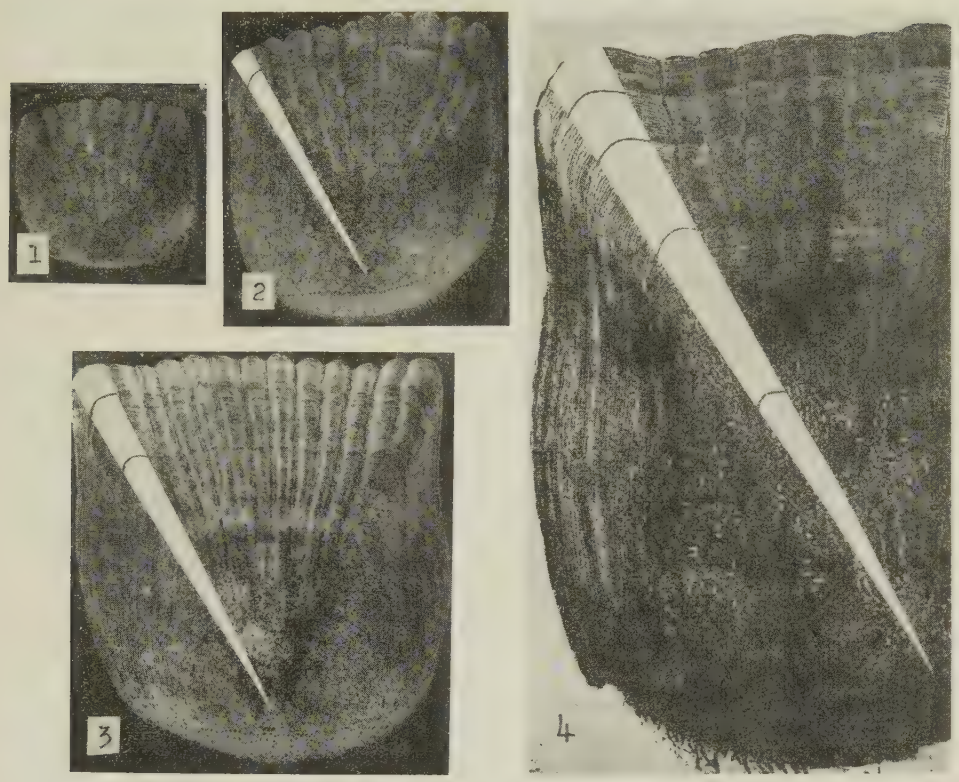

Fig. 1. Photographs of the scales.
1: Apr., 12, 1956. L=105 mm. 2: Jan., 18, 1957. L=142 mm.
3: Jan., 18, 1957. L=165 mm. 4: Sep., 18, 1956. L=238 mm.

size (r) are measured on the longitudinal-axis from the origin of growth (center of nucleus) by means of projector (magnified 20 times).

The relationship between R and r (similarity) is examined for each scale group taken from six different body portions respectively (Fig. 2 and Fig. 3). Although the similarity is well recognizable in every scale group, the

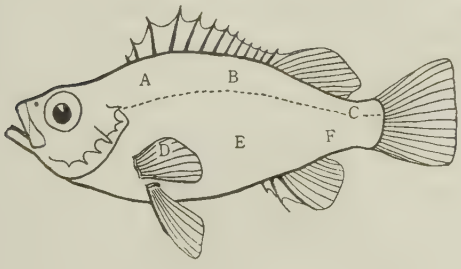

Fig. 2. Body portion sampling scales.

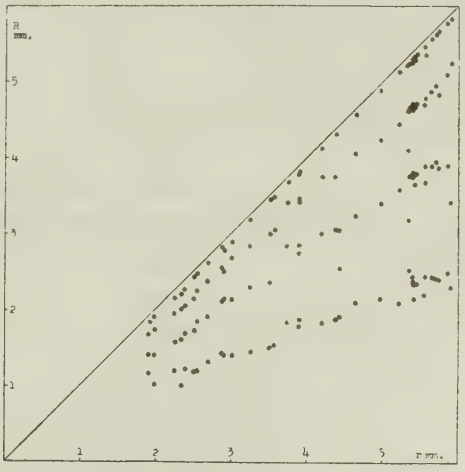

Fig. 3. Similarity of the marks of scales.

probability of mark formation is nearly 1 only among the group taken from portion D but less than 1 among those in other portions, being 0.95 on an average (Table 1). Regenerated scales are very many in every portion, but less in portion D comparative with other portions (Table 2). In addition, it is difficult to measure the scale-size exactly since scales are smaller in these portions than those in portion D and E (Table 3).

Table 1. The rate of the mark-formation in each portion.

Indiv.	Portion					
	A	B	C	D	E	F
1	0.90	0.87	0.95	1.00	0.92	1.00
2	0.90	0.93	0.75	1.00	0.87	1.93
3	0.90	0.93	0.80	1.00	1.00	1.00
4	1.00	1.00	0.90	1.00	0.96	1.93
Mean	0.93	0.93	0.85	1.00	0.94	0.97

Table 2. The rate of the regenerated scale in each portion.

Indiv.	Portion					
	A	B	C	D	E	F
1	0.96	0.98	1.00	0.92	1.00	1.00
2	0.96	0.96	0.78	0.74	0.76	0.90
3	0.84	0.94	0.84	0.66	0.72	0.84
4	0.72	0.82	0.68	0.46	0.74	0.68
5	0.92	0.94	0.82	0.70	0.86	0.94
6	0.72	0.76	0.62	0.52	0.66	0.70
7	0.84	0.64	0.70	0.46	0.82	0.84
8	0.66	0.54	0.64	0.34	0.38	0.70
9	0.68	0.64	0.76	0.36	0.42	0.83
10	0.42	0.64	0.34	0.24	0.58	0.58
Mean	0.77	0.79	0.70	0.55	0.69	0.80

Table 3. The scale-size in each portion.

Indiv.	Portion					
	A	B	C	D	E	F
1	2.41	3.00	3.50	5.64	5.20	4.01
2	2.19	2.66	3.16	4.91	5.56	3.90
3	2.76	3.58	3.31	4.73	5.12	4.16
4	2.90	3.47	3.83	5.68	6.17	3.86
Mean	2.57	3.18	3.45	5.24	5.51	3.99

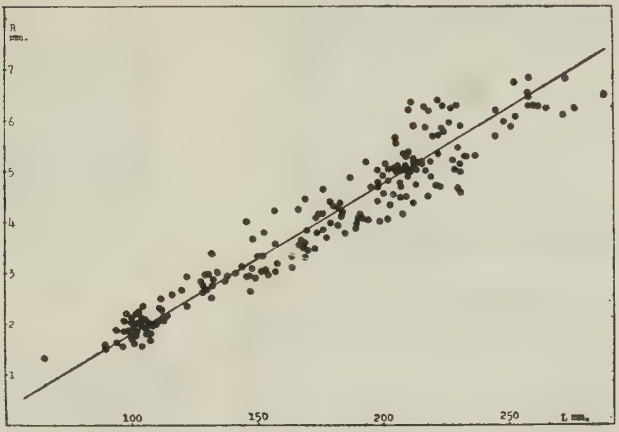

Fig. 4. Relationship of the scale-size to the total length.

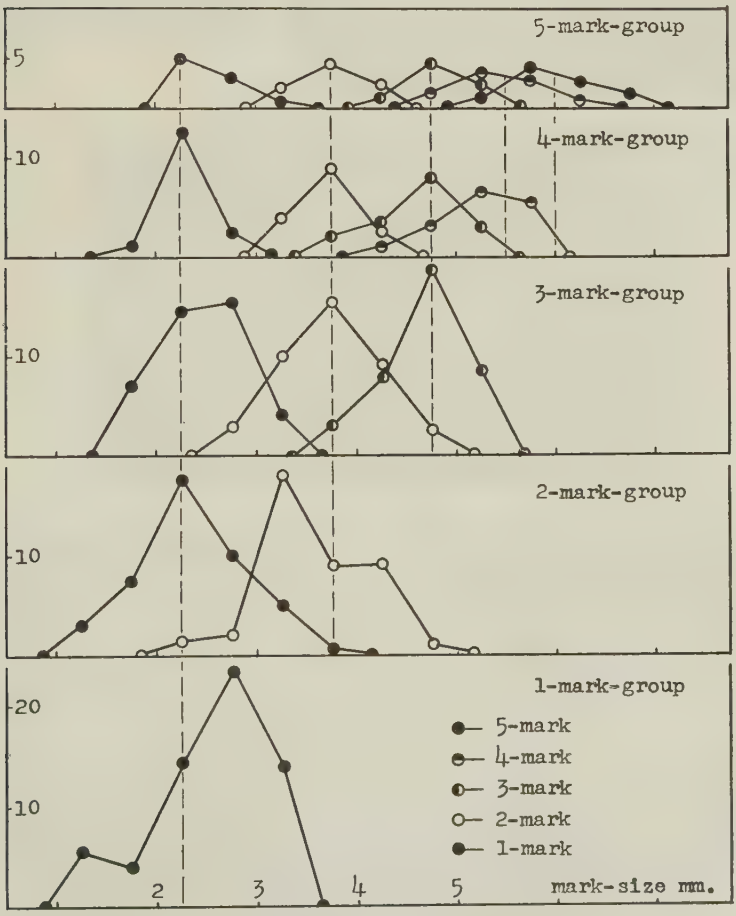

Fig. 5. Correspondency of the mark-size of scale.

Relationship of total length (l) to scale-size (R) is approximately expressed by the equation 1, though the points of l against R are considerably scattered along l-R line (Fig. 4).

$$l = 34.20\,\hat{R} + 37.3 \quad \ldots\ldots\ldots\ldots\ldots\ldots \quad 1$$

All R and r measurements had better be standardized by multiplying with factor, $\hat{R}/R$, because the similarity is recognizable as mentioned above. This treatment is also tried for each mark group and the relationship of standardized mark-size to total length (correspondency) is expressed linearly (Fig. 5 and Table 4).

Table 4. Modes of standard mark-sizes in each mark group (scale method).

Mark-group	r_1	r_2	r_3	r_4	r_5
I	2.75				
II	2.25	3.75			
III	2.50	3.75	4.75		
IV	2.25	3.75	4.75	5.50	
V	2.25	3.75	4.75	5.50	6.00
Mode	2.25	3.75	4.75	5.50	6.00
(l)	(114.3)	(165.6)	(200.8)	(225.2)	(243.0)

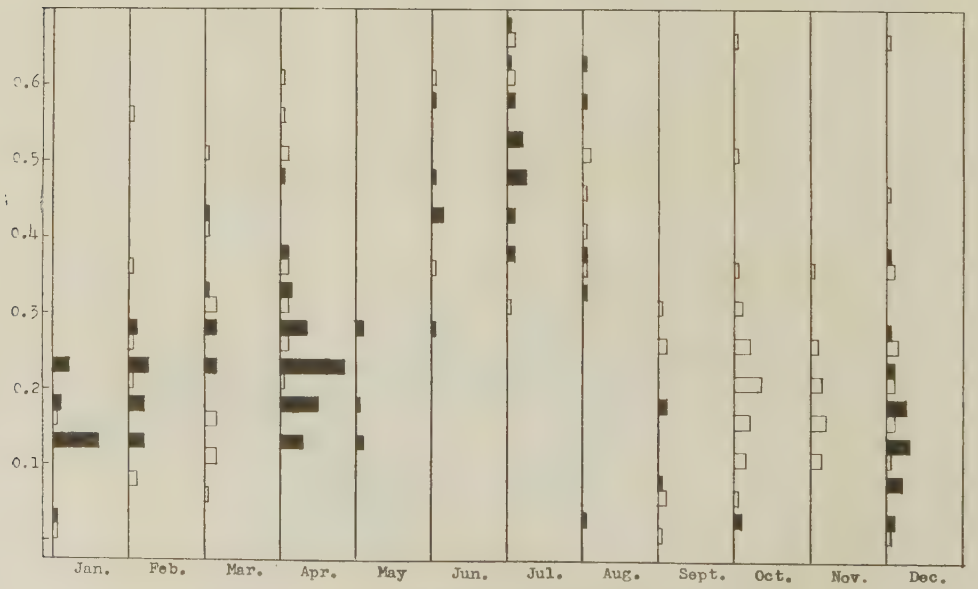

Fig. 6. Monthly changes of marginal growth rate (scale, ■$=R-r_1/R$, □$=R-r_n/r_n-r_{n-1}$).

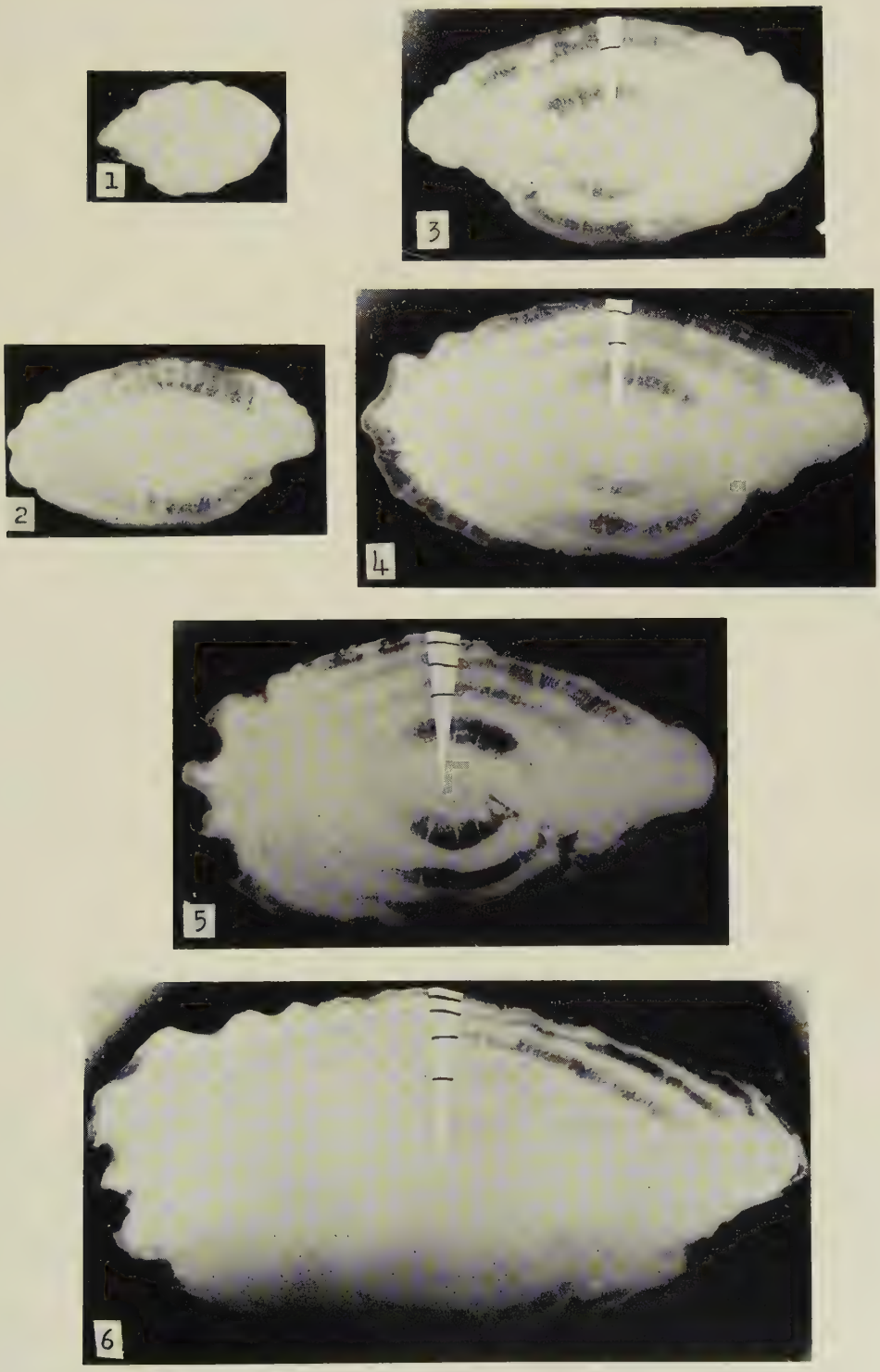

Fig. 7. Photographs of the otolith.

1: May, 3, 1956. L= 37 mm.
2: Mar., 23, 1956. L=148 mm.
3: Mar., 23, 1956. L=168 mm.
4: Mar., 23, 1956. L=197 mm.
5: Mar., 23, 1956. L=240 mm.
6: Feb., 1, 1956. L=253 mm.

Lastly, following to Walford's graphic method is obtained the equation as below,

$$r_{n+1}=0.682\,r_n+2.23 \quad \ldots\ldots\ldots\ldots\ldots\ldots \quad 2$$

Then, these marks are formed at the same time interval. The value of $R-r_1/R$ and of $R-r_n/r_n-r_{n-1}=\alpha$ change seasonaly, attaining the minimum value in September (Fig. 6). The mark is formed in this month every year. The total length, l_n, when the n-th mark is just formed in September, is computable by the equation 1.

2. Age-determination by otolith method

The otoliths washed with water and cleaned well, are immersed in creosote xylol for about 30 seconds and mounted with Canada balsam on the slide glass. The otolith is elliptical in shape and provided with both transparent and opaque zones alternately around opaque central portion, all zones running in parallel with margin (Fig. 7). The marks are defined as the boundaries from outer margin of the opaque zone to transparent one. Otolith-size (R) and mark-size (r) are measured from the center of growth on the short axis.

Relationship of otolith-size to the mark-size among the available

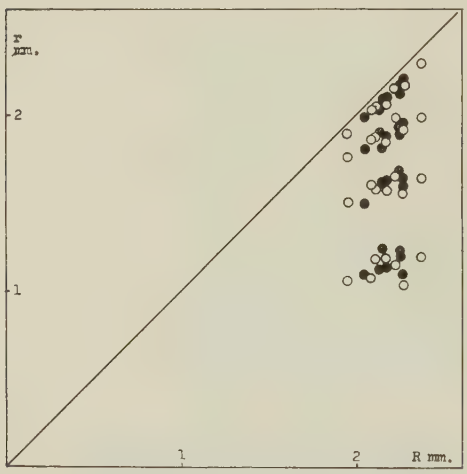

Fig. 8. Similarity in the marks of the otolith of seven specimins (220–241 mm.)

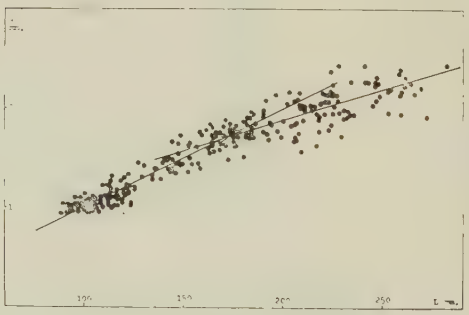

Fig. 9. Relationships of the otolith-size to the total length.

specimens (210–241 mm. in February) are quite similar between left and right otoliths (Fig. 8). Relationship of r to R is expressed approximately in a linear regression, showing similarity.

Relationships of total length to otolith-size are expressed by the following two equations (Fig. 9).

$$l=81.3\,\hat{R}-2.5 \quad \ldots\ldots \quad 90<l<170 \quad \ldots\ldots\ldots \quad 3$$

$$l=132.4\,\hat{R}-108.2 \quad \ldots\ldots \quad 170<l \quad \ldots\ldots\ldots\ldots\ldots \quad 4$$

Then, all the measurements of mark-size are standardized by factor, $\hat{R}/R$. Correspondency is expressed as linearly as that in scale method (Fig. 10 and Table 5).

Table 5. Modes of standard mark-size in each mark group (otolith method).

Mark-group	r_1	r_2	r_3	r
I	1.25 mm.	mm.	mm.	mm.
II	1.30	1.95		
III	1.30	1.95	2.25	
IV	1.30	1.80	2.20	2.45
Mode	1.30	1.95	2.25	2.45
(l)	(103.3)	(156.3)	(189.8)	(216.0)

The standardized mark-size are tested by Walford's graphic method and equation below is obtained.

$$r_{n+1}=0.673\ r_n+0.973 \quad \ldots\ldots\ldots\ 5$$

It is cleared here that the marks are formed at every same time interval. By tracing the seasonal changes in the marginal growth rate, the marks are formed in April every year (Fig. 11).

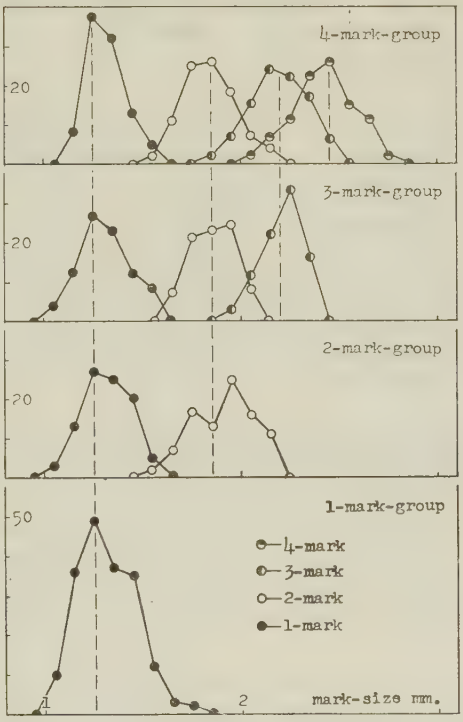

Fig. 10. Correspondency of the mark-size of otolith.

3. Growth

The sizes of total length, L, (see Table 4 and 5) obtained by the scale and otolith method are tested together by Walford's graphic method and expressed by a equatiou as below,

$$L_{n+1}=0.698\ L_n+85.3 \quad \ldots\ldots\ 6$$

The height of spawning season is considered in December. Here, l_1 with the first mark just formed is not attained in September or April in 0-age but in these month of 1-age. Thus, putting $t=0$ at the spawning time, the growth in length is given as,

$$L_t=283\ (1-e^{-0.359t+0.1058}) \quad \ldots\ldots\ldots\ 7$$

Where L_t is the total length after t years since spawned, and two equations are nearly equal to each other.

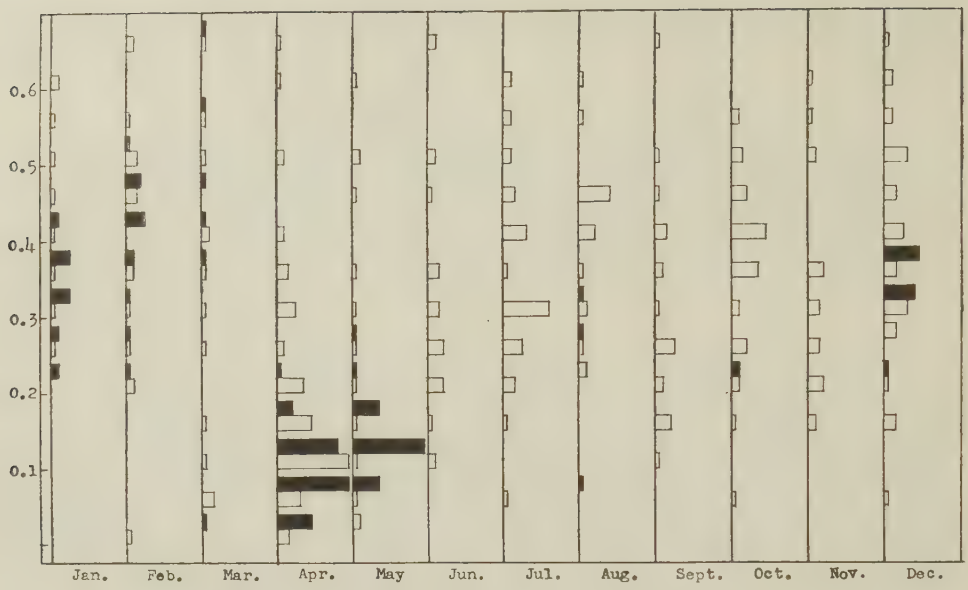

Fig. 11. Monthly changes of marginal growth rate (otolith, ■$=R-r_1/R$, □$=R-r_n/r_n-r_{n-1}$).

Relationship of the body weight to the total length is approximately,

$$W=1.77\cdot10^{-2}\cdot L^3 \quad \ldots\ldots\ldots\ldots\ldots\ldots \quad 8$$

Hence, the growth of body weight is derived from the equations 7.

$$W_t=402\ (1-e^{-0.359t+0.1058})^3 \quad \ldots\ldots\ldots\ldots \quad 9 \quad (L_T=189\ \text{mm.})\ (W_T=120\ \text{g.})$$

Where the time of the maximum growth rate (T) is 3.35 years.

Table 6. Total length and body weight at t years after spawning.

t	L_t mm	W_t g.
1	63	4.5
2	130	39.2
3	176	96.0
4	208	159
5	231	218

4. Maturity

The testis weight attaines maximum (2.1g) in November, while the ovary weight of this ovoviviparous fish in December (Fig. 12).

The right and left ovaries are nearly equal in weight and just same in egg-size compositions which do not differ between the egg-masses of different portions. Small samples can be taken from any portion to estimate the total number of intra-ovarian eggs with Hensen's method.

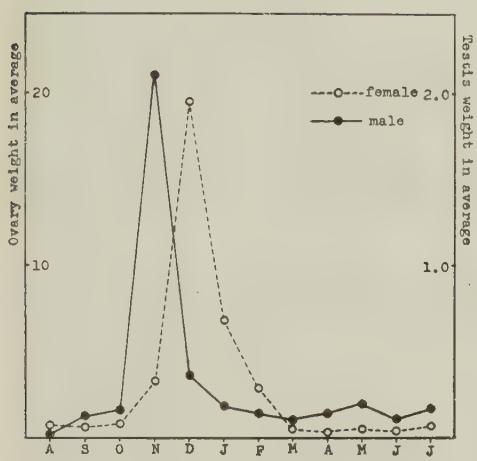

Fig. 12. Monthly changes of gonad weight in average.

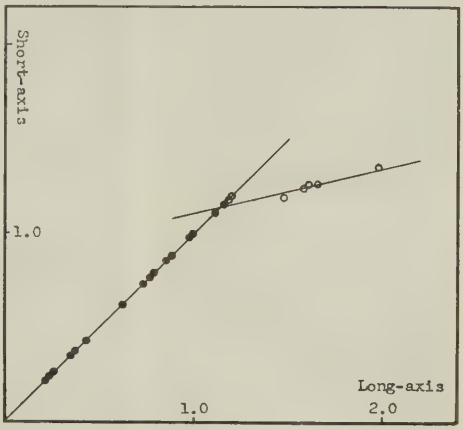

Fig. 13. Rationship of major axis to minor axis.

Table 7. Comparison of egg-size composition at each portion.

Sample No.	Portion (left ovary)			Portion (right ovary)		
	A	B	C	A'	B'	C'
3	0.97±0.33	0.99±0.22	1.02±0.39	0.96±0.38	0.95±0.25	0.98±0.33
2	1.00±0.18	0.89±0.17	0.97±0.20	0.99±0.18	0.98±0.17	0.98±0.19
1	0.98±0.27	1.00±0.15	0.99±0.21	0.99±0.19	0.99±0.24	0.98±0.23
18	1.11±0.15	1.09±0.26	1.11±0.22	1.12±0.25	1.12±0.20	1.12±0.26
20 major axis	1.52±0.89	1.48±1.02	1.50±0.68	1.45±0.51	1.51±0.67	1.45±0.51
20 minor axis	1.09±0.36	1.18±0.45	1.21±0.39	1.18±0.33	1.22±0.37	1.17±0.45

Note: Sample No. refer to Table 9.

Egg-mass of developmental phase, showing an unimodal distribution, appears first at the end of October and grows rapidly. Eggs of developmental phase are spherical in shape when they are smaller than 0.8 mm. in diameter. Eggs above 0.8 mm. in diameter, become ellipsoidal and attain 2.0 mm. in major axis and 1.4 mm. in minor axis just before hatching out (Fig. 13). Thus, entire intra-ovarian eggs of developmental phase become ripe and progenies produced at one time. As a functional females appears first among 2-age group, greater than L_2, but fur smaller than L_T (199 mm.) (Fig. 14 and 15).

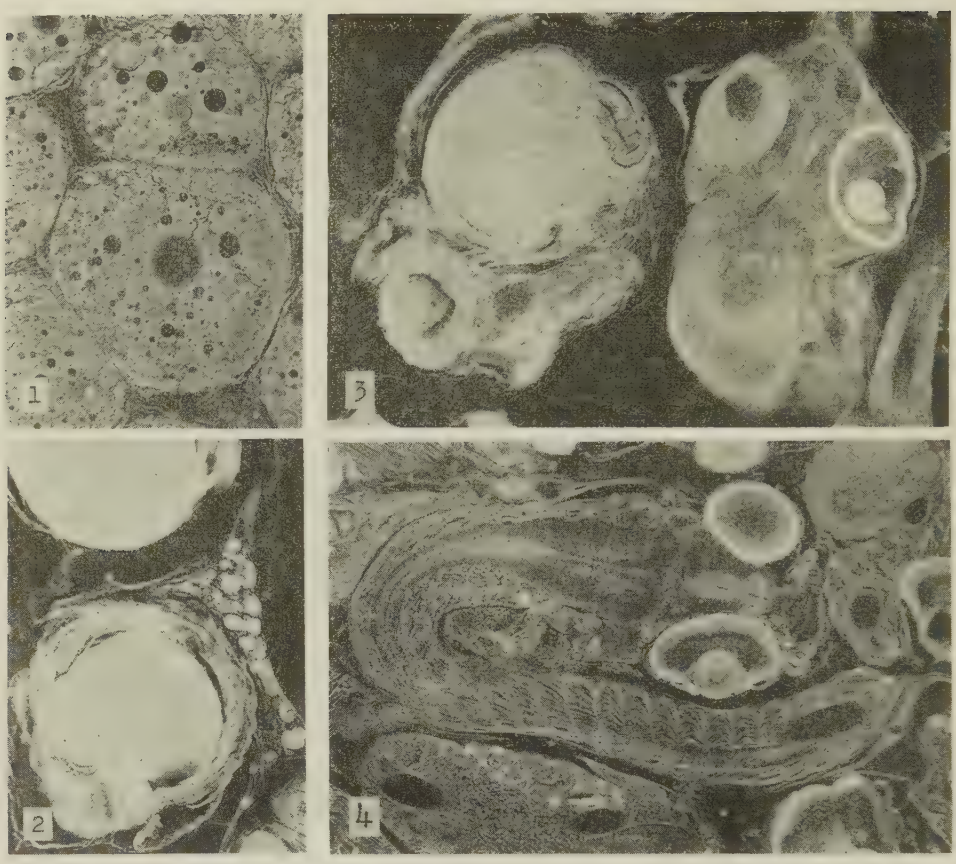

Fig. 14. Photographs of the intra-ovarian eggs of *Sebastes inermis*.
1: Matured eggs in ovary.
2: Fertlized eggs in ovary.
3: Eggs of advanced embryonic stage.
4: Progenies in ovary.

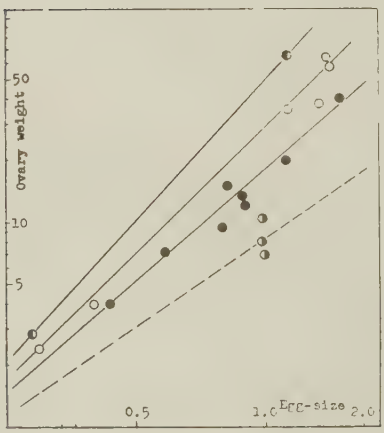

Fig. 15. Relationship of egg-size to gonad weight
◑; 2-age, ●; 3-age,
○; 4-age ◐; 5-age

Tobe 8. Estimate of ovary.

Sample No.	Date	Length	Ovary weight	Age	Number of eggs	Mean of egg diameter
1	Dec. 27. '56	166 mm.	7.0 g.	II	9,750	0.99 mm.
2	〃	167	10.5	II	8,834	0.98
3	〃	172	8.0	II	12,555	0.98
4	Dec. 4. '56	158	0.2	II	3,740	0.21
5	Dec. 27. '56	199	20.0	III	33,000	1.15
6	〃	210	42.2	III	24,000	1.65
7	Dec. 4. '56	198	12.0	III	25,650	0.88
8	〃	206	15.4	III	33,000	0.77
9	〃	210	9.5	III	31,150	0.74
10	〃	204	1.0	III	18,060	0.37
11	〃	212	13.7	III	35,000	0.86
12	Nov. 19. '56	199	7.2	III	57,168	0.62
13	Nov. 3. '56	206	4.0	III	39,284	0.42
14	〃	213	2.4	III	27,600	0.25
15	Nov. 9. '56	232	3.9	IV	71,040	0.37
16	Dec. 4. '56	233	14.4	IV	41,500	0.77
17	Jan. 18. '57	216	15.4	IV	7,425	1.14
18	〃	222	23.2	IV	15,200	1.11
19	〃	210	36.0	IV	20,350	1.18
20	〃	224	36.6	IV	19,555	1.48
21	Dec. 27. '56	230	58.5	IV	27,850	1.60
22	〃	230	64.0	IV	43,850	1.58
23	Nov. 9. '56	240	2.8	V	72,820	0.24
24	Jan. 18. '57	232	10.1	V	2,491	1.97
25	Dec. 27. '56	234	67.2	V	62,300	1.17

Relationship of the number of intra-ovarian eggs to the total length is

$$E = \frac{1}{8.37} \cdot L^{5.56} \quad \ldots\ldots\ldots\ldots\ldots\ldots \quad 10$$

The number of progenies is 9,000 in 2-age, 30,000 in 3-age and 40,000 in 4-age. Spawning groups, from 2-age to 4-age groups, comprise dominantly 3-age group.

Records of Oceanographic Works
in Japan Vol. 5, No. 2,
March 1950

An Ider on the Maximum Permissible Concentration of Radio-active Materials in Sea-water

By
Yoshio HIYAMA
(Prof. University of Tokyo)

INTRODUCTION

With regard to the maximum permissible ionizing radiation dose-rate for the human body, the International Commission on Radiological Protection (I.C.R.P.) has made Recommendations not only for the exposure dose-rate but also for the total body burden, as well as the amount of daily intake through air and water for various kinds of radio-nuclides. In some countries legislation along this line to limit the total effects of radiation from various sources within the country has already been established or proposed. This kind of control can be accomplished either by monitoring the radiation level directly or by the chemical analysis and radioassay of the various materials taken in by the people of the country.

Even assuming that technical developments in the disposal of waste radio-active materials in the sea could limit the amount of flow-out of these materials into the food-producing parts of the ocean to some degree, if the possibility of contamination of the food-producing areas still existed, it would be necessary for the sound and economical development of atomic energy utilization in the future to reserve a share of the total national permissible radiation dose for internal radiation exposure by radio-nuclides of marine origin. This would be particularly the case in those countries which geographically are oceanic islands, where marine products are important in the national diet and where the adjacent seas are likely to be used internationally as important places for waste disposal.

The author in the present paper has tried to find a relationship between the level of sea-water contamination by several radio-nuclides and the level of radiation dose-rate inside the human body caused by these radio-nuclides of marine origin, using the Recommendation of the I.C.R.P. and the few data on the chemical analysis of sea water and of the human body presently available

* The idea of this paper was spoken by the author in Symposium 'Radiation Effects to Human in Atomic Age' by Japan Science Council, 1958. This paper was wrote early 1959 to contribute to this publication after that. The similar content was read by the author in 'Scientific Conference on the Disposal of Radio-active Wastes' by IAEA and UNESCO in Monaco, November 1959.

to the author. However, even if the idea of this calculation were to be recognized by scientists in the fields of oceanography, public health, nutrition, radiation biology, and others, it would still be necessary to get further data on the amounts of trace elements in sea water, in marine products, and in the human body in order to complete a table of the maximum permissible concentrations in sea water of various radio-nuclides. Here the idea is merely advanced and a few examples are described.

RADIO-NUCLIDES

As it is difficult to get the necessary data for determining the maximum permissible concentrations in sea water for all of the nuclides included in the Recommendation of the I.C.R.P., it may be wise to start with some radio-nuclides which are important in view of the character of the waste and their effect on public health. The evaluation of the importance of radio-nuclides in this sense cannot be made merely on the basis of the amount of discharge and the speed of decay. In addition consideration should be given to the fact that some elements are concentrated more than others from sea water by marine organisms and from marine products by the human body. Furthermore, in the estimation of physical decay from the time of discharge to the time of human intake, the period of preservation and storage of the marine products, which possibly differs according to national food habits, must be considered in addition to the period of time required for the physical and biological transmission of the materials from the place of discharge to the food-producing zone of the sea. The speed of uptake of radio-nuclides from the environmental sea water is higher in micro-organisms, which also collect nuclides adhering to the body surface, than in macroorganisms. The latter, which generally have more value as human food than the former, are contaminated either by intake of macroorganisms or by direct material exchange through the gill membranes to and from the sea water. The time required to get equilibrium between the sea water and the body of a fish varies according to the nature of the element and the physiological activity of the fish. Numerous experiments have shown that this time is rarely on the order of several hours but commonly several days or weeks. Thus short-lived radio-nuclides, with half-lives of less than a day, cannot enter into consideration for this problem.

The radio-nuclides known to the author as having been hitherto discovered in marine products made from organisms living in contaminated water are as follows: ^{90}Sr, ^{137}Cs, ^{60}Co, ^{65}Zn, ^{144}Ce, Cd*, Fe*, ^{131}I, ^{103}Ru, ^{99}Mo, ^{140}Ba, and ^{140}La.

SEA-WATER TO MARINE ORGANISMS

Continuous liquid waste disposal will give rise to a characteristic pattern

of the distribution of concentration through the action of currents. Solid waste disposal to deep bottoms would also give rise to a characteristic pattern due to the effects of currents and the rate of flow-out. In both cases the distribution of contamination and its concentration in food-producing parts of the sea must be under constant survey to supply information needed for public health considerations. However, it is much more expensive and technically difficult to survey the bottom in deep waters than to survey shallow bottoms or surface areas.

In considering the quantitative equilibrium between sea water and marine organisms, it must be noted that there are some variations in the physiological behavior of the elements. Most of the elements maintain rather constant concentrations in any given part of the organism under normal physiological conditions, without showing any correlation with their concentrations in the environmental water. These are elements that are considered to be necessary to the maintenance of the normal physiology of the organism. On the other hand, there are some elements whose place can be taken by other elements of similar chemical character, when the concentrations of these elements in the environmental water varies. In both cases the *concentration factor* [1], a ratio of the concentration in the organism to the concentration in the sea water, is available with a certain degree of accuracy like that of the relation between radiation dose and the biological effects, because the oceanic sea water has a rather constant concentration of almost all of the elements normally contained in it. In the latter case the *discrimination factor* or *observed ratio*[2] provides a convenient way to see the relation of relative concentrations between one step (e.g. the environmntal medium) and the next step (e.g. the organism) in any biological procedure, when the concentration of a rare element is obtained as a ratio to the amount of a commoner and similar element, for example, the amount of Sr in that of Ca. However, in the case of sea water to marine organisms it is not necessary to get the discrimination factor in order to see the quantitative equilibrium, because normal oceanic water has rather constant constituents. Thus the concept of the *concentration factor* is more convenient for denoting the quantitative equilibrium between sea water and marine organisms.

However, there are a few other elements, like Pu in animal intake, that would accumulate in a part of the body by continuous uptake from the environment. For this type of element, neither the *concentration factor* nor the idea which the author is going to introduce here can be applied.

SEA-WATER EQUIVALENT FOR DAILY HOMAN INTAKE

The level of contamination of a marine organism by a certain radio-nuclide can be computed by the *concentration factor*, if the concentration of the radio-nuclide in the environmental sea water has been ascertained, and if the organism

has remained in it long enough to come to equilibrium. If human beings took only one single species of marine organism as food, the maximum permissible concentration for sea water could be obtained simply by extending the idea of the *concentration factor* up to the human body. We are, however, in actuality taking in various kinds of marine products in various amounts. Moreover, some elements which we require for normal physiology are taken in mineral form. without passing through the biological process, as for example NaCl as marine table salt in Japan. Therefore, in order to determine the maximum permissible concentration for sea water, we need a more comprehensive view than is provided by the *concentration factor**. The author's idea on this is as follows.

For some elements, we already know the average amount of daily intake by one person (I g per day person) and the fraction of it which originates from either sea water or marine organisms (M). If the concentration of that element in sea water (S g per l) is known, the *Sea Water Equivalent for Daily Human Intake* (Wd l per day per person) can be obtained by the following formula:

$$Wd = M \times I/S \quad \ldots\ldots (1)$$

As the Recommendation of the I.C.R.P. has a table of the maximum permissible concentrations for drinking water based upon the average volume of daily intake by a single person as 2.2 l, if Wd could be 2.2 l for all of the elements, then the maximum permissible concentration which the author is trying to establish for sea water could be exactly the same as the I.C.R.P.'s maximum permissible concentration for drinking water. But this only happens coincidentally with a few elements. Taking NaCl (table salt) as a simple example, 15 g is known to be roughly the average intake per day per person. In some countries rock salt is used as table salt, but in Japan almost all of the salt consumed by human beings is of marine origin. As the Cl concentration in sea water is 18 g per l, and that of Na is 10 g per l, Wd for Cl is 2 l, and for Na is 1.6 l. For this reason, the maximum permissible concentration for sea water can not be the same as that for drinking water.

The Recommendation of the I.C.R.P. has a table of the maximum permissible amounts of daily intake for numerous nuclides (MPDI micro-curie per day per person). From this the maximum permissible concentration of a certain radio-nuclide in sea water (MPCS micro-curie per l) can be obtained as follows:

$$MPCS = MPDI/Wd \quad \ldots\ldots (2)$$

---

*After this is printed, the author could read 'Radioactive Waste Disposal into Atlantic and Gulf Coastal Waters' published by US National Academy of Sciences-National Research Council, Publication 655, 1959. There is a chapter, p. 26, on permissible concentration of radioisotopes in sea-water. As this method is based merely upon the concentration factor, the author's method is considered to be better by the reason here mentioned.

Taking ^{24}Na as an example, as the MPDI for this radio-nuclide is 1.76 micro-curie per day person, the MPCS is 0.11 micro-curie per *l*, while the maximum permissible concentration in drinking water, according to the I.C.R.P.'s 1954 Recommendation, is 0.8 micro-curie per *l*.

However, to get the MPCS for a large number of radio-nuclides, comparable to those covered in the I.C.R.P. table, would take a long time, even if much effort could be concentrated on the task, for at the present moment our information of figures of I for many nations (or international averages) is poor. There is, however, another way to obtain the MPCS, as follows.

SEA-WATER EQUIVALENT FOR THE HUMAN BODY

In the case of elements for which little is known about I but for which the average amount of the element in an individual human body (B g) or in the critical organ (Bc g) is available (see Tipton et al. (3)), the *Sea Water Equivalent for the Human Body* (Wd *l*) or *for the Critical Organ* (Wbc *l*) can be obtained as follswos:

$$Wb = M \times B/S \quad \ldots\ldots\ldots (3) \quad \text{or} \quad Wbc = M \times Bc/S \quad \ldots\ldots\ldots (4)$$

Then the I.C.R.P. Recommendation can be used to get the maximum permissible total body burden (MPTB micro-curie) and that in the critical organ (MPBC micro-curie) for various radio-nuclides. Then the MPCS can be obtained as followos:

$$MPCS = MPTB/Wb \quad \ldots\ldots (5) \quad \text{or} \quad MPCS = MPBC/Wbc \quad \ldots\ldots (6)$$

APPLICATION OF MPCS

When the maximum permissible concentration of a radio-nuclide in sea water obtained in this way is to be applied to a real case of ocean contamination, it is important to know whether or not the nation is actually exposed to other radiation sources which should be considered along with this one from the standpoint of public health. If such other sources exist or are expected to exist at some future time, the maximum permissible radiation dose-rate caused by internally existing radio-nuclides of marine origin must be held to a reasonable fraction of the total, and accordingly the MPCS must be reduced proportionally.

Leaving external radiation and contamination through the air surrounding the human body out of consideration, we must also think of the situation on the land in considering the entire human food contamination, as not all human food is of marine origin. The MPCS obtained by the two methods described in the preceding section is valid only for circumstances where the sea alone is contaminated but the land is not. In cases where the land is also contaminated or expected to be so, as more of the materials in the human body originating

from the land than from the sea, some reasonable maximum permissible concentrations of radio-nuclides in the soil must be considered, and the MPCS must be reduced to a reasonable level accordingly. However, as the composition of the soil varies so greatly from one locality to another, and as carrier free contamination so often occurs in plants, it is hard to obtain the maximum permissible concentrations of radio-nuclides in the soil in general. Though it is possible, leaving carrier free contamination out of consideration, to get a figure for a particular type of soil, it is almost impossible to get a general equilibrium value between the soil and the human body, except in some particular case, because the foods that human beings consume come from various localities with various types of soil. Therefore, foods originating on land must be monitored constantly by chemical analysis and radio-assay in order to know the level of their contribution to contamination of the human body.

The modification of the MPCS to apply in cases where the radioactive contamination also extends to the land is only possible provided that the isotopic

Table I.

	MP TB μc	B μg	M	S μg/ℓ	WB ℓ	WB′ ℓ	MPCS μc/ℓ	MPCS μc/ℓ
$^{90}Sr+^{90}Y$	0.1 (Bone)	450,000 (10)	6.0	7,000	40	65	15×10^{-3}	9×10^{-3}
$^{137}Cs+^{137}Ba$	0.1			0.5				
$^{144}Ce+^{144}Pr$	0.1			0.4				
$^{106}Ru+^{106}Rh$	0.4							
^{60}Co	0.3 (Liver)	0.19 (Stomach, Diaphragma) 0.16 (Aorta Intestine) (100)						
^{55}Fe	100							
^{59}Fe	1.3 (Blood)	300 (Spleen) (10)		10				
^{99}Mo	1.7 (Bone)	0.89 (Liver) (10)		10		0.09		19
^{144}Cd								
^{65}Zn	40 (Bone)	180 (Prostate) (10)		10		18		2.2
^{131}I	0.06 (Thyroid)			50				

dilution ratio([4]) is similar in foods from both land and sea. Then the modified MPCS (MPCS') can be obtained by removing M from the formulae (1), (3) and (4), as follows:

$$MPCS' = MPCS \times M \quad \ldots\ldots (7)$$

$$Wd' = Wd/M \quad \ldots\ldots (8)$$

$$Wbc' = Wbc/M \quad \ldots\ldots (9)$$

Actually, for many elements adequate values of M are not yet known. Therefore it is easier to get MPCS' than to get MPCS at present.

The following table shows MPCS values and the data for calculations by formulae (3) to (9) for some important radio-nuclides. This table shows little beyond the need for more data on this subject.

NOTE

The figures in brackets under column B are the rounded values of the ranges of variation of B obtained from the table of Tipton et al., and the smaller the figure is the more constantly the level of the element is maintained in the human body in normal physiology. This range of variation must be considered in evaluating the accuracy of the average of B to obtain MPCS.

It must be noted that the MPCS obtained here is the concentration of the radio-nuclide in sea water necessary to bring the internal radiation in the human body to the permissible dose-rate level when equilibrium has been established between the sea water and the human body through a sufficiently long period of continuous intake of marine products. Therefore, this idea cannot be applied either to temporary contamination of the sea nor to partial contamination of certain areas. In these cases, examination of the marine products can supply the data to show their contribution to internal radiation in the human body.

Very often actual contamination of the sea is due to radio-nuclides of more than one kind. As the total internal radiation in a critical organ is what we are interested in, if more than one of these radio-nuclides accumulate in the same critical organ, the total maximum permissible radiation dose-rate must be properly apportioned to each of the nuclides.

Finally, the author wishes to point out again that the maximum permissible radiation dose-rate for a human being must not be assigned completely to this source alone, but some part of it must be reserved for other possible future needs with respect to other radiation sources.

LITERATURE

(1) The Effects of Atomic Radiation on Oceanography and Fisheries. 1957. U.S. National Academy of Science. Publication No. 551.

(2) Report of the UN Scientific Committee on the Effect of Atomic Radiation. 1958 pp. 102-108.

(3) Tipton, L. H. & others:— Spectrographic analysis of normal human tissues. ORNL. Central File Number, 56-3-60, 1956, 57-2-2, 57-2-4, 57-11-23, 1957, 58-10-15, 1958.

(4) Hiyama, Y.:— Maximum permissible Concentration of Sr^{90} in food and its environment. Rec. Oceanogr. W. in Japan. III-1, 1957.

Records of Oceanographic Works
in Japan Vol. 5, No. 2,
March, 1960

Morphometric Comparison of the Yellowfin Tuna from the Banda Sea and its Adjacent Waters*

By
Kenji KUROGANE

Abstract

Measurements of various morphometric characters on 60 specimens of yellowfin tuna from the Banda Sea were compared with similar data for yellowfin tuna from waters adjacent to the Banda Sea, namely the western equatorial Pacific, the southern area of the Lesser Sunda Islands and the Coral Sea, in order to analyse the relationship between the Pacific and the Indian tuna resources.

It is apparent from these comparisons that the specimens from the Banda Sea during the season from March to May are similar in morphometrical features with that from the western equatorial Pacific, but are different, so far as the present data indicate, from those taken from the southern area of the Lesser Sunda Islands and from the Coral Sea. However, the inter-relationship of the yellowfin tuna resources of the Indo-Australian Archipelago must be more carefully analysed in the future, by considering the seasonal variations as well as the regional ones.

This study offers the further confirmation of the conclusions that each population of the yellowfin tuna is distributed in rather localized waters, comparing with the albacore population, and that the two species of yellowfin tuna, from the Indian Ocean, *Neothunnus argentivittatus* and from the Pacific, *N. macropterus* may be regarded as belonging to a single species, though this taxonomic question is still being debated.

Introduction

The sea waters of the Indo-Australian Archipelago, especially the Banda Sea, are well known to be excellent fishing grounds for the tunas. However, we have scarcely had informations on the fishery biology of the tunas taken from these areas. Basing the study on the variation of the fishing condition in these waters, it will be considered that the scattered location of the islands and the very complicated nature of the sea current may affect the seasonal migration of the tunas. The fact that in these areas the small sized and the

* A part of the author's thesis work for Doctor's degree.

larval stage yellowfin tuna are frequently found and the gonads of the yellowfin tuna are rather mature, indicate the possibility that the spawning of yellowfin tuna occurs in these areas.

As a fundamental problem in order to understand the fishery biology of the yellowfin tuna of the Indian and the western Pacific Oceans, the proper identity of yellowfin tuna populations throughout the range of Indo-Australian Archipelago have to be clearly analysed. Basing their studies on the size composition and the species composition of the catches of tuna fishery boats, these relationship have been referred to by few researchers, but there is much to be still explained and analysed.

KUROGANE and HIYAMA have reported before on the relationship between the yellowfin tuna populations taken from the equatorial Pacific Ocean(1) and between the tuna populations from the Indian Ocean(2). In this report on the yellowfin tuna from the Banda Sea and its adjacent waters, together with the morphometric data on the specimens from the Banda Sea and the Coral Sea, the author has included the morphometric data of the specimens from the equatorial Pacific and the Indian Oceans, which authors used in their earlier reports on the yellowfin tuna.

The author wishes to express his thanks to Prof. Yoshio HIYAMA for his guidance and gratefully acknowledges and sincerely extends his gratitude to the director and staff of the Nankai Regional Fisheries Research Laboratory, who have given him all the facilities for the collection of the data.

Materials and Methods

Four samples, each consisting of 25 to 35 individuals, were taken from the following waters; two from the Banda Sea in 1956 and 1957 and others from the Coral Sea in 1956 and 1957. All specimens in the samples were caught by long-line fishing boats and were landed at the Tokyo Central Fish Market. These samples are tabulated in Table 1, showing the fishing ground, fishing date, number of specimens, range and average of body length. As regards the yellowfin tuna from the western equatorial Pacific Ocean and from the southern area of the Lesser Sunda Islands, the samples are those that were used in author's previous reports on the yellowfin tuna. The fishing stations of these samples are shown in Fig. 1.

Methods of measurement and analysis of data of the non-meristic characters are idential with that employed in previous reports on the yellowfin tuna. Seventeen body characters were measured in millimeters with slide calipers and a pair of dividers, according to the procedures employed by American tuna researchers. Then the covariance analysis was applied to test and estimate the sample difference.

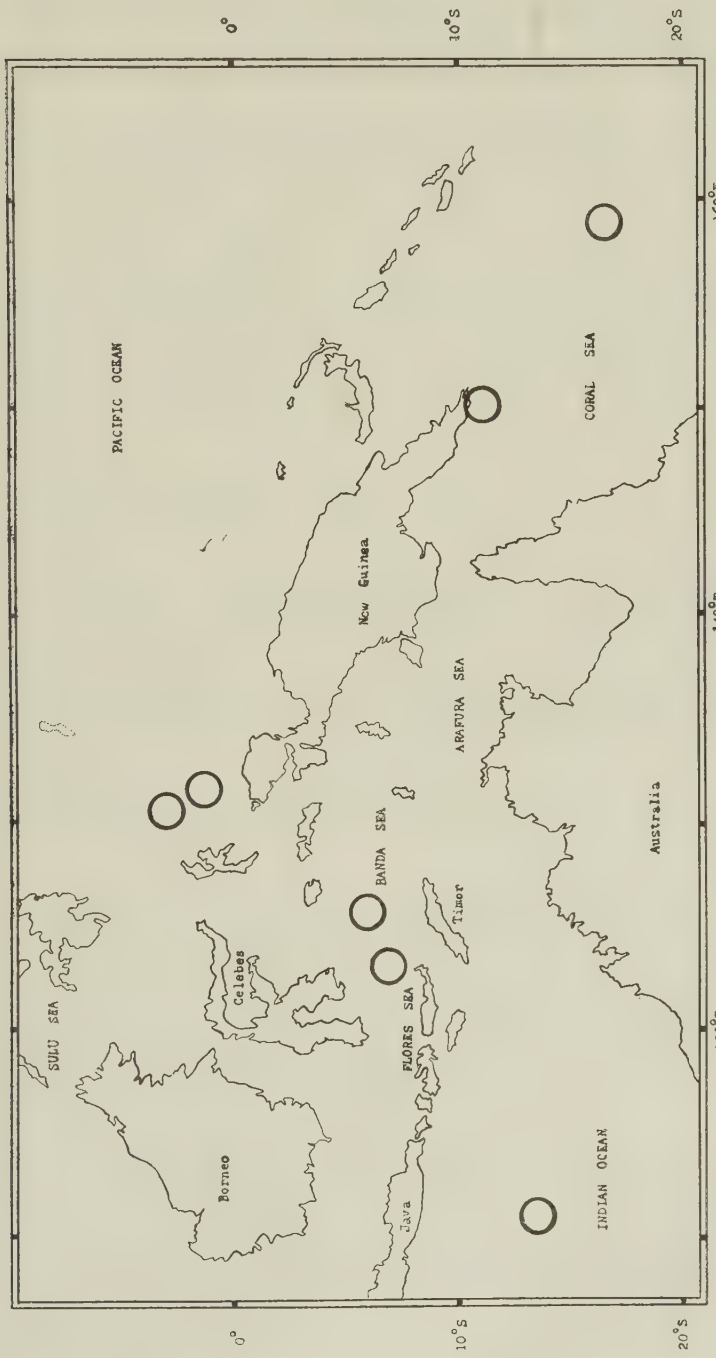

Fig. 1. Sampling stations of the yellowfin tuna.

Results

The yellowfin tuna taken from these areas have been reported before by the author.* The report was based on the morphometric data obtained during his preliminary survey in 1954. In this survey all the specimens were measured by T. SOEJIMA.** The results are summarized as follows:

1) The specimens from the Banda Sea show morphometrical differences with that from the Caroline Islands waters, namely the former have a relatively larger head and more posteriorly positioned fins than the latter. The yelloyfin tuna from these two areas seem to belong to different populations.
2) The specimens from the Banda Sea have morphometrical features similar to that from the southern waters of the Great Sunda Islands and those from these two areas show remarkable differences when compared with those specimens from the Lesser Sunda Islands, in the head lengths and the fin positions. The latter have smaller heads and more anteriorly positioned fins than the former.
3) The specimens from the New Caledonian waters, in the South Pacific Ocean, have morphometrical features different from those of the Banda Sea and the Lesser Sunda Islands, but they show relatively similar features with that from the equatorial Pacific Ocean in the same longitudes.

These raw data have not been used in this report, because of the possible individual error in the measurements which have not been checked yet. However, only the above mentioned results have been tested for their validity by basing on the data measured by the author.

Prior to the comparison of the samples from different areas, it was attempted to analyse the problem whether or not samples from the same area show variation in morphometrical characters.

(A) Morphometrical Variations of the Yellowfin Tuna taken from the Same Area

Authors have pointed in their previous reports on the yellowfin tuna from the equatorial Pacific and the albacore from the Pacific and the Indian Oceans[3], that there are variations in some characters between the samples from the same area. When the variations are small in many of the characters, one may be able to consider the samples to be representative of the population from which they are drawn, and the measurement and the sampling errors small. However, even if one finds great differences in these samples, he cannot analyse these promising factors to produce such great variability. Such differences may be introduced by many factors, for example, seasonal and annual variation

*The author reported orally at the 1955 annual meeting of the Japanese Society of Scientific Fisheries.

**At present, in the service of Kyokuyo Hogei Co., Ltd.

of the same population in morphometrical features, or different populations migrating at different seasons to the same area, or measurement and sampling errors etc. Such many factors may be confounded so complicatedly that one cannot analyse the effect of each factor under the present sampling method.

i) *Comparison of the Two Samples from the Banda Sea*

As shown in Table 1, two samples were taken from the catches of tuna fishing boats operating mainly in the Banda Sea and partially around the Lesser Sunda Islands during the season between March and May.

Table 1. Fishing ground, date taken, number of fish, range and average of body length for each sample taken from the Banda Sea and the Coral Sea.

Sample number	Fishing ground	Date taken	No. of fish	Average of body length (mm)	Range of body length (mm)
I	3°S–11°S 118°–128°E	1956, Mar.–Apr.	25	1220	874–1573
II	3°S–14°S 115°–130°E	1957, Apr.–May	35	1227	1036–1427
III	14°S–19°S 157°–161°E	1956, June–July	26	1272	1002–1560
IV	10°S–12°S 149°–151°E	1957, Sept.–Oct.	30	1311	1106–1530

Because of damage of the tip of the divider, the author could not measure three of the seventeen characters for the 1957 sample, namely first dorsal spine length, maxillary length and diameter of iris. Accordingly in this section, the comparison of the samples have been tested on the relative growth of thirteen body parts against the body length, excepting for the exclusion of the three small characters, above mentioned.

The variance ratio to test the significance of the difference in the sample regression lines of each body character on body length are shown in Table 2. The differences of regression lines are not significant at the 1 percent level in any characters, but the regression of the distance from snout to pectoral fin insertion and the three characters connected with the position of the second dorsal fin, such as snout to second dorsal fin insertion, first dorsal base and second dorsal to caudal, are in each case slightly but significantly different at the 5 percent level. These differences at the 5 percent level are not considered sufficient to detect the population difference, because as previously pointed out in earlier papers, samples taken from the same area show such a difference. At any rate, each sample size is rather small, and hence it will be better to treat these two samples as one from the same population. But in future, these samples from one area must be re-examined from seasonal viewpoints, because of possible migrations of different populations to the same area under complex oceangraphic conditions.

ii) *Comparison of the Two Samples from the Coral Sea*

As shown in Table 1, two series of measurement data from the Coral Sea

were taken from the catches of tuna fishing boats. The fishing was operated during the season between June and July in 1956 and between September and October in 1957 respectively. The results obtained by the comparison of these two samples are as follows (Table 2).

Table 2. Comparison of body proportion by covariance analysis for the samples taken from the same area. This significance shows the difference of the regression lines.

Body character \ Area	Banda Sea	Coral Sea	Western equatorial Pacific
Head length	—	—	—
Snout to 1st dorsal	—	—	—
Snout to 2nd dorsal	○	—	○
Snout to anal	—	—	—
Snout to ventral	—	◉	—
Snout to pectoral	○	—	—
1st dorsal base	○	—	—
2nd dorsal to caudal	○	—	—
Anal to caudal	—	—	—
Spread caudal	—	—	◉
1st dorsal spine length		—	○
2nd dorsal length	—	—	—
Anal length	—	—	◉
Pectoral length	—	○	—
Maxillary length		—	—
Diameter of iris		—	—

Note. —: Not significant at the 5 percent level
○: Significant at the 5 percent level
◉: Significant at the 1 percent level
Blanc is the missing item because of damage to the measuring scale.

In snout to ventral fin insertion on body length, the difference of the regression lines is significant at the 1 percent level and in pectoral fin length at the 5 percent level. The specimens in 1957 have somewhat posteriorly positioned ventral fin and shorter pectoral fin length than those in 1956. However, the regressions of other fourteen characters are not to be regarded as different for the two groups of tunas since covariance analysis shows that the probability of the two samples arising from a same homogeneous population is greater than one chance in twenty.

In general it does not appear that these two sample difference is great, when one considers that these are taken in different years and seasons. So, the author assumes that these two samples are representative of the same population inhabiting the Coral Sea and treat them as one and the same population from the Coral Sea by combining these two series of data in the following sections.

ii) *Comparison of the Two Samples from the Western Equatorial Pacific*

A comparison of these two samples has been reported in earlier reports on the equatorial Pacific yellowfin tuna. These two samples were taken during the season between April and May in 1956 and 1957 respectively. Results obtained are as follows: In anal fin length and spread caudal, the differences are recognized significantly in the 1 percent level and in snout to second dorsal fin insertion and first dorsal spine length in 5 percent level. But authors treated these two samples as one representative sample of this area and compared them with other samples from several other localities of the equatorial Pacific. From these examinations it was found that such differences between samples within an area are in general smaller than the one between areas.

From these results, it becomes apparent that samples taken repeatedly from the same area have slight but quite significant difference in a few characters. Such differences occur more frequently than the one expected from simple random samples from a homogeneous universe. Various possible reasons for this sort of differences between samples may be considered, but the author has not any concrete information for the causes of such differences. Strictly speaking, he may not assume that the specimens from each area constitute a random sample. However, as he saw in the morphometrical study on the albacore and the yellowfin tuna, in general, the samples from the same area, in even different years, show the less differences in many characters compared with the between-area differences. Accordingly, as a step to analyse the between-area differences, he treated the samples from the same region as a unit sample representative of the area.

(B) On the Comparison of the Yellowfin Tuna from the Banda Sea and its Adjacent Waters

As may be seen from Table 3, comparing four yellowfin tuna samples from the Banda Sea, the western equatorial Pacific, the Coral Sea and the southern waters of the Lesser Sunda Islands in the Indian Ocean by usual methods of covariance analysis, significant differences were found at the 1 percent or 0.1 percent level in the eleven of the characters, namely: head length, snout to the insertions of second dorsal, anal, ventral and pectoral fins, first dorsal base, anal to caudal, spread caudal, diameter of iris, length of the second dorsal and anal fins. It can be surely said that these yellowfin tunas do not seem to be drawn from a single homogeneous population.

Following to the test of the significance of the sample differences, the adjusted mean was estimated with its 99 percent confidence interval of each body character which does not show the significant difference in the regression coefficient, basing on the representative regression coefficient estimated from the four samples. These values are tabulated in Table 4 and illustrated in

Table 3. Comparison of body proportion of yellowfin tuna by the covariance analysis for four samples taken from the Banda Sea and its adjacent sea waters. F_r is the variance ratio to test the significance of the regression line difference, F_b to test the regression coefficient difference and F_a to test the adjusted mean difference.

Body character	F_r	F_b	F_a
Head length	5.46***	2.90*	(7.81***)
Snout to 1st dorsal	2.60*	2.53	2.62
Snout to 2nd dorsal	5.04***	5.95***	(3.86**)
Snout to anal	4.86***	1	9.36***
Snout to ventral	3.35**	1	6.34***
Snout to pectoral	3.75**	1.41	6.06***
1st dorsal base	4.39***	5.56***	(3.02*)
2nd dorsal to caudal	1	1.32	1
Anal to caudal	4.37***	3.39*	(5.17**)
Spread caudal	5.61***	3.45*	(7.89***)
1st dorsal spine length	2.36*	2.19	2.47
2nd dorsal length	6.29***	3.65*	(8.59***)
Anal length	6.77***	1.46	12.00***
Pectoral length	1.10	1.63	1
Maxillary length	1.52	1.33	1.70
Diameter of iris	17.15***	1	34.52***

Note. In the case where the regression coefficient difference is significant, the test of the adjusted mean difference becomes inappropriate, i.e. those figures within brackets under F_a.

*: Significant at 5 percent level

**: Significant at 1 percent level

***: Significant at 0.1 percent level

Fig. 2 on head length, the distance from snout to the insertions of ventral and pectoral fins and anal length. Then, the Banda Sea sample was compared again with each of the other sample by the covariance analysis, and the results of F test are shown in Table 5. Basing on these tables and figures the relationship between the specimens from the Banda Sea with those from other waters was analysed.

i) *Comparison of the Samples from the Banda Sea and the Western Equatorial Pacific*

As shown in Table 5, the difference of regression lines, between the samples in the two areas, is significant at the 1 percent level in head length and first dorsal base and significant at the 5 percent level in snout to second dorsal fin insertion, anal to caudal, spread caudal and diameter of iris. These differences are mainly caused in the regression coefficients. The western equatorial Pacific sample is composed of somewhat smaller body sized specimens on the average when compared with other samples. As shown in Table 3,

Table 4. Adjusted mean value of body part, its 99 percent confidence limits, mean standard length in millimeters and estimated regression coefficient.

Statistics / Sample / Body character	Adjusted mean and its 99 percent confidence limits				Estimated regression coefficient	Mean standard length (mm)
	Banda Sea	Western equatorial Pacific	Lesser Sunda Island	Coral Sea		
Head length	321.4±1.57	(319.5)	318.8± 2.19	317.3±1.61	0.2257	1261.0
Snout to 1st dorsal	342.5±1.98	342.8±2.09	343.0± 2.82	339.4±2.12	0.2469	1208.2
Snout to 2nd dorsal	637.4±2.48	(636.3)	639.4± 3.47	634.4±2.56	0.4795	1261.0
Snout to anal	682.9±2.72	683.8±2.86	680.0± 3.87	676.3±2.91	0.5248	1208.2
Snout to ventral	348.2±2.35	349.6±2.48	343.4± 3.35	345.1±2.52	0.2569	1208.2
Snout to pectoral	314.2±1.75	312.9±1.84	310.5± 2.48	310.3±1.87	0.2239	1208.2
1st dorsal base	291.7±2.25	(292.1)	294.0± 3.12	291.0±2.30	0.2421	1260.2
2nd dorsal to caudal	624.1±3.02	625.1±3.18	624.2± 4.30	625.8±3.23	0.5574	1208.2
Anal to caudal	582.3±2.90	(576.9)	586.1± 4.06	584.5±2.99	0.5093	1261.0
Spread caudal	485.7±7.43	(479.6)	463.0±10.38	477.6±7.66	0.5244	1261.0
1st dorsal spine length	2.1468±0.0111*	2.1530±0.0076*	2.1440±0.0108*	2.1560±0.0078*	1.0143	3.0739*
2nd dorsal length	2.5421±0.0158*	(2.5355*)	2.5082±0.0223*	2.5591±0.0161	2.5269	3.0977*
Anal length	2.5387±0.0165*	2.5481±0.0165*	2.4994±0.0223*	2.5610±0.0168*	2.5233	3.0773*
Pectoral length	334.2±3.79	333.6±3.99	330.0±5.39	333.5±4.05	459.87	3.0773*
Maxillary length	116.6±1.20	117.5±0.75	117.2±1.11	117.9±0.80	0.3716	307.0
Diameter of iris	37.6±0.63	38.3±0.38	37.3±0.54	38.3±0.40	0.0778	308.1

Note. As shown in Table 3, the significant differences are recognized in the regression coefficients of several characters. Because these differences depend mainly on particular values of the western equatorial Pacific sample, this sample was excluded from others and the representative regression coefficient of the other three samples and their confidence limits of the adjusted means were estimated. As regards the western equatorial Pacific sample, the point estimation was made using its regression coefficient and these values are inserted within brackets.

*: The logarithmic transformation is applied to the raw data.

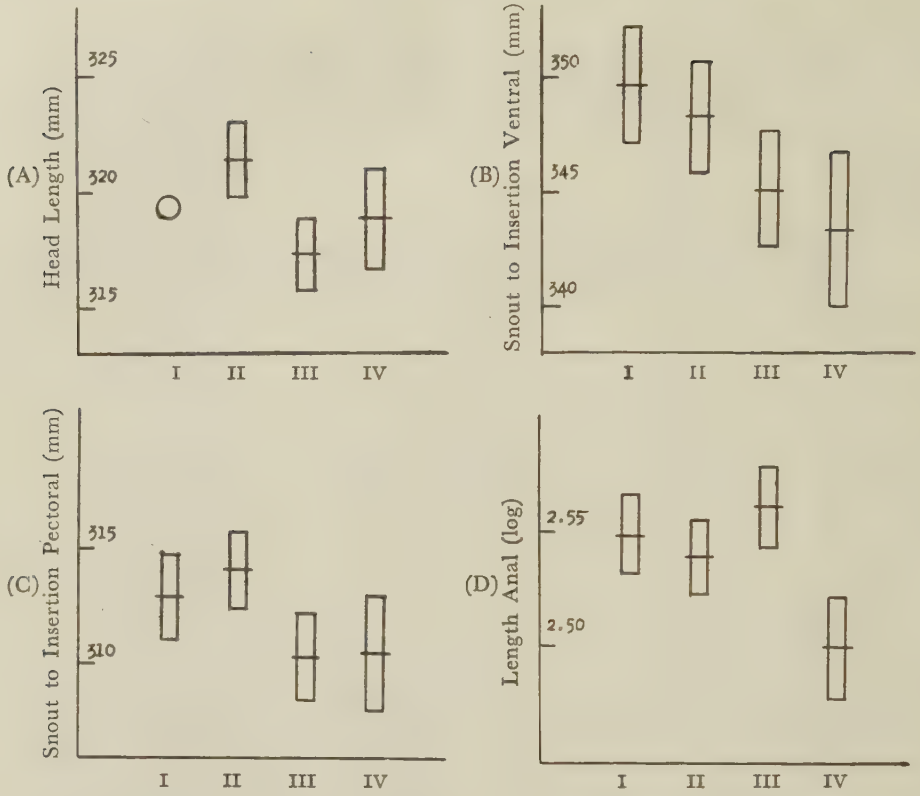

Fig. 2. Adjusted mean of body part and its 99 percent confidence interval.
(A): Head length at 1261 mm. body length
(B): Snout to ventral fin insertion at 1208 mm. body length
(C): Snout to pectoral fin insertion at 1208 mm. body length
(D): Anal length at 1195 mm. body length
I: Yellowfin tuna from the western equatorial Pacific
II: Yellowfin tuna from the Banda Sea
III: Yellowfin tuna from the Coral Sea
IV: Yellowfin tuna from the southern waters of the Lesser Sunda Islands

the significant differences in the regression coefficients are mainly affected by the values of the regression coefficient of the western equatorial Pacific sample. Accordingly, in the estimation of the adjusted means on these characters, the point estimation was carried out on the western equatorial Pacific sample. In the adjusted means there does not seem to be any remarkable difference between these two samples. Thus, on particular values which are produced by the western equatorial Pacific sample, it is necessary to examine in greater detail how much the size composition of samples influence morphometrical study.

The above results are considerably different from that of the preliminary survey conducted in 1954. Previous research has shown that there are marked differences in morphometrical characteristics of specimens from the Banda Sea

Table 5. Comparison of body proportion by the covariance analysis between the Banda Sea sample and each one from its adjacent sea waters. The significance shows the difference of the regression lines.

Compared samples / Body character	Banda Sea		
	Western equatorial Pacific	Lesser Sunda Islands	Coral Sea
Head length	◉	○	●
Snout to 1st dorsal	—	—	◉
Snout to 2nd dorsal	○	—	○
Snout to anal	—	—	●
Snout to ventral	—	◉	—
Snout to pectoral	—	◉	◉
1st dorsal base	◉	—	—
2nd dorsal to caudal	—	—	—
Anal to caudal	○	—	○
Spread caudal	○	●	—
1st dorsal spine length	—	—	—
2nd dorsal length	—	◉	—
Anal length	—	●	—
Pectoral length	—	—	—
Maxillary length	—	—	○
Diameter of iris	○	—	—

Note. —: Not significant at the 5 percent level
○: Significant at the 5 percent level
◉: Significant at the 1 percent level
●: Significant at the 0.1 percent level

and from the Caroline Islands. The Banda Sea sample in the preliminary survey were taken from the catches of tuna fishery boats which operated in August and the present sample from the Banda Sea during the season from March to May. Such differences in season, when the sample is taken in waters where the questions in island locations and sea currents are complicated, may produce possible disagreement in morphometrical results. In such areas the seasonal factors cannot be neglected in morphometrical analysis.

ii) *Comparison of the Samples from the Banda Sea and the Southern Area of the Lesser Sunda Islands*

Between-area differences are observed at the 1 percent or 0.1 percent significant level in the distance from the snout to the ventral, pectoral fin insertions, spread caudal, second dorsal and anal fin lengths. And the relative growth of the head length to body length shows difference at the 5 percent level. These regression line differences do not depend mainly on the regression coefficient differences as shown in the previous section in the comparison between the Banda Sea and the western equatorial Pacific samples, but on the adjusted means.

These results obtained by the test of the significant difference agree rather well with the results from the preliminary survey. However, from comparing the estimated values of each character size in these samples, their disagreement was easily observed. On all above characters excepting the spread caudal, the discrepancies of the adjusted means between these samples in 1954 are shown in Table 6. As shown in Tables 4 and 6, the differences between the Banda Sea sample and the Lesser Sunda Islands sample, taken in 1955-1957 somewhat disagreed with samples taken in the same areas in 1954. However, they agreed rather well with the samples taken from the Caroline and the Lesser Sunda waters in 1954. This phenomena was guessed from the fact that the sample from the Banda Sea in 1955-1957 had morphometrical features rather similar to that from the western equatorial Pacific. Such facts may show the probability that into the Banda Sea different populations of yellowfin tuna are migrating seasonally, though this fact may be confirmed after an elaborate survey in the near future.

Table 6. The discrepancies of the adjusted means of each character at about 1220 mm body length between the samples from the Banda Sea, the Lesser Sunda Islands and the Caroline Islands sea waters in the preliminary survey on the yellowfin tuna.

Body character	Banda Sea>Lesser Sunda	Caroline>Lesser Sunda
Head length	10.6 mm	2.0 mm
Snout to ventral	8.6	4.8
Snout to pectoral	8.1	2.1
2nd dorsal length	38.6	26.1
Anal length	59.2	45.0

iii) *Comparison of the Samples from the Banda Sea and the Coral Sea*

In head length, the distance from snout to first dorsal, anal, pectoral fin insertions, significant differences at the 1 percent or 0.1 percent level, and in the distance from the snout to second dorsal fin insertion, anal to caudal and maxillary length at the 5 percent level have been observed. As seen obviously in the estimated value of the adjusted means, the specimens of the Banda Sea have a larger head and more posteriorly positioned fins than the Coral Sea ones.

Considering these results together with the one obtained in the previous report on the yellowfin tuna from the equatorial Pacific, ranging from 130°E to 130°W, it may be reduced that the Banda Sea yellowfin tuna, during the season from March to May at least, have a relationship with that from the western equatorial Pacific, and the Coral Sea sample with that from the Marshall Islands waters. But as to the fin length, the results are not always in agreement, so the validity of such relationship needs further detailed analysis from the morphometrical and the fishery biological viewpoints.

In general, the data presented herein may support the following relationships between the yellowfin tuna from the Banda Sea and its adjacent sea waters.

1) The specimens of yellowfin tuna taken from the western equatorial Pacific area and from the Banda Sea during the season from March to May, have relatively similar morphometrical features, though in a few characters it is necessary to analyse in more detail the regression coefficient differences of the relative growth. These results do not agree with the ones from the preliminary research on the yellowfin tuna taken from the Banda Sea and the Caroline Islands in a period during July and August. Accordingly, it is to be desired to examine more exactly the pattern of the seasonal migration of the yellowfin tuna inhabiting in the Banda Sea, by gathering more informations on the fishery biological properties of the tunas.
2) Basing on the materials taken from the southern area of the Lesser Sunda Islands in 1956 as well as the one in 1954, it appears that the specimens of the yellowfin tuna have a relatively smaller head, shorter fin and anteriorly positioned fins than the one from the Banda Sea and the Caroline Islands. These results may indicate the existence of a distinct population of the yellowfin tuna in this area.
3) The specimens from the Coral Sea have a somewhat smaller head and more anteriorly positioned fins than the one from the Banda Sea, and these differences are rather well agreed with the one between the samples from the western area and from the central area of the equatorial Pacific. It is probable that the yellowfin tuna from the Banda Sea have a relationship with the western equatorial Pacific yellowfin tuna, and the Coral Sea yellowfin tuna with the central equatorial Pacific one. These possibilities are rather well founded but for confirming these facts more elaborate studies are required.

Discussion

Previous studies on the yellowfin tuna from the equatorial Pacific and from the Indian Ocean have shown that the yellowfin tuna within each ocean are separated into a number of independent or semi-independent populations.

In the present study, the biometric data from specimens of the Banda Sea have been compared with that from specimens of its adjacent waters situated in the Pacific and the Indian Ocean. This area was chosen because it is an important area to analyse the relationship between the tuna resources of the Pacific and the Indian Ocean.

In these areas the yellowfin tuna are richly distributed and the commercial vessels operate with big catches. However, there are very scanty informations about the fishery biological properties of the tuna from these areas. The spawn-

ing of the yellowfin tuna may surely occur in these areas, for ripening adults of this species are taken by long-line fishery boats, the swimming of small sized yellowfins at the surface waters is observed from the board of vessel, the large sized yellowfin tuna of the Banda Sea and of the Coral Sea seem to be migrating to the Arafura Sea for the spawning during summer in the southern hemisphere,[4] and the larval stage yellowfin tuna are collected from the northern area of these seas.[5],[6] As regards the relationship between the yellowfin tuna from these areas, NAKAMURA (1951)[7] recognized marked differences in the ponderal index of specimens from the Sulu Sea and from the Celebes Sea and suggested the necessity of racial investigations. And then he recognized, basing on the materials collected by commercial tuna long-line boats, that the yellowfin tuna from the adjacent waters of the Lesser Sunda and the Timor Islands are rather similar with those from the Banda Sea and the Froles Sea in the seasonal variations of the size composition of this species and of the species composition of the catches. On the contrary, basing on the materials collected in December of 1952, YABUTA (1954)[8] has reported that there are marked differences in the fishing conditions of these two areas. In general, it was said that the fishing condition in the Banda Sea shows remarkable change at about March and September. Considering these facts, in the study of the relationship of the yellowfin tuna resources in the Indo-Australian Archipelago, the seasonal analysis must be much emphasized together with the regional study. The yellowfin tuna from the southern area of the Lesser Sunda form a separate fishing ground from other yellowfin grounds in the Indian Ocean. The magnitude of the difference which is recognized between the samples from the Lesser Sunda and from the equatorial Indian Ocean is quite large in comparison with the difference between the one from the Lesser Sunda and from the Banda Sea and the western equatorial Pacific area, though here too statistically this difference is significant.

Even now, the Indian yellowfin tuna is called *Neothunnus argentivittatus* (CUVIER and VALENCIENNES) 1831, and the Pacific tunas, *Neothunnus macropterus* (TEMMINCK and SCHLEGEL) 1842. Basing on these morphometrical data only, it seems to be dengerous to settle the problem whether or not these tuna species should be considered races of a single species of world-wide distribution. However, these studies on the variations within and between oceans offer further confirmation of the conclusion that these specimens belong to the same species, as pointed out by SCHAEFER (1952),[9] ROYCE (1953)[10] and TSURUTA (1955).[11] This problem must be settled carefully basing on more informations on the detailed external and internal characters of the specimens from various places, particularly on the Atlantic specimens.

Authors have before shown that the albacore from the North Pacific, the South Pacific and the Indian Ocean, form unit populations respectively, and they

are widely distributed and migrate east and westwards. On the contrary, the yellowfin tuna belonging to unit populations seem to be rather localized, hatching, fin tuna belonging to unit populations seem to be rather localized, hatching, growing and dying in relatively confined waters. These properties of the tuna populations are observed, though not sufficiently, from the tagging results and from other fishery biological informations on the spawning, fishing conditions etc.

However, the magnitude of the differences in morphometrical features between the adjoining populations of yellowfin tuna, which are identified basing on the morphometrical data, are not so great as seen in the albacore, and the repeated samples of the yellowfin tuna from the same or nearby waters have somewhat large variability comparing with the albacore samples.

Considering these matters, it may be said that the population of the yellowfin tuna is not distinctly separated but rather intermingling with its adjoining population, and that the existence of morphometrically different population is probable in rather confined waters. With regards to the organization of the separation and intermingling of the populations, these must be analysed not only from morphometrical but also fishery biological viewpoints.

References

(1) Kurogane, K. and Y. Hiyama (1957): Morphometric comparison of the yellowfin tuna taken from the Equatorial Pacific. Bull. Jap. Soc. Sci. Fish., 23 (7 & 8).
(2) Kurogane, K. and Y. Hiyama (1958): Morphometric comparison of the yellowfin tuna from six grounds in the Indian Ocean. Bull. Jap. Soc. Sci. Fish., 24 (6 & 7).
(3) Kurogane, K. and Y. Hiyama (1959): Morphometric comparison of the albacore from the Indian and the Pacific Ocean. Records, Oceano. Works, Japan, 5 (1).
(4) Nomura, T. (1957): Results of landings survey on the tuna (April, 1954—March, 1955). The Investigative Society of Tuna Fishery.
(5) Wade, C. B. (1950): Juvenile forms of Neothunnus macropterus, Katsuwonus pelamis and Euthynnus yaito from Philippine seas. U.S. Fish and Wildlife Service, Fish. Bull. 53.
(6) Wade, C. B. (1951): Larvae of tuna and tuna-like fishes from Philippine waters. U.S. Fish and Wildlife Service, Fish. Bull. 57.
(7) Nakamura, H. (1951): A review on the fishing ground of tuna longline based on the past data. Report, Nankai Regional Fish. Research Lab., No. 1.
(8) Yabuta, Y. (1954): Average year's fishing condition of tuna long-line fisheries. Nankai Regional Fish. Research Lab.
(9) Schaefer, M. B. (1952): Comparison of yellowfin tuna of Hawaiian waters and of
(10) Royce, W. F. (1953): Preliminary report on a comparison of the stocks of yellowfin the American west coast. U.S. Fish and Wildlife Service, Fish, Bull. 72.
tuna. I. P. F. C. 4th Meeting, Section 2.
(11) Tsuruta, S. (1955): Morphometric comparison of yellowfin tuna of Southwestern Great Sunda Islands and of the Pacific waters. Jour. Shimonoseki College, Fish., 4 (3).

Records of Oceanographic Works
in Japan Vol. 5, No. 2,
March, 1960

Strontium-Calcium Discrimination in the Rainbow Trout

By
Ryushi ICHIKAWA
(National Institute of Radiological Sciences)

Abstract

In order to find the rate of discrimination between strontium and calcium when fish takes them from the water or the diet, the author investigated about this problem using the labelled water or diet with Ca^{45} and Sr^{90}. So, the present paper is concerned with (a) the strontium-calcium discrimination observed between fish body and the water, (b) the influence of the amount of calcium and strontium in the water to the rate of discrimination, (c) the strontium-calcium discrimination observed between the fish body and the diet, (d) estimation of maximum probable concentration of strontium-90 in this fish derived from the contamination of the water and diet by the artificial radioactivity such as the radioactive fall-out or the liquid waste effluence released from the nuclear energy plant.

1. Introduction

Calcium is one of the most important elements for every living life. And strontium which has the similar property with calcium always co-exists with calcium in various materials, though its amount is usually quite small comparing with that of calcium. The ratio between them varies according with the kind of materials which containes these elements.[1)4)11)20)]

When strontium-90 from atomic fission debris falls upon earth's surface, it will be taken into the fish bodies via their environmental water and the food in relation to the strontium and calcium exist naturally in the water or food. And it should be reasonable to be assumed that strontium might be discriminated against with respect to calcium at the time of passing into fish body from the environment such as the water and food. For example, the ratio of strontium to calcium in fish body should be expected to be lower than that in water or food in some extent.

Therefore, it is essential for the people who take the fishes for their food to get the exact figure of the rate of discrimination which fishes make between strontium and calcium up-take in order to estimate the maximum probable de-

position of strontium-90 into fishes caused by the accumulation of strontium-90 on the surface of the earth from the fall-out.

But, since the calcium and strontium content and the the ratio between them vary greatly especially in fresh-water area as usual[12], there is no appreciable knowledge about the discrimination factor which is defined as Sr/Ca in fish: Sr/Ca in water.

The author has begun to investigate about this factor using the rainbow trout *Salmo gairdneri irideus* by the experimental methods stated in the next chapter.

The present paper is concerned with (a) the strontium-calcium discrimination observed between fish body and the water, (b) the influence of the amount of calcium and strontium in the water to the rate of discrimination, (c) the strontium-calcium discrimination observed between the fish body and the diet, (d) estimation of maximum probable concentration of strontium-90 in this fish derived from the contamination of the water and diet caused by the artificial radiactivity such as the radioactive fall-out or the liquid waste effluence released from the nuclear energy plant.

This work was investigated by the author at the Laboratory of Radiation Biology, University of Washington, Seattle, Wash., U.S.A. Particular thanks are due to Dr. Lauren R. DONALDSON, director of the Laboratory, who gave the opportunity of this work to the author.

2. Method

The double tracer technique using calcium-45 and strontium-90 was applied in this experiments .

In order to get the each amount of calcium-45 and strontium-90 in each sample separately, 90.5 mg/cm^2 of alminium absorber at which β-ray of calcium-45 was absorbed completely, was used to measure only strontium-90 activity using a certain correction factor caused by the absorber. This factor which was used for multiplying the strontium-90 activity reduced by the absorber varied according with the amount of each sample. It might be caused by the different amount of self-absorption between strontium-90 and calcium-45 contained in sample. After that, amount of calcium-45 was obtained simply by the substraction of strontium-90 (including yttrium-90) activity from the whole activity.

Decay and self-absorption of calcium-45 and strontium-90 was corrected appreciably. Counting for the activity of every sample was begun after more than 2 weeks at least in order to eliminate the yttrium-90 activity taken from the water or the diet into the fish body and to get the growth of yttrium-90 from the strontium-90 which was taken into the fish body.

3. Over all discrimination observed in case of uptake from the water

As will be stated later, it is well known that the fishes can utilize the dissolved calcium in the water enough for their nutrient salt required by absorbing through their gill membrane. And they excrete it through their gill other than the urinary excretion through the kidney. Therefore, at the first step, "the strontium-calcium observed ratio" between the wate rand the fish body which was defined as strontium-calcium ratio taken in the body to that found in water was investigated by labeling the calcium and strontium in water with calcium-45 and strontium-90 respectively.

This term was proposed by C. L. Comar[7] to denote the actual differentiation in tissues or excreta. And this differentiation found as the observed ratio is produced by various physiological processes such as the absorption or the excretion through the various menbrane, at which the individual discrimination should occurr.

3.-1. In case of natural water which contains small amount of strontium

The rainbow trout *Salmo gairdneri irideus* (body length 15 cm approximately) was reared in the natural freshwater which contained 12 mg calcium per liter and was added calcium-45 and strontium-90. The ratio of radioactivity of strontium-90 (including yttrium-90) to calcium-45 was 0.431 for tank 1, and 0.180 for tank 2.

After 52 hours, they were dissected into the muscle and the bone and prepared as the ash sample for the radioassay after getting yttrium-90 growth. The water temperature during this experiment was approximately 60°F. Strontium-90/calcium-45 ratio found in bone, muscle and observed ratio of discrimination between the water and these tissues were shown in table 1. The average value obtained in case of bone was 0.36 ± 0.01 and for muscle 0.37 ± 0.02. The fact that the same value for bone and muscle was obtained means that strontium calcium ratio in both tissues is not different as was supposed. This fact is of pretty importance because the strontium content in muscle could be estimated from strontium-calcium ratio in bone and calcium content in muscle without the chemical analysis accompanied with its difficulty caused by its small quantity.

This strontium-calcium observed ratio between the water and tissues obtained here means that when the fresh water would get strontium-90 concentration A expressed in strontium unit (Sr^{90}/Ca), the rainbow trout living in it could get that of 0.4A as the maximum probable concentration without regarding to the uptake of strontium-90 from their diet which will be discussed later.

Table 1. Strontium-calcium observed ratio between natural water and rainbow trout.

Tank 1. Sr 90/Ca 45 in water.....0.431

Fish No.	Sr 90/Ca 45 in tissues		Observed ratio (Sr 90/Ca 45 : Sr 90/Cr 45) in tissues in in water	
	Bone	Muscle	Bone	Muscle
1	.144	.169	.33	.39
2	.150	.191	.35	.44
3	.186	.194	.43	.45
4	.139	.116	.32	.22
5	.175	.183	.41	.42
Tank 2. Sr 90/Ca 45 in water.....0.810				
6	.273	.308	.34	.38
7	.324	.261	.40	.32
8	.265	.256	.33	.32
9	.266	.317	.33	.39
10	.269	.256	.33	.32
Mean			.36±.01	.37±.02

3.-2. The influence of calcium and strontium concentration in the water

In order to find the influence of variation of strontium and calcium concentration in water to the strontium-calcium discrimination ratio in fish body, the amount of both elements in lake water was changed by adding strontium and calcium ion artificially. Under such conditions, strontium-calcium discrimination observed ratio and the actual amount of them taken up into the fish bodies were investigated in this experiment.

The rainbow trout (about 0.5 grs. body weight) was reared in the following 4 glass tanks which contained various amount of strontium and calcium prepared artificially by adding $CaCl_2$ and $Sr(NO_3)_2$ into the natural lake water. The amount of strontium found in lake water and $CaCl_2$ reagent used in this experiment was negligible compared with the amount of strontium added artificially. The lake water used here contained 12 mgs per liter of calcium naturally. And strontium and calcium in rearing water were labelled with strontium-90 and calcium-45 respectively.

Five fishes in each tanks were killed at 7th day since beginning and ashed and then calcium-45 and strontium-90 taken into fish body simultanously during this period was measured by radioassay. Then, the total amount of calcium and strontium taken into fish body from the water during this rearing period was

obtained by calculation from the ratio between calcium and calcium-45, and strontium and strontium-90 in water respectively. Five fishes remained in each tanks were treated in same way at 11th day since beginning.

Table 2. Calcium and strontium concentration in each rearing water prepared for this experiment.

Tank	Calcium mg/*l*.	Strontium mg/*l*.	Sr/Ca in weight ×100
I	12	12	100
II	18	6	33.0
III	21	3	14.3
IV	23	1	4.35

Water temperature during this rearing period was about 56°F. The amount of storntium and calcium taken into fish body and the ratio between them are shown in table 3 concerning to the individual fish.

Table 3. The amount of strontium and calcium taken in fishes, the ratio between them and the discrimination which fish made in case of uptake from the artificial water.

Period of rearing	Fish No.	Sr mg/Ash g	Ca mg/Ash g	Sr/Ca taken in fish ×100	Sr/Ca fish : Sr/Ca water
Tank 1. (Sr/Ca ×100.....100)					
7 days	1	3.62	15.8	23.0	0.23
	2	3.67	14.9	26.0	0.26
	3	2.58	13.5	19.1	0.19
	4	3.26	15.0	21.8	0.22
	5	3.51	17.1	20.5	0.21
11 days	6	5.18	23.2	22.4	0.22
	7	4.82	21.5	22.4	0.22
	8	4.81	21.2	22.7	0.23
	9	4.47	21.3	21.0	0.21
	10	3.97	20.6	19.2	0.19
Tank 2. (Sr/Ca ×100.....33.3)					
7 days	1	1.68	27.2	6.18	0.19
	2	1.50	22.4	6.71	0.20
	3	1.41	23.6	5.97	0.18
	4	1.55	23.4	6.63	0.20
	5	1.57	26.4	5.98	0.18
11 days	6	2.09	35.0	5.98	0.18
	7	2.16	33.8	6.39	0.19
	8	2.11	34.3	6.15	0.18
	9	2.09	35.5	5.88	0.18
	10	2.12	34.4	6.16	0.18

Tank 3. (Sr/Ca ×100.....14.3)

7 days	1	0.732	25.1	2.92	0.20
	2	0.881	27.0	3.26	0.2ε
	3	0.607	22.8	2.67	0.19
	4	0.669	25.5	2.63	0.18
	5	0.635	23.2	2.73	0.19
11 days	6	0.865	32.7	2.64	0.18
	7	0.750	32.9	2.28	0.16
	8	0.924	35.2	2.62	0.18
	9	0.01	37.9	2.67	0.19
	10	1.03	37.9	2.70	0.19

Tank 4. (Sr/Ca ×100.....4.35)

7 days	1	0.215	25.9	0.829	0.19
	2	0.217	24.5	0.885	0.20
	3	0.249	28.8	9.862	0.20
	4	0.230	29.5	0.779	0.18
	5	0.198	26.1	0.788	0.18
11 days	6	0.280	37.5	0.740	0.17
Mean					0.2±0.02

The amount of both strontium and calcium taken into fish body was found as proportional with their concentration in rearing water as was observed in case of marine fishes from the sea water[10)13)], and therefore the ratio of strontium to calcium taken into fish body was almost exactly proportional to that in water. And from these results we can get the value 0.2±0.02 as the almost constant strontium-calcium observed ratio which was defined as strontium/calcium taken in fish: strontium/calcium in water among the wide range of strontium-calcium ratio from 4.35 to 100 (expressed in strontium/calcium×100 in weight) in water.

But, this value 0.2 obtained in case of natural water experiment, in other words, strontium was discriminated against more at this time. Though strontium content in this fresh water used in this experiment was unknown, it is reasonably supposed to be quite small in quantity such as 0.01 mg per little or less for example and hence 0.1 or less for strontium/calcium ratio (× 100 in weight).

So, it could be said that if strontium content would increase in natural fresh water, the rate of discrimination which fish made should raise up some extent, in other words, the strontium content in water was so small, but, when pretty high concentration of strontium was found in water like in this experiment such as 1 to 12 mg per liter, the rate of discrimination would be almost constant, even if the strontium content or its ratio to calcium would change considerably.

4. Discrimination observed in case of uptake from the diet

The fishes take calcium (and at the same time strontium also) from the diet also even if its amount would be small compared with that from the water[19]. And this experiment stated here was concerned with the discrimination which fishes made between strontium and calcium uptake from their diet.

The diet used in this experiment is the mixed material of 60% vacuum dried fish meal (made from the spawned salmon), 20% frozen shrimp waste (almostly, their head) and 20% fresh liver and spleen of cow or pig.

Calcium-45 and strontium-90 (yttrium-90) solution which had the activity ratio of strontium-90/calcium-45 as 0.639, was added to this diet and mixed up until the homogenous condition of activity was obtained perfectly in every part of the diet.

The labelled diet made in such a way was inserted carefully into the stomach of the rainbow trout using the small polyethylene tube. And these fishes were kept in running water during this experiment to eliminate the reabsorption of the excreted strontium-90 and calcium-45 from the water. And after 24 hours, they were dissected into the muscle and bone for the radioassay.

The ratio of strontium-90 to calcium-45 in both tissues and the observed ratio between the diet and these tissues (Sr^{90}/Ca^{45} in tissue: Sr^{90}/Ca^{45} in diet) obtained in this treatment were shown in Table 4.

Table 4. Strontium-calcium observed ratio between the diet and rainbow trout bone and muscle.

Fish No.	Sr^{90}/Ca^{45}		Observed Ratio	
	Bone	Muscle	Bone	Muscle
1	.403	.401	.63	.63
2	.402	.311	.63	.48
3	.426	.449	.67	.70
4	.506	.473	.69	.74
5	.538	.489	.84	.77
Mean			.71±.05	.67±.06

As seen in the table, the observed ratio of strontium-calcium discrimination in case of uptake from the diet was approximately 0.7. This observed ratio seems to be pretty larger than that obtained in case of uptake from the water, in other words, the rate of discrimination is lower than that.

And as will be discussed later in detail, the amount of calcium taken from the diet is pretty smaller than that from water, but the contribution of the activity in diet to the deposition of strontium-90 into fish would be pretty important when the strontium-90 content in the diet in much higher (for example, more than 10 times) than that in water.

5. Discussion

The studies about strontium-calcium discrimination in living life have become quite important recently in order to estimate the transmission of strontium-90 into human body through the various food chain. And numerous works in detail have been done about this problem in case of mammals[6)7)8)9)14)16)18)21)]. But, the quite few works about this phenomenon in case of fishes were found up to the present.

BOROUGHS[2)3)] stated that the fish discriminated against strontium in comparison with calcium considering from his results that the concentration ratio of strontium-89 from the water was only about a half of that with calcium-45 in the same rearing condition using *Tilapia* reared in the sea water.

But, ROSENTHAL[15)] reported that no discrimination against strontium in favor of calcium was found in his experiment using several freshwater fishes such as *Lebistes, Danio, Tanichthys* getting the same concentration ratio of strontium-90 and calcium-45 taken from the water respectively. And he supposed that these results were caused from some physiological difference between the freshwater and marine fishes in absorption of the isotopes by the gill, skin and intestinal tract comparin gwith BOROUGHS' results.

The mammals take calcium and strontium from ther diet only, and COMAR *et al* have found the various strontium-calcium discrimination factors at each physiological processes in the rat, rabbit and human body. And that differential absorption at the gastrointestinal tract ($DF^{*}_{absorptive}=0.34$) and the differential urinary excretion ($DF^{**}_{urinary}=0.86$) were found as two major discrimination processes in case of rat by the commercial diet[7)]. And the value 0.78 for $DF_{absorptive}$ and 0.87 for $DF_{urinary}$ in case of man investigated using strontium-85 and calcium-45[8)]. And that the excretion of calcium and strontium from the blood into the gastrointestinal tract via the bile, pancreatic juice and the secretion of intestinal mucosa would not contribute in a major way to the over all discrimination. And any discrimination at the movement of calcium and strontium from the blood to skeleton could not be recognized appreciably.

In present investigations, the situation of calcium-strontium uptake is quite different with that of the mammals because the fishes take calcium from their environmental water directly and excrete it through their gill membrane other than intake from the diet and excretion into urine. So, it is a little more complicated to estimate the probable strontium-90 deposition into fish body which takes it from both the water and the diet in natural living condition than that a mammals which take it only from their diet.

If the fishes will grow up in the water which contains SrW (the concentra-

* Discrimination factor observed at the time of the absorption

** The same at the time of urinary excretion.

tion of strontium-90 in the water expressed in strontium unit, Sr^{90}/Ca) of strontium-90, and that in their diet is denoted by SrD, the maximum probable concentration of strontium-90 in fish body (denoted by SrF) should be estimated as follows:

$$SrF = \frac{Sr^{90}\,(\text{from water}) + Sr^{90}\,(\text{from diet})}{Ca\,(\text{from water}) + Ca\,(\text{from diet})}$$

and $Ca\,(\text{from diet})/Ca\,(\text{from water}) = k$,

$$SrF = \frac{Sr^{90}\,(\text{from water})}{(k+1)\,Ca\,(\text{from water})} + \frac{Sr^{90}\,(\text{from diet})}{(1+1/k)\,Ca\,(\text{from diet})}$$

$$= \frac{1}{k+1} SrW \cdot OR_{\text{water-fish}} + \frac{k}{k+1} SrD \cdot OR_{\text{diet-fish}}$$

$$= \frac{1}{k+1} (SrW \cdot OR_{\text{water-fish}} + k \cdot SrD \cdot OR_{\text{diet-fish}})$$

In the formula, k is the ratio of the amount of calcium taken from the diet to that from the water, and $OR_{\text{water-fish}}$, $OR_{\text{diet-fish}}$ are strontium-calcium observed ratio between water and fish, and between diet and fish respectively which are available from the results of experiments.

As the value of k, Tomiyama *et al*[19] have reported approximately 1/50 in case of the gold fish feeding the worm. The yalso found that the assimilability of calcium in fish from the diet was only 8 to 15% though albino rat utilized 79% of calcium from the same diet, and this low assimilability of calcium in diet was the reason why the value of k was so small. And it was concluded that the gold fish took calcium required for the nutrition mostly from the water.

When the value of k, 1/50 is applied for this case, and 0.4 for $OR_{\text{water-fish}}$ and 0.7 for for $OR_{\text{diet-fish}}$ which were shown already, are used in the present formula shown above, SrF could be estimated by the following calculation.

$$SrF = \frac{1}{0.02+1} (0.4\ SrW + 0.02 \times 0.7\ SrD) = 0.4\ SrW + 0.014\ SrD$$

From this result, unless the value of SrD is more than 10 times of SrW, strontium-90 concentration (SrF) mostly depends on that of water. But, if the water would lose its strontium-90 by some reason such as the running out or others and the living lives as the diet for fish would have still high concentration of strontium-90, the value of SrF (concentration of strontium-90 in the diet) would become the quite important factor for the deposition of that into the fish body.

In case of marine fishes, since the ratio of strontium to calcium in sea water is observed to be pretty constant in everywhere, strontium-calcium observed ratio between the water and the fish bone could be estimated by the ratio of strontium

to calcium in fish bone, and that in the sea water which are available from the result of chemical analysis, on the assumption of that the uptake of strontium and calcium from their diet would be quite small in quantity compared with that from the water like that in case of fresh water fishes.

For example supposing that strontium concentration in sea water is 7 to 8 mg per liter[5] and calcium 400 mg per liter [17] approximately, the ratio of strontium to calcium should be 0.02 in weight. And using some strontium-calcium ratio (in weight) of various marine fishes' bones [11] such as black marline *Makaira mazara* 0.0018, alaskan pollack *Theragra chalcogramma* 0.0057, horse mackerel *Trachurus japonicus* 0.0042, skipjack *Katsuwonus pelamis* 0.0025 and croaker *Sciaena sp.* 0.0016, strontium-calcium observed ratio between sea water and fish bones would be estimated as 0.1, 0.3, 0.2, 0.1 and 0.1 respectively without regarding to the influence of the food.

These observed ratios found in case of marine fishes seem to be a little smaller, in other words, the rate of discrimination is a little higher, than that obtained experimentally in rainbow trout. And this fact seems to be caused by the pretty high concentration of strontium and calcium in sea water.

6. Summary

1. In natural lake water which containes 12 mg calcium per liter, the rainbow trout discriminates against strontium in favour of calcium at the rate of 0.4 expressed in the strontium-calcium observed ratio between water and bone or muscle (defined as Sr/Ca taken in fish: Sr/Ca in water) in case of uptake from the water.

2. Getting the same strontium-calcium observed ratio for bone and muscle from this experiment, strontium-calcium ratio in both tissues should be considered to be the same as have been expected. From this fact strontium concentration in muscle could be estimated from calcium concentration in muscle and strontium-calcium ratio in bone.

3. In artificial water which was prepared to have higher strontium concentration than that of natural water (strontium—1 to 12 mg 1, Sr/Ca × 100 in weight —4.35 to 100), the observed ratio of discrimination was found to be 0.2 almost constantly during this wide range of strontium and calcium concentration.

4. From these results, it could be known that strontium concentration in water made the discrimination a little higher, but, it could not be more than twice even if any amount of strontium would be added more.

5. In case of uptake from the diet, strontium-calcium observed ratio between diet and bone or muscle was found to be 0.7 approximately.

6. When the fishe is living in the water which contained SrW of strontium-90 concentration and feeding on the diet which has SrD of that, the probable maximum concentration of strontium-90 in this fish (SrF) should be estimated by

the following formula,

$$SrF = 0.4\ SrW + 0.014\ SrD$$

if 0.4 is used for the observed ratio of discrimination between water and fish, 0.7 for that between diet and fish, and 1/50 for the ratio of the amount taken from diet to that from the water.

7. Strontium-calcium discrimination observed ratio between freshwater and fish seems to be lower than that of marine fishes which can be estimated by strontium-calcium ratio in sea water and fish bones.

7. References

1. Asari, T. (1950): The geochemical distribution of strontium. IV. animal bones Bull. Jap. Soc. Chem. Vol. 70, pp. 12-13.
2. Boroughs, H., S. J. Townsley, and R. W. Hiatt. (1956): The metabolism of radionuclides by marine organisms. I. the uptake, accumulation and loss of strontium-89 by marine fish. Biol. Bull. Vol. 111, pp. 336-361.
3. Boroughs, H., S. J. Tomnsley, and R. W. Hiatt (1957): The metabolism of radionuclides by marine organisms. III. the uptake of calcium-45 in solution by marine fish. Limnology and Oceanography Vol. 2, no. 1, pp. 28-32.
4. Chow, T. J. and T. G. Thompson (1955): The strontium-calcium atom ratio in carbonate secreting marine organisms. Papers in marine biology and oceanography. pp. 20-39. Pergamon Press Ltd., London.
5. Chow, T. J. and T. G. Thompson (1955): Flame photometric determination of strontium in sea water. Analytical Chem. Vol. 27, pp. 18-21.
6. Comar, C. L., I. B. Whitney and F. W. Lengemann (1955): Comparative utilization of dietary Sr. 90 and calcium by developing rat fetus and growing rat. Proc. Soc. Exp. Biol. Med. Vol. 88, pp. 232-236.
7. Comar, C. L., R. H. Wasserman and M. M. Nold (1956): Strontium-calcium discrimination factors in the rat. Proc. Soc. Exp. Biol. Med. Vol. 92, pp. 859-863.
8. Comar, C. L., E. H. Wasserman, Sven Ullberg and C. A. Andrews (1957): Strontium metabolism and strontium-calcium discrimination in man. Proc. Soc. Exp. Biol. Med. Vol. 95, pp. 386-391.
9. Comar, C. L., R. S. Russell and R. H. Wasserman (1957): Strontium-calcium movement from soil to man. Science. Vol. 126, pp. 485-492.
10. Hiyama, Y. and R. Ichikawa (1957): Uptake of strontium by marine fish from the environment. Rec. Oceanogr. Works in Japan. Vol. 3, no. 1, pp. 78-84.
11. Hiyama, Y. (1957): Radiological data in Japan II. Concentration of Sr 90, Cs 137, Pu 239 and others in various materials on earth's surface. Jap. Sci. Monthly. Vol. 10, no. 9.
12. Hutchinson, G. E. (1957): A treaties on limnology. Vol. 1, geography, physics and chemistry. John Wiley & Sons, Inc. New York.
13. Ichikawa, R. and Y Hiyama (1957): The amount of uptake of strontium by marine fish from the environment of various concentration of calcium and strontium. Rec. Oceanogr. Works in Japan. Vol. 4, no. 1.
14. Langemann, F. W., C. L. Comar and R. H. Wasserman (1957): Absorption of calcium and strontium from milk and nonmilk diets. Jour. Nutrition, Vol. 61, no. 4.
15. Rosenthal, H. L. (1957): Uptake of Ca^{45} and Sr^{90} from water by fresh water fishes. Science, Vol. 126, pp. 669-700.

16. Sanger, L., M. Maqsood, A. B. Medlen and C. L. Comar (1957): Endogenous and biliary excretion of calcium-45 and Strontium-89. Arch. Biochem. Biophys. Vol. 66, no. 2.
17. Sverdrup, H. U., M. W. Johnson and R. H. Fleming (1949): The Oceans. Prentice-Hall, Inc. New York.
18. Talmage, H. V., J. C. Schooley and C. L. Comar (1957): Differential removal of strontium-85 and calcium-45 from rat skeleton by peritoneal lavage. Proc. Soc. Exp. Biol. Med. Vol. 95, pp. 413-417.
19. Tomiyama, T., S. Ishio and K. Kobayashi (1956): Absorption by *Carassius auratus* of Ca^{45} contained in *Rhizodrilus limasus*. Research on the effects and influences of nuclear test explosions. Jap. Soc. Promotion of Science.
20. Vinogradov, A. P. (1953): The elementary chemical composition of marine organisms. Sears Foundation for marine Research, Yale Univ., New Haven.
21. Wasserman, R. H., C. L. Comar, M. M. Nold and F. W. Lengeman (1957): Placental transfer of calcium and strontium in the rat and rabbit. Amer. Jour. Phsiol. Vol. 189, no. 1.

Records of Oceanographic Works
in Japan Vol. 5, No. 2,
March, 1960

The Feeding Mechanism in Young Fishes

By
Fujio YASUDA
(Fisheries Department, Faculty of Agriculture, University of Tokyo)

Abstract

In this work, the author made a study of the feeding mechanism that take place before the filtering of food by gills in plankton-feeders and before the trapping of food by the mouth cleft in carnivorous fishes.

In another report, the author said that the cleft does the function of trapping and the mouth breadth determines the size of food. Taking this to be true a comparative study on the development of the cleft and the mouth breadth was made.

As the materials, four marine fishes, red barracuda, mackerel, horse mackerel and anchovy and three tropical fishes, *ticto, sumatra* and *blue gourami* were studied. The results obtained are reported here as follows:

1. In the feeding mechanism of fish in their young stages, the mouth structure, especially the cleft and the breadth are very important factors.
2. In the development of the cleft and the breath there can be observed two types. One, where the cleft length and the breadth cross at some stage after hatching. The other, where the crossing does not occur or is not clearly visible.
3. In the first type, during the stage before the crossing has occured, the fish is not active in its feeding habits and only feeds on non active micro food particles. However, the other type begins feeding actively immediately after hatching.

Introduction

The structure of gills in plankton feeders and the mouth structure in carnivorous fishes have already been reported [1][2][3] as the important organs in the feeding mechanism in fishes. In the present work the author made a study of the feeding mechanisms in young stage of fishes that take place before the filtering of food by gills in plankton feeders and before the trapping of food by the mouth in carnivorous fishes. It was also mentioned in the other report that in the trapping of food by carnivorous fishes, the mouth cleft has the function of trapping the prey and the mouth breadth determines the size of the prey. On the other hand, in the case of young stage of plankton feeders it is thought that the gills do not work as the filtering organs of food but the required food is trapped by the mouth. As these fish grow to become adults they differ from the carnivor-

ous fishes in that their food order being very low and in order to obtain sufficient quantity of food to maintain life it becomes necessary to filter large quantities of food by the gills. As such, the feeding mechanism in young fish, both plankton feeders and carnivorous fishes, is mainly the trapping of food by the mouth. Even in their young stages there is certain period when some fishes cannot actively carry on the trapping function. During these stages the size of the prey and its activity becomes an important problem. Thus far in the other reports author has said that the cleft does the function of trapping and the mouth breadth determines the size of food. Taking this to be true a comparative study on the development of the cleft and the mouth breadth was made.

Materials and Methods

The sampling or experimenting of young or larval forms of marine fish is an exceptionally difficult task. A lot of difficulties were experienced in the collecting of these samples. The smallest possible body size of the following fishes were sampled: red barracuda (*Sphyraem pinquis*), mackrel (*Scomber japonicus*), horse mackrel (*Trachurus japonicus*) and anchovy (*Engraulis japonica*). The size of the cleft and the mouth breadth of these samples were measured. To check the measurements made in this experiment a sub-experiment along with the first was carried out on the following samples of tropical fish: ticto (*Barbus ticto*), sumatra (*Barbus tetrozona*) and blue gourami (*Trichogaster tricopterus*). These tropical fish easily lend themselves to laboratory experimentations.

Of the two tropical fresh water species, blue gourami (*Trichogaster tricopterus*) and ticto (*Barbus ticto*), the graph showing the growth of cleft and the growth of the mouth breadth cross when the total length of the fish is between 4

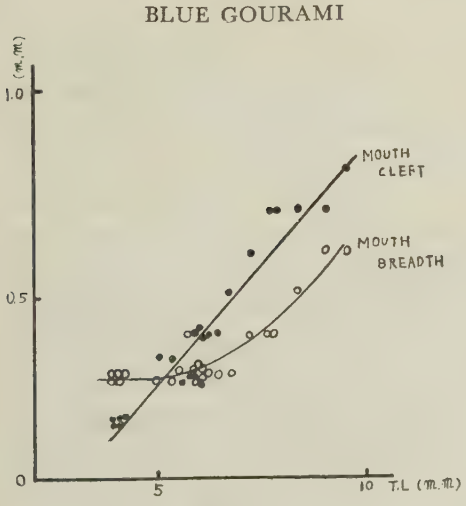

Fig. 1.

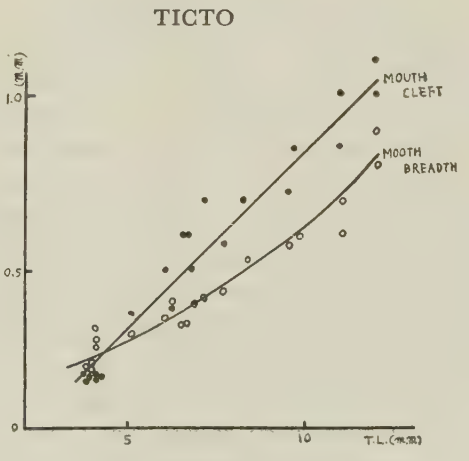

Fig. 2.

to 5 mm. From this crossing point onwards the cleft grows faster than the mouth breadth (Fig. 1 & 2). In sumatra (*Barbus tetrozona*) the cleft and the mouth breadth are of the same size from the beginning and they grow at equal rates (Fig. 3). However, to determine this crossing point in marine fish, i.e. the size of fish when the cleft length and the mouth breadth length are equal, no small samples were available. As such this crossing point was estimated from the graph. The crossing point in anchovy (Fig. 4) was estimated to be when the

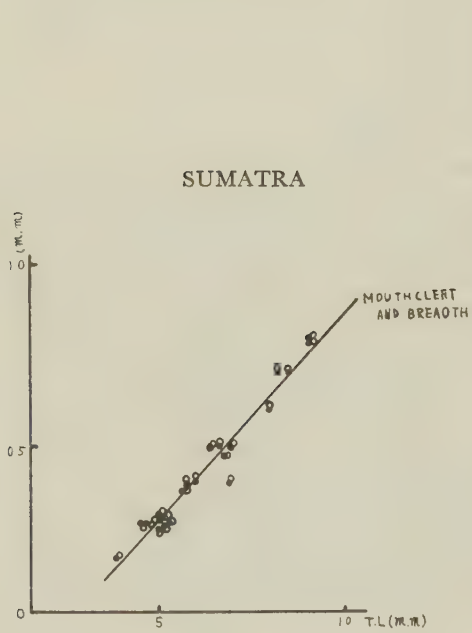

Fig. 3.

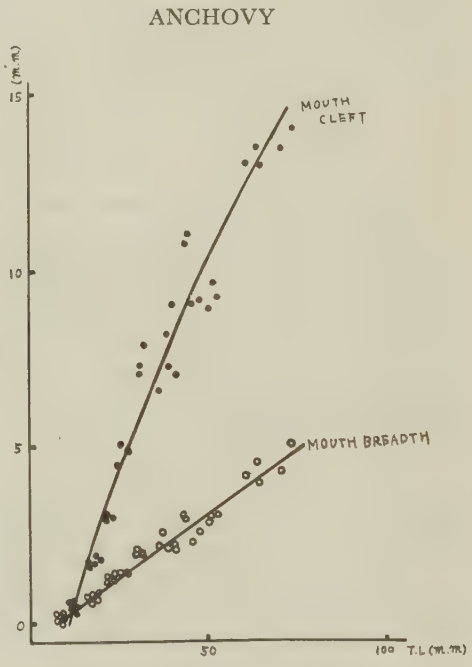

Fig. 4.

total length of the fish is about 10 mm. In the case of red barracuda, (Fig. 5), mackrel (Fig. 6) and horses mackrel (Fig. 7) the crossing point could not be obtained from the graph and this was thought to be because the two measurements do not cross at any time or other. If from the point of trapping mechanism the above mentioned facts are considered, it is possible that for lengths less than those crossing point the food taken is not the function of the trapping mechanism but the food is taken in by the mouth by chance. Hence when the total length of the fish is above those crossing point the cleft grows faster than the mouth breadth and it becomes possible to trap food. And the total length of the fish when it is possible to trap the food is: in ticto about 4 mm. in blue gourami 5 to 6 mm. and in anchovy about 10 mm. At this length the trapping of food becomes active. In red barracuda, mackrel and horse mackrel the changing over from the postlarval to the larval form may be considered as the period from when the trapping of food becomes active.

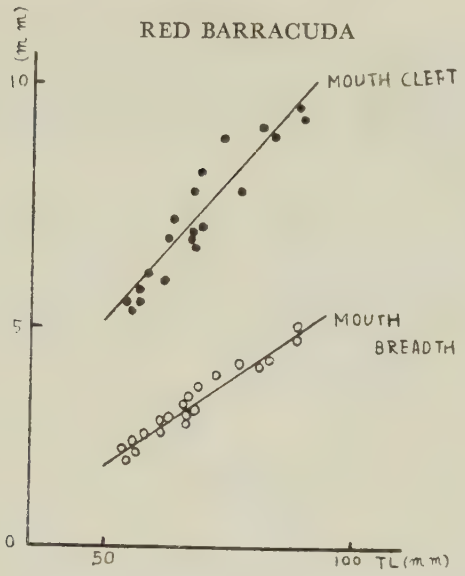

Fig. 5.

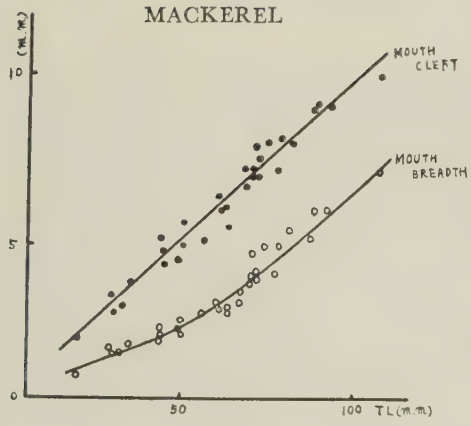

Fig. 6.

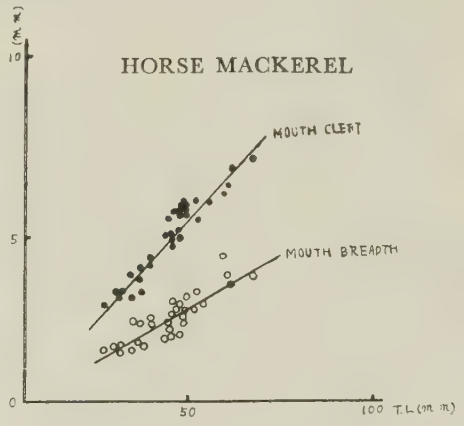

Fig. 7.

Experiment

The above mentioned facts were clarified experimentally. The samples for this experiment were: blue gourami, sumatra, and ticto. Adults of the two sexes of these samples were bred and the hatched out larval ones were fed on *Paramecium caudatium* (8.18 × 0.06 mm) and brine shrimp (*Artemia salina*) (0.38 × 0.16 mm). These were selected as food for the fish because it was thought that *Paramecium* is a non active food and brine shrimp is a good example of an active food. In ticto the total length immediately after the absorption of the yolk sack was almost 4 mm. From the figure (Fig. 2) it appears that from this length

onwards the trapping of food begins. Hatched out ticto was hence put in two tanks and one was fed on *Paramecium* only and the other on brine shrimp. The group that was fed on brine shrimp ate well from the beginning. After one month when the total lengths of the two groups were measured it was found that both were closely equal.

Total length (mm.) after one month (95% confidence limits).

Fed on *Paramecium*	11.16 ± 0.84
Fed on brine shrimp	10.96 ± 0.26

The results of the experiment substantiate the fact that after 4 mm. of total length, the trapping function becomes active.

The same kind of experiment was also conducted for blue gourami. The total length after the absorption of the yolk sack for this fish is about 3 mm. Even from the consideration of the size of the mouth breadth it is not possible for this fish to feed on brine shrimp. As such the fish were first fed on *Paramecium*, and later brine shrimp was added gradually every day. This was done to find out when the fish started to eat brine shrimp. This was observed to be after 10 days of hatching out when the total length was about 5 to 6 mm. This length agreed very closely with the length at the crossing point that was determined graphically.

In the case of sumatra it was observed that, immediately after the absorption of the yolk sack the fish actively feeds on brine shrimp. This experimental result agreed closely with that obtained graphically. In this graphically method it was shown that the total length of the fish when trapping for food begins and becomes active is that length when the cleft length and breadth length are equal. This shows that the experimental results are in full agreement with the theoretical hypothesis. From these results it will be seen that, in some fishes where at a certain stage the cleft length and the breadth length cross, it is very necessary to feed these fishes with a large amount of minute sized food till the crossing point is reached. This is necessary so that the chances of eating the food particles become great.

Results

From the length measurement analyses and the experiment results of the young fishes, whether at a certain stage the cleft length and breadth length are equal (crossing point), if these lengths are equal at a certain stage, the stage at which they are equal, and the relation of this to the feeding mechanism have become clear. In this experiment some fishes did not show the crossing point. In such cases the crossing point has to be determined graphically and also by a survey of the stomach contents. Other than these the author feel that there

are no other possible methods. In anchovy this stage as determined graphically is about 10 mm. From this length onwards it is believed that the anchovy traps food actively. Anchovy's post-larval stage has been said to be between 4 to 18 mm. Hence between this range is the period when the trapping for food is begun actively. In the survey made on young anchovy under 18 mm. total length, the stomachs were mostly empty. This may be because in this length range the anchovy feeds mostly on minute food particles and as such these were not observable in the stomach contents. In red barracuda, mackrel and horse mackrel, similar to sumatra, the food is actively trapped immediately after the absorption of the yolk sack. Hence from these results to conclude that the trapping function begins after the crossing point is a reasonable hypothesis.

Discussion

For a clear understanding of the breeding and culturing possibilities of fish, studies on their feeding habits is of prime importance. Nevertheless in the study of the feeding habits of fish, the study on the feeding habits of young fish, especially in the larval stages of marine fish, are very difficult. This is so because the sampling of the larval forms in the sea cannot be easily carried out and further the transportation of these larval forms to the laboratory has always resulted in happy consequences. Also the artificial insemination of oceanic fishes in the laboratory is very difficult.

In a study of the resources of fish and its population dynamics, along with other factors, a study of the feeding habits of the larval forms is very important. In this work the feeding mechanism of the samples mentioned were studied earlier. As marine samples were difficult to be obtained and studied, from the results obtained by the study of tropical fish, the feeding mechanism of the marine fishes were assumed. The mouth structure (cleft and breadth) is an important factor in the feeding mechanism of carnivorous and omnivorous fishes. In the case of plankton feeders the gill structure is the most important factor. During the young stages, even in plankton feeders the filtering action by the gills in the feeding mechanism does not occur. In the surveyed young stages there were two types. One type is that where the cleft length and the breadth length cross at some stage. The other is that where this crossing does not occur or is not clearly visible as in the former. The type where crossing occur are plankton feeders. The other type are either carnivorous or omnivorous. In the case of the plankton feeders the availability of micro food particles both in quality and quantity are important factors that determine the future life of the fish. That these types of food, both in quality and quantity are available in ample amounts in the oceans show that the fish in the oceans have enough food for survival and growth.

Summary

(1) In the feeding mechanism of fish in their young stages, the mouth structure, especially the cleft and the breadth are very important factors.

(2) In the development of the cleft and the breadth there can be observed two types. One where the cleft length and the breadth length cross at some stage after hatching. The other where the crossing does not occur or is not clearly visible.

(3) In the first type, during the stage before the crossing has occured, the fish is not active in its feeding habits and only feeds on non active micro food particles. However, the other type begins feeding actively immediately after hatching.

Literature

(1) Y. Hiyama & F. Yasuda (1957): The mechanism of utilization of plankton by fishes. Records of Oce. Works Jap. Sp. No.)

(2) F. Yasuda & Y. Hiyama (1957): Mechanism of utilization of plankton by some fishes. Records of Oce. Works Jap. Vol. 3 No. 1)

(3) F. Yasuda (1960): The feeding mechanism in some carnivorous fish (in press)

(3) M. V. Lebour (1920): The food of young fishes (iii) J.M.B.A. 12 (2).

(5) T. Chiba (1956): Studies on the development and systematics of copepoda (Jour. of the Shimonoseki Fish. College, Vol. 6, No. 1).

Records of Oceanographic Works
in Japan Vol. 5. No. 2,
March, 1960

The Relationship of the Gill Structure and Food Habits of Some Coastal Fishes in Japan.

By
Fujio YASUDA
(Fisheries Department, Faculty of Agriculture, University of Tokyo)

Abstract

The gill in fishes, in the case of plankton-feeders are important organs for filtering food.

It has been said that structure and number of gill rakers differ with different fishes, and the more active the feeding habits of the fishes is, the less developed the gill rakers are. There has also been cases where the gill rakers are absent and in all such cases the fish have been found to be very active feeders, feeding on anything.

The author in this study examined the developmental changes of the gills and its relationship to the food habits of the fish in 21 species of coastal fishes of Japan.

Introduction

The gill in fishes are important organs of respiration. Apart from this main function, they also perform the work as filtering organs of food in the case of plankton-feeders. In the respiratory function, the gill filaments play the most important part, and in the filtering of food the gill rakers are all the more important. The gill rakers are on the upside of the gill arch and on the under side of the gill arch are the gill filaments (Fig. 1).

In the feeding mechanism of the plankton-feeders, which regards as the filtering function are the gill rakers and the gill sieves and the processes* found on these two parts. These together with the processes form a mesh and thereby filter food. It has been said that the structure and number of gill rakers differ with different fishes, and the more active the feeding habit of the fish is, the less developed the gill rakers are. There has also been cases where the gill rakers are absent and in all such cases the fish have been found to be very active feeders, feeding on anything.

The author in this study examined the developmental changes of the gills and its relationship on the food habits of the fish in 21 species of coastal fishes in Japan. The results of this study are reported here.

The author wishes to exprese his thanks to Prof. Yoshio HIYAMA for his guidance.

* E. SCOFIELD (1934) has named it "straining processes."

Materials

The 21 species studied here are the following:

No.	Scientific name	Common name	Local name
1	*Etrumeus micropus* (T & S)*	Round herring	Urume-iwashi
2	*Sardinops melanosticta* (T & S)*	Sardine	Ma-iwashi
3	*Harengula zunasi* Bleeker*		Sappa
4	*Engraulis japonica* (Houttuyn)*	Anchovy	Katakuchi-iwashi
5	*Cololabis saira* (Brevoort)*	Skipper or Saury	Sanma
6	*Allanetta bleekeri* (Gunther)		Togoro-iwashi
7	*Mugil cephalus L*	Mullet	Bora
8	*Sphyraena pinguis* Gunther	Red barracuda	Aka-kamasu
9	*Scomber japonicus* Houttuyn*	Mackerel	Ma-saba
10	*Trachurus japonicus* (T & S)*	Horse mackerel	Ma-aji
11	*Seriola quinqueradiata* T & S	Yellowtail	Buri
12	*Oplegnathus fasciatus* (T & S)	Japanese parrot fish	Ishi-dai
13	*Upeneus bensasi* (T & S)	Goatfish	Himeji
14	*Apogon niger* Döderlein		Kuro-ishimochi
15	*Apogon lineatus* (T & S)	Indian perch	Tenjiku-dai
16	*Scombrops boops* (Houttuyn)		Mutsu
17	*Sillago sihama* (Forskal)	Smelt	Kisu
18	*Girella punctata* Gray		Mejina
19	*Mylio macrocephalus* (Basilewsky)	Black snapper	Kuro-dai
20	*Acanthogobius flabimanus* (T & S)	Goby	Ma-haze
21	*Hypodytes rubripinnis* (T & S)	Tiny stinger	Ha-okoze

Shape and structure of the gills and the shape of the processes on the gill rakers

It has already been mentioned earlier that the structure which carry out the feeding mechanism is the gill rakers, the gill sieves and the processes on these two parts. These form a mesh and do the filtering function necessary in the feeding mechanism (Fig. 1-3).

In the elasmobranchs there are 5-7 pairs of gill arches, but in teleostei the gill arches are cartilage and the first four pairs are similar to that of the elasmobranchs and the last rudimentary pharyngobranchial cartilage is changed to the suspensory pharyngeal and this is mostly toothed.

The most posterior gill arches are small in size. The upper gill arch is made up of the epibranchial and pharyngobranchial and the lower gill arch

* Already reported by F. YASUDA and Y. HIYAMA (1957).

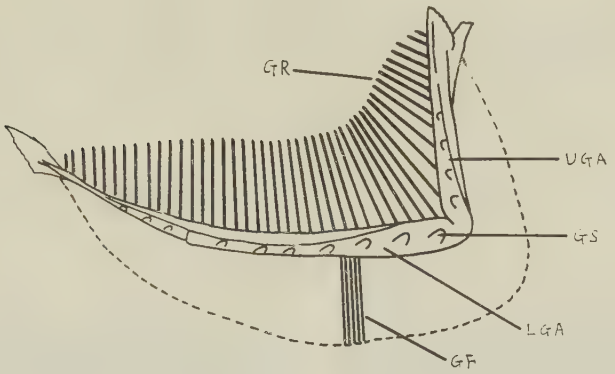

Fig. 1. Structure of the gill (plane figure 1st gill arch)
GR—Gill raker GS—Gill sieve GF—Gill filament
UGA—Upper gill arsh LGA—Lower gill arch

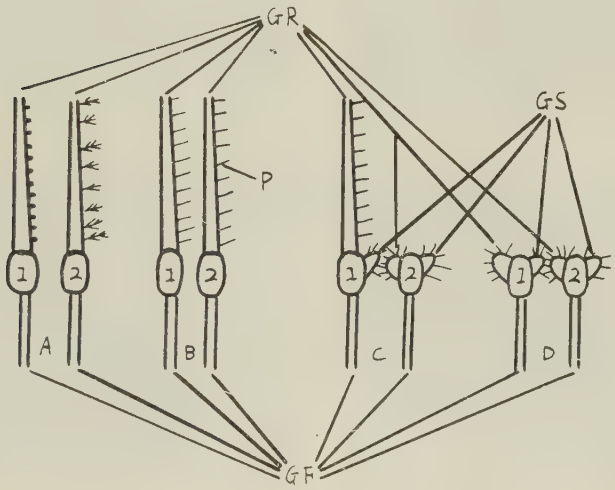

Fig. 2. Structure of the gill (Cross section)
GR—Gill raker GS—Gill sieve GF—Gill filament P—Process
1—1st gill arch 2—2nd gill arch A—Herbivorous fish
B & C—Plankton feeder D—Carnivorous fish

is made up of the hypobranchial and ceratobranchial. The upper and lower gill arches are jointed by a hinge joint which facilitates movement. In sardine and such plankton-feeders that have to open their mouth widely in order to draw a large amount of water for filtering the plankton, or in Apogonidae, a mouth breeder and hence has to open its mouth widely, there is another joint in the lower gill arch to enable the mouth to be opened more widely. However, even in the mackerel species, the vestiges of a joint in the lower gill arch could be seen if it is dyed with alizarin sodium sulfonate.

The movement of the upper and lower gill arches controls the mesh size of gills. The processes on the gill rakers are placed pointing upwards and

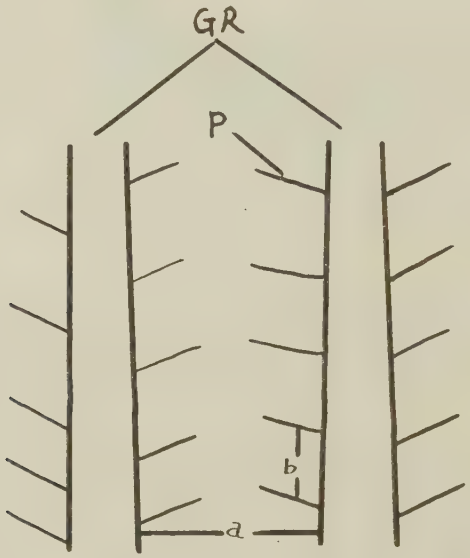

Fig. 3. Structure of the gill mesh (plane figure)
GR—Gill raker P—Process a—Interval of gill raker b—Interval of process

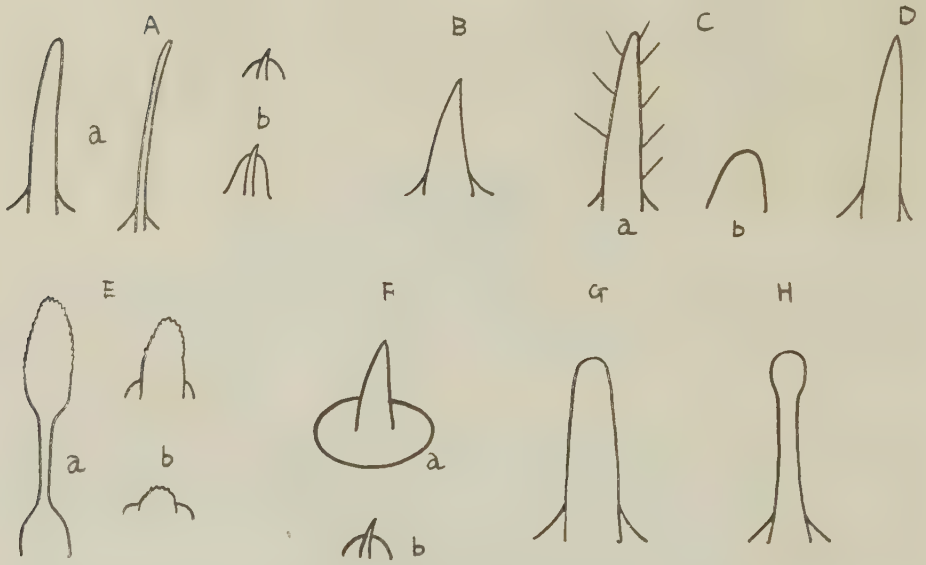

Fig. 4. Shape of the processes
A—Mackerel (a–adult b–young) B—skipper C—Mullet (a–2nd gill arch, b–1st gill arch)
D—Yellowtail E—Sardine (a–adult b–young) F—"SAPPA" (a–adult b–young)
G—Tiny stinger H—"KUROISHIMOCHI"

toward the mouth opening. The arrangement of the processes on the gill rakers are not completely symmetrical and are of various types (Fig. 4). The second and consequent gill arches are sometimes similar to the first gill arch, but generally are degenerated. However in *Mugil cephalus*, on the contrary, the first gill arch is generally degenerated and the consequent gill arches are well developed (Plate 1 A-C). Further, as in sardine (Plate 2), there are fishes where the processes on the gill rakers change in shape with the growth of the fish.

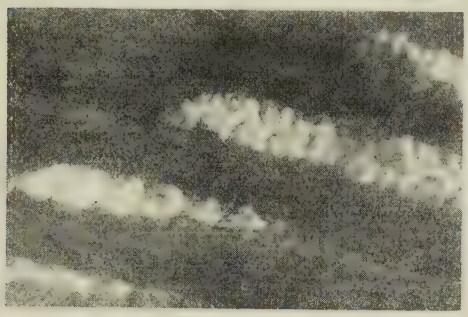

Plate 1–A.

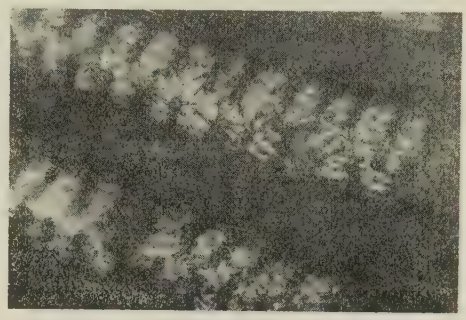

Plate 1–B.

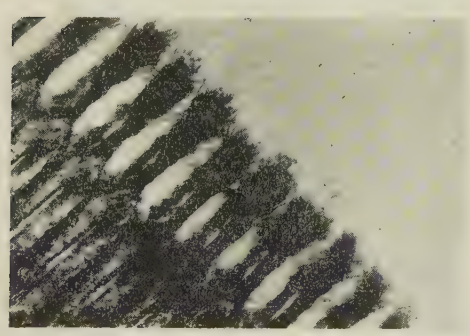

Plate 1–C.

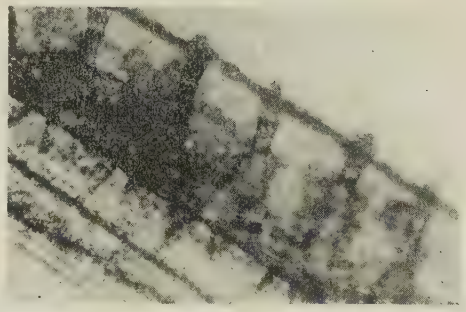

Plate 2.

Plate 1. Processes of *Mugil cephalus* L
A, Processes and gill raker of 1st gill arch (BL. 3.4 cm) B, Processes and gill raker of 2nd gill arch (BL. 6.0 cm) C, Side view of gill raker of 2nd gill arch (BL. 22.4 cm).

Plate 2. Processes of *Sardinops melanosticta* (T&S)
Processes and gill raker of 1st gill arch (BL 19.2 cm)

NAKAI (1938) has pointed out that the changes in the shape of the processes have a difinite relationship to the changes in the food habits of sardine.

The gill sieves are on the inside of the gill and they are situated on the each gill arch at the base of the gill rakers. The number of these gill sieves are very few and they are irregularly arranged. From the observations made, it was generally found, that the gill sieves of the 2nd and consequent gill arches were undeveloped in all cases where the gill rakers were developed and vice-versa (Table 1.) The gill rakers and the gill sieves together on each gill arch per-

form the function of filtering. These structures are shown in Figure 2.

Table 1. Characteristics of gills.

No.	Species / Character	Gill rakers other than 1st gill arch	Gill sieves other than 1st gill arch	No. of joints in 1st gill arch	Arrangement of processes	Time of development of process BL. (cm)	Time the gill raker become constant BL. (cm)
1	*Etrumeus micropus* (T & S)	+	−	2	×	3	*
2	*Sardinops melanosticta* (T & S)	+	−	2	○	3	9〜
3	*Harengula zuuasi* Bleeker	+	−	2	×	3	*
4	*Engraulis japonica* (Houttuyn)	+	−	2	×	3	8〜
5	*Cololabis saira* (Brevoort)	−	+	1	×	4	5〜10
6	*Allanetta bleekeri* (Gunther)	−	+	1	×	*	*
7	*Mugil cephalus* L	+	−	1	○	3	*
8	*Sphyraena pinguis* Gunther	−	−	2	※	※	5
9	*Scomber japonica* Houttuyn	−	+	1	×	3	7〜9
10	*Trachurus japonicus* (T & S)	−	+	1	×	3	6〜9
11	*Seriola quinqueradiata* (T & S)	−	+	1	×	3	5
12	*Oplegnathus fasciatus* (T & S)	−	+	1	×	3	3
13	*Upeneus bensasi* (T & S)	−	+	1	×	*	*
14	*Apogon niger* Döderlein	−	+	2	×	*	*
15	*Apogon lineatus* (T & S)	−	+	2	×	*	*
16	*Scombrops boops* (Houttuyn)	−	+	1	×	3	5〜7
17	*Sillago shihama* (Forskal)	−	+	1	×	2	5
18	*Girella punctata* Gray	−	+	1	×	2	*
19	*Mylio macrocephalus* (Basilewsky)	−	+	1	×	2	3
20	*Acanthogobius flabimanus* (T & S)	−	+	1	※	※	*
21	*Hypodytes rubripinnis* (T & S)	−	+	1	×	*	*

Note: + Developed − Undeveloped ○ Mostly symmetrical × Asymmetrical
※ No process * Data insufficient

From these it may be seen that in coastal fishes the gills are variously shaped. Especially in the plankton-feeders, the feeding habits and gill structure is closely related. Hence to make it convenient to compare and discuss the gill structure and feeding habit in the next chapter, the gills have been classified as shown in Figure 5. Through this method it was possible to group the 21 species under study as represented in Table 2. Further, from Figure 5 it was learnt that with type D as the demarkation to types, these above it were found to be plankton-feeders and those below were carnivorous fishes.

The developmental changes of the gill structures in relation to growth, of the 21 species of fish surveyed are shown in Figure 6.

Table 2. Classification of gills. (see Figure 5)

Type	Species
A	*Sardinops melanosticta* (T & S)
B	*Engraulis japonica* (Houttuyn) *Harengula zunasi* Bleeker *Etrumeus micropus* (T & S)
B′	*Mugil cephalus* L
C	*Cololabis saira* (Brevoort)
D	*Scomber japonicus* Houttuyn *Trachurus japonicus* (T & S)
D′	*Girella punctata* Gray *Mylio macrocephalus* (Basilewsky) *Oplegnathus fasciatus* (T & S) *Scombrops boops* (Houttuyn) *Seriola quinqueradiata* (T & S) *Sillago shihama* (Forskal)
E	*Apogon niger* Döderlein *Apogon lineatus* (T & S)
F	*Upeneus bensasi* (T & S) *Acanthogobius flabimanus* (T & S) *Hypodytes rubripinnis* (T & S)

Note: B′ and D′ are very similar to B or D respectively but different from C or E type.

Feeding habit

A survey of the stomach contents of the 21 species were made at various localities and at different seasons and from the results obtained the following table was made (Table 3).

As in the fishes examined, there were both young and adult ones, and hence the gill structures being in various stages of development, the table was divided into two categories, namely A and B, where all fishes with considerably well developed gill structures were included in group A and those with undeveloped gill structures in group B. From the stomach contents survey, the stomach contents were classified into five groups, namely:

1. Fish
2. Bottom living animals
3. Large plankton
4. Small plankton
5. Non active food

Table 3. Food organisms.

	Species	Range of B.L. (cm)	1		2			3					4							5						
	Food organisms.		Fish Muscle	Cephalopoda	Shrimp	Annelida	Shell	Euphausia	Mysidacea	Other Crustacea	Megalopa	Amphipoda	Ostracoda	Polychaeta	Isopodae	Phyllopoda	Copepoda	Jelly-fish	Fish-larva	Bivalve shelled larva	Gastropod shelled larva	Sagitta	Thaliacea	Fish-egg	Sea-weeds	Phytoplankton
Piscivorous fish	*Sphyraena pinguis* Gunther	A 6~21	73						27	3							1									
		B 3~ 5	50						66								3									
	Scombrops boops (Houttuyn)	A 6~16	55						21								5									
		B 2~ 5	22						89																	
	Seriola quinqueradiata (T & S)	A 6~18	50																							
		B 2~ 5	30														67									
Omnivorous fish	*Mylio macrocephalus* (Basilewsky)	A 6~19										19					14								5	
		B 2~ 5	25		25												25									50
	Oplegnathus fasciatus (T & S)	A 6~12				13	7					13														
		B 2~ 5			10						20						50									10
	Girella punctata Gray	A 6~16				18			9			9					73								73	21
		B 2~ 5				7						7				7	50								57	7
	Scomber japonicus Houttuyn	A 6~31	33	2	2				33		6	1						6				4				
		B 2~ 5	75						13		6						3					6		10		
Carnivorous fish	*Sillago sihama* (Forskal)	A 6~15			3	62			7			3		7	3									3		
		B 1~15	6						50				11				33			6						
	Hypodytes rubripinnis (T & S)	A 6~ 8			25				13		13	13														
		B 5~			27	18					18	18	9													
	Acanthogobius flavimanus (T & S)	A 9~14				27						9														
Plankton feeder	*Etrumeus micropus* (T & S)	A 7~19							29		3					32	42									
	Trachurus japonicus (T & S)	A 6~26	23	8								4	8			2	2			8		6		13		
		B 2~ 5															62		52	22		4				
	Allanetta bleekeri (Gunther)	A 8~11														7	27			7						
	Apogon lineatus (T & S)	A 6~ 7																						100		
		B 1~ 5															100									
	Cololabis saira (Brevoort)	A 6~31						15					5				82						14			22
		B 2~ 5															50									
	Engraulis japonica (Houttuyn)	A 6~13							2		4	8	12			21	75			2	6	13		4		58
		B 2~ 5														44	83			57	4	4				100
	Sardinops melanosticta (T & S)	A 6~21											39			43	90	2	2	5		4		36		63
		B 3~ 5											76			81	95		5	10				10		43
	Upeneus bensasi (T & S)	A 6~							36			7	57			7	57									
		B 4~ 5							20			20	80				100									

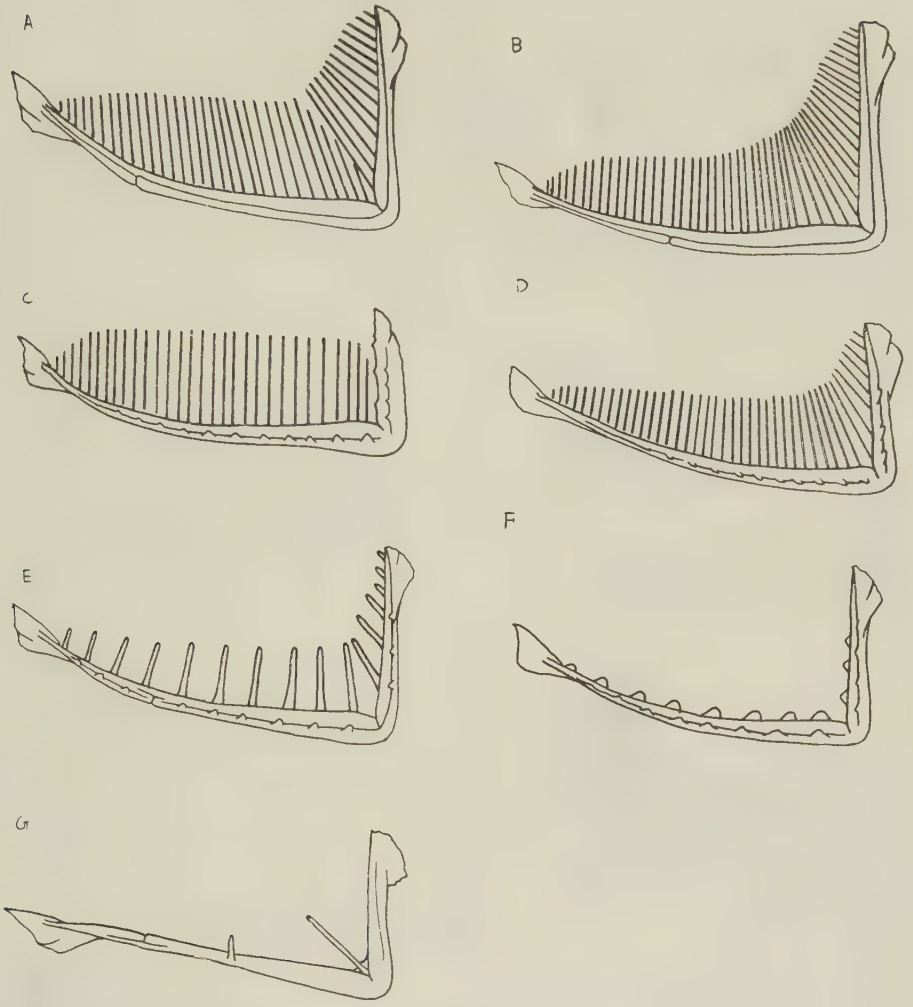

Fig. 5. Classification of gills

The number in the table are in percentages and they have been calculated thus:

$$\frac{\text{Number of fish feeding on a particular organism}}{\text{Number of fish surveyed}} \times 100$$

From the above calculation method it must be understood that the quantity of the fed organism has not been taken into consideration, but only whether the said organism was fed on by the fish or not.

In the case of *Mugil cephalus*, *Harengula zunasi* and *Apogon niger*, the number of individuals surveyed were very few, and hence only whether the fish fed on a particular organism or not has been mentioned in table 4.

Table 4.

Species	Food organisms
Harengula zunasi Bleeker	Mysidacea, Ostracoda, Copepoda, Phyllopoda, Phytoplankton.
Mugil cephalus L	Copepoda, Gastropoda shelled larva.
Apogon niger Döderlein	Mysidacea.

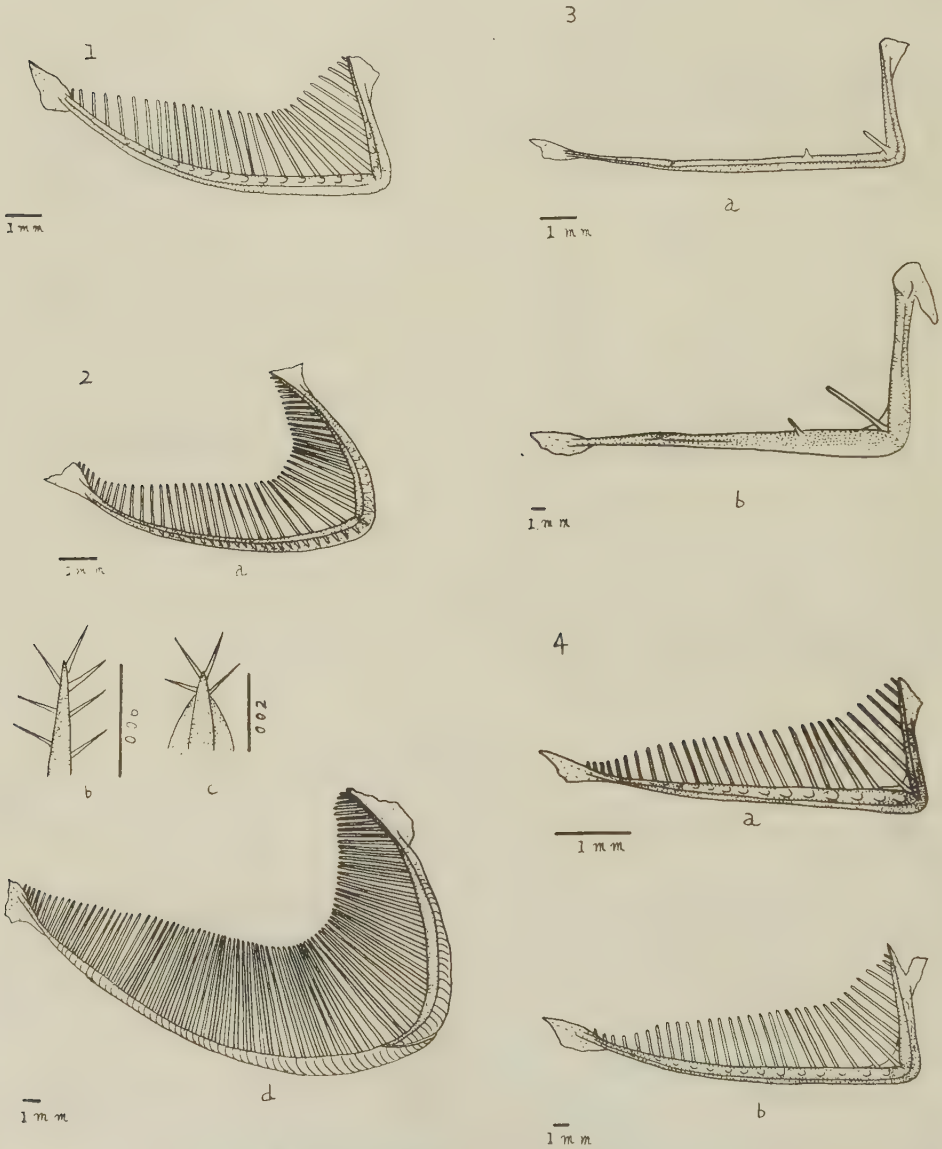

Fig. 6. Gill structure of some fishes

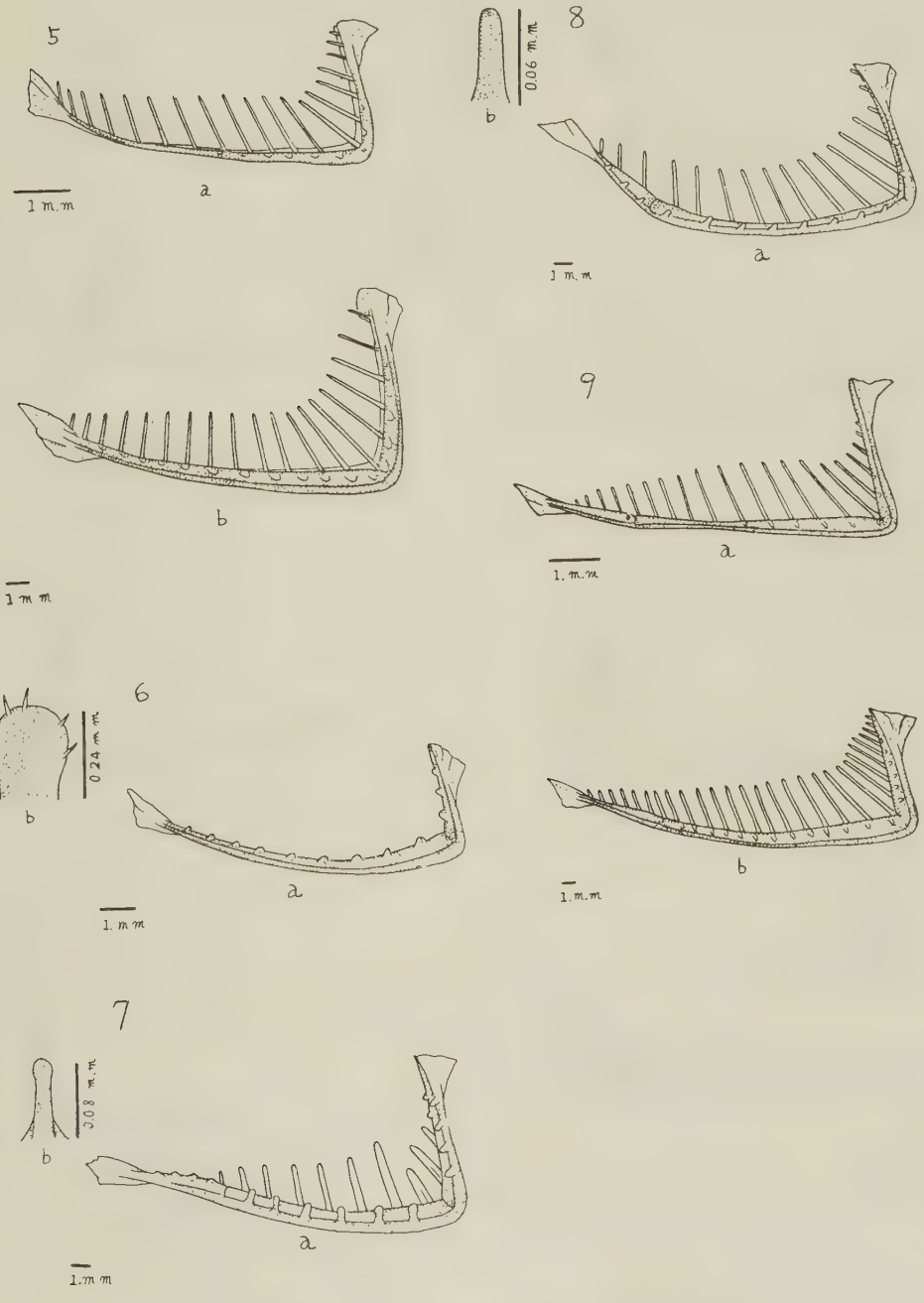
5
1 m.m
a
8
0.06 m.m
b
1 m.m
a
b
1 m m
9
a
1. m.m
6
0.24 m.m
b
a
1. m m
b
1. m.m
7
0.08 m.m
b
a
1. m m

Fig. 6–b.

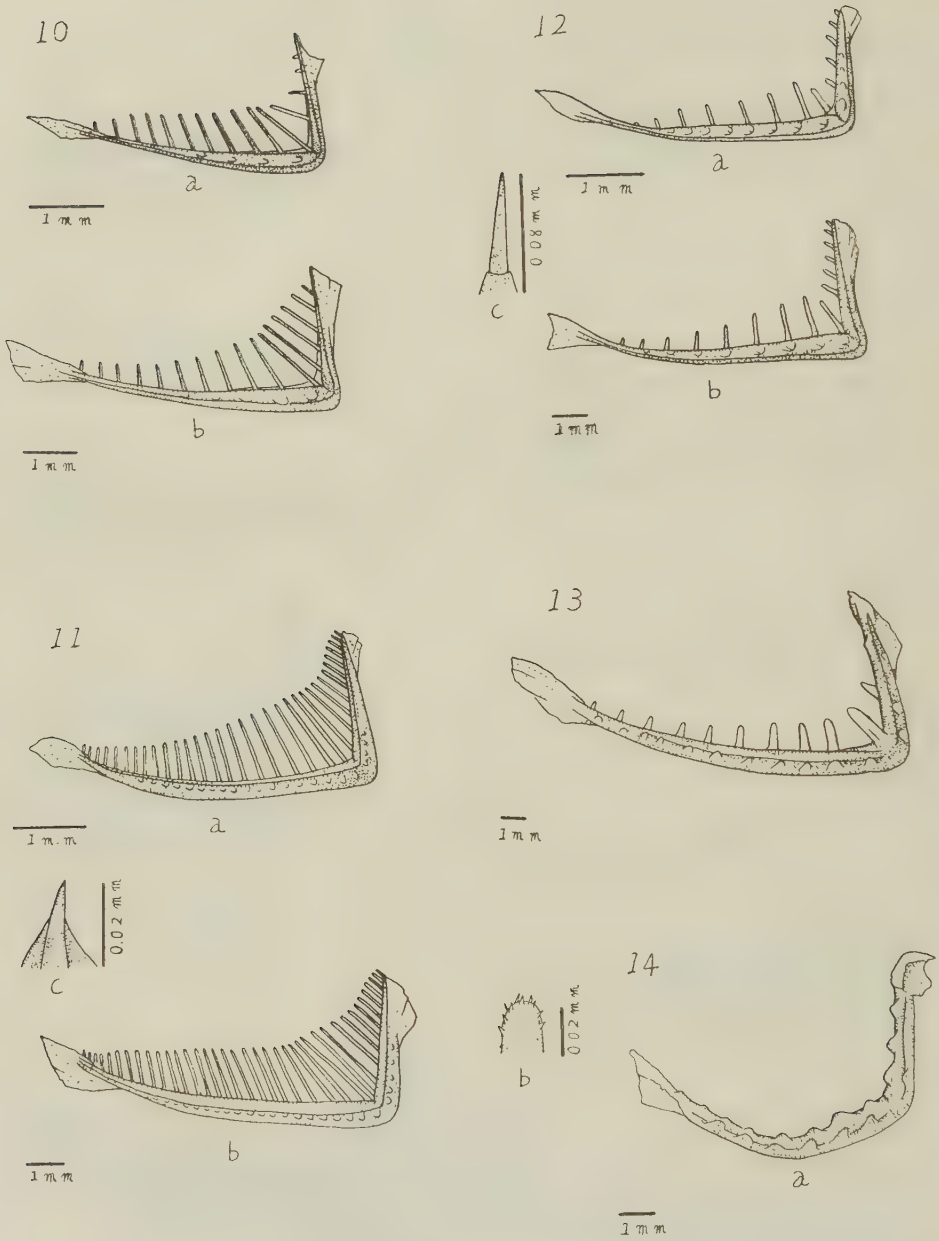
10
a
1 m m
b
1 m m
12
a
1 m m
0.08 m m
c
b
1 m m
11
a
1 m m
0.02 m m
c
b
1 m m
13
1 m m
14
0.02 m m
b
a
1 m m

Fig. 6–c.

Explanation of Figure 6. Gill structure of some fishes

No.	Species	Body length (cm)	Remarks
1	*Etrumeus micropus* (T & S)	10.7	
2 a	*Mugil cephalus* L	6.0	
b		6.0	Process on the gill raker (2nd gill arch)
c		3.4	Process on the gill raker (2nd gill arch)
d		22.4	
3 a	*Sphyraena pinguis* Gunther	6.1	
b		23.8	
4 a	*Seriola quinqueradiata* (T & S)	2.3	
b		13.5	
5 a	*Oplegnathus fasciatus* (T & S)	3.5	
b		11.0	
6 a	*Upeneus bensasi* (T & S)	6.2	
b		6.2	Process and gill raker of 1st gill arch
7 a	*Apogon niger* Döderlein	8.2	
b		8.2	Process on the gill raker (1st gill arch)
8 a	*Apogon lineatus* (T & S)	7.3	
b		7.3	Process on the gill raker (1st gill arch)
9 a	*Scombrops boops* (Houttuyn)	5.9	
b		14.3	
10 a	*Sillago sihama* (Forskal)	3.0	
b		6.0	
11 a	*Girella punctata* Gray	6.0	
b		3.5	
c		6.0	Process on the gill raker (1st gill arch)
12 a	*Mylio macrocephalus* (Basilewsky)	2.4	
b		6.2	
c		6.2	Process on the gill raker (1st gill arch)
13	*Acanthogobius flabimanus* (T & S)	12.5	
14 a	*Hypodytes rubripinnis* (T & S)	7.3	
b		7.3	Process and gill raker of 1st gill arch

* Note: Viewed from inside of gill arch.

Relationship between gill structure and feeding habits

In order to study the gill structure of the 21 species, the interval between gill rakers and the interval between gill processes were supposed to represent

the gill structure sufficiently well and hence a comparative study of these were made. Those fish feed mainly on small planktons. As has been said earlier, the first gill arch is generally well developed and those following are not well developed. There are also cases where the 2nd, 3rd and 4th gill arches are also well developed. In such cases, where the 2nd, 3rd and 4th gill arches overlap, the mesh sizes are even smaller than that in the first gill arch and hence these fishes can filter even minute particles of food organisms. This shows that a study on the development of the gill raker, gill sieves and gill processes of the first gill arch only will be totally insufficient to draw a relationship between gill structure and feeding habit.*

It is still believed that there is not always direct relationship between gill structure and food. However in this study on 21 species, it has been found that the gill structure has a direct bearing on the feeding habit. Like the sardines, fish which have a fine gill structure are all plankton-feeders and those with coarse gill structure, (loose and open mesh) are generally carnivorous fishes. If Figure 5 and Table 2, namely on gill classification, are observed together with Table 3, on stomach contents, the following facts become apparent. Plankton-feeders fall into the A and C types in Figure 5, and carnivorous and omnivorous fishes fall into type D and below, piscivorous fishes especially come under type G. These grouping of types show that there is a difinite relationship between gill structure and the feeding habit. When the gill structure and stomach contents of the adults and the young are treated separately, in the case of plankton-feeders the young fish where the gills are still undeveloped the food is generally trapped by the mouth. As the development of the gill proceed this trapping method of feeding gives way to the filtering of food by the gills. That is, in carnivorous fishes the young fish feed on small food organisms and it grows it begins to feed on large organisms. On the contrary, in plankton-feeders, as we have just seen, the young fish traps food organism and as it becomes an adult it filters even minute planktons. From these facts it becomes very apparent that in a study on the relationship to gill structure and food, another factor, of growth and development of the fish, has to be given every importance.

Literatures

(1) J. NAKAI (1938) Comparative study of the gill structure and food of sardine. (in japanese) (Jour. of Fisheries Research Vol. 33 No. 12)

(2) E. SCOFIELD (1934) Early life history of the california sardine with special reference to distribution of eggs and larvae. (California Fish and Game Comm. Fish Bull. No. 41)

(3) F. YASUDA and Y. HIYAMA (1957) Mechanism of utilization of plankton by some fishes (Rec. Oceanographic Works in Japan. Vol. 3 No. 1)

* These mechanisms have already been reported by F. YASUDA and Y. HIYAMA (1957).

Records of Oceanographic Works
in Japan Vol. 5. No. 2,
March, 1960

The Feeding Mechanism in Some Carnivorous Fishes

By
Fujio YASUDA
(Fisheries Department, Faculty of Agriculture, University of Tokyo)

Abstract

The feeding habits of carnivorous fish (especially the trapping of prey) is mostly controlled by the structure of the mouth, which thereby limits the size of the prey.

The feeding habits and relationship of prey size and mouth structure of four important carnivorous fish, mackerel (*Scomber japonicus*Q, big-eye (*Scomber boops*), yellowtail or amberjack (*Seriola quinqueradiata*) and red barracuda (*Sphyraena pinguis*), and for comparative study the anchovy (*Engraulis japonica*), a true example of a plankton feeder found in the coastal waters of Japan were studied by the author and the following results obtained are reported here:—

1. In the feeding mechanism, namely the trapping of prey, the cleft of the predator serves the most important function, and the mouth breadth limits the size of the prey.
2. As regards the size of the prey, the body depth or body width is more important than the total length or body weight of the prey to the predator in case of their trapping.
3. The "proper size" of the prey (body depth or body width) is that size which is almost equal to the size of the mouth bredth of the predator.

Introduction

As regards the feeding mechanism of fishes and especially the plankton feeders in the previous reports,[1][2] it has already been pointed out that the most important organ is the gill structure. However in the case of carnivorous fish the feeding habits (trapping of prey) is mostly controlled by the structure of the mouth, which thereby limits the size of the prey. Studies on the relation between mouth structure and its size of prey are still fragmentary.

CHIBA (1956) studied on the relationship between growth and the size of cleft and mouth breadth of anchovy (*Engraulis japonica*), but he did not take into consideration the size of food of the anchovy. HAYASŌI (1956) believes that the prey's body shapes (body depth and body width) are important factors.

The feeding habits and the relationship of prey size and mouth structure of four important carnivorous fish mackerel (*Scomber Japonicus*), big-eye (*Scom-*

brops boops), yellowtail or amberjack (*Seriola quinqueradiata*) and red barracuda (*Sphyraena pinguis*) found in the coastal waters of Japan were studied by the author and the findings are reported here.

Mouth structure and feeding mechanism

As material for study the four species mentioned above, and for comparative study the anchovy, a true example of a plankton feeder, were utilised.

The sampling for these species were carried out at various fishing grounds and at different seasons. By thus sampling, about 100 specimens of each species were collected for an analytical study. As those specimens wherein the stomach contents were completely digested or in a decomposed condition are unsuitable for study, several specimens from each species had to be discarded.

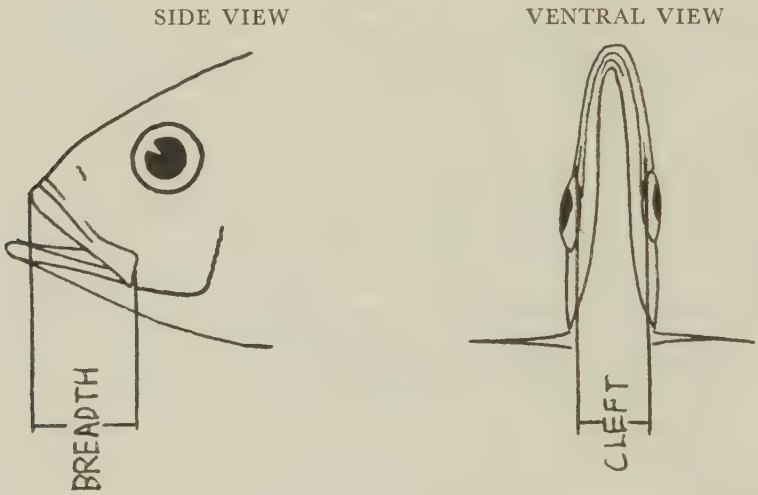

Fig. 1.

In the structure of the mouth, the size of cleft and that of the mouth breadth (Fig. 1) are important factors. The cleft size determins the trapping mechanism or action and the mouth breadth controls the size of prey. Measurements of the mouth breadth of all the specimens from each of the five species were carried out and to know the size of the prey, a survey of the stomach contents were made. From the survey of the stomach contents the maximum and minimum size of the undamaged food (prey) were measured and its relationship to the size of mouth breadth was represented in a graph. In the case of the maximum size of food the total length of the prey was measured and for the minimum size of food the body depth or body width of the prey was measured (Figs. 2-6).

From the graph it may observed that (a) anchovy (Fig. 2), a plankton feeder feeds on food matelials (plankton) that are very much smaller than its mouth breadth. However, (b) for mackerel (Fig. 3) the graph indicating the size of food and the graph indicat ing the mouth breadth overlap. From this graph it may be understood that the size of food and the size of the mouth breadth have very close relationship. In (c) big-eye, yellowtail and red barracuda (Figs. 4-6), while the fish are still young, as in (b) the graph indicating the food size and the graph showing the mouth breadth overlap. However in the adult stage the minimum size of food, i.e. the body depth or body width of the prey (generally fish) falls in line with the mouth breadth. From these results

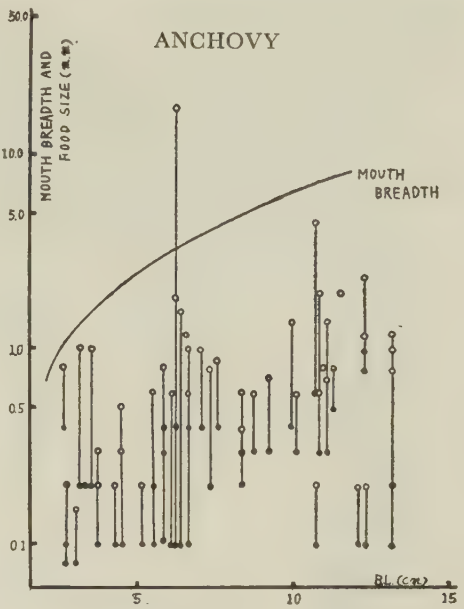

Fig. 2.
○ Maximum size of food
● Minimum size of food

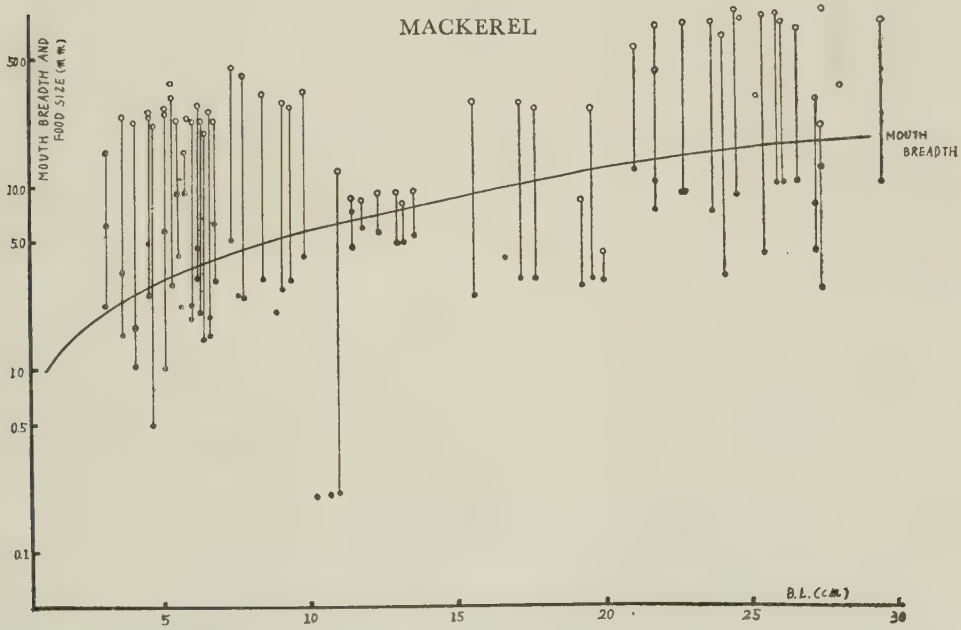

Fig. 3.
○ Maximum size of food ● Minimum size food

it may be inferred that:

(i) Fish which feed on food very much smaller than its mouth breadth, e.g. anchovy, are all plankton.

(ii) Fish, wherein the food size and the mouth breadth overlap are all carnivorous or omnivorous species.

(iii) Fish, wherein the minimum size of food is close to but seldom smaller than the mouth breadth, are all carnivorous and mostly piscivorous species.

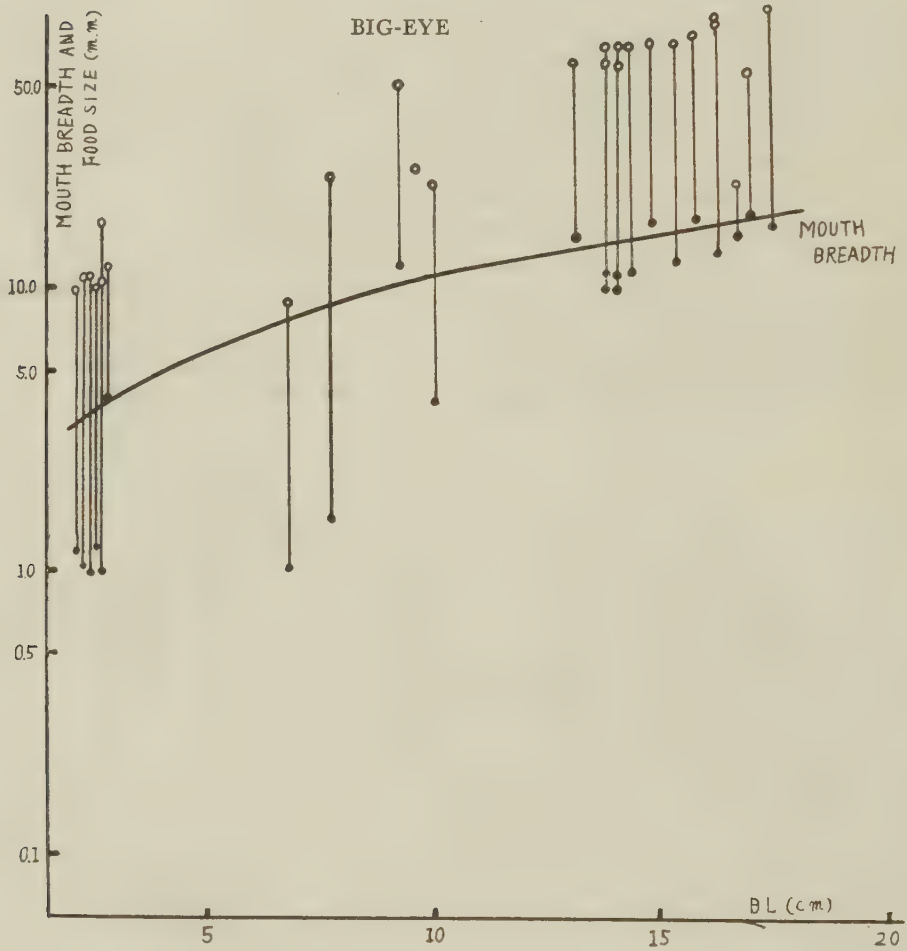

Fig. 4.

○ Maximum size of food ● Minimum size of food

Hence from these results it may be emphasised that in carnivorous or omnivorous types, the mouth breadth is more important factor than the gill structure in the study of its feeding habits. This may be one reason why in

some carnivorous or omnivorous fishes the gill is still primitive or undeveloped.

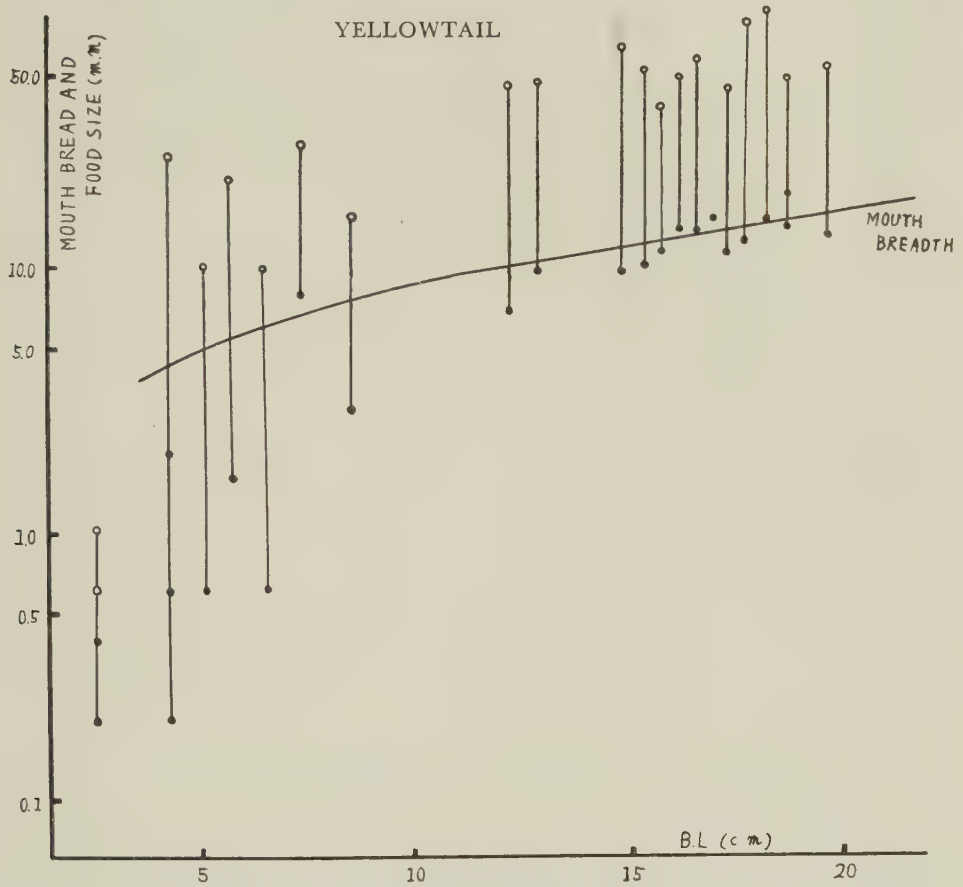

Fig. 5.

○ Maximum size of food ● Minimum size of food

Experiment

From these analytical results it was observed that in carnivorous fish the mouth breadth determines the size of food. To confirm these observations, experiments were carried out.

20 mackerels of body length ranging from 5 to 9 cm. were kept in a tank at the Misaki Marine Biological Laboratory of Tokyo University for about two weeks. Two days prior to the starting of the experiment in aim the fish were left unfed. As the experiment started the fish were fed only on goby of body length ranging from 2 to 7 cm and it was observed that the mackerel fed on goby that were only about 1/4 to 1/3 of its total length. Above this size limit any goby were hardly eaten. Though the survey made in sea, showed

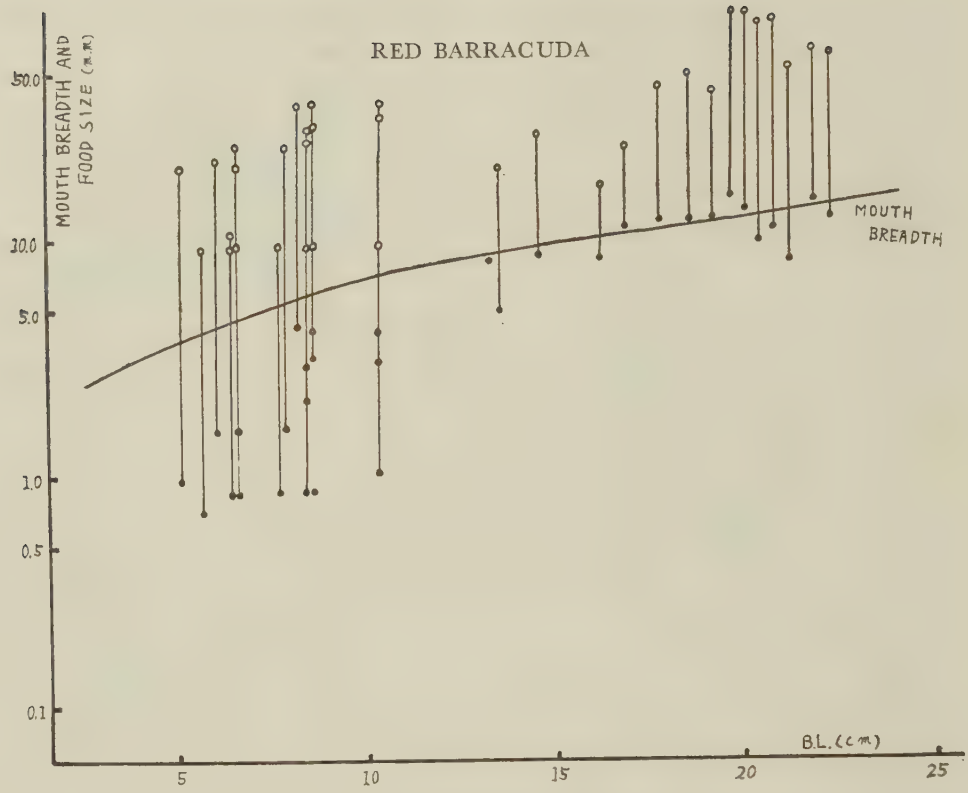

Fig. 6.

○ Maximum size of food ● Minimum size of food

that mackerels' food (shirasu=the young of sardines) size was about $\frac{1}{2}$ the total length of the mackerel, nevertheless in this case the body depth of the prey (Shirasu) was very much smaller than that of goby. When the total length of shirasu and goby of same body depth (3 mm.) were compared, it was seen that the average total length of shirasu was 33 mm., and tbat of goby was 20 mm. From this fact it appears that the body depth or body width is more important factor than the total length in the study of the size of food in fishes. The mouth breath of the mackerels in this experiment was about 5 mm. and there was hardly any difference between this size and the body depth of the prey. Earlier it was pointed out that the mouth breadth determines the size of prey. Now it may be safely said that size of prey should be taken to mean the body width or the body depth of the prey.

Discussion

In carnivorous fish the size of the prey is mostly determined by the size of the mouth breadth of the predator. The author surveyed five different species

of fishes of the carnivorous, omnivorous and plankton feeders and also made a study on the relationship of mouth breadth to food size. In carnivorous and omnivorous fishes the cleft and mouth breadth serve the same purpose as that of the gills in plankton feeders. However, though the structure of the gills may take different forms and may be either simple or complicated, the cleft and mouth breadth are simple structures and their sizes only vary in proportion to the size of each individual fish. It could be assumed that the teeth in carnivorous or omnivorous fish serves an important function in the feeding mechanism. However, if it is so it should be expected that the form and size of the prey should vary according to the size, form and shape of the teeth. This being not so the author believes that the teeth in carnivorous and omnivorous fishes have no direct relation to the feeding mechanism of these fishes. In the case of piscivorous fishes the prey is first trapped by the cleft, then it is taken into the mouth and fed on. In this series of feeding action the size of the prey (body depth or body width) becomes an important factor to the predator.

HAYASHI (1956) in his study on the relation of the size of prey to the predator remarked that the size of the prey is indicated not by the total length or body weight of the prey, but by its body depth or body width. He went on to say further that of the range of sizes that a predator can feed on, it is the larger sizes of the prey that a predator generally feeds on. This size of the prey is referred to as the "proper size" by HAYASHI.

From these experiments and survey the author has already shown that the minimum size of prey (body depth or body width) overlaps with the size of the mouth breadth. This fact indicated that the mouth breadth is a limiting factor on the size of the prey. Hence the author firmly believes that the "proper size" of the prey, is not the larger sizes of the prey that a predator can feed on, as had been referred to by HAYASHI, but it is that size of the prey (body depth or body width) which is almost equal to the size of the mouth breadth of the predator.

Summary

(1) In the feeding mechanism, namely the trapping of prey, the cleft of the predator serves the most important function, and the mouth breadth limits the size of the prey.

(2) As regards the size of the prey, the body depth or body width is more important than the total length or body weight, to the predator.

(3) The "proper size" of the prey (body depth or body width) is that size which is almost equal to the size of the mouth breadth of the predator.

Literature

1. Y. Hiyama & F. Yasuda (1957): The mechanism of utilization of plankton by fishes. (Rec. of Oce. Works Jap. Sp. No.)
2. F. Yasuda & Y. Hiyama (1957): Mechanism of utilization of plankton by some fishes. Rec. of Oce. Works Jap. Vol. 3 No. 1)
3. T. Chiba (1956): Studies on the Development and the Systematics of Copepoda. (Jour. of the Shimonoseki Fish. College, Vol. 6, No. 1)
4. T. Hayashi (1955): Quantitative relationship between piscivorous fish and the variety its food. (in Jap.)
   (Naikai Regional Fish. Resh. Lab.)
5. T. Hayashi (1956): On the feeding habits of fish. (in Jap.)
   (Naikai Regional Fish. Resh. Lab.)

Records of Oceanographic Works
in Japan Vol. 5. No. 2,
March, 1960

Notes on Some Edible Marine Fishes Collected between the Bonin Islands and the Mouth of Sagami Bay. II

By
Tokiharu ABE
(Tokai Regional Fisheries Research Laboratory, and Zool. Inst., Fac. Sci., Univ. Tokyo)

(With 1 Plate)

Abstract

Pristipomoides auricilla (JORDAN, EVERMANN & TANAKA) of the subfamily *Etelinae* is believed not to have been recorded from the Japanese waters. On the night of February 9, 1959, a fine example of this fish was taken by hook and line, 5 miles northeast of Torishima (southernmost island of Tokyo Prefecture). A description of this specimen is given together with some notes on other specimens of the species purchased in 1955 at the Central Wholesale Market of Tokyo. Additional notes on *Pristipomoides filamentosus roseus* (CASTELNAU) (*cf.* ABE & TAKASHIMA, 1956; ABE, 1957) are also given.

As stated by Prof. J. L. B. SMITH (1954, pp. 485 & 486) and the present writer (ABE, 1957, pp. 1160-1162), the species of *Pristipomoides* are in a state of confusion. Recently the writer has received for study a fine example of *Pristipomoides auricilla* (JORDAN, EVERMANN & TANAKA) from Mr. Yôji KURATA, Ôshima Branch, Tokyo Prefectural Fisheries Experiment Station, Habu, Ôshima (south of Tokyo), and found that it is distinct from *P. filamentosus roseus* (CASTELNAU) and *P. sieboldi* (BLEEKER). Further, he has learned that JORDAN & JORDAN (1922, p. 48) had pointed out the incorrect account of the dentition of *Pristipomoides violescens* (JORDAN & EVERMANN) in the original description (JORDAN & EVERMANN, 1903, pp. 182 & 183). According to the former authors, the tongue is toothless in *violescens*. In the present paper, the writer wishes to give an account of the specimen of *P. auricilla* just mentioned together with some notes on other specimens of this species and some notes, again, on *P. filamentosus roseus* (*cf.* ABE & TAKASHIMA, 1956; ABE, 1957). He expresses here his sincere thanks to Mr. KURATA for his kindness, and to Mr. Teizô ISA and his brother, Mr. Kin-ichi MATSUDA (middlemen at the Central Wholesale Market of Tokyo) for the trouble of picking up specimens of *P. auricilla* and congeners for study. It was in 1955 that they kindly sold him two specimens of *auricilla* which had been fished undoubtedly between the Bonin Islands and Hachijô Is-

land. It is also with pleasure that he expresses his sincere thanks to Dr. T. Kamohara for cordial cooperation.

A. A description of *Pristipomoides auricilla*

Pristipomoides auicilla (Jordan, Evermann & Tanaka)

"Kimadra*-himedai**, new Japanese name

Arnillo auricilla Jordan, Evermann & Tanaka, 1927, pp. 667-670. Hawaii.

Study material.——

1 specimen (Cat. No. Abe '59-28), measuring 370 mm. in total length, 332 mm. in fork length and 300 mm. in standard length. Taken by hook and line, 5 miles northeast of Torishima (midway between Hachijô Island and the Bonin Islands), at a depth of 260-350 m., above (or on) a bank, on the night of February 19, 1959. Fished by one of the crew of the 'Tonan-maru", research vessel of Tokyo Prefectural Fisheries Experiment Station, and presented by Mr. Yôji Kurata, along with a colored photograph (pl. I) of the specimen taken while fresh. The surface temperature of the sea was 19.4°C (after Mr. Kurata).

2 specimens (Cat. Nos. Abe '55-93 & '55-94), measuring 345 mm. and 305 mm., respectively, in standard length. Purchased at the Central Wholesale Market of Tokyo, on March 29, 1955, through courtesy of Mr. Teizô Isa and his brother. Judging by the activity of some Japanese fishermen bringing in considerable quantity of food fishes, mostly of the subfamily *Etelinae*, from southerly waters, these specimens were undoubtedly taken between Hachijô Island and the Bonin Islands. One of the specimens (Cat. No. Abe '55-93) has recently been lost sight of because of the confusion at the refrigerator where it has been kept; the other specimen (Cat. No. Abe '55-94) has recently been moved from the refrigerator to alcohol for future osteological study. The latter specimen is not in a good state, and proportional dimensions are not given of it below.

Proportional dimensions, expressed in perentages of standard length, of the formalin-preseved specimen (Cat. No. Abe '59-28).——

Greatest depth of body (between dôrsal and ventral origins) 29.2, gratest breadth of body (below dorsal origin) 17.3 least depth of caudal peduncle 8.7, length of head 29.3 (left) & 30.0 (right), horizontal diameter of eye 7.8 (left) & 7.7 (right), vertical diameter of eye 6.8 (left) & 7.0 (right), length of snout 9.7 on each side, interorbital breadth (not bony) above eye-centers) 10.7, least depth of preorbital (with skin) 3.0 on each side, length of upper jaw (from snout tip to postero-dorsal corner of maxillary) 12.0 (left) & 11.8 (right),

* Meaning motted with yellow.

** Meaning *Pristipomoides sieboldi* (Bleeker); "hime" is young lady or princess; "dai" is "tai", porgy.

greatest depth of upper jaw (at hind end) 3.3 on each side, length of longest (5th from top; on each side) pectoral fin-ray 28.0 (left) & 27.5 (right), length of ventral spine 13.3 (left) & 14.0 (right), length of longest (outermost) ventral fin-ray 21.5 (left) & 21.7 (right), length of longest (3rd) dorsal spine 12.0, length of longest (hindmost) dorsal fin-ray 12.5, length of longest (3rd) anal spine 8.7, length of longest (hindmost) anal fin-ray 14.0, length of longest (probably uppermost branched) caudal fin-ray *ca.* 26.7, length of longest (uppermost of lower limb; not the one at the junction between the upper and lower limbs) 4.0 (left & 3.7 (right).

General appearance and coloration.——

The keys a, b, cc, ee, f, gg and hh in "Analyses of genera of *Etelinae und Verilinae*" given by JORDAN, EVERMANN & TANAKA, 1927, pp. 666-668, and the account given by them on the type of *auricilla* well apply to the present specimens. Discrepancy in the width of preorbital may have been caused by the difference in the method of measuring this width. The pale and brownish violet parts (in formalin) of the photographed specimen were, after Mr. KURATA, a little deeper in color while fresh. In another specimen (Cat. No. ABE '55-94), the ground color was purplish while fresh, and there was a yellow part on the lower lobe of the caudal fin as well. Whether this coloration is characteristic for the male or not, is not certain.* Excepting for the coloration, narrow (or, low) preorbital and less produced hindmost fin-rays of the dorsal and anal, the present specimens resemble *Pristipomoides filamentosus roseus* fairly closely.

Fin-formulae.——

D. X 11 (=i+10 in 1 specimen; all soft rays branched in 2 specimens; last soft ray not bifid to base). A. II 8 (all soft rays branched in 3 specimens; last soft ray not bifid to base). P. 16 (=ii+12+ii) on each side in 2 specimens; 16 (left) & 15 (right) in 1 specimen, V. I 5 (all soft rays branched) in 2 specimens. C. 8/7 (branched soft rays) in 2 specimens.

Scales.——

The scales are ctenoid. The number of pored scales in the lateral line is 73 (of which 3 are behind the posterior end of the vertebral column and on the proximal part of the caudal fin) on each side. The number of scales in the oblique row from the dorsal origin down and rearward to the one just above the lateral

* It may be added here that this alcoholic specimen is believed to be a male and that the dention of the jaws, vomer and palatines is slightly different from that of the formalin-preserved specimen (Cat. No. ABE '59-28) which is believed to be a female (the gonads are in a poor state). The teeth of the vomer, palatines and the inner jaw teeth (inside of the canine-like outer larger teeth) are much larger in the male specimen than in the female, and the foremost canine-like teeth of the lower jaw are fairly larger in the male sPecimen than in the female. For dentition, *vide* pp. 105 & 106.

line is 1 (very small) +1 (fairly smaller than the lower scales) +7 on each sides. The number of scales in the oblique row from the anal origin up and forward to the scale just below the lateral line is 1 (fairly smaller than the upper scales) +15 (left) and 1 (very small) +1 (fairly smaller than the upper scales) +16 (right). The number of predorsal scales in and near (posteriorly) the mid-dorsal line is 17. Cheek with 7 rows of scales; the lowermost scales very small. Suboperculum with 4 (left) and 3 (right) horizontal rows of scales. Operculum with 8 (left) and 7 (right) vertical rows and 11 oblique (rising up and forward) rows of scales (on each side). The outside of the proximal part of the pectoral fin and the proximal part of the caudal fin are covered with small scales. The account of the scales given above is of the single specimen preserved in formalin.

Branchiostegals, pseudobranchiae and gill-rakers.——

The following account under this caption is based on 2 specimens (Cat. Nos. Abe '59-28 & '55-94). The left branchiostegal membrane laps over the right anteriorly. The number of branchiostegals is 7 on each side.

Pseudobranchiae are well developed, and the elevation in front of them on either side of the head is not pronounced.

Gill-rakers are rather stout, and number 7 (without any rudiments above) +1+18 (lowermost fairly small) left) and 8 (without any rudiments bove) +1+16 (without any rudiments below) (right) in 1 specimen; 1 (very small+9+1+19 (left) and 1 (extremely small) +9+1+18+1 (very small) (right) in 1 specimen.

Teeth, tongue and isthmus.——

The following account is based on two speciments (Cat Nos. Abe '59-28 & '55-94). Teeth are present on the jaws, palatines and vomer. There is a single row of canine-like teeth on the upper jaw. They are set rather sparsely, and those near the snout tip are a little larger than the posterior one. Inside of this row is a band of very small (villiform) teeth, which tapers posteriorly. The greatest width of the band (near the snout tip) is much larger than the greatest width of the band of the similar villform teeth of the lower jaw and the greatest width of the band of palatine teeth, and nearly equals (in the female), or, is fairly smaller (in the male) than, the height of the triangular patch of the vomerine teeth (measured parallel to the longitudinal axis of body). On the lower jaw, the foremost short single row of afew canine-like teeth,* which are set rather sparsely as in the upper, is separated laterally by a band of very small (villiform) teeth. The latter band of teeth on either side of the lower jaw does not extend posteriorly, and is continuous with a row of closely-act, canine-like teeth. Inside of this row of cannine-like teeth, there are no villiform

* In the larger male specimen, these teeth are fairly larger than the other teeth, some nearly flaring outwards. (*cf* p. 104).

teeth; in other words, the villiform teeth are confined to the anterior part of the lower jaw. The vomerine teeth are very small (villiform in the female specimen) or small (canine-like in the male specimen), forming a triangular patch, the posterior margin of the patch being nearly straight and perpendicular to the longitudinal axis of body. On each side of the posterior margin just mentioned, separated by a narrow naked area, is the head of the band of the villiform (in the female specimen) or small canine-like (in the male) palatine teth. This band gradually tapers rearwards. The tongue is not very broad anteriorly, forming a high trapezoid in smaller specimen, and slightly pointed anteriorly in larger one, and, though not very smooth, is toothless. Thus the dentition in *auricilla* resembles that of *filamentosus roseus*.

The isthmus is scaled, and keeled for a short distance along the mid-ventral line.

B. Again on *Pristipomoides filamentosus roseus*

a) Since the publication of an account of *Pristipomoides filamentosus roseus* (CASTELNAU) in 1957 (ABE, 1957), the writer has seen incresingly numerous individuals of this food fish at the Central Wholesale Market of Tokyo. This increase is caused perhaps by the profits and by the intensified activity of certain groups of fishermen who are familiar with handline fishing in the waters between the Bonin and the northerly islands. He has tried to find any examples and records of this fish in the waters around the mainland of Japan (namely, Honshu), but so far not been able to see any specimens and records. In 1957, he was inclined to suspect (ABE, 1957, p. 1155) that Dr. KAMOHARA's two small specimens recorded under the name of *Pristipomoides argyrogrammicus* might be *P. filamentosus roseus*. Recently, the present writer has examined these specimens kindly sent on loan from Dr. KAMOHARA, and found that they differ from *roseus* in having much larger scales (52 scales along lateral line) and remarkably fewer gill-rakers (5+1+12).

b) In discussing the species of *Pristipomoides*, Prof. J. L. B. SMITH (1954) and the present writer (1957) overlooked the account of the dentition of *Pristipomoides violescens* (JORDAN & EVERMANN) given by JORDAN & JORDAN (1922 p. 48). As stated above (p. 102 of the present paper), the original description of *violescens* is said to comprise incorrect account of the dentition. If this is true, it becomes more and more probable that *violescens* is a synonym of *roseus*, or, that they are very closely allied one to another.

References

ABE, T. 1957. In TOMIYAMA & ABE's Figures and descriptions of the fishes of Japan, vol. 1vi, pp. 1155-1163, pl. 227, figs. 578 & 579.

ABE, T. & Y. TAKASHIMA, 1956. Notes on some edible marine fishes collected between the

Bonin Islands and the mouth of Sagami Bay. — I. Bull. Tokai Regional Fisheries Research Laboratory, no. 14, pp. 15-19.

Jordan, D. S. & Evermann, B. W. 1903. Descriptions of new genera and species of fishes from the Hawaiian islands. Bull. U. S. Fish Commn., vol. xxii (1902), pp. 163-208.

Jordan, D. S. & Evermann, B. W. 1905. The aquatic resources of the Hawaiian islands. I. The shore fishes of the Hawaiian islands, with a general account of the fish fauna. Bill. U. S. Fish Comm., vol. xxii, pp. 1-574, 138 pls.

Jordan, D. S., Evermann, B. W. & Tanaka, S. 1927. Notes on new or rare fishes from Hawaii. Proc. Calif. Acad. Sci., 4th ser., vol. xvi, no. 20, pp. 649-680, pls. 22-24.

Jordan, D. S. & Jordan, E. K. 1922. A list of the fishes of Hawaii, with notes and descriptions of new species. Mem. Carnegie Mus., vol. x, no. 1, pp. 1-92, pls. 1-4.

Kamohara, T. 1953. Marine fishes newly found in Prov. Tosa, Japan, with descriptions of a new genus and species. Research Rep. Kôchi Univ., vol. ii, no. 11, pp. 1-10, 2 pls.

Smith, J. L. B. 1954. Fishes new to Africa obtained by deep line fishing in Kenya waters, with a revision of the East African species of the genus Pristipomoides Bleeker, 1852. Ann. Mag. Nat. Hist., ser. 12, vol. vii, pp. 481-492, pls. 10 & 11.

Explanation of Plate I.

Pristipomoides auricilla (Jordan, Evermann & Tanaka). Total length 370 mm. Captured by hook and line, 5 miles northeast of Torishima, on the night of February 19, 1959. Photograph by Mr. Yôji Kurata.

Records of Oceanographic Works
in Japan Vol. 5. No. 2,
March, 1960

On the Larva Possibly Referable to *Marlina marlina* (JORDAN & HILL)

By
Shoji UEYANAGI & Hiroshi YABE
(Nankai Regional Fisheries Research Laboratory)

Abstract

An istiophorid larva with rigid pectoral fin and short snout, about 26 mm. in total length, was collected from the equatorial area of western Pacific. As a result of the examination based on the diagnostic characters (form of pectoral fin, vertebral formula etc.), this larval specimen was identified with *Marlina marlina* (JORDAN & HILL).

It is noteworthy that this larva quite resembles in the profile of head, especially in the short snout, the larva of *Eumakaria nigra* NAKAMURA, in which the morphological change of the snout in his ontogenesis is known as a very characteristic one among the istiophorids.

We mentioned previously in a report(9) about the larvae of the black marlin* *Eumakaira nigra* NAKAMURA that an istiophorid larva, about 26 mm. in total length, which had the rigid pectoral fin and was supposed to be *Marlina marlina* (J. & H.) has been collected. But in subsequent examination of that specimen based on the several morphological characters containing the above diagnostic one (rigid pectoral), we ascertained it must be the larva of Shirokajiki** *Marlina marlina* (JORDAN & HILL).

The description and identification on the above mentioned larva are given in this paper.

Description of specimen

Data on the capture, selected measurements and meristic counts of the specimen are shown in Table 1.

The growth stage of this larval specimen is so advanced that one may recognize it immediately as the larval stage of the istiophorid (Fig. 1).

Body. — The dorsal profile is characteristic in giving the square shouldered impression; — projects conspicuously in the most anterior part of the dorsal fin and descends backward somewhat steeply. Each proportion

* This is the same as "Pacific blue marlin".

** Japanese name "Shirokajiki"; shiro—white, kajiki—marline.

Table 1. Data of capture and measurements for the specimen.

Date, Time	VI–21, 1954 0720–0930
Position	10°–21′ N 159°–35′ E
Water temperature	0 m–28.0° C 10 m–27.99°
Chlorinity	0 m–18.92 o/oo 10 m– 〃
Method of capture	dip-net
Measurements in mm:	
Total length	26.5
Standard length	23.
* V. F.—A. F.	7.7
Snout length	3.8
Dia. of orbit	2.8
Dia. of eye	2.55
Postorbital length	3.3
Upper jaw length	6.4
Lower jaw length	5.8
Head length	9.9
Head width	3.4
Pterotic spine	1.15
Preopercular spine	2.85
Body height:	
at ventral fin origin	4.1
at anal fin origin	2.8
Body width	2.65
Pectoral fin-ray length	4.0
Ventral fin-ray length	6.9
Anal fin-ray length	2.4
Dorsal fin-ray length:	
4th	2.45
5th	4.3
6th	5.0
10th	3.4
Counts:	
No. of pectoral fin-rays	21
No. of anal fin-rays	23
No. of dorsal fin-rays	ca. 50

* The distance from the ventral fin origin to the anal fin origin.

Fig. 1. Larva of *Marlina marlina*, total length 26.5 mm.

of head, trunk and tail is approximately 43, 33.5 and 23.5 % of standard length.

Head. — The profile of head is very similar with that of the larva of *Eumakaira nigra* in same growth stage as this specimen. Snout is slightly elongated (snout length is about 16 % of body length) and extends a little beyond the tip of the mandible. The eye is large with a diameter about one-quarter the head length. The spination of head is in the process of degenerating. The serrations on the orbital crest and the lower edge of the lower jaw are considerably diminished. Pterotic spine and preopercular spine are no more so prominent (length of the latter is approximately equal to the diameter of orbit). Small process is discernible on the upper side of the supracravicle. A small slit is found just anterior to the nostril. About ten fanglike teeth are present on the tip of the snout and also of the mandible, and follow to which approximately twenty teeth of varied sizes, forming two rows which turn inward and outward, and further, small teeth occur between the two rows. On the paratine also teeth are found. Both right and left branchiostegal membrane fuse into one, with seven branchiostegal-rays respectively.

Scale. — Minute spinelike scales are covering over the surface of postorbital portion, operculum and the trunk of body; however, are not yet found on the tail. The part without scale is discernible as the stripe like the lateral line pattern on the lateral side of the body. This stripe originates at the upper part of pectoral fin, descends posteriorly, and then it runs in an approximately straight line along the center of the side of body, and besides that another stripes are found under the former, like a branch pattern (Fig. 2).

Fig. 2. Showing the distributions of dermal spinelike scales on the lateral side of the body.

Fins. — Fin formation is advanced on each fin. Though the profile of dorsal fin is not exactly known because of the half-shutting condition caused by the fixation in formalin, dorsal fin seems not so high over its entire base

as those — sail-like type[9]—of the same sized sailfish larva or *E. nigra* larva. The anterior portion of the fin is the most highest* — formation of the anterior lobe — and posterior to which seems to lower gradually. That fin is not separate yet into two parts; however, the rear seven rays which may become the 2nd dorsal fin are more thicker than the anterior ones and distinguished from the latters. Fin-ray

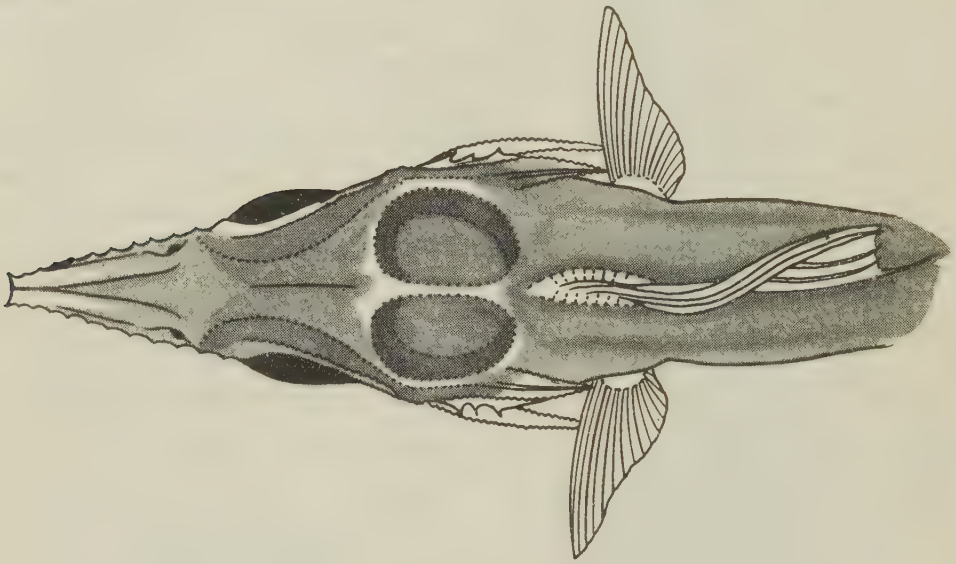

Fig. 3. Showing the rigid pectoral fin with dorsal view.

numbers are estimated approximately 50. Sheath of fin is formed along its entire base. Anal fin with 23 rays is not separate yet too, however, the seven rays of posterior part are thick as well as the case of dorsal fin and the tendency of differentiation is recognized. Pectoral fin is remarkably characteristic. The base of fin twists anteriorly and fin stands out from the side of the body at a right angle and spreads itself horizontally, bending the outer surface. As a result of this structure, fin cannot be folded against the side of the body without breaking the joint between the fin and the shoulder girdle. Pectoral fin has 21 rays. Ventral fin is very long and reaches to nearly 90 % of the abdominal length.** The third ray is little longer than the first ray. Ventral fin groove is formed over the entire length of the abdomen. Caudal fin is forked and articulations in the rays are discernible. Lateral keel on the caudal peduncle is not yet formed.

* The 6th ray is the longest.

** The distance from the ventral fin insertion to the anal fin insertion (indicated in Table 1. as "V.F. — A.F.").

*Pigmentation.** — The pattern of pigmentation extends over almost all the surface of body (assuming a brownish colour). The parts without pigment only remain in the upper and lower jaw (except the anterior portion of them), branchiostegals membrane, orbit, spines and serrations and in the tip of the tail. Anterior portions of inner side of both jaws are coloured with dark brown, and ventral side of body with yellow-white. Fins have no colour except the dorsal fin. In the dorsal fin membrane are dispersed many dark-brown spots densely, however, the most anterior part (anterior to the 4th ray) and the rear part (about ten rays) have no pigments. Stripes or band-like pattern is not found.

Identification of the specimen

Examination of this specimen comparing to the already known istiophorid larvae was done, paying attention to the characters, namely, the profile of head and dorsal fin etc., which are thought to be effective in the diagnosis of the larval stages of istiophorids, and consequently it was found that this specimen hardly resembles the larvae of sailfish (*Istiophorus*)[1, 10, 11] or striped marlin (*Makaira mitsukurii*)[8] in the above mentioned characters and also looks different from the larva of *Eumakaira nigra*.[9] In regard to the last one, this specimen bears a striking resemblance to that in the profile of head and in the long ventral fin, however, differs obviously from that in the shape of dorsal fin.

As mentioned above, this specimen seems not to belong to the any of former three istiophorid species, and it is noticeable that this specimen quite differs in the form of pectoral fin from them. Such a characteristic — rigid — pectoral fin as observed in this specimen is only found on *Marlina marlina* of all marlins and its character has been recognized as a important diagnostic one for this marlin.[2, 3, 4] From this point, this specimen is supposed to be the larval stage of *Marlina marlina* (J. & H.).

Then the following examination was made to confirm this presumption.

The vertebral numbers of this specimen was counted by the method of taking a soft X-ray photograph, and as a result the vertebral formula was calculated 11+13 (Fig. 4). It is known that the marlins with such vertebral formula are the *E. nigra* or *M. marlina*.[2, 4, 6] But the possibility for this specimen to be the larva of *E. nigra* is negated by reason of the facts mentioned already. That is, the above presumption is supported on this basis. The calculation results of the each fin-ray numbers also support that presumption.

* Observation was made in the condition of specimen preserved in alcohol for a long time after fixation by formalin. On fresh specimen, dorsal and lateral surface of body colored with steel-blue; ventral side of body, silver-white.

Fig. 4. Vertebrae of the specimen, soft X-ray photograph.

From the whole results of variable examinations, this specimen is recognized as the larva of *Marlina marlina* (Jordan & Hill).

If this identification is right, from the appearances of this larva and adult of *M. marlina* it seems to us that the morphological change of the snout in the ontogenesis on *M. marlina* is the similar type of that of *E. nigra*,[7, 9] (although we can't say conclusively, because of the entire lacking of informations for the both anterior and posterior growth stages of this specimen, namely the larval and young stages). And if it is so, the interesting questions seem to rise in respect of the relationships or systematic problems on the Istiophoridae and we wish to discuss this subject in future.

References

(1) Gehringer, J. W. (1956): Observations on the development of the Atlantic sailfish *Istiophorus americanus* (Cuvier) with notes on an unidentified species of Istiophorid. Fishery Bull. 110. Vol. 57, 33 pp, 40 figs, U. S. Fish and Wildlife Service.

(2) Howard, J. K. (1959): Contribution to the determination of the valid scientific name for the rigid-pectoraled marlin of the Pacific. Spe. Ser. Bull. No. 15, Program for Research of Istiophoridae, Mar. Lab., Univ. of Miami.

(3) Morrow, J. E. (1957): On the morphology of the pectoral girdle in the genus *Makaira*. Bull. of Bingham Oceanogr. Collection. 16 (2), pp. 18, figs. 4.

(4) Nakamura, Hiroshi. (1938): Report of an investigation of the spearfishes of Formosan waters. Repts. Taiwan Govt., Gen. Fish. Exp. Stat. 1937 (10), 15 pls., 12 figs.

(5) Royce, W. F. (1957): Observations on the Spearfishes of the Central Pacific. Fishery Bull. 124. Vol. 57, pp. 58, figs. 27, U. S. Fish and Wildlife Service.

(6) Ueyanagi, Shoji. (1957): Young of the black marlin, *Eumakaira nigra* Nakamura. Rept. Nankai Reg. Fish. Res. Lab., 6: 91-102, 3 pls., 5 figs.

(7) Ueyanagi, Shoji. (1957): Morphological changes occurring through the growth of the Black Marlin, *Eumakaira nigra* Nakamura. Rept. Nankai Reg. Fish. Res. Lab., 6: 103-106, 5 figs.

(8) UEYANAGI, Shoji. (in press): Larvae of the striped marlin, *Makaira mitsukurii* JORDAN & SNYDER.

(9) UEYANAGI, Shoji. & Hiroshi, YABE. (1959); Larva of the Black Marlin (*Eumakaira nigra* NAKAMURA). Rep. Nankai Reg. Fish. Res. Lab., 10: 151-169, 1 pl., 18 figs.

(10) VOSS, G. L. (1953): A contribution to the life history and biology of the sailfish, *Istiophorus americanus* Cuv. and Val., in Florida waters. Bull. Mar. Sci., Gulf and Caribbean, 4 (3), pp. 206-240, figs. 1-6.

(11) YABE, Hiroshi. (1953): On the larvae of sailfish, *Istiophorus orientalis* collected in the South-western Sea of Japan. Contributions of Nankai Reg. Fish. Res. Lab., No. 1, 10 pp. 6 figs.